Fall 12-17-2021

Design and Synthesis of Small Molecular probes for CNS and Kidney Disorders

Swagat H. Sharma
University of Nebraska Medical Center

Design and Synthesis of Small Molecular probes for CNS and Kidney Disorders

by

Swagat Sharma

A DISSERTATION

Presented to the Faculty of

the University of Nebraska Graduate College

in Partial Fulfillment of the Requirements

for the Degree of Doctor of Philosophy

Pharmaceutical Sciences

Graduate Program

Under the Supervision of Professor Corey Hopkins

University of Nebraska Medical Center

Omaha, Nebraska

November, 2021

Supervisory Committee:

Jonathan L. Vennerstrom, Ph.D.   Ram Mahato, Ph.D.

Amarnath Natarajan, Ph.D.   Paul Trippier, Ph.D.

ACKNOWLEDGEMENTS

Design and Synthesis of Small Molecular probes for CNS and Kidney Disorders

Swagat Sharma, Ph.D.

University of Nebraska Medical Center, 2021

Supervisor: Corey Hopkins, Ph.D.

The G protein regulated inwardly rectifying potassium channels (GIRK) are a family of inwardly rectifying potassium channels and are key effectors in signaling pathways. GIRK 1/2 channel subunit, predominantly found in the brain, is involved pathophysiology of various neurological disorders including, but not limited to, epilepsy, anxiety, Parkinson's, pain, reward, and addiction. Previously, our laboratory had identified a series of urea containing molecules as GIRK1/2 preferring activators. Unfortunately, the urea series suffers from significant PK liabilities (solubility, brain penetration and high clearance). The chapter 1 of the dissertation describes our efforts in developing three new series of activators with improved pharmacokinetics properties while retaining activity.

Human Mas-related G protein-coupled receptor X1 (MRGX1) is a part of the larger GPCR family of receptors and has restricted expression in nociceptors within the peripheral nervous system. Allosteric activation of Mrgx1 inhibits the high voltage acting Ca^{2+} (HVA) channel necessary for nociception. This makes it a promising target for non-addictive pain therapy. Previous efforts in our lab for optimization of hits obtained from high-throughput screening (HTS) had led to the development of a selective MrgX1 allosteric agonist, ML382. Chapter-2 shows our SAR studies around ML382 to overcome potential pharmacokinetic liabilities of ML382 and identify newer and more potent MrgX1 allosteric agonists. Through our medicinal chemistry based efforts we were able to identify 10 fold more potent agonists compared to ML382.

Progressive chronic kidney disease (CKD) is characterized by a total or considerable loss in kidney function, affects approximately 1 in 10 people around the world. Previous work in our

collaborator's laboratory has established the role of the transient receptor potential canonical-5 (TRPC5) ion channel in mediating calcium influx in podocyte leading to cytoskeletal changes and loss of functionality. Chapter-3 describes our medicinal chemistry based approach for the design, synthesis and characterization of novel benzimidazole basedTRPC5 inhibitors We were able to bring the activity from micro-molar to low nano molar.

Table of Contents

LIST OF FIGURES

LIST OF TABLES

LIST OF SCHEMES

ABBREVEATIONS

ACN/CH$_3$CN	Acetonitrile
AcOH	Acetic acid
AUC	Area under the curve
BAM 8-22	Bovine adrenal medulla peptide
BBB	Blood-brain barrier
BBr$_3$	Boron tribromide
BINOL	1,1′-Bi-2-naphthol
CDCl$_3$	Deuterated chloroform
CDI	*N,N'*-carbonyldiimidazole
CHS	Cholesteryl hemisuccinate
CKD	Chronic kidney disease
CL$_{HEP}$	Hepatic Clearance
CL$_{INT}$	Intrinsic Clearance
CNS	central nervous system
CryoEM	Cryogenic electron microscopy
Cs$_2$CO$_3$	Cesium carbonate
CTD	cytoplasmic domain
CuI	Copper Iodide
CVD	Cardiovascular disease
D1	Dopamine 1
DAG	Diacylglycerol
DAMGO	Ala^2-MePhe^4-Glyol^5-Enkephalin
DCM	Dichloromethane
DIPEA	N, N-Diisopropylethylamine

DMF	Dimethylformamide
DMSO	Dimethyl sulfoxide
DMSO-d_6	Deuterated dimethyl sulfoxide
DN	Diabetic nephropathy
DRG	Dorsal root ganglion
EC_{50}	Half maximal effective concentration
EDG	Electron donating group
EK	Reversal Potential of K^+
ER	Endoplasmic reticulum
ESI	Electrospray ionization
EtOH	Ethanol
EWG	Electron withdrawing group
FSGS	Focal Segmental Glomerulosclerosis
GIRK	G protein-gated, inwardly rectifying K^+ channels
GABA	γ-aminobutyric acid
GPCRs	G-protein coupled receptors
h	Hour
HATU	Hexafluorophosphate azabenzotriazole tetramethyl uronium
hCL_{INT}	Human Intrinsic clearance
hCL_{HEP}	Human Hepatic clearance
HEK293	Human embryonic kidney 293 cells
HEPES	(4-(2-hydroxyethyl)-1-piperazineethanesulfonic acid)
hERG	human Ether-à-go-go-Related Gene
HLM	Human liver microsomes
HPLC	High-performance liquid chromatography

HSQC	Heteronuclear single quantum coherence
HTS	High throughput screen
HVA	High voltage active
IC_{50}	Half maximal inhibitory concentration
IP	Intraperitoneal
IP3	Inositol triphosphate
IPSP	Inhibitory postsynaptic potential
IRK/Kir	Inwardly rectifying potassium channels
IV	Intravenous
JHICC	Johns Hopkins Ion Channel Center
K_2CO_3	Potassium carbonate
KATP	ATP sensitive potassium channels
LCMS	Liquid chromatography–mass spectrometry
MDCK	Madin-Darby Canine Kidney
MeOD/CD_3OD	Deuterated methanol
MeOH	Methanol
Met-ID	Metabolite-ID
MLM	Mouse liver microsomes
MLSMR	Molecular Library Small Molecule Repository
Mrg	Mas-related G-protein–coupled receptor
MW	Molecular Weight
$NaCNBH_4$	Sodium cyanoborohydride
NADPH	Nicotinamide adenine dinucleotide phosphate
$NaHCO_3$	Sodium bicarbonate
NaOEt	Sodium Ethoxide

n-BuLi	n-butyl lithium
NMP	n-methyl-2-pyrrolidone
NMR	Nuclear Magnetic Resonance
PAM	Positive allosteric modulator
PAMP	Pro adrenomedullin amino-terminal 20 peptide
PCl_5	Phosphorus pentachloride
$PdCl_2$	Palladium(II) chloride
$PdCl_2$.dppf.DCM	[1,1'-Bis(diphenylphosphino)ferrocene]palladium(II) dichloride
PIP2	Phosphatidylinositol 4,5-bisphosphate
PK/PD	Pharmacokinetics and pharmacodynamics
PLC	Phospholipase C
PNS	peripheral nervous system
$POCl_3$	Phosphoryl chloride
PPB	Plasma Protein Binding
Prep-HPLC	Preparative high-performance liquid chromatography
PSA	Polar surface area
PyClu	chlorodipyrrolidinocarbenium hexafluorophosphate
Rac	Rho GTPases
RBF	Round bottom flask
RED	Rapid Equilibrium Dialysis
RT	Room temperature
R_T -	Retention time
SAR	Structure-activity relationship
SPE	Solid phase extraction
T3P	Propanephosphonic acid anhydride

TBAI	Tetra-n-butylammonium iodide
TBDMSCl	Tert-Butyldimethylsilyl chloride
tBu_3PHBF_4	tri-tert-butyl phosphonium tetrafluoroborate
TEA	Triethyl amine
TEA-HCl	Triethyl amine-Hydrochloric acid salt
TFA –	Trifluoro acetic acid
T_{half}	Half-life
THF	Tetrahydrofuran
Tmax	Transport maximum
TMD	Transmembrane domain
$TMSN_3$	Trimethylsilyl azide
TR-MCD	Treatment-resistant minimal change disease
TRP	Transient receptor potential
TRPC	Transient receptor potential cation channels
UNMC	University of Nebraska Medical Center
VSLD	Voltage sensing-like domain
VTA	Ventral tegmental area

CHAPTER 1. GIRK1/2 Activators

1.1. INTRODUCTION TO GIRK CHANNELS

GIRK Channels

In the last few centuries, humans have learned to utilize artificial magnetic fields to create a flow of electrons. This is primarily achieved by mobilizing the valence electrons in metals and conductors. The flow of electrons from high to low voltage creates a current which can be utilized in various ways to transport energy or conduct a message. Long before the development of the process to create currents, mankind knew about body-generated current. Throughout different civilizations, there have been mentions of these currents. Current in the body is predominantly a result of gradient differences between the prominent water-soluble cations such as sodium (Na^+), potassium (K^+), calcium (Ca^{+2}), and anions such as chloride (Cl^-). Excitable cells such as neurons and cardiomyocytes utilize this concentration gradient to create a small but measurable electric voltage across the cellular membrane; known as the membrane potential. The potential across the cellular membrane in neurons is approximately -70 mV. Ion channel proteins in the cellular and intracellular membranes passively and actively regulate the pores permeable to various water-soluble ions involved in sustaining life. Ion channels exploit ion concentration gradients and generate changes in the membrane potentials of excitable cells. The current produced is utilized to send and receive signals from the brain. The signals for sleep, emotions, voluntary movements, involuntary movements, and many more physiological phenomenon are operated by virtue of this small yet measurable current.[1]

These ion channels are operated primarily by two mechanisms, direct modulation by an endogenous or an exogenous trigger ranging from a single ion to small molecules, peptides, and hormones. And second is mediated through a secondary modulation based on signals from other membrane-bound receptors such as G-protein coupled receptors (GPCRs). Ion selectivity,

membrane expression, and responsiveness to biological or external stimuli are some of the main features that influence the role of ion channels in various physiological process.[2]

A family of proteins capable of modifying the ability of an electrical signal to form is the G protein-gated, inwardly rectifying K^+ channels (GIRK). Nearly 100 years ago, the first observation linking a physiological response modulated by GIRK channels was published.[3] As their name describes, GIRK channels are gated by G proteins, display inward rectification, and are K^+ selective. G Protein gated inwardly rectifying potassium channels (Ki3/GIRK) are part of a larger family of inwardly rectifying potassium channels (Kir). These GIRK channels coupled to numerous G protein-coupled receptors regulate cellular excitability and inhibitory neurotransmitters. These channels act as a mediator for the effects of many neurotransmitters, neuromodulators, and hormones, contributing to general homeostasis, synaptic plasticity, learning memory, and pain signaling. Inwardly rectifying potassium channels (IRK/Kir) are a diverse set of potassium channels in eukaryotic species, classified into seven subfamilies (Kir1-Kir7) encoded by different *KCNJ* genes. These are divided into four functional groups based on their mechanism of action: (1) Kir2 are the classical rectifier channels; (2) G protein gated inwardly rectifying potassium channels (Ki3/GIRK); (3) ATP sensitive potassium (KATP); and (4) Potassium transport channels (Kir1, Kir2, Kir5, Kir7). Due to their connection with the GPCRs, it is believed that many approved CNS drugs such as desimipramine, fluoxetine, haloperidol, thioridazine, pimozide and do interact with the GIRK channels.[4] A better understanding of the physiological role of GIRK channels is vital to understanding their role in health and diseases. The discovery and development of novel selective activators and inhibitors of these GIRK channels will pave the way towards a better understanding of the physiological functions of this vital potassium channel. There is strong evidence of the relationship between GIRK channels and various neurological and psychiatric conditions. The development of a selective channel activator will be of great value to understand the physiology, pathology, and pharmacology of these interesting channels and develop possible CNS active drugs.[5-7]

Structure and Distribution

The basic topology of all Kir channels consists of four subunits combining to form a canonical K⁺ pore-forming transmembrane domain (TMD) and a large cytoplasmic domain (CTD). Two gates in series regulate ion conduction: one created by the inner helices of the TMD, and the other by the G loop at the apex of the CTD. Protein cascade usually interacts with the N- and C-terminus in the CTD, as shown in **Figure 1**.**1**.[8, 9]

GIRK channels are assembled in a tetrameric unit, formed by four essential subunits: GIRK1 (Kir3.1/KCNJ3), GIRK2 (Kir3.2/KCNJ6), GIRK3 (Kir3.3/KCNJ9), and GIRK4 (Kir3.4/KCNJ5). These subunits assemble into either heterotetramers or homotetramers channels, depending upon the specific GIRK subunits expressed within a cell. GIRK subunits have different N- and C- terminal domains, affecting their trafficking and membrane localization.[10] Owing to this, only GIRK2 and GIRK4 can form functional homotetramers in the brain and the heart, respectively, due to the presence of endoplasmic reticulum (ER) export motif in the CTD that permits their homotetrameric assembly and promotes channel trafficking to the cell surface. GIRK1 and GIRK3 subunits lack this motif and thus, only appear in the form of heterotetramers mostly with GIRK2.[10] Differential GIRK subunit expression throughout various organs leads to specific channel combinations and physiological role/significance.[11]

Initial structural studies for GIRK channels were predominantly site-directed mutagenesis experiments to pinpoint the amino acids involved in binding. Whorton *et. al.* were the first to solve a GIRK2 homotetramer by X-ray crystallography.[12] The findings are as follows: GIRK is a transmembrane protein with extracellular loops, but its C- and N-terminals are located intracellularly. Each subunit has two transmembrane helices, designated TM1 and TM2, and a pore region that constitutes the inner lining of the channel. The extracellular loops serve as an ion selectivity filter for the channel, while both the C- and N- terminals exposed to the cytoplasm inside the cell are the binding sites for G protein subunits and other structural proteins involved in

signaling cascades and channel gating. In the hinge region, the G-loop gate connects the transmembrane (TMD) and cytoplasmic domain (CTD) and acts as the physical barrier for ion penetration. The open and closed state of the G-loop gate controls the flow of ions due to conformational changes upon binding of other co-factors to the channel. The TM1 and TM2 helices contain multiple positive amino acid residues (e.g., Arg, Lys), which act as the binding sites for the negative phosphate head group of phosphatidylinositol 4,5-biphosphate (PIP2), a very important lipid that stabilizes the conformation of the channel, as shown in **Figure 1.2.** There are other multiple sites where sodium ions are also bound, stabilizing the channel. Overall GIRK channel is a part of a larger supramolecular assembly in the membrane, tightly associated with the signaling GPCR, G-proteins, and co-factors such as PIP2. The filter preference for alkali metal cations across GIRK channel is $K^+ \approx Rb^+ > Cs^+ > Na^+ > Li^+$.[12, 13]

GIRK2 (Kir3.2) forms functional homotetramers and are thus a good candidate for crystallographic structure determination. A recent structural characterization for GIRK2 was performed by Yamuna *et al.* using cryo-electron microscopy (CryoEM) technology. The aim was to figure out cholesterol binding in GIRK2, providing new therapeutic sites for modulating these channels. Structures of GIRK2 in the presence and absence of the cholesterol analog cholesteryl hemisuccinate (CHS), and PIP2 revealed that CHS binds near PIP2 in lipid-facing hydrophobic pockets of the transmembrane domain (TMD). CHS potentiates the effects of PIP2, which stabilizes the inter-domain region and promotes the engagement of the cytoplasmic domain (CTD), suggesting it to be a positive allosteric modulator (PAM). Apart from identifying novel therapeutic sites for modulating GIRK channels in the brain using cholesterol analogs, one major implication of this study is towards neurodegenerative diseases characterized by elevated cholesterol levels in the brain, primarily AD, Parkinson's, and Huntington's diseases.[14]

In the CNS, GIRK1-3 subunits are widely expressed in the olfactory bulb, hippocampus, cortex, thalamus, and cerebellum, as well as in the spinal cord.[15] GIRK1/2 heterotetramers are the

prominent variation of GIRK channels in neurons. GIRK2 is critical for generating GIRK currents in neurons, as mice lacking this subunit exhibit reduced GIRK currents in different parts of the brain.[6] Dopamine neurons in the ventral tegmental area (VTA) express a GIRK2/3 heteromer. GIRK1/4 is another predominant channel; however, its location is limited to the heart.[16] Alternative splicing of the Kcnj gene transcripts reveals multiple isoforms of the GIRK2 subunits (GIRK2a-d), assembled either into homotetrameric or heterotetrameric combinations. Several isoforms of GIRK1 and GIRK3 subunits are also cloned, but their expression patterns and functional relevance have not been established yet.[17]

Figure 1.1. Crystal structure of the GIRK2 (Kir3.2) In complex with the beta-gamma G protein subunits. Looking from top. K+ ion can be seedn in the middle of the pore. PDB-4KFM**.**
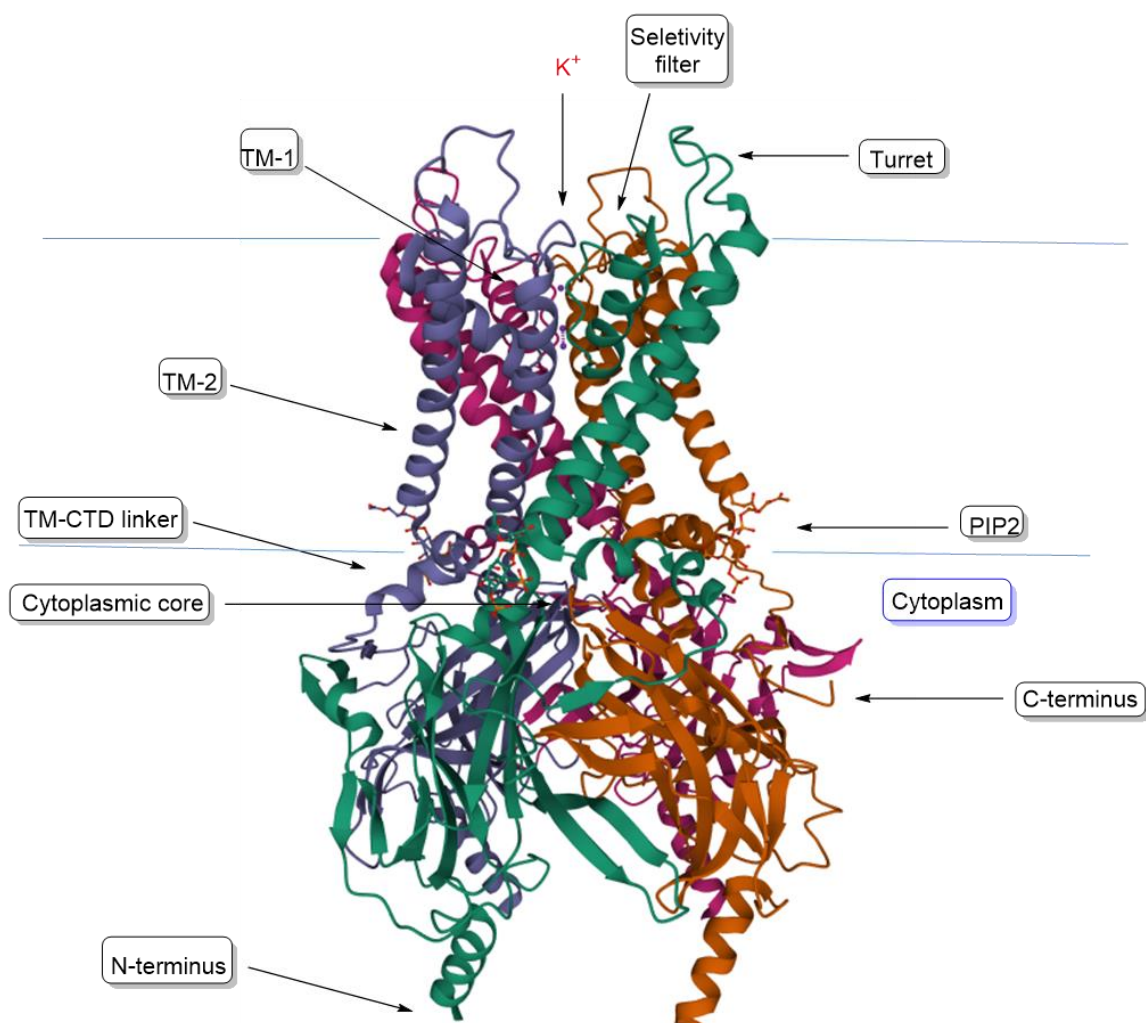
Figure 1.2. CryoEM structure of the G protein-gated inward rectifier K+ channel GIRK2 (Kir3.2) in complex with PIP2. (PDB: 6XIT)[13]

Mechanism of Action

The mechanism of GIRK channel activation/inhibition mediated by different modulators, signaling pathways, and the consequences of those activation/deactivation open the door towards the understanding of targeting GIRK in various CNS-related diseases states.

GIRK channel activation elicits the flow of K^+ ions across the cell membrane and thus drives the membrane voltage toward the Nernst potential for K^+. At Nernst potential, there is no net current flow of ions through a membrane. This leads to a stabilization of the K^+ membrane potential at the reversal potential of K^+ (EK), making depolarization more difficult to accomplish and, therefore, making action potentials more difficult to generate. In this way, GIRK channels can mediate an inhibitory postsynaptic potential (IPSP) in neurons. Near the K^+ Nernst potential, voltage-dependent Na^+ and Ca^{2+} channels tend to be silenced, and therefore electrical excitation is diminished. This is an essential signaling mechanism by which hormone and neurotransmitter stimulation GPCRs regulates many essential physiological processes.[18]

GIRK channels are predominantly expressed in dendrites, where they mediate slow inhibitory postsynaptic effects (IPSPs) after activation by GPCRs, which contributes to the suppression of neuronal excitability by hyperpolarizing membrane potential and slowing down the repolarization of cell membranes.[6]

A wide variety of neurotransmitters and neuromodulators such as γ-aminobutyric acid (GABA), serotonin, adenosine, dopamine, opioids and somatostatin, can induce the activation of GIRK channels. The GIRK channels require the presence of the co-factor PIP2 for their functioning. The G-proteins are heterotrimers composed of α, β, and γ subunits. Gα contains GTPase domain which transforms GTP into GDP upon GPCR activation, and in this way, it mediates the time for which channel remains in an open state since GIRK channels are only active in the presence of GTP. The binding of the neurotransmitter to its respective GPCR, in the presence of GTP and PIP2, causes a conformational change or dissociation of the G-protein into Gα(i/o) and

Gβγ, allowing the interaction between Gβγ and GIRK, which mediates the opening of the channels gates and allows potassium conductance The hydrolysis of GTP to form GDP reverts back the conformational change of the G protein, causing the separation of the Gβγ subunit from its GIRK binding sites leading to the deactivation of the GIRK channel. In contrast, molecules such as acetylcholine, substance P, or TSH-releasing hormone interact with GPCRs that are coupled to a different G-protein (Gq), and its activation reduces the activity of GIRK channels after the molecule binds to the GPCR, Gq activates phospholipase C (PLC). PLC reduces the local concentration of PIP2 by hydrolysis to inositol triphosphate (IP3) and diacylglycerol (DAG), which decreases GIRK currents due to the necessity for PIP2 for channel opening, as shown in **Figure. 1.3.**[7, 11, 19]

GABA receptors. In pyramidal cells, activation of GIRK currents by GABAB receptors induces cell hyperpolarization and is mainly involved in postsynaptic inhibition, thus modulating hippocampal excitability and plasticity. In Down's syndrome mouse models, animals have a third copy of the GIRK2 subunit, resulting in augmented GIRK2 expression in the brain (and particularly CA1 pyramidal cells). In the opposite scenario, Amyloid-β (Aβ) peptides decrease GABAB currents in CA3 pyramidal neurons. This effect is most likely observed due to a reduction in the expression of some GIRK subunits and GIRK channels conductance. This ultimately leads to hippocampal hyperexcitability, which characterizes the early stages of Alzheimer's disease. [20]

Serotonin receptors: GIRK channels modulate depressive behaviors through serotonin signaling. GIRK1-3 channel subunits are co-expressed with 5-HT_{1A} receptors in most cells of the hippocampus, cerebral cortex, septum, and dorsal raphe nucleus. Activation of GIRK channels by 5-HT induces membrane depolarization and mediates a slow excitatory response. 5-HT_{1A} and GIRK2 knockout mice exhibit depression-resistant behavior and decreased anxiety. While only 5-HT_{1A} knockout animals display increased anxiety.[21]

Dopaminergic receptors: Dopamine receptors are metabotropic receptors divided in two classes: D1-like (D1 and D5) receptors that activate stimulatory $G_{\alpha olf}$ subunit (guanine nucleotide-binding protein subunit alpha) and D2-like (D2, D3, D4) receptors that operate through inhibitory

Gαi/o proteins. GIRK signaling mediates effects of both classes of dopamine receptors in the striatum and midbrain. GIRK2 knockout mice have a higher susceptibility to seizures and exhibit hyperactivity and increased D1 receptor signaling. Transient motor hyperactivity in GIRK1-knockout and GIRK2-knockout mice can be inhibited by application of the D1 receptor antagonist SCH23390 or a high dose of GIRK1/2 activator **ML297**.[22, 23]
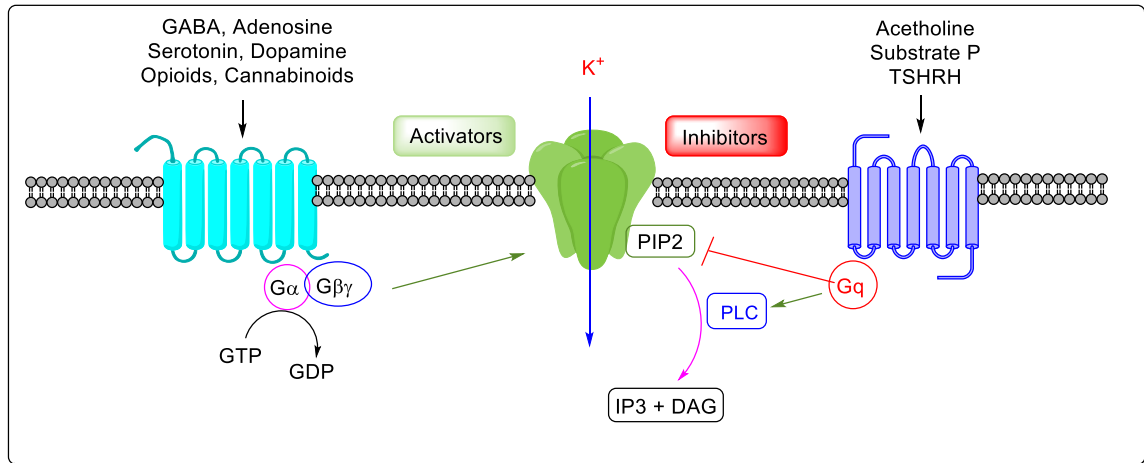
Figure 1.3. Mechanism of GIRK activation and inhibition by GPCRs and exogenous modulators. Exogenous modulators may exhibit their effects via interaction with the GPCR cascade or direct interaction with the channel.

GIRK Channels in Diseases

G protein-gated inwardly rectifying potassium (GIRK) channels provide a primary source of inhibition in the brain and have been implicated in a variety of neurological disorders. Loss of GIRK channel function leads to hyperexcitability and susceptibility to seizures, changes in alcohol consumption, and increased sensitivity to psychostimulants. Over the years, there have been extensive studies on various GIRK subunit knockout mice, which demonstrate a wide array of phenotypes resulting in many physiological processes. Some of the studies are shown in **Table 1.1.**

Pain and Addiction: GIRK channels are not only crucial in homeostatic and synaptic plasticity processes but also in reward signaling and drug addiction since they are present in many dopaminergic, GABA-ergic and glutamatergic neurons of the mesocorticolimbic pathway.[24] Behavioral memory (e.g., in hippocampus and amygdala) and reward-related behavior (in the mesocorticolimbic pathway), drug addiction or basically any type of addiction is considered as the aberrant form of learning and memory. Psychotropic drugs hijack normal processes of learning and memory and are shown to alter GIRK-dependent signaling, which drives pathological plasticity processes in the reward system that are crucial for the development of addiction. GIRK channels are also important in the spinal and supraspinal pain signaling since they are expressed not only in the brain but also in the spinal cord and in the sensory neurons of the dorsal root ganglion (DRG) cells. They mediate analgesic effects of the GABAB cannabinoid-, opioid- and norepinephrine receptor agonists.[25] Activation of GIRK2-containing channels is necessary for analgesia since weaver, and GIRK2 knockout mice do not respond to the analgesic effects of drugs that act through cannabinoid, GABAB, or opioid receptors. Additionally, GIRK2-, GIRK3- and GIRK2/3-knockouts are characterized by increased sensitivity to pain (hyperalgesia) and generally do not respond to the morphine treatment.[26-29]

Epilepsy: Epilepsy is caused due to neuronal hyperexcitability thus reducing cell excitability is a potential method to treat epilepsy. GIRK channels are important inhibitory regulators in reducing cell excitability through hyperpolarizing membrane potential in the central

nervous system.[6, 30] GIRK2$^{-/-}$ knockout mice develop spontaneous convulsion and show a increased propensity for generalized epileptic seizures when given a GABA$_A$ receptor antagonist injection. Pentylenetetrazol (PTZ) a commonly used convulsant, when injected results in higher severity score and short latency time in GIRK2$^{-/-}$ mice compared to wildtype.[31] Tertiapin (TPQ) a GIRK antagonist increases the probability of spontaneous seizures in the kindling model.[32] This findings show that GIRK channels especially GIRK1 and GIRK2 subunits play crucial role in the pathogenesis of epilepsy and thus a functional increase in the GIRK channel activity should help in decreasing the convulsion level during epileptic seizures.

Table 1.1. GIRK Gene Manipulation studies

Genetic manipulation	Resulting Phenotype	Reference
Kcnj3 (GIRK1) knockout	↓ antinociceptive effects of opioids ↑ Baseline and cocaine-induced motor activity ↓ anxiety	15 24 22
Kcnj3 (GIRK1) knockin	↓ anxiety, hyperactivity and impaired nociception, spatial learning and memory	33
Weaver mice (point-mutation in *Kcnj6* (GIRK2))	Increased motor activity Symptoms of Parkinson's disease Seizures, hyperalgesia, learning impaiments	34 29
Kcnj6 (GIRK2) knockout	↓ antinociceptive effects of opioids, ethanol, nicotine, baclofen, cannabinoids, and α2-agonists (clonidine). ↓ self-administration of cocaine ↓ anxiety ↑ depression-resistant behavior ↑ Baseline motor activity	35 36 24
Kcnj9 (GIRK3) knockout	↓ antinocioceptive effects of opioids ↓ withdrawal symptoms (handling-induced convulsions) from zolpidem and pentobarbital ↓ withdrawal from ethanol	37 15

GIRK 1/2 Channel Activators

GIRK1/2 are the most prominent of the GIRK channels in the CNS. Genetic ablation studies over many years have shown it has major pharmacological utility in epilepsy, seizure, and pain. GIRK 1/4 is another predominant channel which is present in the heart and its activation leads to the slow down of heartbeats and is a target for the treatment of atrial fibrillation. The presence of a GIRK1 subunit in the heart makes it very important for the molecules to be selective for a tetrameric GIRK1/2 channel. Unfortunately, the lack of subtype selective GIRK channel activators has impeded its utilization and characterization.[38]

GIRK channels can be activated by a few diverse sets of compounds, independently of the GPCR or G proteins. There are various allosteric GIRK channel activators, such as intracellular Na^+ and low molecular weight alcohols (C1-C4, e.g., ethanol), that interact with the CTD of the channel. An increase in intracellular Na^+ concentration leads to the activation of GIRK2- and GIRK4-containing channels, strengthening PIP2 binding or increasing receptor affinity for Gβγ. Methanol, ethanol, 1-propanol, and 1-butanol also activate GIRK channels in a Gβγ-independent manner, especially those containing GIRK2, while 1-panthenol and other long-chain length alcohols have inhibitory effect. Structural studies with GIRK2 homotetramer has led to the discovery of more than one discrete hydrophobic alcoholic binding pocket in the CTD.[39, 40]

Some natural compounds have also been identified to nonselectively activate GIRK channels, such as the bioflavonoid Naringin. It is a poor, non-selective activator (EC_{50} >100 μM) for GIRK1/2 and GIRK1/4.[41] Ivermectin, a widely used antiparasitic drug also shows some activity towards GIRK2 directly in a Gβγ-independent manner, but the activation is dependent on PIP2.[42]

Many volatile anesthetics, like halothane and isoflurane, are GIRK activators.[43] Chloroform activates GIRK1/2 and GIRK1/4 in a G-protein-independent manner. But these are of limited use due to their adverse effects, diverse activity, and not well understood mechanisms.[44]

The discovery of ML297 **(2)** (VU0456810, *N*-(3,4-difluorophenyl)-*N′*-(3-methyl-1-phenyl-1*H*-pyrazole-5-yl)urea) as a first-in-class selective and potent (EC$_{50}$ ~160 nM) PIP2 dependent GIRK1/2 channel activator paved the way for new promising investigations around the utility of GIRK channels. ML297 was discovered after a structure-activity relationship (SAR) optimization of high throughput screen (HTS) lead CID736191 (**1**), as shown in **Figure 1.4**. An HTS compatible thallium flux assay coupled with Gi/o couple GPCR protein to GIRK 1/2 was used for easy, fast, and efficient assay readout. The development of thallium flux assay has greatly facilitated the rapid screening of ion channels. Traditionally these assays are performed via the patch clamp method.[45, 46] As shown in **Figure 1.4**, an elaborate SAR around the urea lead molecule was performed. Starting with the 1-phenyl position, the most tolerated group were phenyl, benzyl and to a somewhat extent a trifluoropropane. Although direct benzyl replacement into ML297 gives two-fold improvement in the potency (70 nM vs. 160 nM), the selectivity is lost. For potency assignment, the R substitution on the right-hand phenyl ring proves to be most fruitful. Multiple halogens and alkyl substitutions were performed and the overall pattern depicts 3-mono- or 3,4-dihalogen or 3-CF$_3$ substitutions gives the best result. But there are certain anomalies, such as the chlorine atom which does not fit into that generalization. Overall, 3,4-difluoro substitution proves to be most potent. The urea part, shown in red, is almost untouchable at this stage, and any attempt to methylate the urea leads to inactive molecules. The most exciting phenomenon occurs over the 3-pyrazole (R') substitution. A CYP450 metabolism study of ML297 shows the 3-methyl position is a site of oxidative metabolism. In order to prevent this oxidation, various cyclopropyl groups were tried. C-2 substitution on cyclopropyl retains the activation property although not as active as methyl. But any attempt of C-1 substitution switches the molecule from activator to inhibitor. A detailed SAR is performed keeping either of the R', R, phenyl, and benzyl as constant and changing the other groups. But, overall, from these urea series ML297 has the best balance of activity and selectivity against GIRK1/4.[47, 48]

A detailed pharmacological and pharmacokinetic and pharmacodynamic (PK/PD) exploration was done around ML297 to best gauge its drug-like properties so that it can be used in various GIRK animal disease models. Pharmacokinetics (PK) is concerned with the processes that govern a drug's path through the body and its resulting concentration in different body compartments. Pharmacodynamics (PD) is concerned with the physiological and behavioral consequences produced by the drug molecules. The relationship between PK and PD is described as PK/PD analysis which relates drug concentration to drug effect.[49] First, the activity of ML297 was checked with both thallium flux and regular voltage patchclamp, though the values don't match exactly, the pattern remains the same. Next, ML297 was tested against other CNS targets with close structural resemblance to GIRK1/2. It performed well and showed only little activity against hERG channels at very high concentrations as shown in **Table 1.3**. The pharmacokinetic properties of ML297 were somewhat lacking for a tool compound designed for CNS diseases. ML297 showed good solubility (17.5 μM), modest plasma protein binding (mouse f_u, 0.026) with high mouse liver microsome clearance (CL_{HEP} = 88 mL/min/kg). The major concern along with rapid clearance is the poor brain to plasma ration of 0.2, as shown in **Table 1.4**.[50]

Mutagenesis studies have revealed two critical amino acids in the GIRK1 subunit (F137 and D173), in the pore helix and the second in the membrane-spanning domains essential for GIRK1 activity. ML297 requires PIP2 for activation of the channel, but, interestingly, ML297 can activate the channel in the absence of G protein. ML297 lacks good subtype selectivity for GIRK1/2 and activates both GIRK1/3 and GIRK1/4 channels, which could lead to off-target effects, thus limiting ML297's therapeutic utility.[51]

The effect of ML297 *in vivo* has been investigated in several different behavioral assays for epilepsy, anxiety, and insomnia. ML297 (60 mg/kg, i.p.) exhibited improved efficacy compared with the anticonvulsant sodium valproate in both an electroshock and a pentylenetetrazol-induced mouse model of epilepsy, increasing the latency of seizure onset and preventing convulsions and lethality.[52] ML297 reduced cyclothiazide-induced enhancement of neuronal excitability in cultured

hippocampal neurons and reduced Racine score and extended seizure latency in a pilocarpine-induced mouse model of epilepsy.[53]

ML297 does not affect locomotor activity in the open field test and did not show any reinforcing effects in the condition place preference test, indicating the anxiolytic effects are not related to reduced locomotion or the rewarding effect of ML297. Systemic injection of ML297 (30 mg/kg, i.p.) reduce wakeful activities, locomotion, and increased non-rapid eye movement (NREM) sleep in mice without inducing spike-wave discharges (an absence of seizure activity) or memory impairment.[51, 54] VU0466551 (**3**) a more potent GIRK activator (2-fold more potent than ML297), showed anxiolytic and analgesic effects, when applied either alone or with morphine.[27]

Xu *et al.* performed a chemical optimization around ML297 replacing the right side halogenated phenyl with 5-membered halogenated heterocycles and some biaryl rings. One of the compounds from this study, GAT1508 (**6**), showed comparable potency to ML297 (75 nM vs. 111 nM) in their electrophysiological assay. GAT1508 is claimed to be lacking complete activity towards GIRK1/4 the cardiac ion channel. However, independent testing in our collaborator's lab does not produce the same result. They also perform a homology modeling with the GIRK2 homotetramer, showing that the major interaction if GAT1508 is π-stacking with multiple Phe residues in the TM1 region.[55]

Finally, very recently, Zhao *et al.* reported a novel GPCR independent GIRK activator named GiGA1 that directly binds to the alcohol-binding pocket in GIRK1/2 and discovered through virtual screening.[56] GiGA1 (**5**) induced activation is G-protein independent and does not alter inward rectification of GIRK1/2, and has specificity towards GIRK1/2 compared to GIRK1/4. Mutation of 2 amino acid residues in GIRK2 equivalent to that in GIRK1 enables its activation by ML297.[57] But since the GiGA1 was identified based on the alcohol binding pocket, these mutations do not alter its activity. Mutagenesis study and molecular dynamic simulations point towards an R43 on mGIRK1 and D346 on mGIRK2 to be interacting with the GiGA1.[56] Even though the two

new urea leads claim to be more potent and selective, the presence of the urea functional group itself leads to many pharmacokinetic and brain penetration issues.

A. Natural product based GIRK activators
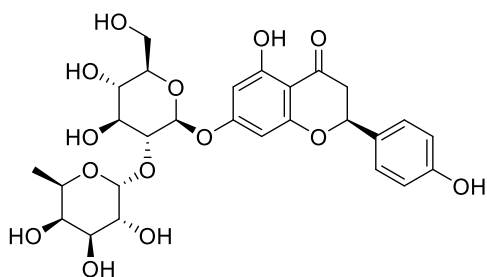
Naringin
GIRK 1/2 EC$_{50}$ > 100 μM
Non-slective
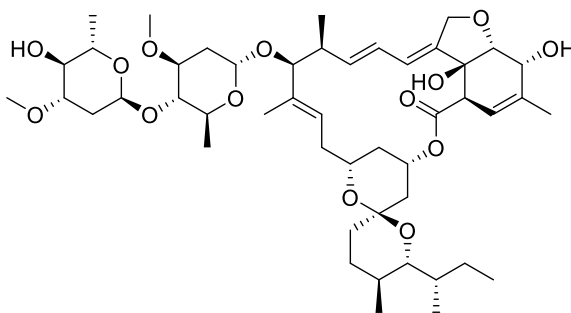
Ivermectin
GIRK EC$_{50}$ = 3 to 8 μM
PIP2 dependent

B. SAR studies leading to ML297
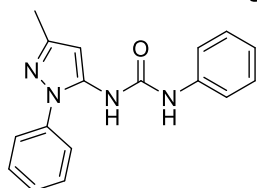
VU0032230, CID **736191 (1)**
GIRK 1/2 EC$_{50}$ = 1.4 μM
GIRK 1/4 EC$_{50}$ = 0.69 μM
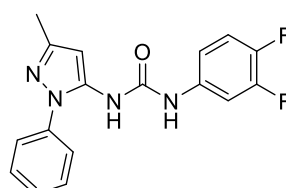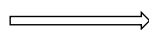
VU0456810, **ML297 (2)**
GIRK 1/2 EC$_{50}$ = 0.16 μM
GIRK 1/4 EC$_{50}$ = 1.8 μM
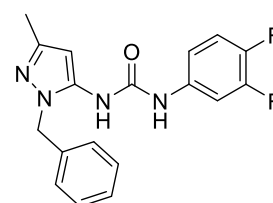
VU0466551 **(3)**
GIRK 1/2 EC$_{50}$ = 0.07 μM
GIRK 1/4 EC$_{50}$ = 0.11 μM

R' =
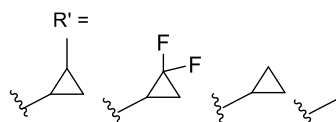
Activator "Molecular switch"

Inhibitor "Molecular switch"
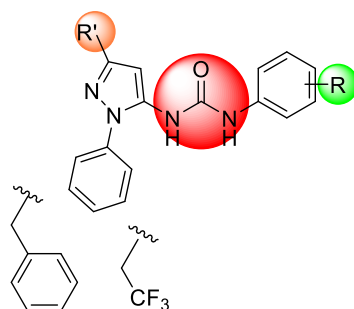
GIRK 1/2 EC$_{50}$, R' = Me	
<0.2 μM	**>0.2 μM**
3- Br	3-Cl
4-Br	4-Cl
3-F	2-Br
3-CF$_3$	2-CF$_3$
4-CF$_3$	3-CH$_3$
3,4-F,F	3,4- Cl,Cl

R =

C. Other active GIRK 1/2 activators
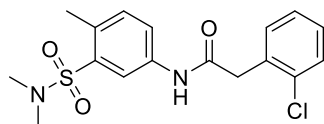
VU0259369 (4)
GIRK 1/2 EC$_{50}$ = 1.4 μM
GIRK 1/4 EC$_{50}$ = 0.69 μM
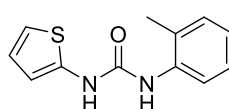
GiGA1 **(5)**
GIRK 1/2 EC$_{50}$ = 0.16 μM
GIRK 1/4 EC$_{50}$ = 1.8 μM
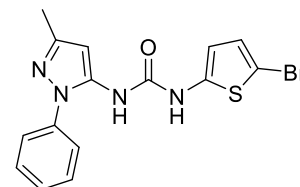
GAT1508 (6)
GIRK 1/2 EC$_{50}$ = 0.075 μM
GIRK 1/4 E$_{MAX}$ = 0%

Figure 1.4. Background of GIRK 1/2 small molecule activators

Table 1.2. Thallium flux vs voltage clamp obtained EC$_{50}$ of ML297

Cell Line	EC$_{50}$ Thallium flux (nM)	N	EC$_{50}$ Voltage clamp (nM)	N
GIRK 1/2	162 ± 89	6	584 ± 175	9
GIRK 1/4	887 ± 266	3	1400 ± 1200	9
GIRK 2	Inactive	4	Inactive	3
GIRK 2/3	Inactive	3	Inactive	3

Table 1.3. ML297 selectivity

Cell Line	Potency (µM)	N
Kir2.1	Inactive	3
Kv7.4	Inactive	4
hERG	10.1 ±7.0	4
GABA$_A$	Inactive	3

Table 1.4. ML297 PK properties

Assay in	Result
Plasma protein binding (f_u) mPPB	0.026
Solubility	17.5 µM
Mouse Intrinsic Clearance (mCL$_{INT}$)	2951 mL/min/kg
Mouse Hepatic Clearance (mCL$_{HEP}$)	88 mL/min/kg
Brain concentration at T$_{max}$ (30 min) (IP, 60mg/kg)	130 nM
Plasma concentration at T$_{max}$ (30 min)	640 nM
Brain:Plasma	0.2

1.2. Amide Series

Design

The urea-based GIRK1/2 activators previously identified after SAR studies of the hits obtained through HTS played a vital role in establishing the GIRK pharmacology. However, to develop GIRK activators as *in vivo* probes and potential therapeutics, we need activators with improved brain penetration and better pharmacokinetic profile, primarily the intrinsic stability. Since a vast amount of SAR was done around the urea based activators, Dr. Hopkins' lab at Vanderbilt University thought to combine two different type of compounds: a urea, **3** and an phenylacetamide, **4**, to come up with a hybrid molecule which can potentially address the PK liabilities of the previous activators. Thus a new class of amide activators, **7**, was designed by merging the pyrazole privileged scaffold from the urea, **3**, and the acetamide from **4**, was incorporated. As has been seen with the previous SAR study of ureas, pyrazole *N*-substitution and the 3-position R_1 replacement can have dramatic changes in the activity; thus, a comprehensive plan was developed to test the best suitable substitution to obtain potent, selective and stable amide class-I activators. As shown in **Figure 1.5**, the optimization began with Class-IA type of molecules primarily focusing towards the right-hand phenyl substitutions R_2. Once an optimized phenyl substitution is identified, various pyrazole substitutions in Class-IB can be tested, and the best pyrazoles will be subjected to extensive right-hand phenyl substitutions R_2 study. Along with it, the central amide moiety will also be explored to see if any changes are tolerated.

3
GIRK 1/2, EC$_{50}$ = 73 nM
Poor brain penetration

4
GIRK 1/2, EC$_{50}$ = 1.1 mM
weak potency

Amide Series, **7** Class-I

Class-**IA**
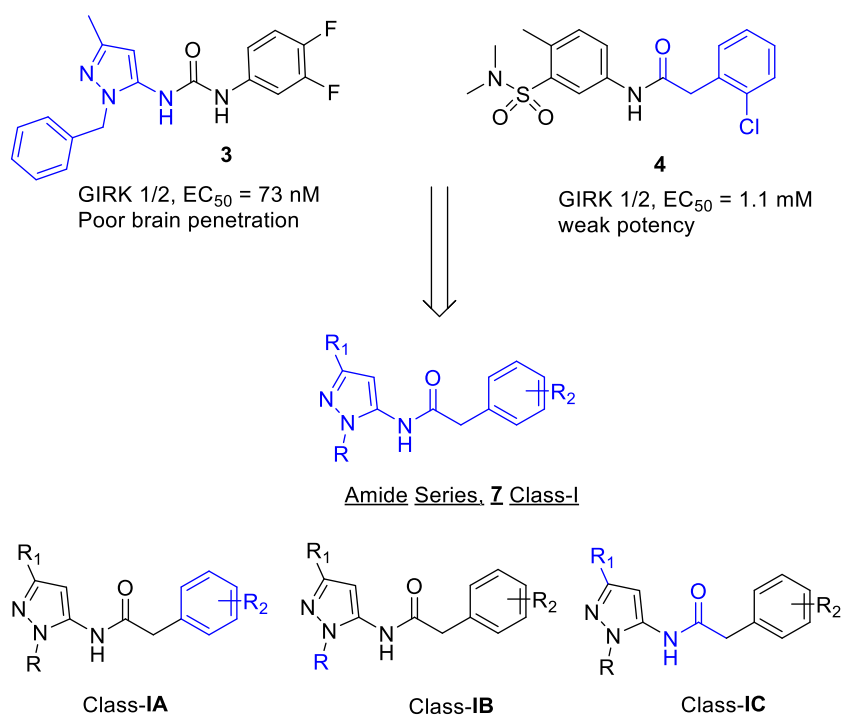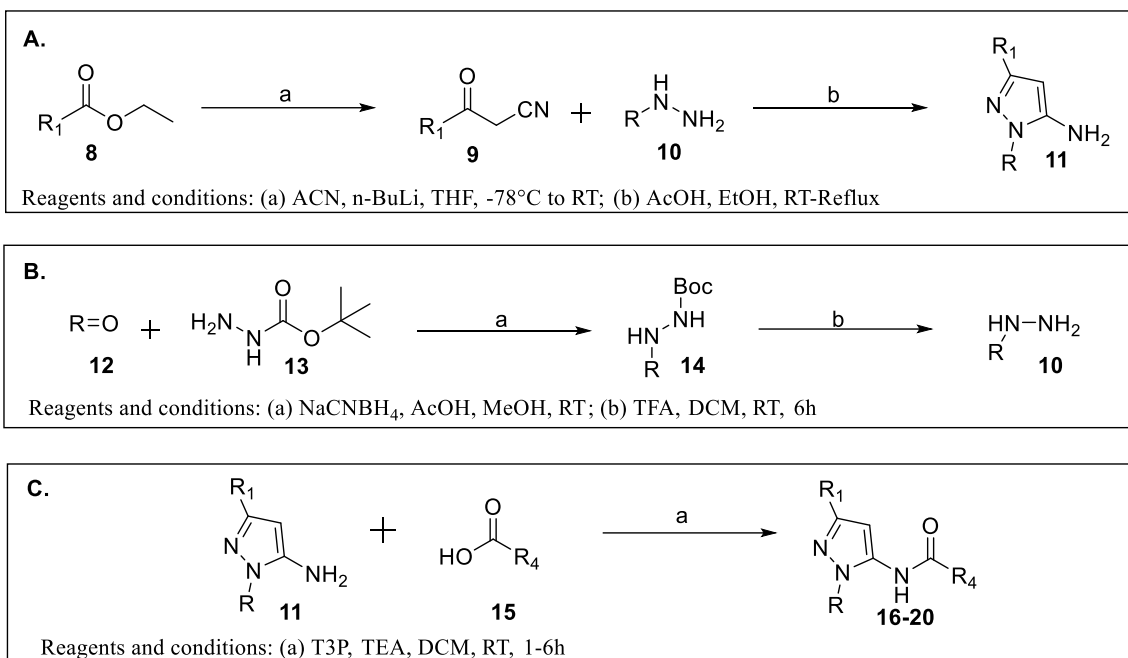
Class-**IB**

Class-**IC**

Figure 1.5. Design and SAR plan for amide series (Class-I)

Synthesis and methods

The synthesis for the amide scaffold activators primarily involved late stage amide bond formation since substituted phenylacetic acids are readily available. Substituted amino pyrazole, **11**, are obtained through cyclization of an substituted hydrazine, **10**, with an appropriate 3-oxoalkanenitrile, **9**, under acidic conditions. Compound **9** can be obtained through n-BuLi mediated reaction of appropriate ethyl ester, **8**, with acetonitrile (CH_3CN) as shown in **Scheme 1.1.A**. Non-commercial hydrazines can be made by reductive amination between substituted carbonyl compounds, **13**, and an appropriate Boc-hydrazine followed by deprotection under acidic conditions to yield hydrazine, **10**, **Scheme 1.1.B**. The previous synthesis of the amide used chlorodipyrrolidinocarbenium hexafluorophosphate (PyClu) as the coupling agent, and although the reaction proceeded, the resulting compounds required column purification and 15-20 min of active ester formation of PyClu with the respected acid coupling partner. To improve on the reaction, we used propanephosphonic acid anhydride (T3P, 50% in ethyl acetate), which has gained quite a good reputation as a coupling reagent in recent years. The by-products are water-soluble, the reagent is cheap and is shipped in a solvent of choice ranging from dichloromethane (DCM) to dimethyl sulfoxide (DMSO). For most small scale reactions the coupling is extremely fast and reliable. And contrary to other coupling reagents, there is no need for making an active ester first, as T3P can be added to a mixture of acid, amine and base yields very clean reactions. [58]

The compounds thus prepared were sent to the lab of Dr. Weaver in the Department of Pharmacology, Vanderbilt University School of Medicine. The compounds were tested using HEK293 cells expressing both GIRK1/2 and 1/4 channels, using a standardized automated thallium flux assay, which enables fast and reliable testing of multiple GIRK activators simultaneously. Once the activation data is received, based on the activity future molecules where designed and tested, but mostly the design followed the plan mentioned above to conduct the SAR studies primarily focused on right-hand side phenyl substitution and the pyrazole substitution on the left-

hand side. The active molecules, and some structurally diverse but inactive molecules, were subjected to first-line pharmacokinetic studies wherein the molecules were incubated into human and mice liver microsomes and their degradation was quantified using LCMS-MS. Metabolic elimination rate constant k was obtained from the first order plot of the percentage of drug remaining at each timepoint. The rate constant k thus obtained was placed in various equations mentioned in detail in the supplemental section to obtain half life $T_{1/2}$, intrinsic clearances hCL_{INT} (human), mCL_{INT} (mice) and free fraction $\%f_u$. The pharmacokinetic studies were conducted at UNMC in the lab of Dr. Yazen Alnouti or were outsourced to Q2 solutions based in Indianapolis. Detailed synthetic procedures, characterization data, biological assay, and PK calculations are mentioned in the supplemental information at the end of this chapter.

A.

Reagents and conditions: (a) ACN, n-BuLi, THF, -78°C to RT; (b) AcOH, EtOH, RT-Reflux

B.

Reagents and conditions: (a) NaCNBH$_4$, AcOH, MeOH, RT; (b) TFA, DCM, RT, 6h

C.

Reagents and conditions: (a) T3P, TEA, DCM, RT, 1-6h
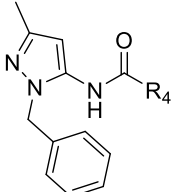
Scheme 1.1. General synthesis of amide series (Class-I)

Results

The initial structure-activity relationship (SAR) library focused on evaluating a variety of phenyl acetamides keeping the *N*-benzyl pyrazole constant to test whether these were the viable replacement of the urea moiety as shown in **Table 1.5**. The initial shift to amide **16a** was shown to lose significant activity compared to the urea analog, **3** (EC_{50} = 1.97 μM vs EC_{50} = 0.073 μM). Replacing the 3,4-difluorophenyl with a 3-chloro-4-fluorophenyl, **16b**, produced a ∼4-fold increase in potency (EC_{50} = 0.478 μM), still ∼5-fold less potent than the urea analog. However, **16b** only provided a slight improvement in the selectivity for GIRK1/2 versus GIRK1/4 channel subtypes (∼4-fold selectivity vs ∼2-fold selectivity for **3**). Other modifications of the phenyl portion such as 1,4; 1,5 halogen substitution, phenyl, naphthyl, pyridyl, or substituted pyridyl did not lead to an improvement over **16b.** The unsubstituted phenyl derivative (**16c**, EC_{50} = >10 μM) lost significant activity. Having identified a somewhat beneficial substitution to make the amide moiety work, in the next phase, 3-chloro-4-fluorophenyl is kept constant, and pyrazole *N*-substitution was explored, as shown in **Table 1.6**

Table 1.5. Initial SAR of Class-IA Pyrazole-5-yl-phenylacetamides

Cmpd	R$_4$	GIRK1/2 EC$_{50}$ (µM ± SEM^a; % activation ± SEM^b)	GIRK1/4 EC$_{50}$ (µM ± SEM^a; % activation ± SEM^b)
3		0.073 ± 0.007; 96.0 ± 1.1	0.150 ± 0.021; 94.0 ± 1.5
16a		1.967 ± 0.325; 74.7 ± 7.8	3.975 ± 0.189; 46.0 ± 4.0
16b		0.478 ± 0.077; 94.5 ± 5.5	2.0 ± 0.8; 100 ± 0
16c		>10; >25	>10; >15
16d		1.35 ± 0.17; 36.3 ± 4.9	2.75 ± 0.74% 17.0 ± 0.7
16e		Inactive	Inactive
16f		1.193; 33	1.523; 12%
16g		1.844; 67	2.415; 38%
16h		3.877; 58	5.984; 36%
16i		>22.0; >25	inactive

^{a}Potency values where obtained from triplicate determinations; values are average of n=3.
^{b}reported efficacy values shown are obtained from triplicate determinations; value are average of n=3 normalized to a standard compound, **3**

Replacement of the *N*-benzyl with trifluoromethyl, **17a**, led to drastic decrease in the activity (EC_{50} = 5.5 µM), but replacing the benzyl group with cyclohexyl, **17b**, proved to be an effective change as the potency increased ∼3-fold over the *N*-benzyl pyrazole analog (**17b**, EC_{50} = 0.165 µM vs **16b**, EC_{50} = 0.478 µM). The potency was maintained after the insertion of a flexible methylene linker to the cyclohexylmethyl **17c** (EC_{50} = 0.135 µM). These changes, although offering an improvement in GIRK1/2 channel potency, did not drastically alter the selectivity profile of the compounds. Further scanning with branched, and <6-membered cycloalkyl substitutions had no beneficial outcomes. The addition of nitrogen to the benzyl moiety (4-pyridylmethyl, **17f**, EC_{50} > 10 µM) led to a ∼20-fold reduction compared to the benzyl counterpart; and the addition of an oxygen to the cyclohexyl analog (4-pyran, **17g**, EC_{50} = 3.07 µM) also led to a ∼20-fold reduction in activity, as shown in **Table 1.6.**

To fully explore the scope of the phenylacetamide substitution tolerance, as well as other urea replacements, several alternative analogs branching the methylene group of the phenylacetamide were studied, with both quaternary center (cyclopropyl, **18a**) and (*R*)- and (*S*)-methyl substitution, **18b** and **18c**. Truncation of the phenylacetamide to the benzamide, **18d** as well as reverse amide analogs, **18e** and **18f**; both with and without the methylene spacer, were examined. Unfortunately, none of these derivatives were active, as shown in **Table 1.7**.

Having the cyclohexane and cyclohexylmethyl as the best *N*-substitution on pyrazole, 3-position R_1 methyl was replaced with some of the previously used "molecular switches".[48] As expected cyclopropyl or substituted cyclopropyl were not active >10-fold less potent compared to methyl, with an only exception of 2,2-difluorocyclopropyl, **19a**, however, this only had a <2-fold selectivity. Removal of methyl, **19f**, still retains some activity. And additional carbon on the phenylacetamide side led to an almost 10-fold decrease in potency, as shown in **Table 1.8**.

Table 1.6. SAR of Class-IB Pyrazole *N*-substitution
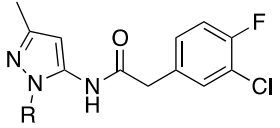
Cmpd	R	GIRK1/2 EC$_{50}$ (μM ± SEM[a]; % ± SEM[b])	GIRK1/4 EC$_{50}$ (μM ± SEM[a]; % ± SEM[b])
17a	F$_3$C	5.575 ± 0.660; 77.0 ± 11.4	>10; >63%
17b		0.165 ±. 0.012; 87.3 ± 0.9	0.720 ± 0.213; 50.5 ± 5.5
17c		0.135 ± 0.024; 82.0 ± 3.5	0.534 ± 0.285; 52.3% ± 7.4
17d		0.536 ± 0.444; 97.8 ± 4.8	3.26 ± 1.410; 111.5 ± 6.5
17e		5.775 ± 1.524; 66.8 ± 6.8	>10; >33
17f		>10; >42	>10; >25
17g		3.067 ± 0.791; 86.0 ± 5.6	>10; >35
17h		2.633 ± 0.732; 97.3 ± 10.4	6.70 ± 1.68; 100.3 ± 10.0
17i		1.40 ± 0.27; 89.7 ± 9.1	5.925 ± 1.359; 80.0 ± 4.6
17j		0.840 ± 0.180; 82.3 ± 5.8	1.950 ± 0.519; 91.7 ± 8.4
17k		0.483 ± 0.084; 57.3 ± 6.3	1.485 ± 0.313; 55.3 ± 2.5
17l		3.100 ± 1.776; 55.0 ± 4.9	3.250 ± 0.867; 48.7 ± 2.9
17m		1.515 ± 0.410; 102.0 ± 5.5	5.40 ± 1.34; 97.7 ± 6.8
17n		Inactive	Inactive
17o		0.518 ± 0.091; 87.0 ± 7.3	2.150 ± 0.555; 80.3 ± 8.5

[a]Potency values where obtained from triplicate determinations; values are average of n=3. [b]reported efficacy values shown are obtained from triplicate determinations; value are average of n=3 normalized to a standard compound, **3**

Table 1.7. SAR of Class-IC Amide substitution/replacement
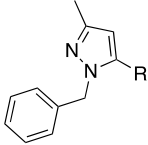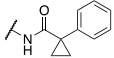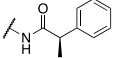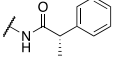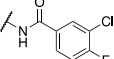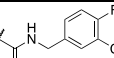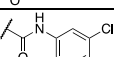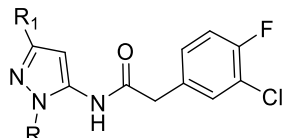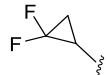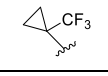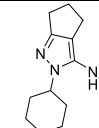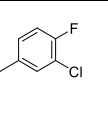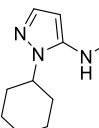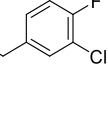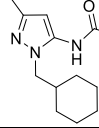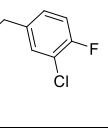
Cmpd	R	GIRK1/2 EC$_{50}$ (µM ± SEM[a]; % ± SEM[b])	GIRK1/4 EC$_{50}$ (µM ± SEM[a]; % ± SEM[b])
18a		Inactive	inactive
18b		Inactive	inactive
18c		Inactive	Inactive
18d		Inactive	inactive
18e		Inactive	Inactive
18f		Inactive	Inactive

[a]Potency values where obtained from triplicate determinations; values are average of n=3. [b]reported efficacy values shown are obtained from triplicate determinations; value are average of n=3 normalized to a standard compound, **3**

Table 1.8. SAR of Class-IC 3rd position R1 substitution

Cmpd	R	R1	GIRK1/2 EC$_{50}$ (µM)	GIRK1/4 EC$_{50}$ (µM)
19a			0.4	0.62
19b			inactive	inactive
19c			>2.3	inactive
19d			3.03	inactive
19e			inactive	inactive
19f			1.015	3.55
19g			1.6	1.3
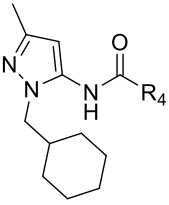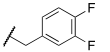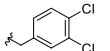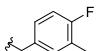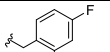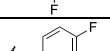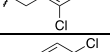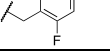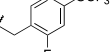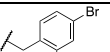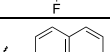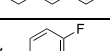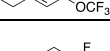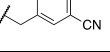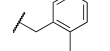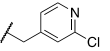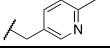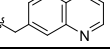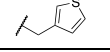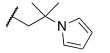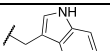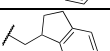
[a]Potency values where obtained from triplicate determinations; values are average of n=3. [b]reported efficacy values shown are obtained from triplicate determinations; value are average of n=3 normalized to a standard compound, **3**

Having identified methyl cyclohexyl as the best *N*-substitution for the amide series, we carried out an extensive right-hand side phenyl substitution to establish the best possible substitution pattern. The 3,4-dihalo substitution was the first to be explored, similar to the 3-chloro-4-fluoro substitution, **17c**, (EC$_{50}$ = 0.135 µM, selectivity ~ 4-fold); 3,4-difluoro, **20a**, had similar potency and somewhat better selectivity (EC$_{50}$ = 0.149 µM, selectivity ~ 5.7-fold). Overall, most of the 3,4-substitution **20a,b,c,j,k** were active (<0.5 µM). 2,4-disubstitution were also active, but not as potent as the 3,4-analogs. However, none of these active molecules crossed the selectivity barrier set by **20a** (~5.7 fold). In addition to di-halogen, 2-Me, **20l** and 3-chloropyridine, **20m** were also active and had EC$_{50}$ of <0.5 µM. Additional 5-membered heterocyclic replacement of phenyl or the naphthyl ring did not show any significant activity, as shown in **Table 1.9**.

With the majority of SAR trends around the new class of amide-based GIRK activators being established, we subjected selected compounds to *in vitro* PK studies. Various *N*-pyrazole substitutions and some right-hand side phenyl derivatives were chosen to be tested. Amongst 3-chloro-4-fluoro phenyl derivatives the stability (lower clearance values) decreased in order from isobutyl **17d**, cyclohexyl **17b**, cyclohexylmethyl **17c** and benzyl **16b**. Overall the molecules were not stable, except cycloheteroalkyl substitution such as tetrahydrothiophene-1,1-dioxide, **17e**, and 4-tetrahydropyran, **17g**. **17e** was the most stable of the compounds tested and had the highest free fraction in humans and mice. Amongst *N*-cyclohexyl methyl pyrazole derivatives, 3-chloro-4-fluorophenyl, **17b**, was the most stable compared to napthyl, **20i**, 3-trifluoromethoxy-4-fluoro, **20j**, and 3-cyano-4-fluoro, **20k**. Unfortunately, the stable molecules **17e** and **17g** were not active (EC$_{50}$ >3 µM); however, this observation shall help in designing future activators. A smaller set of selected compounds **16c**, **17b**, and **17c** were evaluated in a mouse IP cassette study to assess their ability to cross the blood-brain barrier (BBB).[59] All of the compounds were brain penetrant with K_p values > 0.5−0.9 (K_p = total brain/total plasma concentrations). This represents a significant

improvement over the previously reported urea scaffolds, where many of those analogs had low brain penetration ($K_p < 0.2$), as shown in **Table 1.10**.

Table 1.9. Extensive SAR of Class-IA Phenyl substitution

Cmpd	R4	GIRK1/2 EC$_{50}$ (μM ± SEM[a]; % ± SEM[b])	GIRK1/4 EC$_{50}$ (μM ± SEM[a]; % ± SEM[b])
20a		0.149 ± 0.009; 71.3 ± 2.6	0.850 ± 0.475; 47.3 ± 7.5
20b		0.30 63	0.40 37
20c		0.25 42	0.80 25
20d		0.63 49	1.70 20
20e		0.343 ± 0.127; 50.0 ± 4.6	0.462 ± 0.019; 21.3 ± 3.3
20f		0.382 ± 0.165; 51.0 ± 2.3	1.01 ± 0.05; 28.7 ± 4.7
20g		0.600 ± 0.201; 53.7 ± 2.9	1.22 ± 0.03; 27.3 ± 3.7
20h		0.800 ± 0.130; 50.0 ± 5.0	0.925 ± 0.220; 18.7 ± 2.8
20i		0.405 ± 0.105; 59.0 ± 5.6	0.923 ± 0.162; 28.0 ± 5.3
20j		0.245 ± 0.063; 81.3 ± 4.4	0.751 ± 0.142 65.3 ± 09
20k		0.126 ± 0.013; 82.3 ± 3.5	0.295 ± 0.071; 75.0 ± 3.6
20l		0.293 ± 0.085; 44.0 ± 2.1	0.930 ± 0.222; 29.7 ± 4.6
20m		0.396 ± 0.029; 79.3 ± 2.0	1.28 ± 0.02; 61.3 ± 4.7
20n		>9.4; >40	inactive
20o		>10 47	6.40 29%
20p		2.38 ± 0.77; 61.7 ± 3.4	<10; >21%
20q		0.892 ± 0.107; 59.5 ± 0.5	2.59 ± 0.25; 28.0 ± 3.3
20r		inactive	inactive
20s		inactive	inactive
20t		1.10 ± 0.04; 25.5 ± 0.5	inactive
20u		2.04 ± 0.74; 73 ± 21	>10; >79

[a]Potency values where obtained from triplicate determinations; values are average of n=3. [b]reported efficacy values shown are obtained from triplicate determinations; value are average of n=3 normalized to a standard compound, **3**

Table 1.10a. *In Vitro* DMPK properties of selected amide Class-I compounds

Cmpd	Structure	GIRK1/2 EC$_{50}$ (µM ± SEM)	hCL$_{INT}$	mCL$_{INT}$	hPPB	mPPB
			mL/min/kg		$f_u{}^a$	
16b		0.478 ± 0.077	ND	690	ND	0.071
17b		0.165 ±. 0.012	246	622	0.009	0.136
17c		0.135 ± 0.024	1390	>5930	0.003	c
17d		0.536 ± 0.444	156	1070	0.016	0.172
17e		5.775 ± 1.524	14.3	18.0	0.348	0.362
17g		3.067 ± 0.791	23.6	85.7	0.211	0.423
20i		0.405 ± 0.105	2080	>5930	0.003	c
20j		0.245 ± 0.063	1900	>5930	0.002	c
20k		0.126 ± 0.013	648	2970	0.020	0.071

Table 1.10b. *In vivo* PK properties of Class-I

	Mouse cassette (IP, 0.25 mg/kg, 0.25 h)		
	Plasma (ng/mL)	Brain (ng/g)	$K_p{}^b$
16c	101	63.4	0.61
17b	87.6	75.5	0.87
17c	190	104	0.55

$^a fu$ = fraction unbound, $^b K_p$ = total brain/plasma ratio, ^{c}unstable in mouse plasma, ND-not determined

1.3. Tetrazole Series

Design

In the previous amide class-I series, we achieved some notable milestones primarily in increasing the brain penetration K_p value for class-I compounds 2- to 3-fold more than that of urea. Although we saw some stability improvement, achieving the right balance of an active and PK tool molecule was still lacking. Some cycloheteroalkyl substitution as in **17e** and **17g** were stable but lacked activity. Hence the pursuit to find a suitable combination that can utilize such stability promoting attribute of this privileged scaffold was underway. As previously, we went back to the HTS data to find some unique structural moiety that can be incorporated into our existing pyrazole acetamides. One such compound was **21**, as shown in **Figure 1.6** which has a bicyclic ring instead of pyrazole and a 5-phenyl tetrazole linked with an acetamide linker. From our previous experience, it was easy to figure out that the poor activity of **21** (EC_{50} = 3.6 μM) was due to the lack of the pyrazole moiety in its structure which has been pivotal for good activity. Thus we planned to merge the amide **7** and **21** to come up with a new tetrazole series, class-II compounds **22.** The initial plan was to incorporate pyrazoles and scan the R_1 and R positions in class-IIA compounds. In the urea series, *N*-benzyl was active and in the amide series cyclohexyl/methyl were the most active and heterocycloalkyl gave very good stability. Thus, if the class-IIA compounds were to be active, we would explore class-IIB and try various 5-phenyl tetrazole substitution and modify/replace the tetrazole moiety itself.
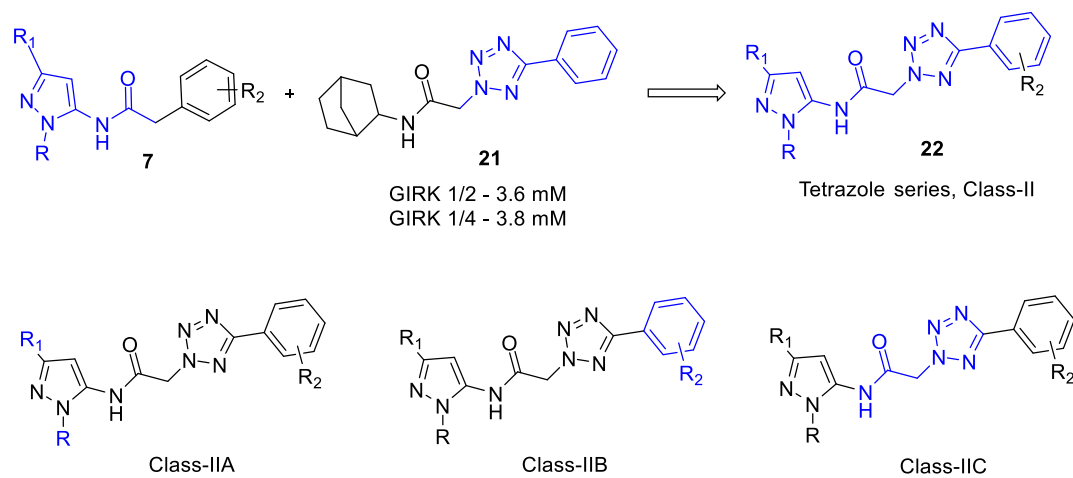
Figure 1.6. Design and SAR plan for tetrazole series (Class-II)

Synthesis and methods

The first step towards the synthesis of the tetrazole derivatives was to come up with an efficient synthesis of the 5-substituted tetrazole, **24**. We needed a protocol that can yield desired tetrazoles in >80% purity without any purification since it's very difficult to purify tetrazoles over normal phase columns. And in case we need to scan multiple tetrazole derivatives, the protocol should allow for hassle-free, easy setup, and not requiring long reflux conditions which prevents from keeping multiple reactions at the same time. Surprisingly, not many of the reported methods work as described, especially those involving metal catalysts. We tried some of the following protocols on benzonitrile to make a 5-phenyl tetrazole. 1. TBDMSCl, NaN_3, NMP, 220 ℃, µW; 2. $ZnBr_2$, NaN_3, water, 24h reflux. In both cases, the reaction becomes sluggish.[60, 61] Thus, we adopted a protocol from an industry report utilizing a 1998 paper from Koguro *et al.* to synthesize large quantities of 5-phenyl tetrazole via flow chemistry.[62] This TEA-HCl, NaN_3, toluene protocol yields tetrazole in >80% yield with >95% purity just out of a simple workup.

To assemble the tetrazole class-II scaffold, **22**, two main directions were designed based on the side of the molecule being explored. To explore pyrazole side, **Scheme1.2B**, shall be utilized wherein an acid derivative of substituted tetrazole would undergo amide bond formation with various pyrazoles. In order to scan the tetrazole, an α-chloro acetamide derivative of pyrazole shall be utilized to act as a leaving group for substitution type of reaction, **Scheme 1.2C**. And to perform these reaction in parallel on multiple tetrazoles at the same time, an original protocol for alkylation of tetrazole under reflux conditions was optimized to be performed under microwave reaction conditions.[63] Thus multiple reactions to make **29a-v** can be set up at the same time and microwave irradiated on an Anton Parr microwave system equipped with an auto sampler. The same alkylation protocol under basic condition was used to prepare various heterocyclic replacements of tetrazole attached to the pyrazole acetamide via C-N linkage. As shown in **Scheme 1.2D**, a carbon swap from acetamide towards 5-phenyl substitution in tetrazole, **29t**, was achieved via benzyl bromide

to alkylate commercially available sodium 5-(ethoxycarbonyl)tetrazole **31**. Some modifications could be done at the end stage such as the conversion of carbonamide to thioamide, **27a** to **30d**, using Lawesson's reagent. Solvent choice plays a crucial role in this reaction, as it works best with xylene and toluene. To achieve heterocyclic replacement of tetrazole without a C-N linkage to the pyrazole acetamide such as **30m**, the preferred route was to perform α-arylation of diethyl malonate with a halogenated heterocycle and subsequent decarboxylation and hydrolysis in basic condition followed by amide bond formation. Some of the oxazole/isooxazole type of heterocycles can be built onto malonate derivatives and cyclized such as in **30k** and **30n.** To make pyridine and phenyl replacements of tetrazole such as **30r**, appropriate phenyl/pyridyl acetic acid with a halogen handle is condensed to pyrazole amine, and later the molecule is built using Suzuki type of reactions to achieve C-C bond formation.

Similar to the amide series, compounds once prepared, were sent to the Weaver lab for testing, and once we start getting some active compounds, select few compounds would be subjected to PK profiling.

A.

23 → a → **24** → b → **25**

Reagents and conditions: (a)NaN₃, TEA.HCl, Toluene, 120°C; (b)1. Br-ethyl acetate, NaOEt, Ethanol. NaOH, Water, THF

B.

11 + **25, 26** (n=0,1,2) → a → **27a-x**   Z = N/O/C/S

Reagents and conditions: (a)T3P, TEA, DCM, RT

C.

11 → a → **28** → Z=N,C,O,S, b → **29a-v**

Reagents and conditions: (a)TEA, DCM; (b) NaOEt, EtOH, MW, 90°C

D.

31 → a → **32** → b → **29t**

Reagents and conditions: (a) Benzyl Br, TEA, DMF, RT (b) 1. LiOH 2. T3P, TEA, **11**

E.

27a → a → **30d**

Reagents and conditions: (a) Lawesson's reagent,*O*-xylene, 75°C

F.

33 → a → **34** → b → **30m**

Reagents and conditions: (a) diethyl malonate, CuI (b) K₂CO₃, T3P, TEA, DCM, **11**

G.

Reagents and conditions: (a) T3P (b) Suzuki, phenyl boronic acid

Scheme 1.2. General synthesis of tetrazole series (Class-II)
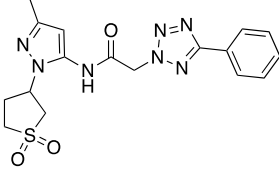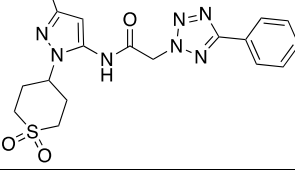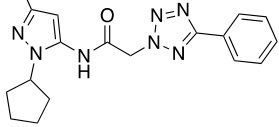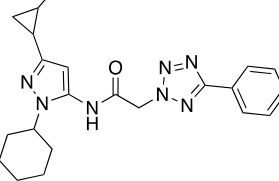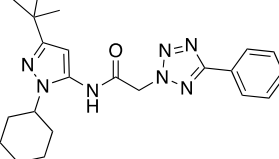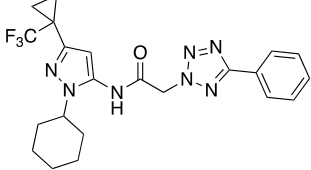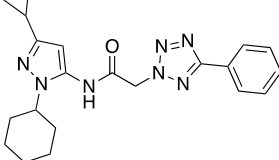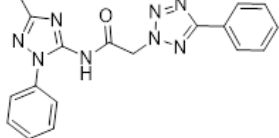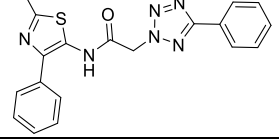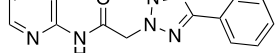
Results
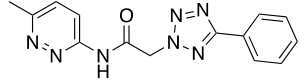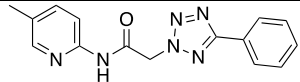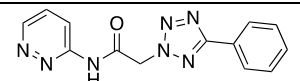
The SAR exploration for class-IIA was started with utilizing some of the active substitutions from the previous series, cyclohexyl **27a**, $(EC_{50} = 96$ nM) came out to be 1.5-fold more potent than the cyclohexyl methyl, **27b**, $(EC_{50} = 176$ nM). However, both of these active compounds had only ~2.5-fold selectivity towards GIRK1/4. Benzyl **27d** $(EC_{50} = 495$ nM) was 6-fold better than phenyl **27c** $(EC_{50} = 3,019$ nM), but less potent than **27a**. Once again, the reversal in trend in amide series compared to urea series wherein cycloalkyl were better than phenyl/benzyl substitutions was maintained. The 4-tetrahydropyran, **27e**, $(EC_{50} = 435$ nM) was more active in the tetrazole series compared to the previous amide $(EC_{50} = >3,000$ nM). This was promising, as *N*-4-tetrahydropyran substituted pyrazole phenyl acetamide was one of the two metabolically stable compounds. Initially, the incorporation of oxygen into the cyclohexyl ring was made to explore any beneficial H-bonding interaction on that molecular end. In a similar fashion, 4,4-difluorocyclohexyl, **27f**, was made to explore the fit in the pocket where cyclohexyl might be resting/interacting, and this modification came out to be active, **27f** $(EC_{50} = 84$ nM) and was one of the most potent compounds. Branched alkyl such as **27h** and **27i**; and small cycloalkyls such as **27j** were not active substitutions, although isopropyl, **27g** $(EC_{50} = 556$ nM) and cyclopentyl, **27m** $(EC_{50} = 163$ nM) were active compounds. Incorporating another stability promoting heterocycloalkyl substitution as in **27k**, $(EC_{50} = 1,003$ nM) turned out to be only moderately active. We then tried to incorporate the sulfone moiety in a 6-membered ring, **27l**, compared to 5-membered as in **27k**, to see if it would impart stability along with potency, however, it was not active. Substitution of the pyrazole 3-position R_1 substitution with methylated cyclopropyl **27n** and **27o** retained the molecular switch phenomenon observed with the previous urea series shown in **Figure 1.4**. Wherein 2-methyl cyclopropyl in **27n**, $(EC_{50} = 843$ nM) was an activator and 1-methyl cyclopropyl in **27o**, $(EC_{50} = >10,000$ nM) was an inhibitor switch. Unsubstituted cyclopropyl, **27q** $(EC_{50} = 271$ nM), was well tolerated. An attempt to replace the pyrazole with different heterocycles such as triazine, **27r**, isothiazole, **27s**, pyridine,

27t, **27v**, and pyridazine, **27u** and **27w**, resulted in completely inactive compounds, as shown in

Table 1.11.

Table 1.11. SAR of class-IIA series around pyrazole substitution

Cmpd	Structure	GIRK1/2 (nM ± SEM[a]; % ± SEM[b])	GIRK1/4 (nM ± SEM[a]; % ± SEM[b])
21		1,983 ± 546; 13 ± 1	2,761 ± 753; 7 ± 1
27a		96 ± 7; 92 ± 2	259 ± 25; 63 ± 2
27b		176 ± 16; 77 ± 2	283 ± 26; 58 ± 2
27c		3,019 ± 517; 66 ± 3	4,093 ± 528; 25 ± 1
27d		495 ± 75; 74 ± 2	848 ± 121; 48 ± 2
27e		435 ± 22; 115 ± 2	2,037 ± 114; 109 ± 3
27f		84 ± 9; 68 ± 2	383 ± 36; 52 ± 2
27g		556 ± 55; 107 ± 3	>4,000; >96
27h		>5,000; >69	>10,000; >20
27i		>6,000; >105	>10,000; >97
27j		>5,000; >78	>10,000; >39

27k		1,034 ± 66; 93 ± 1	2,168 ± 172; 75 ± 2
27l		>10,000; >25	inactive
27m		163 ± 7; 105 ± 1	612 ± 32; 84 ± 2
27n		843 ± 139; 78 ± 4	>10,000; >19
27o		>10,000; >10	Inactive
27p		Inactive	inactive
27q		271 ± 17; 45 ± 1	659 ± 57; 15 ± 0
27r		Inactive	inactive
27s		Inactive	Inactive
27t		inactive	inactive
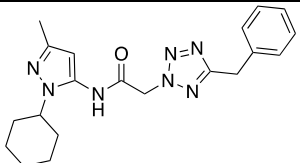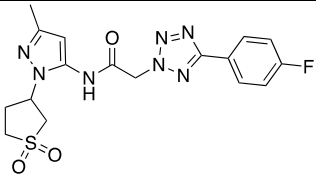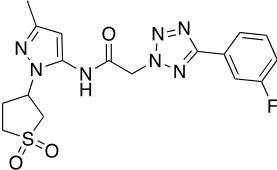
27u		inactive	inactive
27v		inactive	inactive
27w		inactive	inactive
[a]Potency values where obtained from triplicate determinations; values are average of n=3. [b]reported efficacy values shown are obtained from triplicate determinations; value are average of n=3 normalized to a standard compound, **3**			

Having identified some potent compounds in the initial left-hand side pyrazole exploration, the focus shifted to optimizing the 5-phenyl substitution on the tetrazole ring. Primarily, a halogen scan was performed to find the ideal site for halogenation on the phenyl ring and replace the phenyl with pyridyl, cycloalkyl, and benzyl to see if those substitutions are tolerated. As shown in **Table 1.12**, replacing phenyl with pyridyl in **29a** and **29b** resulted in the loss of activity, but 3-pyridyl **29a** was 7-fold more active compared to 2-pyridyl, **29b**. 3,4-dichloro, **29c** and 3,5-dichloro, **29d** were only modestly active. Shifting to 3,4-difluoro, **29e** resulted in a more active compound with $EC_{50} = 116$ nM, which was similar in potency to phenyl **27a**, $EC_{50} = 96$ nM. In a mono fluoro scan, meta-F compound **29f**, $EC_{50} = 81$ nM was more active than ortho and para-substituted fluoro **29h** and **29g**, respectively with $EC_{50} \sim 180$ nM. Except for methyl substitution wherein p-Me, **29k**, $EC_{50} = 111$ nM was better than m-Me, **29j**, $EC_{50} = 129$ nM; the trend of meta substitution being better compared to ortho or para continued with chloro, **29i**; methoxy **29l** vs **29m**; and trifluromethyl **29o** vs **29p**. All resulting in potent compounds with EC_{50} in the range of 150 to 250 nM. Trying to incorporate the active meta-fluoro substitution into pyridine led to 3-fold increase in potency compared to the unsubstituted pyridine **29r** vs. **29a**. Replacing the 5-phenyl from tetrazole with a cyclopropyl, **29s** or benzyl, **29t** resulted in an almost complete loss of activity. Trying to incorporate fluoro substitution in the sulfone containing pyrazole did not resulted into better activity, plain phenyl **27k**, $EC_{50} \sim 1,000$ nM was better compared to **29u** and **29v**, $EC_{50} = 1,034$ nM as shown in **Table 1.12.**

Table 1.12. SAR of class-IIb series around tetrazole substitution

Cmpd	Structure	GIRK1/2 (nM ± SEM[a]; % ± SEM[b])	GIRK1/4 (nM ± SEM[a]; % ± SEM[b])
29a		1,931 ± 89; 96 ± 1	4,908 ± 165; 80 ± 1
29b		14,571 ± 1,379; 81 ± 3	>33,000; >41)
29c		1,217 ± 91; 84 ± 2	2,201 ± 130; 70 ± 1
29d		980 ± 68; 82 ± 1	2,122 ± 331; 51 ± 2
29e		116 ± 6; 93 ± 1	392 ± 23; 79 ± 2
29f		81 ± 7; 96 ± 2	264 ± 22; 80 ± 2
29g		180 ± 11; 92 ± 1	634 ± 45; 74 ± 2
29h		187 ± 22; 88 ± 3	447 ± 42; 60 ± 2
29i		300 ± 29; 89 ± 2	662 ± 75; 66 ± 2

29j		129 ±15; 93 ± 3	435 ± 113; 63 ± 6
29k		111 ± 9; 86 ± 2	408 ± 29; 64 ± 1
29l		175 ± 13; 90 ± 1	779 ± 78; 65 ± 1
29m		117 ± 9; 76 ± 2	299 ± 18; 40 ± 1
29n		712 ± 25; 89 ± 1	1,510 ± 89; 51 ± 1
29o		241 ± 11; 94 ± 1	448 ± 39; 50 ± 1
29p		183 ± 17; 86 ± 2	850 ± 200; 57 ± 4
29q		> 3000 ; > 83	> 10,000; > 38
29r		441 ± 57; 95 ± 4	1,337 ± 181; 68 ± 4
29s		>3,000; >68	>10,000; >25
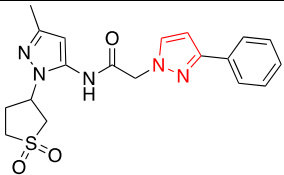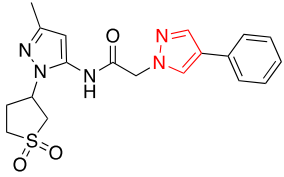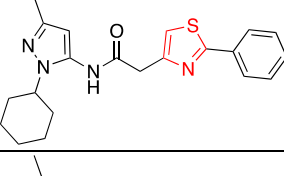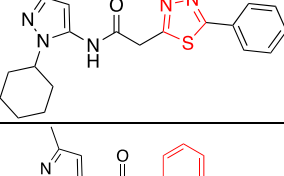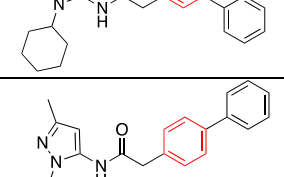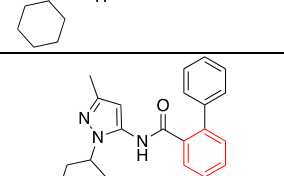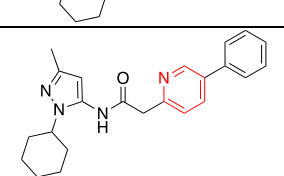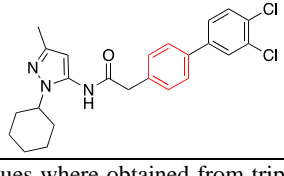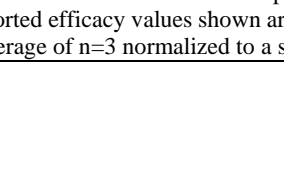
29t		Inactive	inactive
29u		>2,240; >92	>10,000; >65
29v		1,304 ± 76; 109 ± 2	>3,303; >86

[a]Potency values where obtained from triplicate determinations; values are average of n=3.
[b]reported efficacy values shown are obtained from triplicate determinations; value are average of n=3 normalized to a standard compound, **3**

Next, we moved our efforts to modifying the acetamide group, which might help in decreasing enzymatic hydrolysis of the susceptible amide bond and replace tetrazole with other heterocycles in order to decrease the polarity and nitrogen count. An attempt to methylate the amide, **30a**, and the acetamide linker, **30b**, resulted in inactive compounds, reconfirming the SAR that a free secondary amide is required for the activity. Deuteration of the active molecule **27a** did retain the activity in **30c**, EC_{50} = 116 nM. Conversion of amide to thioamide, **30d**, EC_{50} = 623 nM led to 6-fold decrease in potency but still a good control to test for PK stability. If any of these modifications aimed at improving the stability comes out to be fairly stable and active, a SAR could be performed around it to increase the potency. Removal of one nitrogen from **27a** to get triazoles **30e** and **30f** resulted in active molecules with a very distinct regioisomeric requirement activity. The 4-substituted triazole was more active (**30e**, EC_{50} =116 nM); however, the 5-substituted analog did retain some potency (**30f**, EC_{50} = 375 nM). The 5-phenyloxazol-2-ylacetic acid derivative (**30g**, EC_{50} = 631 nM) was much more potent than the 2-phenyloxazol-4-ylacetic acid analog (**30h**, EC_{50} = >11,000 nM). Although, the oxazole was much less active than the tetrazole or triazole. Further exploration of the regiochemistry of the nitrogens and determination of whether these atoms were necessary led us to the pyrazole derivatives (**30i** and **30j**). Interestingly, we identified a distinct regioisomeric requirement for potency. The 4-phenyl-1*H*-pyrazole, **30i** was ∼8-fold more potent than the 3-phenyl-1*H*-pyrazole, **30j**, (EC_{50} = 65 nM vs EC_{50} = 511 nM.). The nitrogen placement in the 4-phenyl-1*H*-pyrazole maintained the nitrogen in a similar arrangement as the triazole (**30e**) and the original tetrazole (**27a**). Incorporation of this active pyrazole into the 5-membered sulfone ring (**30k** and **30l**) did not result in activity, nor did it follow the regioselective trend. Thiazole, **30m**, and thiadiazole, **30n**, did not maintain potency, which may be due to the position of the nitrogen/sulfur in the thiazole and the increased ring size in the thiadiazole or due to the presence of the sulfur atom in general. Replacement of tetrazole by pyridine and non-hetero aromatic phenyl resulted in an interesting observation wherein the *meta*-phenyl substituted analog possessed

moderate activity **30o** (EC$_{50}$ = 370 nM); however, all of the *para and ortho*-substituted analogs were less active or inactive at all, **30p-s** as shown in **Table 1.13**.

Table 1.13. SAR of class-IIC series around tetrazole replacement

Cmpd	Structure	GIRK1/2 (nM ± SEM[a]; % ± SEM[b])	GIRK1/4 (nM ± SEM[a]; % ± SEM[b])
30a		Inactive	inactive
30b		Inactive	Inactive
30c		116 ± 9; 98 ± 2	578 ± 39; 68 ± 2
30d		623 ± 72; 80 ± 3	1,256 ± 92; 36 ± 1
30e		116 ± 3; 87 ± 1	412 ± 26; 76 ± 1
30f		375 ± 33; 87 ± 2	1,027 ± 85; 49 ± 1
30g		631 ± 154; 72 ± 5	1,132 ± 79; 27 ± 1
30h		>11,000; >69	3,979 ± 547; 22 ± 1
30i		65 ± 6; 72 ± 2	348 ± 15; 52 ± 1
30j		511 ± 29; 88 ± 2	998 ± 105; 49 ± 2

Compound	Structure		
30k	*(chemical structure)*	>2,627; >72	>3,207; >32
30l	*(chemical structure)*	>5,421; >64	>10,000; >27
30m	*(chemical structure)*	1,326 ± 227; 44 ± 3	>3,000; >18
30n	*(chemical structure)*	>2,823; >60	>10,000; >21
30o	*(chemical structure)*	370 ± 95; 72 ± 5	>4,000; >51
30p	*(chemical structure)*	1,657 ± 297; 69 ± 6	1,825 ± 424; 20 ± 2
30q	*(chemical structure)*	Inactive	inactive
30r	*(chemical structure)*	1,520 ± 115; 36 ± 1	inactive
30s	*(chemical structure)*	4,471 ± 318; 49 ± 2	4,352 ± 326; 11 ± 1

[a]Potency values where obtained from triplicate determinations; values are average of n=3. [b]reported efficacy values shown are obtained from triplicate determinations; value are average of n=3 normalized to a standard compound, **3**

The most active compounds emerging from the SAR and compounds modified with the intent to improve the stability were subjected to *in vitro* clearance in human and mice liver microsomes. As expected, some of the most active regular *N*-cyclohexyl substituted pyrazole such as **24a, 29d, 29f, 30f,** and **30h** were highly metabolized. Interestingly, the 4,4-difluoro substitution in **27f** decreased the clearance by 2-fold (hCL$_{INT}$ = 77.3 mL/min/kg) compared to regular cyclohexyl. All the efforts to try to mask the free amide by methylation **30a** and **30b**, deuteration **30c,** or bioisosteric replacement with thioamide **30d** did not translate into increased stability. In fact, some of the analogs, like **30d**, were cleared much faster compared to the regular amide. Along with the difluoro, **27f**, one more interesting trend was observed in the triazole **30e**, as it had decent stability – only 2-fold less compared to the 5-membered sulfone **27k,** which has maintained to be stable throughout its incorporation into the various class of GIRK activators. Both **30e** and **27k** had ~3% unbound drug in human plasma protein binding (hPPB) assay. This represents a significant leap as **30e** is also active with EC$_{50}$ = 116 nM. But these results raised an important question about what imparts stability to these class of compounds, the heterocyclic 5-membered ring in **27k** might be offering a bulky resistance for the amide to line up in the active catalytical site of hydrolysis enzyme. Still, masking of free amide did not result in improved clearance. And the data of **30e,** which has a free amide, further contradicts the amide hydrolysis hypothesis. Both **27k** and **30e** after being stable in human liver microsomes and having ~3% unbound drug in hPPB are still highly cleared in mice, and their unbound fraction is so low that's its hard to recover any measurable quantities from the assay. The only outlier, in this case, was amide *N*-methylated compound **30a,** which, in spite of being highly cleared, shows up in mPPB assay (~3.6 %f_u) as shown in **Table 1.14**.

Table 1.14. *In Vitro* DMPK properties of selected tetrazole Class-II compounds

Cmpd	Structure	GIRK1/2 EC$_{50}$ (µM±SEM)	hCL$_{INT}$	mCL$_{INT}$	hPPB	mPPB
			mL/min/kg		%*f$_u$* (unbound)	
27a		96 ± 7	186.4	2917.53	1.09	Poor recovery
27f		84 ± 9	77.3	722.7	1.5	Poor recovery
27k		1,034 ± 66	<23.13	<49.5	3.69	Poor Recovery
29d		980 ± 68	99.9216	489.06	<0.03	Poor recovery
29f		81 ± 7	162.3726	2710.62	0.98	Poor Recovery
29v		1,304 ± 76	<23.1	<49.5	4.7	Poor recovery
30a		inactive	378.4	2338.4	1.7	3.6
30b		inactive	202.6188	2954.16	0.74	Poor Recovery
30c		116 ± 9	208.6	2583.9	Poor recovery	Poor recovery
30d		623 ± 72	346.4874	>5930.1	<0.06	Poor recovery
30e		116 ± 3	54.5868	595.98	2.97	Poor Recovery
30f		375 ± 33	209.0952	3487.77	0.42	Poor Recovery
30h		65 ± 6	113.7996	2356.2	2.4	Poor recovery

1.4. Ether Series

Design

Tetrahydrothiophene 1,1-dioxide moiety on the 3-methyl pyrazole has consistently proven to impart metabolic stability to the GIRK activators over the previous two series. Yet, an appropriate right-hand side combination has not been found which would make the activators with this stability imparting sulfone, also potent. An ether or phenol linked acetamide **37** was an additional scaffold from the HTS and thus, we decided to incorporate this new ether type of linkage into our existing pyrazole. For this series, we first tested the ether linkage on the sulfone containing pyrazole, and if it is potent, then only further SAR would be explored. The plan was made as detailed in **Figure 1.7**. If the sulfone seems to be active with this 2,4-dichloro substituted ether than a comprehensive pyrazole SAR followed by right-hand side ether modifications would be performed.

Synthesis

Similar to previous tetrazole general synthesis, a two-way approach was designed in order to facilitate ease of synthesis based on the part of the molecule being explored. The reaction of substituted phenol with bromoethyl acetate under basic conditions, followed by saponification gives the ether linked acetic acid coupling partner **40,** which can be coupled with the pyrazoles **11** to yield compound **44a-u.** This method is useful in diversifying pyrazole moiety keeping the other part constant. To explore the ether side α-chloro acyl coupling partner, **28**, can be utilized to undergo a nucleophilic substitution reaction with phenol to yield **45-47** series of compounds. While halogenated phenols and anilines, such as **38** are readily available, in order to make heterocyclic linked phenol **43**, a bromo or iodine halogen partner on protected phenol is used to undergo Suzuki or Buchwald type of reactions to form C-C or C-N extension, **42**. The methyl-protected phenol undergoes deprotection in the presence of boron tribromide (BBr$_3$) or sodium thiomethoxide (NaSMe) to get the desired functionalized phenol, **43. (Scheme 1.3)**
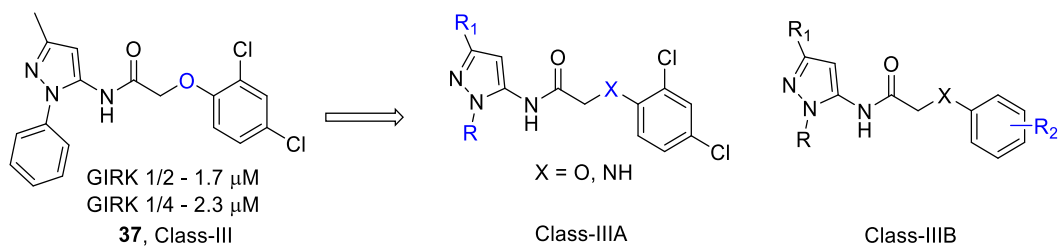
Figure 1.7. Design and SAR plan for ether series (Class-III)

A.

Reagents and Conditions: (a) K$_2$CO$_3$, DMF; (b) LiOH, THF, Water

B.

Reagents and Conditions: (a) Suzuki or Buchwald; (b) HBr or BBr$_3$ or NaSMe

C.

Reagents and Conditions: (a) T3P; (b) K$_2$CO$_3$, DMF
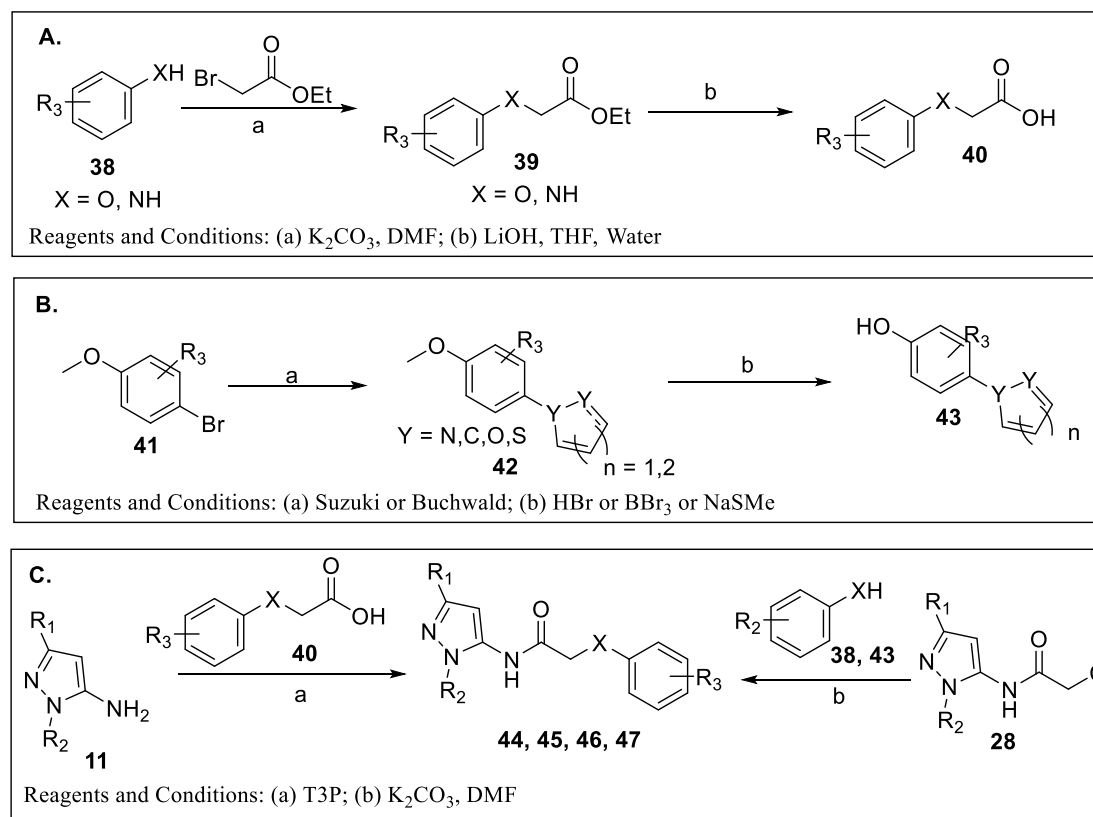
Scheme 1.3. General synthesis of ether series (Class-III)
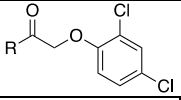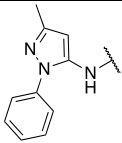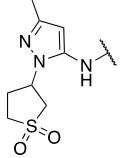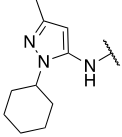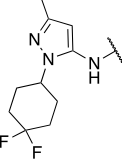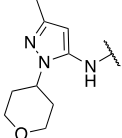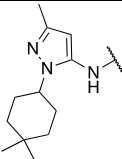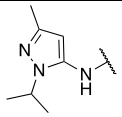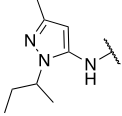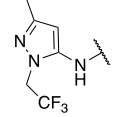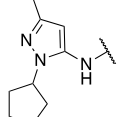
Results

The exploration to utilize the newly found right-hand side ether linkage began with coupling it to the tetrahydrothiophene 1,1-dioxide containing pyrazole. The compound thus obtained, **44a**, was highly potent with EC_{50} = 137 nM, which was comparable to some of the most potent GIRK activators obtained to date. Along with good potency for GIRK1/2, **44a** was 5-fold selective towards GIRK1/4 (EC_{50} = 702 nM). With such a good starting point, we began to explore the pyrazole substitution further. Some of the most active substitutions from the previous studies were utilized. First, the cyclohexyl, **44b** (EC_{50} = 91 nM) and difluoro cyclohexyl, **44c** (EC_{50} = 33 nM) were evaluated and **44c** is the most potent GIRK1/2 activator developed to date. **44d** containing the 4-tetrahydropyran was also highly potent with EC_{50} = 88 nM. 4,4-dimethylcyclohexyl containing compound, **44e**, was not as active, branched alkyl such as isopropyl **44f** (EC_{50} = 133 nM), *sec*-butyl, **44g** (EC_{50} = 163 nM), trifluoromethyl, **44h** (EC_{50} = 220 nM) containing moieties were also active. While *N*-cyclopentyl **44i** (EC_{50} = 147 nM) was active, *N*-cyclopropyl **44j** (EC_{50} = 1,013 nM) was not active. *N*-cyclopentyl containing pyrazole has retained their activity in all the series so far, but if the ring size is smaller than pentyl, the activity is lost. *N*-benzyl, **44k** (EC_{50} = 340 nM) and 6-membered sulfone containing ring, **44l** (EC_{50} = 577 nM) were only moderately active and only 2-fold selective. Since the ether linkage was imparting activity with previously moderately acitve substituted pyrazoles, we tried to incorporate some pyrazole replacement scaffolds as pyrazoles do face some oxidation and hydrolysis problems. 4-Phenyl thiazole, **44m**, and oxadiazole, **44n**, were not active at all. Benzoisoxazole **44o** (EC_{50} = 609 nM) was somewhat active. In order to prevent enzymatic hydrolysis, we came up with a ring closure strategy to make the secondary amide a tertiary one and still maintain some structural resemblance to the active *N*-cyclohexyl moiety. Thus dihydropyrrolo[1,2-*a*]pyrimidine bearing compound, **44p**, was synthesized but was completely inactive. A 6-membered substituted pyridine was utilized to mimic the substitutions on pyrazoles **44q** and **44r**, but they were also not active. Later some bioisosteric replacements of the amide were tried. Converting amide to carbamate, **44s**, led to complete loss of

activity. Thioamide replacement **44t** (EC_{50} = 723 nM) was moderately active, and alkylating the amide-NH **44u** led to a complete loss of activity. Thus assuring the absolute need of secondary amide for GIRK 1/2 activators, as shown in **Table 1.15**

With 5-membered sulfone ring being the active moiety, we tried some 3-position pyrazole substitutions to see if any of those would be tolerated. With an increase in the size of R_1 substitutions activity is lost. On the 2,4 dichlorophenyl ether linkage the activity was in order of methyl **44a** > ethyl **45a** > isopropyl **45b** > cyclobutyl **45c**. To replace the ether moiety an aniline was incorporated as in the case of **45d** (EC_{50} = 592 nM); however, ethers, such as **44a**, are four times more potent compared to anilines. An R_1 substitution around aniline gave almost similar results as ether, except the ethyl **45e** (EC_{50} = 590 nM) was equipotent to methyl, and isopropyl was completely inactive. To check the substitution effect of right-hand halogen, 2,4-dichloro was replaced with 2-chloro-4-fluoro moiety, which resulted in the loss of activity for both methyl **45h** (EC_{50} = 436 nM) and ethyl **45i** (EC_{50} = 553 nM). Still, the pattern of methyl substitutions being better than ethyl was maintained, as shown in **Table 1.16**.

Table 1.15. SAR of class-III ether around pyrazole substitution

Cmpd	Structure	GIRK1/2 (nM ± SEM[a]; % ± SEM[b])	GIRK1/4 (nM ± SEM[a]; % ± SEM[b])
37		1,707 ± 229; 56 ± 2	2,301 ± 251; 21 ± 1
44a		137 ± 23; 95 ± 2	702 ± 211; 76 ± 4
44b		91 ± 8; 98 ± 2	430 ± 43; 94 ± 3
44c		33 ± 3; 84 ± 2	145 ± 21; 71 ± 3
44d		88 ± 7; 108 ± 2	371 ± 27; 86 ± 3
44e		>677; >28	inactive
44f		133 ± 7; 98 ± 1	607 ± 50; 78 ± 2
44g		163 ± 10; 108 ± 2	571 ± 37; 101 ± 2
44h		220 ± 16; 85 ± 2	373 ± 35; 75 ± 2
44i		147 ± 11; 109 ± 2	548 ± 37; 102 ± 2
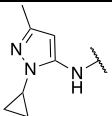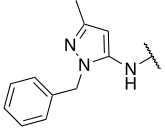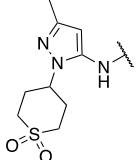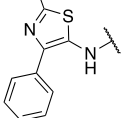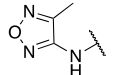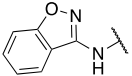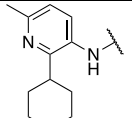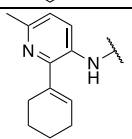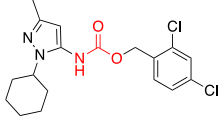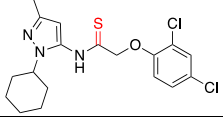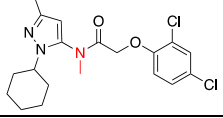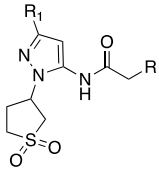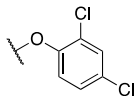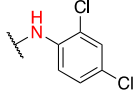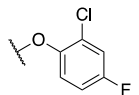
44j		1,013 ± 138; 63 ± 2	>5,000; >26
44k		340 ± 41; 94 ± 3	768 ± 170; 76 ± 7
44l		577 ± 58; 65 ± 2	1,171 ± 89; 44 ± 1
44m		Inactive	inactive
44n		>6,000; >50	>8,000; >52
44o		609 ± 169; 20 ± 1	1,476 ± 2,904; 13 ± 4
44p		Inactive	Inactive
44q		782; 44%	N/A; N/A
44r		N/A; N/A	N/A; N/A
44s		>4,000; >46	inactive
44t		723 ± 88; 103 ± 4	2,869 ± 282; 99 ± 6
44u		Inactive	inactive

[a]Potency values where obtained from triplicate determinations; values are average of n=3.
[b]reported efficacy values shown are obtained from triplicate determinations; value are average of n=3 normalized to a standard compound, **3**

Table 1.16. SAR of Class-IIIA, R$_1$ pyrazole and ether replacement

Cmpd	R$_1$	R	GIRK1/2 (nM ± SEM[a]; % ± SEM[b])	GIRK1/4 (nM ± SEM[a]; % ± SEM[b])
45a	Et		187 ± 34; 79 ± 4	360 ± 98 36 ± 4
45b			1,200; 12%	inactive
45c			1,400; 21%	Inactive
45d	Me		592 ± 51; 98 ± 2	>2,804; >59
45e	Et		590; 76%	1,400; 27%
45f			Inactive	Inactive
45g			Inactive	Inactive
45h	Me		436; 93%	1,752; 64%
45i	Et		583; 79%	888; 30%
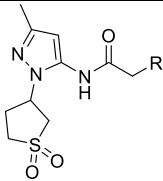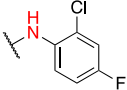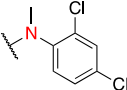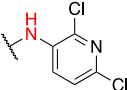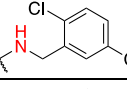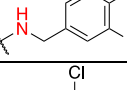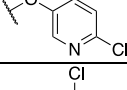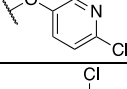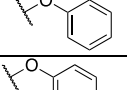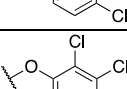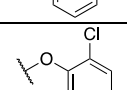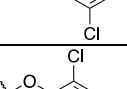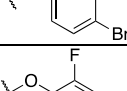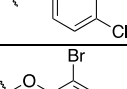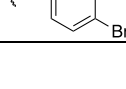
[a]Potency values where obtained from triplicate determinations; values are average of n=3. [b]reported efficacy values shown are obtained from triplicate determinations; value are average of n=3 normalized to a standard compound, **3**

Having established the 3-position methyl to be the most tolerated group, next, we went on to explore the right-hand side ether and aniline substitution. We started with aniline modifications. We tried to swap the 2,4-dichloro with a 2-chloro-4-fluoro moiety in **46a** (EC_{50} = 1,269 nM) as had been observed with the ether in the compound **45h**, this change was not productive, neither was an attempt to methylate the aniline in **46b**. Incorporation of a chlorinated pyridyl aniline led to a complete loss of activity in **46c**. And an adding extra carbon in the form of halogenated benzyl amines **46d** and **46e** were also completely inactive. Thus seeing no scope for immediate improvement with anilines, our focus remained on optimizing the ether linkage itself. Adding nitrogen to the ring in the active 2,4-dichloro moiety led to inactive compounds **46f** and **46g.** To check the importance of 2- and 4- position halogenation, we prepared individual 2-chloro **46h** (EC_{50} = 962 nM) and 4-chloro **46i** (EC_{50} = 4,659 nM) substitutions. The 2-position chlorination seems to be more active overall. But the combination of 2,4-dichloro was much better, almost 7-fold more active than mono-chloro compounds. From the result of 2,3-dichloro compound **46j** (EC_{50} = 239 nM) and 2,5-dichloro **46k** (EC_{50} = 150 nM), it could be concluded that the original 2,4-dichloro is the most active combination. Replacing the 4-chloro in the active combination to make 2-chloro-4-bromo compound **46l** was fruitful since it came out to be active with EC_{50} = 132 nM. A swap with fluorine at the same place was not tolerated. Hence now the 2-position chloro was swapped with a fluorine **46m,** EC_{50} = 1,454 nM to see if that was active but had similar fate as **45h**. Since swapping with bromine retained the activity, we went with a 2,4-dibromo compound **46n**, and this came out to be two-fold more potent (EC_{50} = 63.8 nM) compared to the 2,4-dichloro (EC_{50} = 137 nM). But similar to chloro an effort to find out if the 2-position **46o** (EC_{50} = 493 nM) or the 4-position **46p** (EC_{50} = 4,480 nM) is better led to an overall reduction in the potency. But as similar to the chloro, bromo at 2-position is 10-fold more potent than at the 4-position. Having established the 2,4-dihalogenated moiety to be the optimal, we went with 2,4-dimethoxy **46q** (EC_{50} = >12,000 nM), 2,4-dimethyl **46r** (EC_{50} = 1,739 nM) and 2,4-trifluoromethyl **46s** (EC_{50} = 146 nM). The active trifluoromethyl group was tested once again at the 2-position **46t** (EC_{50} = 484 nm) and we obtained
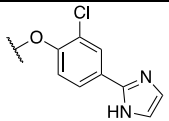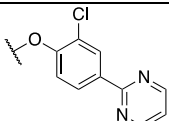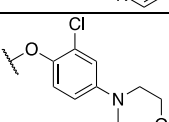
similar results as of mono-chloro and mono-bromo compounds. Having established the ideal substitution position and the best working substitutions, we went with some exploratory work to see if there would be space in the pocket where the right-hand side part of the structure fits into the GIRK1/2 channel and if extending it would be beneficial. Bulkier aromatic ring-containing compounds having a quinoline **46u**, naphthyl **46v**, indole **46w**, indazole **46z**, benzofuran **47a**, and 1*H*-pyrazolo[3,4-*b*]pyridine **47b**, all came out to be inactive except the benzofuran **47a** which had EC_{50} = 3,893 nM. An effort to add an extra carbon as in **47c** was also not productive. To further explore the elongation potential of the molecules, we tried to incorporate some 5 and 6 membered heterocycles with potential for occupying space, making $\pi-\pi$ interactions and also provide some hydrogen bonding potential.

To begin with, a thiazole was attached at the 2-position, **47e** (EC_{50} = 646 nM) and the 4-position, **47d** (EC_{50} = 623 nM). To our surprise, the molecules retained some activity and were almost similar in potency. A pyrazole linked to the 4-position via C-N bond **47f** was somewhat active EC_{50} = 772 nM, but an imidazole linked to the same position via C-C bond **47g** was not active. Incorporation of pyrimidine **47h** and morpholine **47i** at the similar 4th position resulted in compounds with extremely low potency, as shown in **Table 1.17**.

Table 1.17. SAR of Class-IIIB ether substitution

Cmpd	R	GIRK1/2 (nM ± SEM; % ± SEM)	GIRK1/4 (nM ± SEM; % ± SEM)
46a		1,269; 90%	5,875; 52%
46b		2,955 ± 235; 77 ± 9 %	3,839 ± 368; 24 ± 3%
46c		>10,000; >50	>10,000; >8
46d		>10,000; >28	inactive
46e		Inactive	Inactive
46f		>10,000; >65	>10,000; 61
46g		3,472 ± 174; 70 ± 4	5,378 ± 270; 42 ± 2
46h		962 ± 170; 92 ± 5%	3,133 ± 289 ; 59 ± 5%
46i		4,659 ± 18; 101 ± 3%	>10,000 >77
46j		239 ± 50; 84 ± 5%	601 ± 137; 44 ± 4%
46k		150 ± 38; 88 ± 4%	511 ± 73; 47 ± 3%
46l		132 ± 24; 93 ± 9%	427 ± 65; 69 ± 5%
46m		1,454 ± 12; 91 ± 2%	3,919 ± 54; 52 ± 2%
46n		63.8 ± 7; 94 ± 2%	229 ± 28; 77 ± 3%

Compound	Structure	Value 1	Value 2
46o		493 ± 80; 86 ± 4%	1,277 ± 155; 48 ± 2%
46p		4,480 ± 404; 96 ± 11%	>9,400; >54
46q		>12,000; >38%	Inactive
46r		1,739 ± 154; 99 ± 2%	5,541 ± 882; 57 ± 4%
46s		146 ± 21; 88 ± 2%	730 ± 97; 52 ± 2
46t		484 ± 93; 81 ± 4%	1,286 ± 257; 48 ± 4%
46u		Inactive	inactive
46v		4,200; 98%	>8,300; >41%
46w		>12,500; >40	Inactive
46x		N/A	N/A
46y		Inactive	inactive
46z		Inactive	Inactive
47a		3,893; 110	>9,200; >60
47b		Inactive	inactive
47c		2,256; 102	4,710; 39
47d		623; 93	1,966; 53
47e		646; 77%	946; 33%
47f		772; 95	2,573; 49

47g		N/A	N/A
47h		2,199; 91%	5,064; 52%
47i		6,012; 91%	N/A

[a]Potency values where obtained from triplicate determinations; values are average of n=3. [b]reported efficacy values shown are obtained from triplicate determinations; value are average of n=3 normalized to a standard compound, **3**

The pharmacokinetic profiling of the ether series gave some exciting results and thought-provoking insights into the metabolic stability of these types of GIRK1/2 activators. It also raises some important questions on the main metabolizing pathways it is subjected to and what structural attributes prevent it from getting easily degraded. This study was unique as until now the PK studies had only one or two compounds belonging to the stability providing 5-membered sulfone moiety, but this study had multiple sulfone derivatives which provided a deeper insight into what might be happening. Most of the *N*-alkyl, cycloalkyl pyrazole bearing compounds such as **44f, 44c, 44d, 44s,** and **44t** were rapidly metabolized. Whenever there is an amide bond present in an investigative molecule, it is generally held as the culprit for making the molecule metabolically labile – due to the potential for amidolysis, but even with carbamate and thioamide replacement as in the case of **44s** and **44t** absence of amide bond did not improve the stability. 4-Tetrahydropyran, **44d**, did appear to offer some stability and had a good amount of free fraction in the human, indicating that oxidation of N-cycloalkyl in the pyrazole might be one of the metabolic pathways involved. Owing to the size of the sulfone moiety, we hypothesized that it is providing metabolic stability by shielding the amide bond to interact with the hydrolytic enzymes and also preventing the *N*-heterocycle pyrazole oxidation. But some of these stability is lost in the case of 3-ethyl containing pyrazoles such as **45a**, pointing toward the oxidation at the 3-position also to be a metabolic pathway involved. The 5-membered sulfone ring did give equal stability to the aniline class of molecules; in fact the aniline type molecules had much better free fraction available in mouse, compare **45d** to **44a**. But in the case of anilines, 3-ethyl pyrazoles were not as stable as the 3-methyl pyrazole **45e** vs **45d.** Lastly, incorporation of dibromo instead of dichloro also led to 2-fold decrease in stability **46n** vs **44a.** These results strongly suggest that the stability of these types of molecules is not only due to a particular heterocycle replacement but all the structural optimization plays a key role in making **44a** both stable and potent at the same time, as shown in **Table 1.18**. **44a** is further subjected to a LCMS-MS based metabolite identification experiment to figure out where

and what type of metabolism is occurring and using these insights to guide the future development

of GIRK1/2 activators with better stability in mice also.

Table 1.18. *In Vitro* DMPK properties of selected ether Class-III compounds

Cmpd	Structure	GIRK1/2 EC$_{50}$ (µM±SEM)	hCL$_{INT}$	mCL$_{INT}$	hPPB	mPPB
			mL/min/kg		f_u	
44f		133 ± 7	323.82	4950	Poor recovery	Poor recovery
44a		137 ± 23	46.26	594	11.8	Poor Recovery
44c		33 ± 3	295.1	>5930.1	6.6	Poor recovery
44d		88 ± 7	100.4	2970	16.3	Poor recovery
44l		577 ± 58	25.443	294.03	15.95	Poor recovery
44s		>4,000	341.3988	2806.65	0.32	4.9
44t		723 ± 88	250.7292	>5930.1	<0.06	Poor recovery
45a		187 ± 34	165.6	1,174.1	5.4	Poor recovery
45d		592 ± 51	44.9	174.2	8.5	13.1
45e		590	168.0	714.8	3.6	7.9
46n		63.8 ± 7	93.0	672.2	4.8	Poor recovery
46t		146 ± 21	50.9	134.6	6.8	Poor recovery

MLM	0 min	60 min
Parent	97.4%	0.6%
M1	2.6%	95.4%
HLM	**0 min**	**60 min**
Parent	99.9%	54.8%
M1	0.1%	18.3%
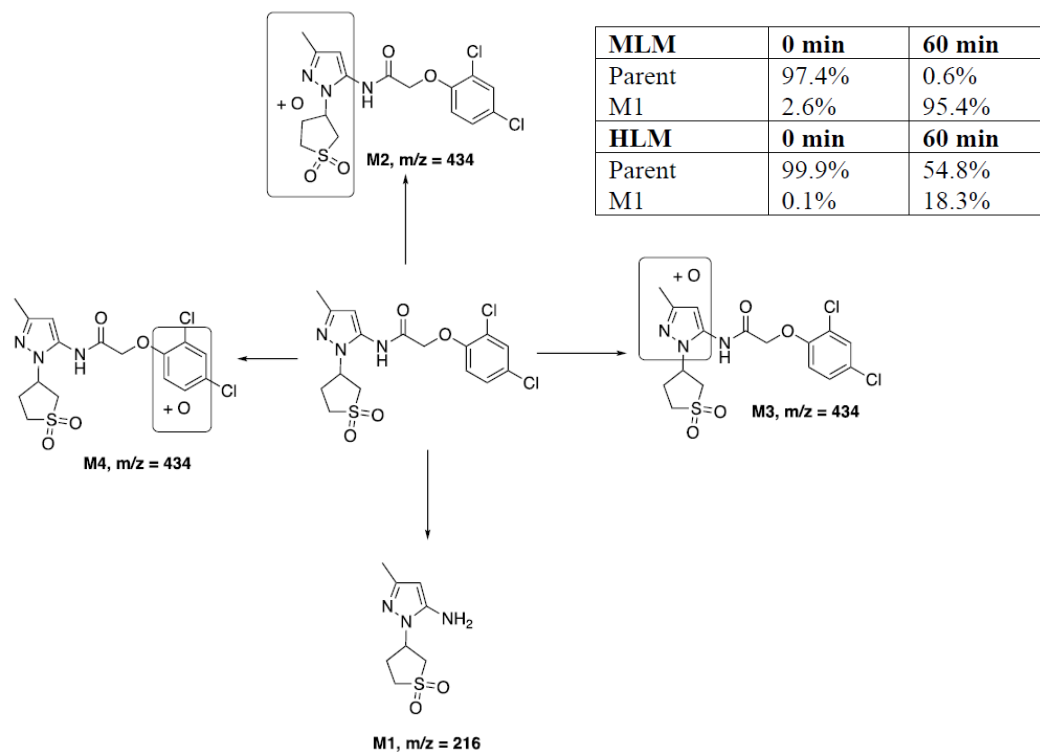
Figure 1.8. Metabolite ID Study of 44a in mouse and human liver microsomes with NADPH

44a is highly metabolized in mouse liver microsomes (MLM) and moderately metabolized in human liver microsomes (HLM). After 60 min of incubation, the metabolite M1 (amide hydrolysis) was the largest component in MLM, and the parent was the largest component in HLM. The amide hydrolysis in MLM was independent of NADPH. All other oxidative metabolites are present in <2% at 60 mins.[64] The metabolite study made it clear why the free fraction in mPPB was not able to get detected most of the time, as the majority of GIRK activators are highly metabolized in mice liver microsomes. Oxidative metabolism is <2%, as shown by the met-ID studies, as shown in **Figure 1.8**. With all this information, it is difficult to pinpoint what role or benefit the 5-membered sulfone ring provides for imparting stability in HLM. Based on these studies the most prominent way to improve mice stability would be to stop the amide hydrolysis, which could be a tough challenge since the importance of a free secondary amide has been reinstated multiple times over the various SAR studies performed on the GIRK1/2 activators.
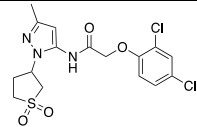
44a was subjected to a detailed selectivity and pharmacokinetic study. The goal of the study was to identify any off-target effects of **44a** and get detailed *in vitro* and *in vivo* PK parameters which shall be helpful while subjecting **44a** to *in vivo* efficacy assays. The values obtained in the study are summarized in **Table 1.19**. A thallium flux assay to functionally evaluate the selectivity of **44a** in a diverse panel of potassium channels was carried by our collaborator. The compound was evaluated against Kir3.2 (homomeric GIRK2), Kir6.2/SUR1, Kv2.1, Kv2.2, Kv7.2, Kv11.1 (hERG), Maxi-K, SLACK, and SLICK, and showed complete selectivity against all ion channels tested. Finally **44a** was profiled against the Psychoactive Drug Screening Panel at the University of North Carolina, Chapel Hill. This panel consists of 45 receptors and transporters that are of importance in the CNS was clean against this larger panel of receptors, confirming **44a** as a selective GIRK1/2 activator.[65]

44a was subjected to Caco-2 permeability assay to assess its permeability and its suitability to be delivered orally. It was determined to be highly permeable and have a low efflux ratio (ER = 1.75). **44a** was also tested in a human liver S9 liver stability assay and was shown to be a low

clearance molecule (CL_{HEP} = 9.0 mL/min/kg) with a $T_{1/2}$ of 106.6 minutes. **44a** in an *in vivo* rat cassette study was shown to be highly cleared with a short half-life ($T_{1/2}$ = 0.35 h), yet it had a brain to plasma ratio of *Kp* = 0.58, indicating a significant portion of what is left was reaching the brain. Finally, **44a** was evaluated in a discrete *in vivo* PK experiment in order to assess the PK properties when dosed individually. When **44a** was dosed via IP route, the compound had improved plasma and brain half-life (plasma, $T_{1/2}$ = 1.6 h; brain, $T_{1/2}$ = 1.7 h) and significantly improved brain: plasma ratio (K_p = 1.8). The study indicated that **44a** could be effectively used for *in vivo* efficacy assay, and various information obtained from the study such as T_{max}, $C_{max,}$ and AUC shall help in deciding the dose and its frequency, as shown in **Table 1.19**.

Table 1.19. Detailed PK-PD profiling of 44a

Compound-**44a**				
GIRK1/2			$137 \pm 23;$	
GIRK1/4			702 ± 211	
Selectivity (µM)			Human S9 metabolic stability	
Kv2.1			$T_{1/2}$ (min)	106.6
Kv2.1/6.4			CL_{HEP} (mL/min/kg)	9.0
Kv2.1/9.1			Hepatic ER	0.45
Kv2.1/8.2 (82D)			% remaining (60 min)	62
Kv7.2	>30		Rat	
Kv2.2			In vivo PK (cassette, 0.5 mpk)	
hERG			CL (mL/min/kg)	169
KCNMA1/B4			$T_{1/2}$ (h)	0.35
SLACK			C_0 (ng/mL)	82.4
SLACK-A934T			V_{ss} (L/kg)	3.3
SLICK			AUC (h*ng/mL)	96.4
Kir6.2			Brain (cassette)	
In vitro PK			Plasma (ng/mL)	39.8
hCL_{INT}	hCL_{HP}	46.3	14.0	Brain (ng/g)	23.1
mCL_{INT}	mCL_{HEP}	594	78.2	B:P	0.58
rCL_{INT}	rCL_{HEP}	278.6	55.9	Discrete PK (10 mpk, IP)	
hPPB (%f_u)	11.8		$T_{1/2}$ (h)	1.6
mPPB (%f_u)	*		T_{max} (h)	0.5
rPPB (%f_u)	*		C_{max} (ng/mL)	44.0
PDSP Selectivity			AUC (h*ng/mL)	92.6
Selectivity panel	Not active[a]		Brain (10 mpk, IP)	
[a]No receptor >50% inhibition at 10 µM for 45 receptors			$T_{1/2}$ (h)	1.7
			T_{max} (h)	0.17
			C_{max} (ng/g)	217
			B:P	1.8
Caco-2 Permeability (10^{-6} cm/s)				
A-B	13.7		*In vivo* PK studies were performed at Pharmaron, Louisville, KY.	
B-A	24.0			
Efflux ratio	1.75			

1.5. Summary and Conclusions

Ion channels play a very crucial role in various physiological processes throughout the body. In the central nervous system, their role becomes very critical due to their association with numerous other receptors. GIRK is also one such type of ion channel whose role in conducting the inhibitory synaptic current is very important. Many scientific groups have been trying to rationalize and establish the role of the GIRK channel in the pathophysiology of various CNS disorders. One of the most important steps in utilizing full potential of this GIRK channels is to develop a selective molecular probe. Developing small molecular probes for ion channels become a challenge since the ligand bound crystal structure of ion channels are hard to obtain. The story of the development of GIRK1/2 activators begin with high throughput screening, the facilities, assays and technology developed to perform those high throughput screening tremendously helps to perform structure-activity relationship. Our collaborators have been pioneers in developing thallium flux assay, which could be run by robots in a high throughput fashion, increasing the speed and accuracy of the workflow. While performing SAR studies, it's very crucial to obtained EC_{50} values and not just % activation. Automation allows for swift flow back of activity and potency data which helps in guiding the design of future molecules.

In studies, the availability of HTS data helped tremendously, as we were able to find new leads by going back to the HTS data. The SAR studies for the three series amide, tetrazole, and ether are shown in **Figure 1.9**. The study highlights a crucial point that with the changes in structure, as it's difficult to generalize the substitution pattern. In the previous urea type of molecules, phenyl and benzyl were the active substitutions on the pyrazole ring. However, since the development and incorporation of an amide bond, cycloalkanes have been the preferred choice of *N* substitution on the pyrazole ring. On the right-hand side of the molecule also a proper substitution scan is critical. As can be seen in the figure in amide series 3,4-substitution was necessary, then with tetrazoles only third position substitution with fluorine was the best suitable

and later on moving to the ether 2,4-dichloro substitution was the best. For most of the early series fluorine substitution was equal or better than chlorine substitution, but now chlorine is the optimal halogen of choice.

SAR of the amide series showed the necessity of secondary amide and 3,4-halogen substitution; moving to the tetrazole series, the structural features of the pyrazole side of the ring remain similar to that of the amide, including the requirement of the central secondary amide. But very interesting observations were made regarding the dependence of activity on the regioselectivity of the nitrogen were in just the two nitrogen showed in color blue, and their specific position was more important for the activity.

In the ether series, we were able to find the right fit for the 5-membered sulfone substitution of the pyrazole, which has been consistently giving metabolically stable molecules. The requirement for right-hand side halogen substitution was different from the previous molecule. As discussed in the results section of the ether series, differences in the stability on various pyrazole derivatives having the same 5-membered sulfone ring gave us thought-provoking insights into what matters for the metabolic stability. After many assumptions, we are still not clear if it is the shielding effect of the sulfone on the amide or the prevention of oxidation of the previously used cyclohexyl on the pyrazole is responsible for better stability.

The table in **Figure 1.9** shows our progress over the different series, moving from urea to amide solved the brain penetration issue. It could be speculated that decreasing the polarity going from urea to an amide might have helped in brain penetration, in addition to eliminating an additional H-bonding NH. An increase in the brain penetration along with 4-fold selectivity towards GIRK1/4 ideally translates into much better control of off-target effects, since quite a significant amount of the compound will reach the brain and will not be circulating in the plasma to react with GIRK1/4, which is present in the heart. Moving from amide to tetrazole, we got many low nanomolar active compounds, but the significant discovery was in establishing the role of 5-

membered sulfone to impact the stability of the molecules. In the ether series, we were able to develop stable molecules, which are active, selective, and at the same time had very good brain penetration. Over the course of these four series, we addressed selectivity, brain penetration, and stability issues.

Figure 1.9. SAR studies of GIRK 1/2 activators and their progress
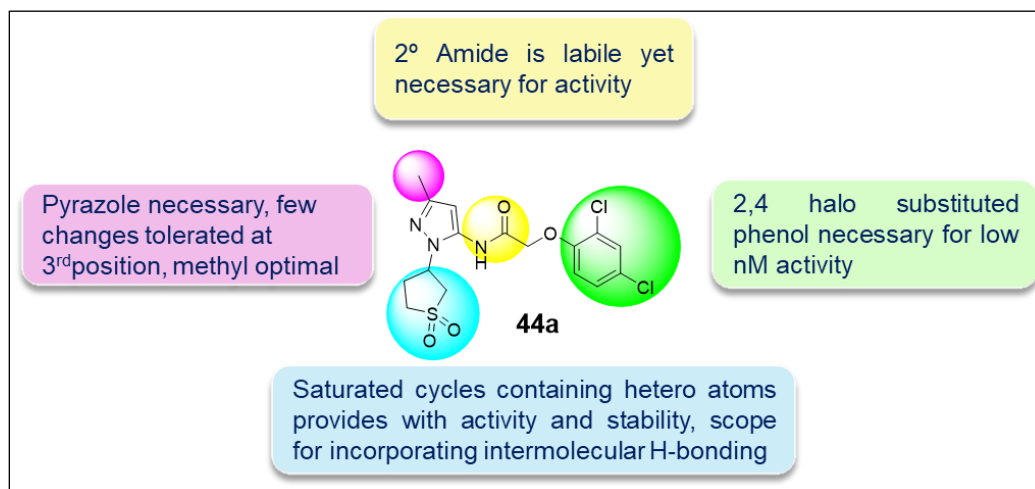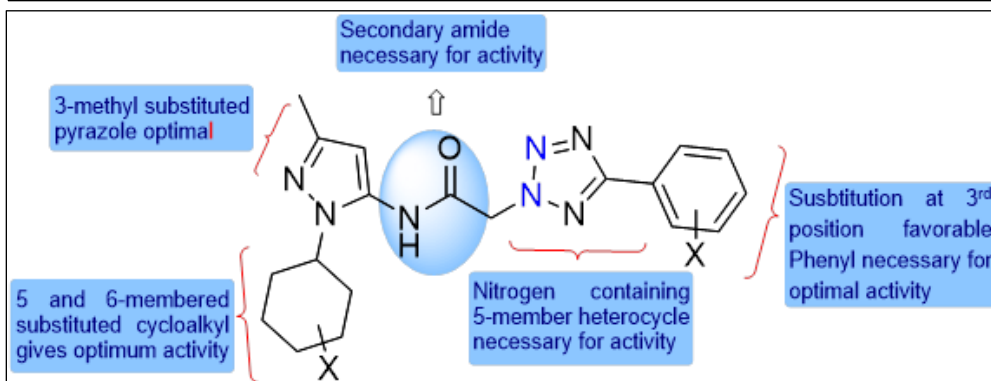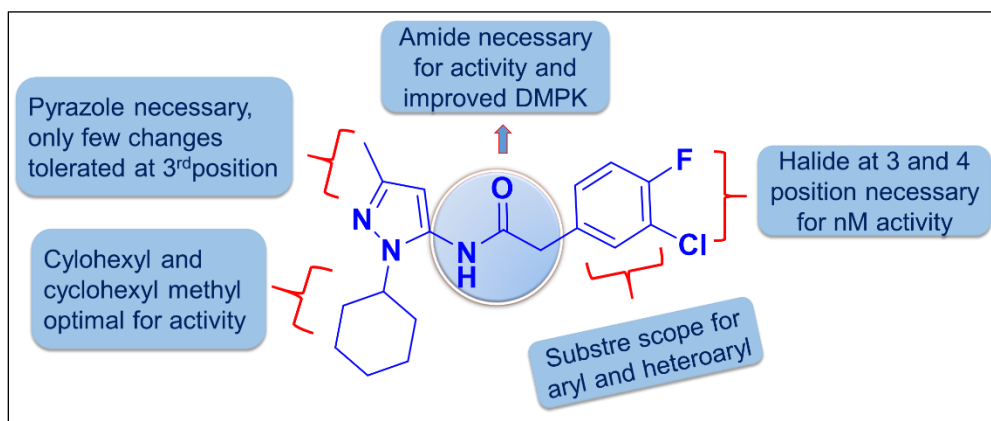
	Urea (**3**)	Amide (**17b**)	Tetrazole (**27k**)	Ether **(44a)**
Potency (EC$_{50}$ nM)	73	165	1034	137
GIRK 1/2 vs 1/4 (~Fold)	2	4	2	5
B:P ratio (Kp)	0.2	0.85	-	1.8
hCL$_{INT}$ (mL/min/kg)	-	246	23	46.3

1.6. Synthesis Protocols and Experimental

In Vitro Pharmacology

Thallium flux assays were preformed in the lab of Dr. David Weaver at Vanderbilt University. Briefly, HEK-293 cells expressing either GIRK1 and GIRK2 or GIRK1 and GIRK4 were cultured in α-MEM (Corning, Corning, NY) containing 10% (v/v) fetal bovine serum (Thermo Fisher Scientific, Waltham, MA) plus 1× glutagro (Corning, Corning, NY) (referred as cell culture medium) at 37 °C in a humidified 5% CO2 atmosphere. Cells at ~90% confluence were dislodged from the tissue culture vessel using TrypLE Express (Thermo Fisher Scientific, Waltham, MA) and plated at a density of 20,000 cells/well in 20 µL/well cell culture medium in 384-well, clear-bottom, black-walled, BD PureCoat Amine plates (Corning, Corning, NY) and incubated overnight at 37 °C in a humidified 5% CO_2 atmosphere. On the day of assay, the medium was removed from the plates and replaced with 20 µL/well of a solution containing assay buffer (Hank's buffered saline solution (Thermo Fisher Scientific, Waltham, MA) plus 10 mM HEPES (Thermo Fisher Scientific, Waltham, MA)-NaOH, pH 7.2), 1 µM Thallos (TEFlabs, Austin, TX), 0.5% DMSO, and 0.036% Pluronic F-127 (Sigma-Aldrich, St. Louis, MO). Cell plates containing Thallos solution were incubated 1 h at room temperature. Following incubation the Thallos-containing solution was replaced with 20 µL/well assay buffer. The Thallosloaded cell plates were transferred to a Panoptic kinetic imaging plate reader (WaveFront Biosciences, Franklin, TN). Images acquired at 1Hz, 480/40 nm excitation, and 538/40 nm emission were collected for 10 s, after which time 20 µL/well of assay buffer containing test compounds at 2-fold over their final concentrations were added.

Imaging continued for 4 min, at which time 10 µL/well of a solution containing 125 mM NaHCO3, 1.8 mM CaSO4, 1 mM MgSO4, 5 mM glucose, 2 mM Tl2SO4, and 10 mM HEPES-NaOH pH 7.2 was added and images were collected for an additional 2 min. To quantify test compound effects on GIRK channel activity, the initial slopes of the thallium-evoked changes in fluorescence were fit to a 4-parameter logistic equation using the Excel (Microsoft, Redmond, WA)

plugin XLfit (IDBS, Guildford, UK) to obtain potency and efficacy values. Efficacies are relative to a maximally effective concentration of **3**. Ten-point concentration series from 30 µM to 1.5 nM were generated using an Echo liquid handler (Labcyte, San Jose, CA). Final DMSO concentration, 0.24% (v/v), in the assay was constant across all compound concentrations. Unless otherwise indicated, all buffer salts were obtained from Sigma-Aldrich, St. Louis, MO.

DMPK Studies

In vitro and *in vivo* drug metabolism and pharmacokinetics study were performed in the lab of Dr. Yazen Alnouti, Dr. Yashpal Chhonker and Prof. DJ Murry's lab at UNMC. Some pharmacokinetics study and metabolite identification were performed by Q^2 Solutions, Indianapolis.

Metabolic stability was assessed using mouse, rat, and human liver microsomes (XenoTech, LLC, Lenexa, KS, USA) for phase I metabolism. Briefly, the bu_er solution was prepared containing potassium phosphate buffer (100 mM, pH 7.4), 25 µL of microsomal protein (20 mg/mL), magnesium chloride (10 mM) and NADPH (2 mM) in a final volume of 0.5 mL was pre-incubated at 37 °C for 10 min in water bath maintaining at 60 rpm. The reaction was started by adding 2 µL of drug (compound). Serial samples (50 µL) were collected at selected time intervals (0, 5, 15, 20, 30, 45 and 60 min) and quenched with 200 µL of acetonitrile spiked with 10 µL of IS (0.5 µg/mL). All the samples were vortexed and centrifuged at 13,000×g for 15 min, supernatant collected and transferred to an autosampler vial and injected (2 µL) onto the LC-MS/MS system. Both the S9 Fraction and HLM metabolic stability was expressed as the percentage of drug remaining at each time point. The *in-vitro* metabolic elimination rate constant was calculated from the first-order plot of a natural logarithm of the area ratio versus time. The slope of the linear regression equation was used to determine elimination rate constant "k" (min^{-1}). The half-life ($t_{1/2}$) was calculated using Equation (1). The *in-vitro* intrinsic clearance (CL_{INT}) was determined by using

Equation (2). The intrinsic clearance was further extrapolated to *in-vitro* hepatic clearance (CL$_{HEP}$: mL/min/kg of body weight) using a scaling factors and Equation (3).

Plasma Protein Binding (PPB) Study. Rapid Equilibrium Dialysis (RED) device system (Thermo Scientific, Rockford IL) was used to evaluate PPB by adding buffer to the buffer chamber and dosing solution to the sample chamber. The buffer chamber contained 350 µL of phosphate-buffered saline (containing 100 mM sodium phosphate and 140 mM sodium chloride, pH 7.4). The sample contained mouse plasma spiked with 1 µM or 10 µM of drug and was added to the sample chamber. The RED kit top was then sealed and incubated at 37 °C on an orbital shaker at 100 rpm for 5 h. At pre-determined times, aliquots (40 µL) were removed from the sample and buffer chambers and mixed with an equal volume of buffer or blank plasma, respectively. The samples were further processed by solid phase extraction (SPE) and analyzed by LC-MS/MS. PPB was calculated using Equation (4).

$$t^{1/2} = 0.693/k \tag{1}$$

$$CL_{int} = \frac{0.693}{t^{1/2}} \times \frac{Volume\ of\ reaction\ mixture\ (mL)}{mg\ of\ protein} \tag{2}$$

$$CL_{HEP} = CL_{int} \times \frac{mg\ of\ protein}{gram\ of\ liver} \times \frac{gram\ of\ liver}{kg\ of\ body\ weight} \tag{3}$$

$$\%Bound = \frac{Concentration\ (donor\ cell) - Concentration\ (receiver\ cell)}{Concentration\ (donor\ cell)} \times 100 \tag{4}$$

Synthesis Procedure and Experimental data

All ^{1}H and ^{13}C NMR spectra were recorded on Bruker AV-400 (500 MHz) instrument. Chemical shifts are reported in ppm relative to residual solvent peaks as an internal standard set to δH 3.31 or δC 49.00 (CD$_3$OD) or δH 2.50 or δC 39.52 ((CD$_3$)$_2$SO). Data are reported as follows: chemical shift, multiplicity (br = broad, s = singlet, d = doublet, t = triplet, q = quartet, m = multiplet), coupling constant (Hz), and integration. Low resolution mass spectra were obtained on an Agilent 1260 LCMS with electrospray ionization, with a gradient of 5-95% MeCN in 0.1% formic acid water over 4 min. Analytical thin layer chromatography was performed on LuxPlate silica gel 60 F254 plates. Visualization was accomplished with UV light, and/or the use of ninhydrin, anisaldehyde and ceric ammonium molybdate solutions followed by charring on a hot-plate. Chromatography on silica gel was performed using Silica Gel 60Å (230-400 mesh) from Sorbent Technologies. Solvents for extraction, washing and chromatography were HPLC grade. All reagents were purchased from Aldrich Chemical Co. (or similar) and were used without purification.

Final compounds were purified by either using Biotage Isolera-1 normal flash chromatography system or a Gilson preparative reversed-phase HPLC system comprised of a 322 aqueous pump with solvent-selection valve, 334 organic pump, GX-271 liquid hander, two column switching valves, and a 159 UV detector. UV wavelength for fraction collection was user-defined, with absorbance at 254 nm always monitored. Column: Phenomenex Axia-packed Luna C18, 50 x 21.2 mm, 5 μm. For Acidic Method: Mobile phase: CH$_3$CN in H$_2$O (0.1% formic acid). Gradient conditions: 2.0 min equilibration, followed by user-defined gradient (starting organic percentage, ending organic percentage, duration, typically 4 mins), hold at 95% CH$_3$CN in H$_2$O (0.1% TFA) for 2 min, 20 mL/min, 23 °C.

General Synthesis for making 5-amino pyrazoles (11)

Reagents and Conditions: (a) ACN, n-BuLi, THF, -78°C to RT
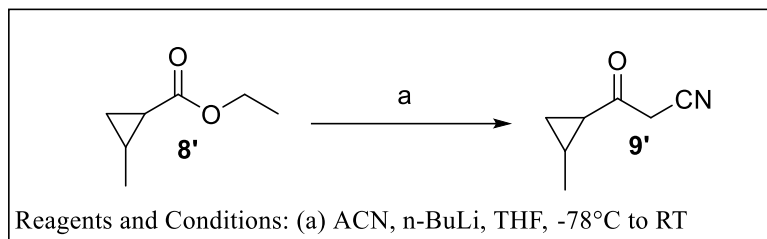
3-(2-methylcyclopropyl)-3-oxopropanenitrile: In an oven dried 50 mL 3-neck RBF, n-BuLi (3.75 mL, 9.37 mmol) was added dropwise to a solution of CH_3CN (0.49 mL, 9.3 mmol) in anhydrous THF (12 mL) under inert gas atmosphere at -78 °C. After stirring for 30 mins, ethyl 2-methylcyclopropane-1-carboxylate (0.60 g, 4.7 mmol) was added and the reaction was allowed to reach rt over a period of 2 h. Reaction completion was determined by TLC. Reaction was quenched with NH_4Cl_{aq} saturated solution. Product was extracted with ethyl acetate (100 mL *2). Combined organic layers were washed with brine, dried over sodium sulphate, concentrated and used as such. Yield = 0.7 g (crude), ^1H NMR (500 MHz, CDCl$_3$) δ 3.60 (d, J = 0.7 Hz, 2H), 1.85 (dt, J = 8.0, 4.2 Hz, 1H), 1.63 – 1.56 (m, 1H), 1.46 – 1.41 (m, 1H), 1.18 (d, J = 6.0 Hz, 3H), 0.99 – 0.93 (m, 1H). ^{13}C NMR (125 MHz, CDCl$_3$) δ 196.88, 114.05, 32.69, 28.96, 22.87, 21.39, 17.92.

Reagents and Conditions: (a) AcOH, EtOH, RT-Reflux
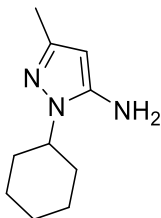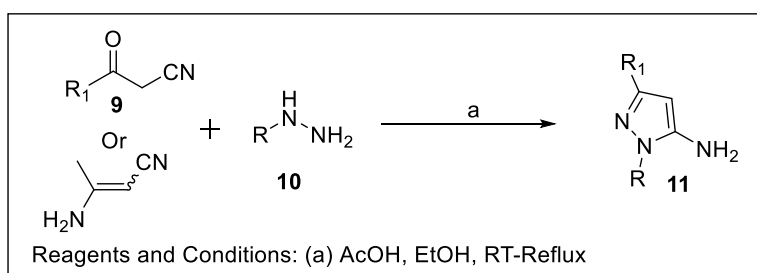
1-cyclohexyl-3-methyl-1*H*-pyrazol-5-amine. In a 250 mL RBF, 3-aminobut-2-enenitrile (2.0 g, 0.24 mole) was added to a stirred solution of cyclohexyl hydrazine hydrochloride (4.0 g, 26 mmole) and acetic acid (0.1 mL) in ethanol (60 mL). The reaction was refluxed for 6 h. Crude was evaporated and loaded on column to elute out product at 40% ethyl acetate in hexane. Yield = 1.74 g (40%) LCMS: R_T = 1.50 min., >98% @ 215 and 254 nm, *m/z* = 180.1 [M + H]$^+$. ^{1}H NMR (500 MHz, DMSO-*d$_6$*) δ 5.02 (s, 1H), 4.92 (s, 2H), 3.86 – 3.78 (m, 1H), 1.94 (s, 3H), 1.78 – 1.68 (m, 4H), 1.63 (dd, *J* = 16.3, 7.4 Hz, 3H), 1.31 (q, *J* = 12.9 Hz, 2H), 1.18 – 1.08 (m, 1H). ^{13}C NMR (125 MHz, DMSO-*d$_6$*) δ 145.90, 144.64, 87.80, 53.50, 32.13, 25.21, 25.05, 14.02.
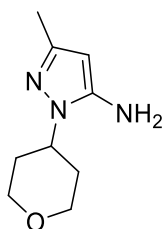
3-methyl-1-(tetrahydro-2*H*-pyran-4-yl)-1*H*-pyrazol-5-amine. Yield = 0.2 g (69%) LCMS: R_T = 0.58 min., >98% @ 215 and 254 nm, *m/z* = 182.1 [M + H]$^+$. ^{1}H NMR (500 MHz, DMSO-*d$_6$*) δ 5.06 (s, 1H), 5.03 (s, 2H), 4.11-4.9 (m, 1H), 3.93 (dd, *J* = 11.2, 4.2 Hz, 2H), 3.39 (td, *J* = 12.3, 1.8 Hz, 2H), 1.97 (s, 3H), 1.91 (ddd, *J* = 24.3, 12.6, 4.6 Hz, 2H), 1.66 (dd, *J* = 12.6, 2.2 Hz, 2H).
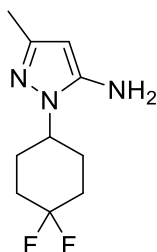
1-(4,4-difluorocyclohexyl)-3-methyl-1*H*-pyrazol-5-amine. Yield = 0.18 g (20%) LCMS: R_T = 1.45 min., >98% @ 215 and 254 nm, *m/z* = 216.1 [M + H]$^+$. ^{1}H NMR (500 MHz, DMSO-*d$_6$*) δ 5.07 (s, 1H), 5.05 (s, 2H), 4.12 – 4.06 (m, 1H), 2.14-2.10 (m, 3H), 1.97 (s, 3H), 1.99 – 1.87 (m, 4H),

1.84 – 1.77 (m, 3H). ^{13}C NMR (125 MHz, DMSO-d_6) δ 146.85, 145.71, 88.45, 51.34, 32.55 (t, J = 24.2 Hz), 28.30 (d, J = 9.7 Hz), 14.49.
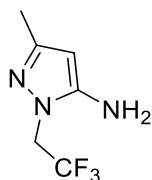
3-methyl-1-(2,2,2-trifluoroethyl)-1*H*-pyrazol-5-amine. Yield = 40 mg (12%) LCMS: R_T = 1.88 min., >98% @ 215 and 254 nm, m/z = 180.0 [M + H]$^+$. ^{1}H NMR (500 MHz, DMSO-d_6) δ 5.35 (s, 2H), 5.10 (s, 1H), 4.68 (q, J = 9.2 Hz, 2H), 1.97 (s, 3H).
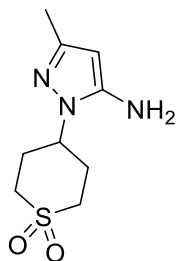
4-(5-amino-3-methyl-1*H*-pyrazol-1-yl)tetrahydro-2*H*-thiopyran 1,1-dioxide. Yield = 40 mg (35%) LCMS: R_T = 0.51 min., >98% @ 215 and 254 nm, m/z = 230.0 [M + H]$^+$. ^{1}H NMR (500 MHz, DMSO-d_6) δ 5.18 (s, 1H), 5.11 (s, 2H), 4.34 (t, J = 10.0 Hz, 1H), 3.29 – 3.20 (m, 4H), 2.39 – 2.28 (m, 2H), 2.13 – 2.03 (m, 2H), 1.99 (s, 3H).
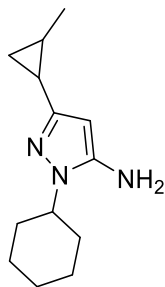
1-cyclohexyl-3-(2-methylcyclopropyl)-1*H*-pyrazol-5-amine. Yield = 0.1 g (18%) LCMS: R_T = 1.84 min., >98% @ 215 and 254 nm, m/z = 220.1 [M + H]$^+$. ^{1}H NMR (500 MHz, DMSO-d_6) δ

6.97 (s, 2H), 5.29 (s, 1H), 4.33 (tt, J = 11.9, 3.7 Hz, 1H), 2.03 – 1.92 (m, 2H), 1.85 – 1.72 (m, 5H), 1.63 (d, J = 12.6 Hz, 1H), 1.42 – 1.31 (m, 2H), 1.27 – 1.16 (m, 2H), 1.12 (d, J = 5.9 Hz, 3H), 1.02 (dq, J = 10.0, 5.0 Hz, 1H), 0.90 – 0.85 (m, 1H). ^{13}C NMR (125 MHz, DMSO-d_6) δ 153.48, 150.47, 86.29, 55.93, 30.81, 25.40, 24.71, 18.50, 18.31, 17.67, 15.38.
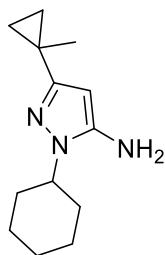
1-cyclohexyl-3-(1-methylcyclopropyl)-1H-pyrazol-5-amine. Yield = 0.2 g (22%) LCMS: R_T = 1.88 min., >98% @ 215 and 254 nm, m/z = 220.1 [M + H]$^+$. ^{1}H NMR (500 MHz, DMSO-d_6) δ 6.95 (s, 2H), 5.47 (m, 1H), 4.27 (t, J = 11.6 Hz, 1H), 1.80 (d, J = 13.1 Hz, 2H), 1.72 (d, J = 9.6 Hz, 3H), 1.61 (m, J = 12.7 Hz, 1H), 1.35 (s, 3H), 1.30 (M, J = 13.0 Hz, 2H), 1.24 – 1.14 (m, 3H), 1.06 (s, 2H), 0.81 (s, 2H).
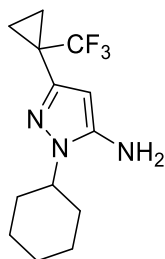
1-cyclohexyl-3-(1-(trifluoromethyl)cyclopropyl)-1H-pyrazol-5-amine. Yield = 40.0 mg (20%) LCMS: R_T = 2.59 min., >98% @ 215 and 254 nm, m/z = 274.1 [M + H]$^+$.
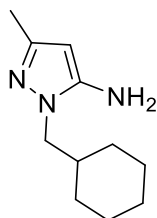
1-(cyclohexylmethyl)-3-methyl-1*H*-pyrazol-5-amine. LCMS: R_T = 1.65 min., >98% @ 215 and 254 nm, *m/z* = 194.0 [M + H]$^+$. ^{1}H NMR (500 MHz, DMSO-*d₆*) δ 5.03 (s, 1H), 4.94 (s, 2H), 3.56 (d, *J* = 7.2 Hz, 2H), 1.95 (s, 3H), 1.77 – 1.70 (m, 1H), 1.68 – 1.63 (m, 2H), 1.63 – 1.59 (m, 1H), 1.53 (d, *J* = 12.9 Hz, 2H), 1.19 – 1.09 (m, 3H), 0.98 – 0.88 (m, 2H). ^{13}C NMR (125 MHz, DMSO-*d₆*) δ 147.62, 145.37, 87.88, 52.26, 38.18, 30.49, 26.54, 25.78, 14.33.

Reagents and conditions: (a) NaCNBH$_4$, AcOH, MeOH, rt, 6 h (b) TFA, DCM, rt, 12 h
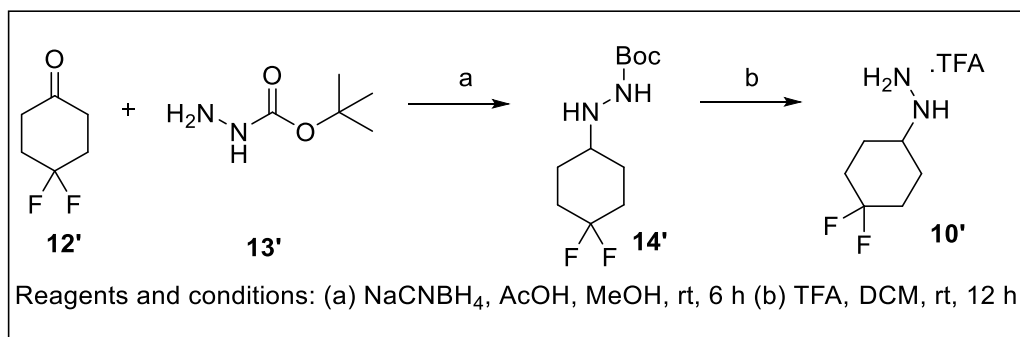
***tert*-butyl 2-(4,4-difluorocyclohexyl)hydrazine-1-carboxylate (14').** In a 50 mL RBF, *tert*-butyl hydrazinecarboxylate (980 mg, 7.5 mmol) was added to a solution of 4,4-difluorocyclohexan-1-one (1.0 g, 7.4 mmol) in MeOH (12 mL). After stirring for 30 mins at RT, acetic acid (1.27 mL, 22.3 mmol) and NaCNBH$_4$ (690 mg, 11.1 mmol) was added at 0 °C. The reaction was stirred at RT for 6h. Crude was basified with 2N NaOH$_{aq}$ and saturated NaHCO$_3$. Product was extracted with DCM (100 mL * 2). Combined organic layer was washed with brine, dried over sodium sulphate, evaporated and purified by flash chromatography (0-40% ethyl acetate:hexane). Yield =1.3 g (69%) ^{1}H NMR (500 MHz, DMSO-*d₆*) δ 8.22 (S, 1H), 4.42 (s, 1H), 2.98 – 2.88 (m, 1H), 2.09 – 1.96 (m, 2H), 1.75 (dd, *J* = 16.3, 11.2 Hz, 2H), 1.68 – 1.61 (m, 2H), 1.51 – 1.43 (m, *J* = 6.8 Hz, 2H), 1.39 (s, 9H).

(4,4-difluorocyclohexyl)hydrazine (10'). In a 10 mL RBF, *tert*-butyl 2-(4,4-difluorocyclohexyl)hydrazine-1-carboxylate (1.3 g) was treated with TFA (4 mL) in DCM (4 mL). The reaction was stirred at rt for 12 h. Crude was evaporated and used as such as a TFA salt. ^{1}H

NMR (500 MHz, DMSO-d_6) δ 3.11 – 3.01 (m, 1H), 2.12 – 2.01 (m, J = 19.8 Hz, 2H), 2.00 – 1.82 (m, 4H), 1.58 – 1.44 (m, 2H).

General Procedure A: T3P mediated amide bond synthesis

Reagents and Conditions: (a) T3P, TEA, DCM, RT
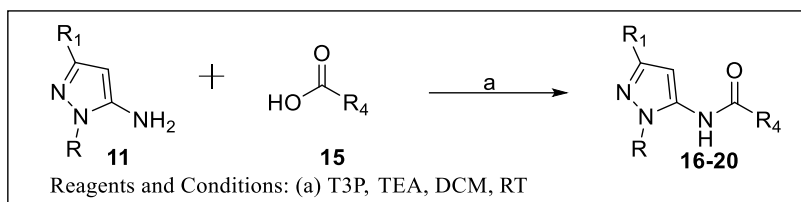
In a 1 dram vial, to a stirred solution of amine **11** (1.0 equiv.), acid (1.0 equiv.), and TEA 3.0 equiv.) in DCM was dropwise added propylphosphonic anhydride solution ≥50 wt. % in ethyl acetate (1.5 equiv.). The reaction was stirred at rt for 1-6 hours. The product was partitioned between ethyl acetate and water. Organic layers were combined, washed with brine, dried over sodium sulphate, concentrated and purified by normal phase flash chromatography (Biotage-Isolera) or reverse phase preparative chromatography (0-100% CH₃CN in water).
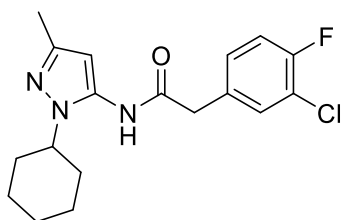
2-(3-chloro-4-fluorophenyl)-*N*-(1-cyclohexyl-3-methyl-1*H*-pyrazol-5-yl)acetamide (17b). Yield =15.3 mg (44%, white solid). ¹H NMR (400 MHz, CDCl₃) The compound exists as a 4:1 ratio of amide rotamers. Signals corresponding to the major rotamer: δ 7.38 (d, J = 6.6 Hz, 1H), 7.21−7.06 (m, 2H), 5.96 (s, 1H), 3.64 (s, 2H), 3.62−3.51 (m, 1H), 2.20 (s, 3H), 1.93−1.58 (m, 7H), 1.32−1.10 (m, 3H), Signals corresponding to the minor rotamer: δ 5.88 (s, 1H), 3.45 (s, 2H), 3.93−3.78 (m, 1H), 2.26 (s, 3H); ¹³C NMR (101 MHz, CDCl₃) only the chemical shifts of the major amide rotamer are reported δ 14.0, 25.0, 25.7, 32.5, 42.4, 57.0, 100.0, 117.2 (J_{CF} = 21 Hz), 121.7

(J_{CF} = 18 Hz), 128.0 (J_{CF} = 7 Hz), 131.2 (J_{CF} = 4 Hz), 131.3, 147.2, 157.6 (J_{CF} = 250 Hz), 168.7;

HRMS (ESI$^+$): calculated for $C_{18}H_{21}ClFN_3O$ [M + H] 349.1357, found 349.1359.
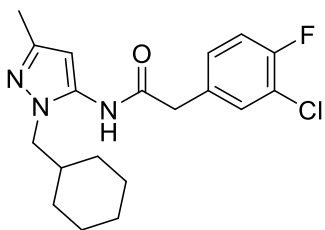
2-(3-chloro-4-fluorophenyl)-*N*-(1-(cyclohexylmethyl)-3-methyl-1*H*-pyrazol-5-yl)acetamide

(17c). Yield = 72.5 mg (76%, white solid). ^{1}H NMR (400 MHz, CDCl$_3$) The compound exists as a

5:1 ratio of amide rotamers. Signals corresponding to the major rotamer: δ 7.36 (d, *J* = 6.6 Hz, 1H),

7.212−7.09 (m, 2H), 6.04 (s, 1H), 3.63 (s, 2H), 3.50 (d, *J* = 7.4 Hz, 1H), 2.18 (s, 3H), 1.72−1.54

(m, 4H), 1.52−1.35 (m, 2H), 1.19−0.99 (m, 3H), 0.94−0.54 (m, 2H), Signals corresponding to the

minor rotamer: δ 5.89 (s, 1H), 3.44 (s, 2H), 3.58 (d, *J* = 7.4 Hz, 2H), 2.26 (s, 3H); ^{13}C NMR (101

MHz, CDCl3) only the chemical shifts of the major amide rotamer are reported δ 13.9, 25.5, 26.0,

30.6, 38.4, 42.5, 54.3, 99.0, 117.2 (J_{CF} = 21 Hz), 121.7 (J_{CF} = 18 Hz), 129.1 (J_{CF} = 7 Hz), 131.1

(J_{CF} = 4 Hz), 131.4, 134.9, 147.4, 157.6 (J_{CF} = 250 Hz), 168.0; HRMS (ESI$^+$): calculated for

$C_{19}H_{23}ClFN_3O$ [M+H] 363.1514, found 363.1518.
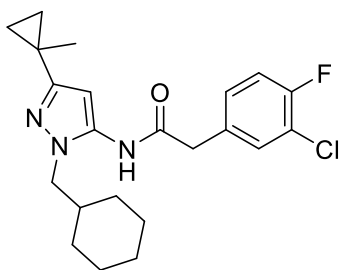
2-(3-chloro-4-fluorophenyl)-*N*-(1-(cyclohexylmethyl)-3-(1-methylcyclopropyl)-1*H*-pyrazol-5-

yl)acetamide (19b). Yield = 7.20 mg (18.9% , white solid). ^{1}H NMR (500 MHz, DMSO-*d$_6$*) δ

9.90 (s, 1H), 7.56 (d, *J* = 7.1 Hz, 1H), 7.40 (t, *J* = 8.9 Hz, 1H), 7.35 − 7.32 (m, 1H), 5.88 (s, 1H)

3.85 − 3.77 (m, 1H), 3.68 (s, 2H), 1.80 − 1.57 (m, 8H), 1.32 (s, 3H), 1.18 (m, *J* = 9.8 Hz, 2H), 0.80

(m, 2H), 0.63 (m, 2H). ^{13}C NMR (125 MHz, DMSO-d_6) δ 169.42, 154.98, 135.12, 134.10, 131.51, 130.36, 130.30, 117.25, 117.09, 96.19, 55.61, 32.70, 25.54, 25.31, 22.71, 16.37, 14.89.
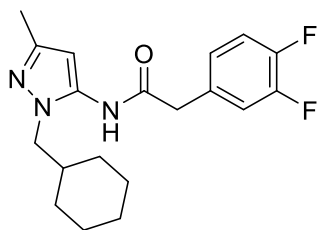
N-(1-(cyclohexylmethyl)-3-methyl-1H-pyrazol-5-yl)-2-(3,4-difluorophenyl)acetamide (20a).

Yield = 3.2 mg; (9%, white solid) LCMS: single peak (254 nm), R_T = 4.342; MS (ESI$^+$) m/z = 348.1. [M + H]$^+$. ^{1}H NMR (500 MHz, DMSO-d_6) δ 9.93 (s, 1H), 7.46 – 7.35 (m, 2H), 7.21 – 7.14 (m, 1H), 5.96 (s, 1H), 3.65 (d, J = 11.8 Hz, 4H), 2.08 (s, 3H), 1.68 – 1.52 (m, 5H), 1.40 – 1.32 (m, 2H), 1.07 (h, J = 9.8, 9.4 Hz, 3H), 0.76 (t, J = 12.6 Hz, 2H).^{13}C NMR (125 MHz, DMSO-d_6) δ 168.81, 145.94, 136.63, 133.83, 126.50, 126.45, 126.42, 118.57, 118.44, 117.81, 117.67, 99.04, 53.65, 41.73, 38.26, 30.29, 26.33, 25.59, 14.21.
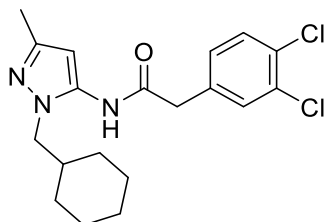
N-(1-(cyclohexylmethyl)-3-methyl-1H-pyrazol-5-yl)-2-(3,4-dichlorophenyl)acetamide (20b).

Yield = 16.0 mg (33%, white solid) LCMS: R_T = 4.45 min., >98% @ 215 and 254 nm, m/z = 380.1 [M + H]$^+$. ^{1}H NMR (500 MHz, DMSO-d_6) δ 9.95 (s, 1H), 7.61 (d, J = 8.1 Hz, 1H), 7.33 (d, J = 8.2 Hz, 1H), 5.95 (s, 1H), 3.67 (s, 2H), 3.62 (d, J = 7.2 Hz, 2H), 2.08 (s, 3H), 1.56 (d, J = 6.7 Hz, 4H), 1.34 (d, J = 12.4 Hz, 2H), 1.06 (s, 3H), 0.71 (d, J = 11.1 Hz, 2H). ^{13}C NMR (125 MHz, DMSO--d_6) δ 168.63, 145.98, 137.24, 136.57, 131.55, 131.32, 130.95, 130.08, 129.97, 99.11, 53.67, 41.73, 38.28, 30.29, 26.31, 25.60, 14.22.

N-(1-(cyclohexylmethyl)-3-methyl-1*H*-pyrazol-5-yl)-2-(4-fluoro-3-methylphenyl)acetamide

(20c). Yield = 14.0 mg (31.8 %, off-white solid) LCMS: R_T = 4.2 min., >98% @ 215 and 254

nm, *m/z* = 344.1 [M + H]⁺. ¹H NMR (500 MHz, DMSO-*d₆*) δ 9.88 (s, 1H), 7.32 – 7.26 (m, 1H),

7.04 (d, *J* = 9.9 Hz, 1H), 6.98 (dd, *J* = 11.7, 5.2 Hz, 1H), 5.95 (s, 1H), 3.69 (d, *J* = 9.8 Hz, 4H),

2.30 (s, 3H), 2.08 (s, 3H), 1.70 – 1.64 (m, 1H), 1.60 (s, 2H), 1.41 (d, *J* = 12.5 Hz, 3H), 1.10 (t, *J* =

8.9 Hz, 2H), 0.83 (dd, *J* = 22.5, 9.4 Hz, 3H). ¹³C NMR (125 MHz, DMSO-*d₆*) δ 169.17, 162.46,

160.53, 145.92, 139.91, 139.84, 136.85, 132.27, 132.20, 131.01, 116.94, 116.77, 112.76, 112.60,

98.89, 53.67, 38.31, 30.36, 26.37, 25.64, 19.75, 14.23.
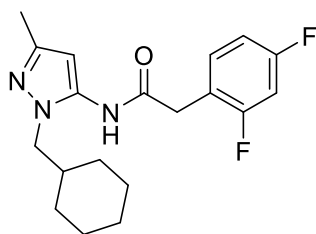
N-(1-(cyclohexylmethyl)-3-methyl-1*H*-pyrazol-5-yl)-2-(2,4-difluorophenyl)acetamide   (20d).

Yield = 15.0 mg (34%, white solid) LCMS: R_T = 4.4 min., >98% @ 215 and 254 nm, *m/z* = 348.1

[M + H]⁺. ¹H NMR (500 MHz, DMSO-*d₆*) δ 9.96 (s, 1H), 7.44 (dd, *J* = 15.5, 8.4 Hz, 1H), 7.27 –

7.20 (m, 1H), 7.07 (t, *J* = 7.7 Hz, 1H), 5.95 (s, 1H), 3.72 (d, *J* = 8.9 Hz, 4H), 2.08 (s, 3H), 1.75 –

1.68 (m, 1H), 1.62 (s, 3H), 1.44 (d, *J* = 12.4 Hz, 2H), 1.12 (t, *J* = 9.1 Hz, 3H), 0.87 (t, *J* = 10.4 Hz,

2H). ¹³C NMR (125 MHz, DMSO-*d₆*) δ 168.24, 162.89, 161.99, 160.94, 160.02, 145.94, 136.78,

133.48, 133.43, 119.60, 119.49, 111.77, 111.60, 104.28, 104.08, 103.87, 98.83, 53.63, 38.31, 35.38,

30.35, 26.39, 25.65, 14.24.
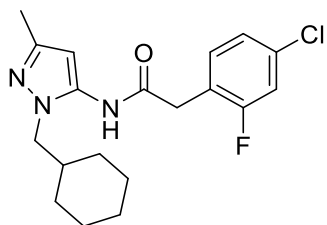
2-(4-chloro-2-fluorophenyl)-*N*-(1-(cyclohexylmethyl)-3-methyl-1*H*-pyrazol-5-yl)acetamide

(20f). Yield = 252.0 mg (67%, white solid) LCMS: single peak (254 nm), R_T = 4.584; MS (ESI$^+$) m/z 364.1. [M+H]$^+$. ^{1}H NMR (500 MHz, DMSO-d_6) δ 9.97 (s, 1H), 7.47 – 7.39 (m, 2H), 7.28 (dd, *J* = 8.3, 2.1 Hz, 1H), 5.95 (s, 1H), 3.74 (s, 2H), 3.71 (d, *J* = 7.2 Hz, 2H), 2.08 (s, 3H), 1.70 (ddp, *J* = 11.2, 7.2, 3.4 Hz, 1H), 1.66 – 1.55 (m, 3H), 1.47 – 1.39 (m, 2H), 1.12 (h, *J* = 10.1, 9.3 Hz, 3H), 0.85 (qd, *J* = 11.7, 3.4 Hz, 2H).^{13}C NMR (125 MHz, DMSO-d_6) δ 168.00, 161.98, 160.00, 145.94, 136.72, 133.70, 133.66, 132.81, 132.73, 124.96, 124.93, 122.52, 122.39, 116.29, 116.08, 53.63, 38.31, 35.52, 30.35, 26.39, 25.65, 14.24.
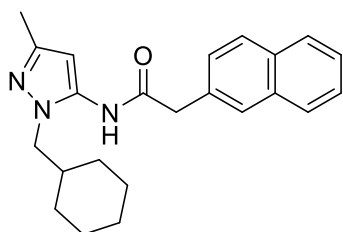
***N*-(1-(cyclohexylmethyl)-3-methyl-1*H*-pyrazol-5-yl)-2-(naphthalen-2-yl)acetamide (20i)..** Yield = 30.0 mg (75%, off- white solid) LCMS: single peak (254 nm), R_T = 4.618; MS (ESI$^+$) m/z 362.3. [M + H]$^+$. ^{1}H NMR (500 MHz, DMSO-d_6) δ 9.97 (s, 1H), 7.95 – 7.82 (m, 4H), 7.50 (pd, *J* = 7.0, 1.5 Hz, 3H), 5.96 (s, 1H), 3.81 (s, 2H), 3.61 (d, *J* = 7.2 Hz, 2H), 2.07 (s, 3H), 1.56 (ddp, *J* = 11.0, 7.5, 3.7 Hz, 1H), 1.50 – 1.40 (m, 3H), 1.33 – 1.22 (m, 2H), 1.02 – 0.80 (m, 3H), 0.69 – 0.56 (m, 2H).^{13}C NMR (125 MHz, DMSO-d_6) δ 169.38, 145.90, 136.77, 133.82, 133.48, 132.39, 128.29, 127.98, 127.93, 127.87, 126.64, 126.14, 99.07, 53.64, 43.10, 38.23, 30.19, 26.17, 25.51, 14.23..
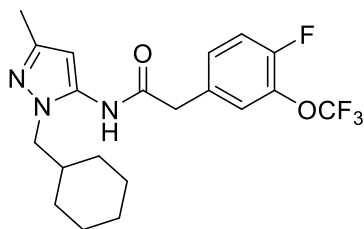
N-(1-(cyclohexylmethyl)-3-methyl-1H-pyrazol-5-yl)-2-(4-fluoro

(trifluoromethoxy)phenyl)acetamide (20j). Yield = 32.0 mg (76.1%, yellow solid). LCMS:

single peak (254 nm), R_T = 4.755; MS (ESI⁺) m/z 414.1. [M + H]⁺. ¹H NMR (500 MHz, DMSO-

d_6) δ 9.96 (s, 1H), 7.54 – 7.46 (m, 2H), 7.41 (ddd, J = 8.6, 4.7, 2.1 Hz, 1H), 5.96 (s, 1H), 3.71 (s,

2H), 3.65 (d, J = 7.2 Hz, 2H), 2.08 (s, 3H), 1.73 – 1.50 (m, 4H), 1.37 (d, J = 12.3 Hz, 2H), 1.07 (h,

J = 11.6, 11.0 Hz, 3H), 0.81 – 0.66 (m, 2H). ¹³C NMR (125 MHz, DMSO-d_6) δ 168.77, 152.03,

145.98, 136.63, 133.99, 130.64, 124.88, 117.88, 117.73, 98.99, 53.62, 41.52, 38.29, 30.28, 26.29,

25.58, 14.22.
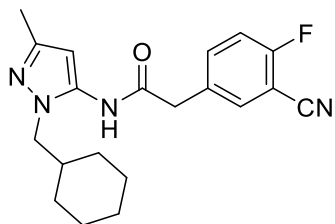
2-(3-cyano-4-fluorophenyl)-N-(1-(cyclohexylmethyl)-3-methyl-1H-pyrazol-5-yl)acetamide

(20k). Yield = 25.0 mg (69%, white solid) l LCMS: single peak (254 nm), R_T = 4.135; MS (ESI⁺)

m/z 355.1. [M+H]⁺. ¹H NMR (500 MHz, DMSO-d_6) δ 9.97 (s, 1H), 7.86 (dd, J = 6.3, 2.2 Hz, 1H),

7.74 (ddd, J = 8.0, 5.3, 2.3 Hz, 1H), 7.53 (t, J = 9.1 Hz, 1H), 5.96 (s, 1H), 3.74 (s, 2H), 3.66 (d, J =

7.2 Hz, 2H), 2.08 (s, 3H), 1.68 – 1.52 (m, 4H), 1.38 (d, J = 12.8 Hz, 2H), 1.07 (q, J = 9.7, 9.0 Hz,

3H), 0.84 – 0.69 (m, 2H). ¹³C NMR (125 MHz, DMSO-d_6) δ 168.54, 145.98, 137.58, 137.50,

136.60, 134.65, 133.87, 133.85, 117.06, 116.91, 114.41, 100.34, 100.22, 98.95, 53.62, 41.12, 38.30,

30.32, 26.33, 25.61, 14.22.
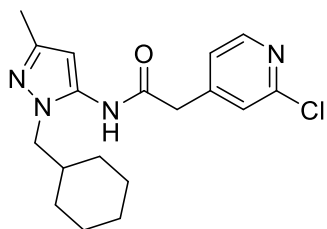
2-(2-chloropyridin-4-yl)-*N*-(1-(cyclohexylmethyl)-3-methyl-1*H*-pyrazol-5-yl)acetamide

(20m). Yield = 47.0 mg (75%, off-white solid) LCMS: single peak (254 nm), R_T = 3.858; MS (ESI$^+$) m/z 347.1. [M+H]$^+$. ^{1}H NMR (500 MHz, DMSO-d_6) δ 10.04 (s, 1H), 8.38 (d, *J* = 5.0 Hz, 1H), 7.49 (s, 1H), 7.40 – 7.34 (m, 1H), 5.98 (s, 1H), 3.76 (s, 2H), 3.67 (d, *J* = 7.3 Hz, 2H), 2.08 (s, 3H), 1.71 – 1.52 (m, 4H), 1.39 (d, *J* = 12.8 Hz, 2H), 1.09 (t, *J* = 9.0 Hz, 3H), 0.79 (tt, *J* = 11.9, 6.0 Hz, 2H). ^{13}C NMR (125 MHz, DMSO-d_6) δ 167.61, 150.74, 150.23, 148.91, 146.01, 136.50, 125.23, 124.54, 98.98, 53.65, 41.54, 38.31, 30.32, 26.33, 25.62, 14.22.
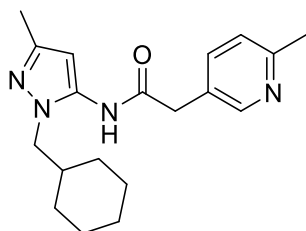
***N*-(1-cyclohexyl-3-methyl-1*H*-pyrazol-5-yl)-2-(6-methylpyridin-3-yl)acetamide (20n).** Yield = 15.0 mg (62%, off-white solid) LCMS: single peak (254 nm), R_T = 2.756; MS (ESI$^+$); m/z 327.1. [M+H]$^+$. ^{1}H NMR (500 MHz, DMSO-d_6) δ 9.95 (s, 1H), 8.39 (d, *J* = 2.3 Hz, 1H), 7.61 (dd, *J* = 8.0, 2.3 Hz, 1H), 7.22 (d, *J* = 7.9 Hz, 1H), 5.95 (s, 1H), 3.64 (d, *J* = 7.8 Hz, 4H), 2.44 (s, 3H), 2.08 (s, 3H), 1.69 – 1.53 (m, 4H), 1.36 (d, *J* = 12.8 Hz, 2H), 1.06 (q, *J* = 9.5, 8.7 Hz, 3H), 0.77 (t, *J* = 12.1 Hz, 2H). ^{13}C NMR (125 MHz, DMSO-d_6) δ 169.09, 156.61, 149.70, 145.91, 137.27, 136.68, 128.71, 123.12, 99.02, 53.64, 38.26, 30.28, 26.33, 25.60, 24.09, 14.23.
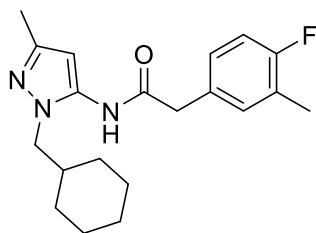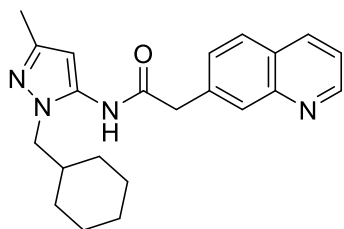
N-(1-(cyclohexylmethyl)-3-methyl-1H-pyrazol-5-yl)-2-(quinolin-7-yl)acetamide (20o). Yield =

13.0mg (27%, white solid) LCMS: single peak (254 nm), R_T = 4.48; MS (ESI$^+$) m/z 363.1. [M+H]$^+$.

^{1}H NMR (500 MHz, DMSO-d_6) δ 10.01 (s, 1H), 8.90 – 8.85 (m, 1H), 8.34 (d, J = 8.2 Hz, 1H), 8.00

(d, J = 8.6 Hz, 1H), 7.92 (s, 1H), 7.76 (dd, J = 8.6, 1.2 Hz, 1H), 7.53 (dd, J = 8.2, 4.2 Hz, 1H), 5.97

(s, 1H), 3.86 (s, 2H), 3.61 (d, J = 7.2 Hz, 2H), 2.08 (s, 3H), 1.60 – 1.51 (m, 1H), 1.44 (d, J = 9.8

Hz, 3H), 1.27 (d, J = 12.0 Hz, 2H), 0.94 (dd, J = 25.0, 12.5 Hz, 2H), 0.85 (dd, J = 16.0, 8.1 Hz,

1H), 0.62 (q, J = 11.2 Hz, 2H). ^{13}C NMR (125 MHz, DMSO-d_6) δ 206.95, 169.18, 150.71, 147.32,

145.94, 136.72, 136.13, 134.54, 131.53, 129.38, 128.27, 128.12, 122.08, 99.10, 53.65, 42.82, 38.21,

31.15, 30.19, 26.16, 25.49, 14.22.
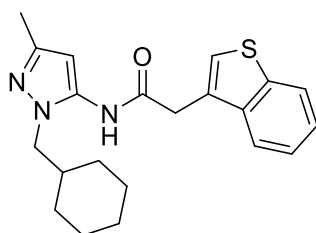
2-(benzo[b]thiophen-2-yl)-N-(1-(cyclohexylmethyl)-3-methyl-1H-pyrazol-5-yl)acetamide

(20u). Yield = 26.0 mg (68%, yellow solid) LCMS: single peak (254 nm), R_T = 4.596; MS (ESI$^+$)

m/z 368.1. [M+H]$^+$. ^{1}H NMR (500 MHz, DMSO-d_6) δ 9.99 (s, 1H), 8.03 – 7.97 (m, 1H), 7.91 (dd,

J = 7.2, 1.8 Hz, 1H), 7.62 (s, 1H), 7.41 (pd, J = 7.1, 1.4 Hz, 2H), 5.96 (s, 1H), 3.94 (s, 2H), 3.63 (d,

J = 7.3 Hz, 2H), 2.08 (s, 3H), 1.67 – 1.46 (m, 4H), 1.36 – 1.26 (m, 2H), 1.02 (t, J = 8.7 Hz, 3H),

0.74 – 0.59 (m, 2H). ^{13}C NMR (125 MHz, DMSO-d_6) δ 168.48, 145.93, 140.01, 139.06, 136.78,

130.33, 125.46, 124.80, 124.51, 123.38, 122.50, 98.92, 53.66, 38.25, 36.16, 30.22, 26.29, 25.59,

14.23.

General Procedure for synthesis of 5-substituted tetrazoles:

Reagents and Conditions: (a) NaN$_3$, TEA.HCl, Toluene, 120°C
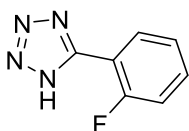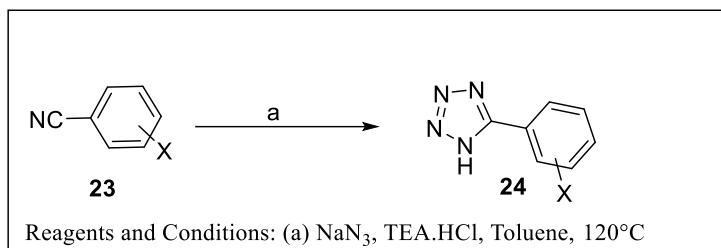
5-(2-fluorophenyl)-1*H***-tetrazole**. In a 10 mL seal tube, 2-fluorobenzonitrile (143 µL, 1.38 mmol), sodium azide (0.10 g, 1.5 mmol), TEA.HCl (0.21 g, 1.54 mmol) were heated at 120 °C for 6 h. Once benzonitrile is completely consumed, reaction is cooled down and ice-cold 1N HCl$_{aq}$ (10 mL) was added to the crude, precipitates formed are filtered, washed with cold water and dried under vacuum to obtain desired product. Yield = 0.16 g (78%) LCMS: R$_T$ = 1.81 min., >98% @ 215 and 254 nm, *m/z* = 165.0 [M + H]$^+$. ^{1}H NMR (500 MHz, DMSO-*d$_6$*) δ 8.07 (td, *J* = 7.6, 1.8 Hz, 1H), 7.71 – 7.65 (m, *J* = 8.4, 7.3, 5.4, 1.8 Hz, 1H), 7.54 – 7.48 (m, *J* = 10.8, 8.4, 0.9 Hz, 1H), 7.45 (td, *J* = 7.6, 1.1 Hz, 1H). ^{13}C NMR (125 MHz, DMSO-d$_6$) δ 160.47, 158.46, 134.01, 133.95, 130.51, 125.89, 125.86, 117.20, 117.04.
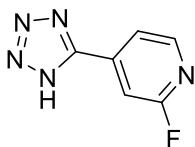
2-fluoro-4-(1*H***-tetrazol-5-yl)pyridine.** Yield = 0.19 g (83%) LCMS: R$_T$ = 1.60 min., >98% @ 215 and 254 nm, *m/z* = 166.0 [M + H]$^+$. ^{1}H NMR (500 MHz, DMSO-*d$_6$*) δ 8.51 (d, *J* = 5.2 Hz, 1H), 7.99 – 7.96 (m, 1H), 7.75 (s, 1H). ^{13}C NMR (125 MHz, DMSO-*d$_6$*) δ 164.97, 163.09, 149.89, 149.77, 119.88, 119.85, 107.62, 107.30.
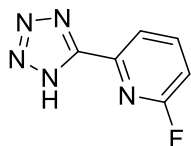
2-fluoro-6-(1*H*-tetrazol-5-yl)pyridine. Yield = 0.18 g (78%) LCMS: R_T = 1.62 min., >98% @ 215 and 254 nm, m/z = 166.0 [M + H]$^+$. ^{1}H NMR (500 MHz, DMSO-d_6) δ 8.28 (dd, J = 15.8, 8.1 Hz, 1H), 8.18 (dd, J = 7.4, 1.9 Hz, 1H), 7.46 (dd, J = 8.2, 1.8 Hz, 1H). ^{13}C NMR (125 MHz, DMSO-d_6) δ 164.20, 162.29, 144.82, 144.76, 121.11, 121.08, 112.93, 112.64.
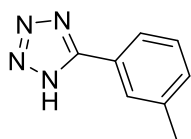
5-(*m*-tolyl)-1*H*-tetrazole. Yield = 0.21 g (83%) LCMS: R_T = 2.04 min., >98% @ 215 and 254 nm, m/z = 161.0 [M + H]$^+$. ^{1}H NMR (500 MHz, DMSO-d_6) δ 7.89 (s, 1H), 7.84 (d, J = 7.7 Hz, 1H), 7.49 (t, J = 7.7 Hz, 1H), 7.41 (d, J = 7.6 Hz, 1H), 2.41 (s, 3H). ^{13}C NMR (125 MHz, DMSO-d_6) δ 139.28, 132.34, 129.78, 127.87, 124.59.
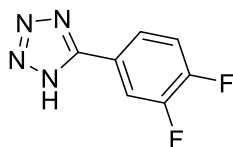
5-(3,4-difluorophenyl)-1*H*-tetrazole. Yield = 0.22 g (80%) %) LCMS: R_T = 2.0 min., >98% @ 215 and 254 nm, m/z = 183.0 [M + H]$^+$. ^{1}H NMR (500 MHz, DMSO-d_6) δ 8.09 (ddd, J = 11.2, 7.6, 2.1 Hz, 1H), 7.97 – 7.90 (m, 1H), 7.72 (dt, J = 10.5, 8.5 Hz, 1H).
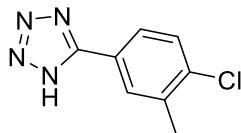
5-(4-chloro-3-methylphenyl)-1*H*-tetrazole. Yield = 0.25 g (86%) LCMS: R_T = 2.23 min., >98% @ 215 and 254 nm, m/z = 195.0 [M + H]$^+$. ^{1}H NMR (500 MHz, DMSO-d_6) δ 8.05 (d, J = 1.6 Hz,

1H), 7.88 (dd, *J* = 8.3, 2.0 Hz, 1H), 7.67 (d, *J* = 8.3 Hz, 1H), 2.43 (s, 3H). ^{13}C NMR (125 MHz,

DMSO-*d$_6$*) δ 137.30, 136.58, 130.43, 129.96, 126.52, 20.10.

General Procedure B for synthesis of tetrazole series (Class-II)

Reagents and Conditions: (a) Br-ethyl acetate, NaOEt, Ethanol (b) NaOH, Water THF
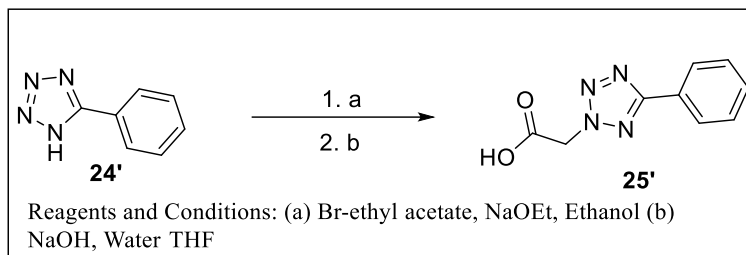
Step-1: ethyl 2-(5-phenyl-2*H*-tetrazol-2-yl)acetate. In a 10 mL RBF, bromo ethyl acetate (0.37

mL, 3.4 mmol) was added dropwise to a solution of 5-phenyl-2*H*-tetrazole (0.50 g, 3.4 mmol) and

NaOEt (0.24 g, 3.5 mmol) in Ethanol (7 mL) at RT. The reaction was refluxed for 12 h. The crude

was filtered while still hot, then filtrate was concentrated. Product was recrystallized in cold

ethanol. Recrystallized product used as such. Yield = 0.50 g (62%) LCMS: R$_T$ = 2.57 min., >98%

@ 215 and 254 nm, *m/z* = 233.0 [M + H]$^+$.

Step-2: 2-(5-phenyl-2*H*-tetrazol-2-yl)acetic acid (25'). In a 10 mL RBF, NaOH (0.12 g, 3.2

mmol) dissolved in water (3 mL) was added to a solution of ethyl 2-(5-phenyl-2*H*-tetrazol-2-

yl)acetate (0.50 g, 2.1 mmol) in THF (7 mL). Reaction was stirred at RT for 12 h. Water (50 mL)

and ethyl acetate (100 mL) were added to the crude and stirred vigorously. Water layer was

partitioned and acidified up to pH-3 with concentrated HCl, product was extracted from the water

layer by washing with ethyl acetate (50 mL*2). Combined organic layer from 2nd extraction (after

acidification) were collected, washed with brine, dried over sodium sulphate and evaporated to

obtain desired product. Yield = 0.38 g (88%) LCMS: R$_T$ = 1.98 min., >98% @ 215 and 254

nm, *m/z* = 205.0 [M + H]$^+$. 1H NMR (500 MHz, DMSO-*d$_6$*) δ 8.09 (dd, J = 7.7, 1.7 Hz, 2H), 7.61

– 7.56 (m, 3H), 5.76 (s, 2H). ^{13}C NMR (125 MHz, CD$_3$CN) δ 166.33, 165.10, 130.61, 129.17, 127.17, 126.58, 53.21.
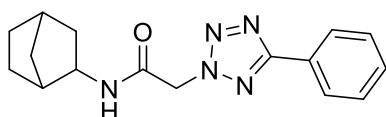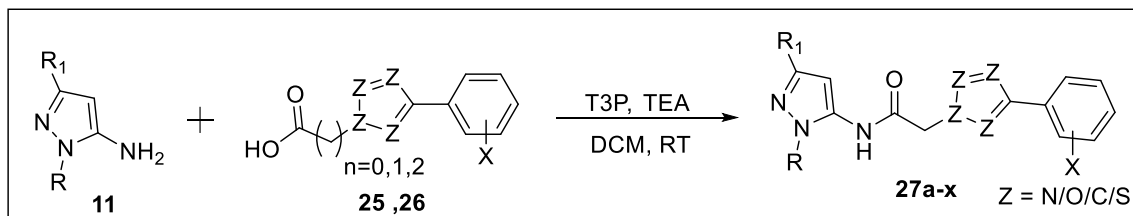
N-(bicyclo[2.2.1]heptan-2-yl)-2-(5-phenyl-2H-tetrazol-2-yl)acetamide (21). In a 1 dram vial, to a stirred solution of bicyclo[2.2.1]heptan-2-amine (15 mg, 0.13 mmol), 2-(5-phenyl-2H-tetrazol-2-yl)acetic acid (27 mg, 0.13 mmol) and TEA (54 µL, 0.40 mmol) in DCM (1 mL) was dropwise added propylphosphonic anhydride solution ≥50 wt. % in ethyl acetate (107 µL, 0.160 mmol). The reaction was stirred at RT for 1 hour. The product was partitioned between ethyl acetate (15 mL * 2) and water (15 mL). Organic layers were combined, washed with brine, dried over sodium sulphate, concentrated and purified by reverse phase preparative chromatography (0-100% CH$_3$CN in water). Yield = 28.0 mg (70%, yellow solid) LCMS: R$_T$ = 2.78 min., >98% @ 215 and 254 nm, m/z = 298.0 [M + H]$^+$. ^{1}H NMR (500 MHz, CDCl$_3$) δ 8.21 – 8.14 (m, 1H), 7.58 – 7.46 (m, 2H), 5.34 (s, 1H), 3.76 (d, J = 4.5 Hz, 1H), 2.32 – 2.19 (m, 1H), 1.80 (dd, J = 12.9, 8.3 Hz, 1H), 1.58 – 1.41 (m, 2H), 1.28 – 1.09 (m, 3H). ^{13}C NMR (125 MHz, CDCl$_3$) δ 165.84, 162.51, 130.78, 129.03, 126.96, 126.74, 55.45, 53.41, 53.28, 42.17, 40.17, 40.12, 35.63, 35.54, 27.99, 26.31.
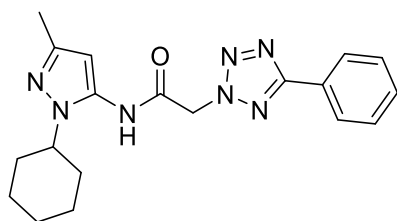
N-(1-cyclohexyl-3-methyl-1*H*-pyrazol-5-yl)-2-(5-phenyl-2*H*-tetrazol-2-yl)acetamide   **(27a).**

Yield = 38 mg (76%, white solid) LCMS: R_T = 2.57 min., >98% @ 215 and 254 nm, *m/z* = 366.1

[M + H]$^+$. ^{1}H NMR (500 MHz, DMSO-*d₆*) δ 10.53 (s, 1H), 8.14 – 8.05 (m, 2H), 7.65 – 7.53 (m,

3H), 6.00 (s, 1H), 5.88 (s, 1H), 5.85 (s, 2H), 4.09 (ddd, *J* = 10.9, 9.4, 3.9 Hz, 1H), 2.11 (s, 3H),

1.86 – 1.73 (m, 6H), 1.66 (d, *J* = 12.3 Hz, 1H), 1.40 – 1.31 (m, 2H), 1.21 – 1.15 (m, 1H). ^{13}C NMR

(125 MHz, CDCl₃) δ 166.33, 161.49, 147.38, 131.14, 129.12, 127.01, 126.29, 99.65, 57.39, 55.45,

32.55, 25.53, 24.95, 13.92.
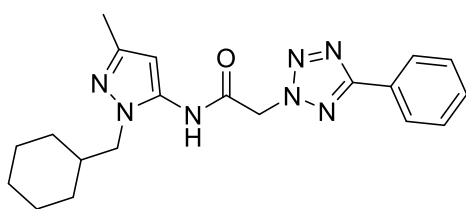
N-(1-(cyclohexylmethyl)-3-methyl-1*H*-pyrazol-5-yl)-2-(5-phenyl-2*H*-tetrazol-2-yl)acetamide

(27b). Yield = 17 mg (32%, White solid) LCMS: R_T = 2.71 min., >98% @ 215 and 254 nm, *m/z* =

380.1 [M + H]$^+$. ^{1}H NMR (500 MHz, CDCl₃) δ 8.20 (d, *J* = 3.7 Hz, 2H), 8.05 (s, 1H), 7.60 – 7.52

(m, 3H), 6.21 (s, 1H), 5.59 (s, 2H), 3.63 (d, *J* = 7.2 Hz, 2H), 2.23 (d, *J* = 8.9 Hz, 3H), 1.74 – 1.64

(m, 1H), 1.55 (d, *J* = 10.6 Hz, 3H), 1.45 (d, *J* = 12.1 Hz, 2H), 1.08 (dd, *J* = 25.5, 12.6 Hz, 2H),

0.96 – 0.87 (m, 1H), 0.70 (q, *J* = 11.5 Hz, 2H). ^{13}C NMR (125 MHz, CDCl₃) δ 166.48, 160.79,

147.67, 133.88, 131.23, 129.18, 127.03, 126.20, 98.87, 55.50, 54.44, 38.59, 30.53, 25.91, 25.45,

13.92.

N-(3-methyl-1-phenyl-1*H*-pyrazol-5-yl)-2-(5-phenyl-2*H*-tetrazol-2-yl)acetamide (27c). Yield = 23 mg (46%, white solid) LCMS: R_T = 2.51 min., >98% @ 215 and 254 nm, *m/z* = 360.1 [M + H]$^+$.^{1}H NMR (500 MHz, CDCl$_3$) δ 8.29 (s, 1H), 7.98 (d, *J* = 7.1 Hz, 2H), 7.60 – 7.48 (m, 3H), 7.25 (d, *J* = 6.4 Hz, 4H), 7.19 – 7.12 (m, 1H), 6.60 (s, 1H), 5.51 (s, 2H), 2.32 (s, 3H). ^{13}C NMR (125 MHz, CDCl$_3$) δ 166.34, 159.75, 149.72, 137.03, 134.56, 131.09, 129.77, 129.02, 128.46, 127.07, 126.18, 124.45, 98.39, 55.34, 13.91.

N-(1-benzyl-3-methyl-1*H*-pyrazol-5-yl)-2-(5-phenyl-2*H*-tetrazol-2-yl)acetamide (27d). Yield = 30 mg (58%, white solid) LCMS: R_T = 2.54 min., >98% @ 215 and 254 nm, *m/z* = 375.1 [M + H]$^+$.^{1}H NMR (500 MHz, CDCl$_3$) δ 8.11 – 8.06 (m, *J* = 6.4, 2.8 Hz, 2H), 7.52 – 7.46 (m, *J* = 3.4 Hz, 3H), 7.20 (dq, *J* = 14.1, 7.1 Hz, 3H), 7.01 (d, *J* = 7.2 Hz, 2H), 6.20 (s, 1H), 5.42 (s, 2H), 5.18 (s, 2H), 2.22 (s, 3H). ^{13}C NMR (125 MHz, CDCl$_3$) δ 165.79, 162.06, 148.12, 136.07, 134.99, 130.78, 128.98, 128.80, 127.83, 126.92, 126.61, 126.55, 100.30, 54.84, 52.08, 13.69.
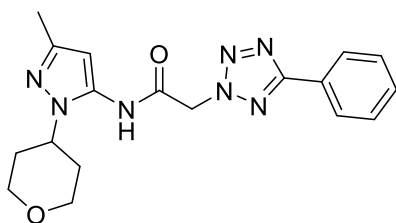
N-(3-methyl-1-(tetrahydro-2*H*-pyran-4-yl)-1*H*-pyrazol-5-yl)-2-(5-phenyl-2H-tetrazol-2-yl)acetamide (27e). Yield = 20 mg (33%, white solid) LCMS: R_T = 2.23 min., >98% @ 215 and 254 nm, *m/z* = 368.1 [M + H]$^+$. ^{1}H NMR (500 MHz, DMSO-*d$_6$*) δ 10.50 (s, 1H), 8.12 – 8.07 (m, 2H), 7.62 – 7.54 (m, 3H), 6.03 (s, 1H), 5.84 (s, 2H), 4.39 – 4.29 (m, 1H), 3.97 (dd, *J* = 11.3, 3.8

Hz, 2H), 3.42 (t, *J* = 11.5 Hz, 2H), 2.12 (s, 3H), 2.00 (qd, *J* = 12.4, 4.5 Hz, 2H), 1.74 (d, *J* = 10.3

Hz, 2H). ^{13}C NMR (125 MHz, DMSO-*d$_6$*) δ 164.73, 163.88, 146.45, 134.78, 131.19, 129.83,

127.21, 126.83, 99.26, 66.76, 55.40, 52.88, 32.97, 14.41.
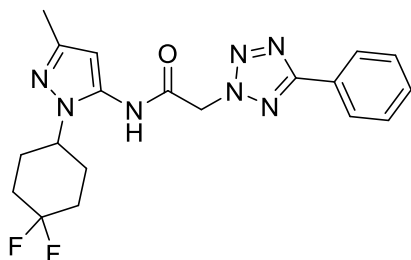
***N*-(1-(4,4-difluorocyclohexyl)-3-methyl-1*H*-pyrazol-5-yl)-2-(5-phenyl-2*H*-tetrazol-2-**

yl)acetamide (27f). Yield = 30 mg (40%, Off-white solid) LCMS: R$_T$ = 2.55 min., >98% @ 215

and 254 nm, *m/z* = 402.1 [M + H]$^+$. ^{1}H NMR (500 MHz, DMSO-*d$_6$*) δ 10.50 (s, 1H), 8.09 (dd, *J* =

7.6, 1.6 Hz, 2H), 7.67 – 7.51 (m, 3H), 6.03 (s, 1H), 5.84 (s, 2H), 4.31 (m, 1H), 2.18 (m, 3H), 2.12

(s, 3H), 1.97 (m, 7H). ^{13}C NMR (125 MHz, DMSO-*d$_6$*) δ 164.74, 164.05, 146.60, 134.89, 131.18,

129.82, 127.20, 126.83, 99.56, 55.37, 52.83, 32.47, 32.27, 28.73, 28.66, 14.39.
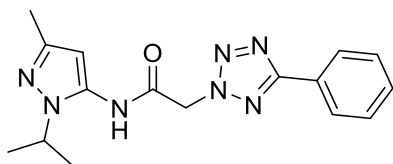
***N*-(1-isopropyl-3-methyl-1*H*-pyrazol-5-yl)-2-(5-phenyl-2*H*-tetrazol-2-yl)acetamide   (27g).**

Yield = 32 mg (34%, Off-white solid) LCMS: R$_T$ = 2.31 min., >98% @ 215 and 254 nm, *m/z* =

326.1 [M + H]$^+$. ^{1}H NMR (500 MHz, DMSO-*d$_6$*) δ 10.46 (s, 1H), 8.09 (dd, *J* = 7.7, 1.5 Hz, 2H),

7.63 – 7.55 (m, 3H), 6.00 (s, 1H), 5.83 (s, 2H), 4.49 (dt, *J* = 13.1, 6.5 Hz, 1H), 2.12 (s, 3H), 1.34

(d, *J* = 6.5 Hz, 6H). ^{13}C NMR (125 MHz, DMSO-*d$_6$*) δ 164.69, 163.85, 146.21, 134.42, 131.15,

129.80, 127.21, 126.82, 99.13, 55.32, 48.30, 22.84, 14.43.
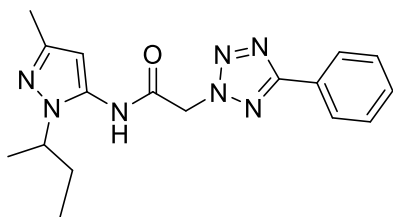
N-(1-(sec-butyl)-3-methyl-1H-pyrazol-5-yl)-2-(5-phenyl-2H-tetrazol-2-yl)acetamide   (27h).
Yield = 16 mg (32%, White solid) LCMS: R_T = 2.40 min., >98% @ 215 and 254 nm, m/z = 340.1
[M + H]$^+$. ^{1}H NMR (500 MHz, DMSO-d_6) δ 10.44 (s, 1H), 8.14 – 8.02 (m, 2H), 7.62 – 7.55 (m,
3H), 5.99 (s, 1H), 5.82 (d, J = 4.0 Hz, 2H), 4.25 – 4.17 (m, 1H), 2.12 (s, 3H), 1.84 – 1.73 (m, 1H),
1.71 – 1.62 (m, 1H), 1.32 (d, J = 6.5 Hz, 3H), 0.68 (t, J = 7.3 Hz, 3H). ^{13}C NMR (125 MHz, DMSO-
d_6) δ 164.71, 163.79, 146.41, 135.37, 131.17, 129.82, 127.22, 126.82, 98.84, 55.34, 54.00, 29.62,
21.00, 14.46, 11.06.
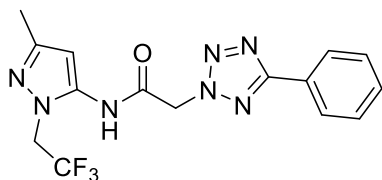
N-(3-methyl-1-(2,2,2-trifluoroethyl)-1H-pyrazol-5-yl)-2-(5-phenyl-2H-tetrazol-2-
yl)acetamide (27i). Yield = 15 mg (50%, Off-white solid) LCMS: R_T = 2.40 min., >98% @ 215
and 254 nm, m/z = 366.0 [M + H]$^+$. ^{1}H NMR (500 MHz, DMSO-d_6) δ 10.72 (s, 1H), 8.21 – 8.00
(m, 2H), 7.72 – 7.50 (m, 3H), 6.20 (s, 1H), 5.85 (s, 2H), 5.08 – 4.86 (m, 2H), 2.13 (s, 3H).
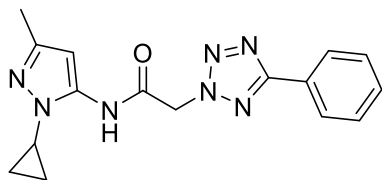
N-(1-cyclopropyl-3-methyl-1H-pyrazol-5-yl)-2-(5-phenyl-2H-tetrazol-2-yl)acetamide   (27j).
Yield = 23.5 mg (39%, Off-white solid) LCMS: R_T = 2.27 min., >98% @ 215 and 254 nm, m/z =
324.1 [M + H]$^+$. ^{1}H NMR (500 MHz, DMSO-d_6) δ 10.62 (s, 1H), 8.21 – 7.99 (m, 2H), 7.70 – 7.48

(m, 3H), 6.05 (s, 1H), 5.86 (s, 2H), 3.50 – 3.39 (m, 1H), 2.07 (s, 3H), 0.98 (s, 4H). ^{13}C NMR (125 MHz, DMSO-d_6) δ 164.72, 163.40, 145.80, 137.15, 131.15, 129.81, 127.21, 126.83, 99.06, 55.35, 29.48, 14.24, 6.79.
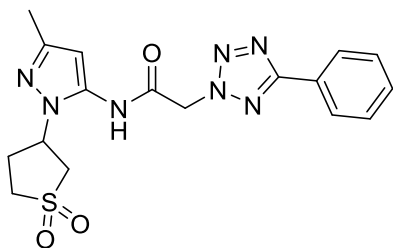
N-(1-(1,1-dioxidotetrahydrothiophen-3-yl)-3-methyl-1H-pyrazol-5-yl)-2-(5-phenyl-2H-tetrazol-2-yl)acetamide (27k). Yield = 24 mg (30%, white solid) LCMS: R_T = 2.27 min., >98% @ 215 and 254 nm, m/z = 402.1 [M + H]$^+$. ^{1}H NMR (500 MHz, DMSO-d_6) δ 10.64 (s, 1H), 8.11 – 8.07 (m, 2H), 7.62 – 7.56 (m, 3H), 6.09 (s, 1H), 5.85 (s, 2H), 5.27 – 5.17 (m, 1H), 3.63 (dd, J = 13.4, 8.4 Hz, 1H), 3.56 – 3.48 (m, 1H), 3.33 – 3.29 (m, 1H), 3.25 – 3.15 (m, 1H), 2.50 – 2.44 (m, 2H), 2.15 (s, 3H). ^{13}C NMR (125 MHz, DMSO-d_6) δ 164.72, 164.08, 148.00, 135.88, 131.17, 129.81, 127.18, 126.83, 99.89, 55.32, 54.95, 52.15, 51.56, 29.56, 14.43.
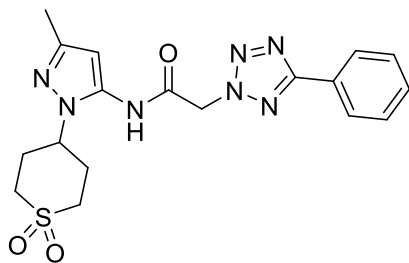
N-(1-(1,1-dioxidotetrahydro-2H-thiopyran-4-yl)-3-methyl-1H-pyrazol-5-yl)-2-(5-phenyl-2H-tetrazol-2-yl)acetamide (27l). Yield = 18 mg (45%, Brown solid) LCMS: R_T = 2.80 min., >98% @ 215 and 254 nm, m/z = 417.1 [M + H]$^+$. ^{1}H NMR (500 MHz, DMSO-d_6) δ 10.02 (s, 1H), 8.09 (dd, J = 7.7, 1.8 Hz, 2H), 7.64 – 7.54 (m, 3H), 5.97 (s, 1H), 4.92 (s, 2H), 4.42 – 4.34 (m, 1H), 3.31 – 3.23 (m, 4H), 2.44 – 2.36 (m, 2H), 2.14 (s, 3H), 2.13 – 2.07 (m, 2H). ^{13}C NMR (125 MHz,

DMSO-*d₆*) δ 167.20, 152.96, 146.92, 135.01, 129.94, 128.48, 125.64, 122.98, 115.75, 100.37, 67.83, 51.38, 49.52, 30.17, 14.40.

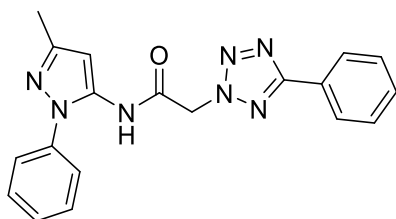
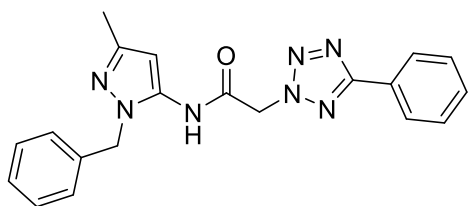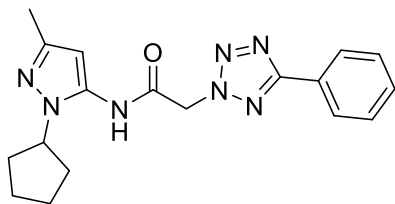***N*-(1-cyclopentyl-3-methyl-1*H*-pyrazol-5-yl)-2-(5-phenyl-2*H*-tetrazol-2-yl)acetamide   (27m).**

Yield = 22 mg (39%, White solid) LCMS: R$_T$ = 2.52 min., >98% @ 215 and 254 nm, *m/z* = 352.1 [M + H]$^+$. ^{1}H NMR (500 MHz, DMSO-*d₆*) δ 10.48 (s, 1H), 8.12 – 8.06 (m, 2H), 7.66 – 7.51 (m, 3H), 6.01 (s, 1H), 5.83 (s, 2H), 4.65 (p, *J* = 7.3 Hz, 1H), 2.11 (s, 3H), 2.03 – 1.93 (m, 2H), 1.92 – 1.79 (m, 4H), 1.65 – 1.54 (m,2H). ^{13}C NMR (125 MHz, DMSO-*d₆*) δ 164.71, 163.74, 146.25, 135.26, 131.17, 129.81, 127.21, 126.82, 99.15, 57.43, 55.35, 32.55, 24.61, 14.45.
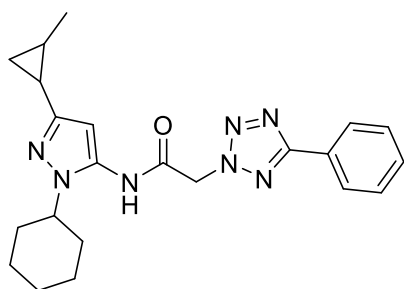
***N*-(1-cyclohexyl-3-(2-methylcyclopropyl)-1*H*-pyrazol-5-yl)-2-(5-phenyl-2*H*-tetrazol-2-yl)acetamide (27n).** Yield = 27 mg (49%, Off-white solid) LCMS: R$_T$ = 2.84 min., >98% @ 215 and 254 nm, *m/z* = 406.1 [M + H]$^+$. ^{1}H NMR (500 MHz, DMSO-*d₆*) δ 10.42 (s, 1H), 8.11 – 8.06 (m, 2H), 7.62 – 7.50 (m,32H), 5.83 (s, 1H), 5.82 (m 1H), 4.15 – 3.92 (m, 1H), 1.84 – 1.70 (m, 6H), 1.65 (d, *J* = 12.3 Hz, 1H), 1.54 – 1.48 (m, 1H), 1.40 – 1.30 (m, 2H), 1.24 – 1.16 (m, *J* = 12.9 Hz, 1H), 1.09 (d, *J* = 5.9 Hz, 2H), 0.99 – 0.90 (m, 1H), 0.73 (dt, *J* = 8.5, 4.4 Hz, 1H), 0.62 – 0.57 (m,

1H). ^{13}C NMR (125 MHz, DMSO-d_6) δ 164.73, 163.81, 152.60, 134.34, 131.17, 129.80, 127.21, 126.82, 95.35, 55.61, 55.39, 32.89, 25.60, 25.36, 18.97, 18.46, 16.25, 16.22.
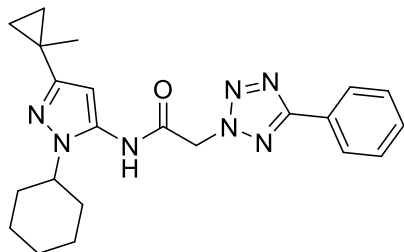
N-(1-cyclohexyl-3-(1-methylcyclopropyl)-1H-pyrazol-5-yl)-2-(5-phenyl-2H-tetrazol-2-yl)acetamide (27o). Yield = 16 mg (42%, White solid) LCMS: R_T = 2.97 min., >98% @ 215 and 254 nm, m/z = 406.1 [M + H]$^+$. ^{1}H NMR (500 MHz, DMSO-d_6) δ 10.49 – 10.40 (m, 1H), 8.16 – 8.04 (m, 2H), 7.67 – 7.49 (m, J = 5.6 Hz, 3H), 5.96 (s, 1H), 5.83 (s, 2H), 4.13 – 3.97 (m, 1H), 1.89 – 1.69 (m, 6H), 1.65 (d, J = 12.3 Hz, 1H), 1.34 (d, J = 17.8 Hz, 5H), 1.27 – 1.15 (m, 1H), 0.84 – 0.77 (m, 2H), 0.71 – 0.62 (m, 2H). ^{13}C NMR (125 MHz, DMSO-d_6) δ 164.72, 163.82, 155.22, 134.38, 131.17, 129.80, 127.20, 126.81, 95.71, 55.65, 55.39, 32.82, 25.55, 25.32, 22.66, 16.40, 14.90.

N-(1-cyclohexyl-3-(1-(trifluoromethyl)cyclopropyl)-1H-pyrazol-5-yl)-2-(5-phenyl-2H-tetrazol-2-yl)acetamide (27p). Yield = 11 mg (22%) LCMS: R_T = 3.01 min., >98% @ 215 and 254 nm, m/z = 460.1 [M + H]$^+$. ^{1}H NMR (500 MHz, CD$_3$OD) δ 8.19 – 8.14 (m, 2H), 7.58 – 7.52 (m, 3H), 6.35 (s, 1H), 5.77 (s, 2H), 4.11 (td, J = 14.5, 7.4 Hz, 1H), 1.93 – 1.83 (m, 6H), 1.72 (d, J

= 12.8 Hz, 1H), 1.51 – 1.39 (m, 2H), 1.35 – 1.21 (m, 6H). ^{13}C NMR (125 MHz, CD$_3$OD) δ 164.48, 145.83, 134.03, 130.34, 128.72, 127.05, 126.44, 100.27, 56.78, 54.49, 32.20, 25.24, 24.92, 9.59.
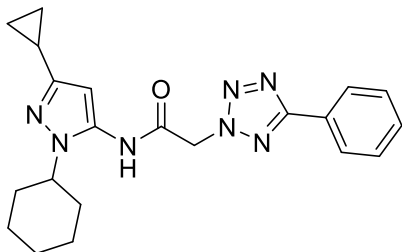
N-(1-cyclohexyl-3-cyclopropyl-1H-pyrazol-5-yl)-2-(5-phenyl-2H-tetrazol-2-yl)acetamide (27q). Yield = 14 mg (34%, White solid) LCMS: R_T = 2.71 min., >98% @ 215 and 254 nm, m/z = 392.1 [M + H]$^+$. ^{1}H NMR (500 MHz, DMSO-d_6) δ 10.43 (s, 1H), 8.14 – 8.07 (m, 2H), 7.63 – 7.53 (m, 3H), 5.87 (s, 1H), 5.82 (s, 2H), 4.08 – 4.00 (m, 1H), 1.86 – 1.70 (m, 7H), 1.65 (d, J = 12.4 Hz, 1H), 1.35 (dd, J = 24.9, 12.5 Hz, 2H), 1.19 (dd, J = 25.7, 12.9 Hz, 1H), 0.85 – 0.76 (m, 2H), 0.60 – 0.50 (m, 2H). ^{13}C NMR (125 MHz, DMSO-d_6) δ 164.72, 163.78, 152.67, 134.39, 131.16, 129.79, 127.20, 126.81, 95.28, 55.63, 55.39, 32.87, 25.59, 25.35, 10.01, 8.11.
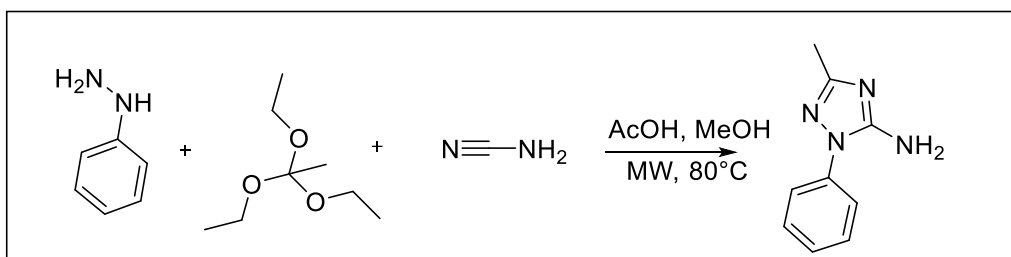
3-methyl-1-phenyl-1H-1,2,4-triazol-5-amine. In a 10 mL microwave vial, phenyl hydrazine (390 mg, 3.69 mmol), triethyl orthoacetate (0.56 mL, 3.0 mmol), cyanamide (129 mg, 3.08 mmol) and acetic acid (10.0 μL, 0.150 mmol) in anhydrous MeOH were subjected to microwave irradiation at 80 ºC for 60 min. Crude was evaporated, product was precipitated in ethyl acetate:hexane (8:2), crude solid thus obtained was purified by reverse phase preparative HPLC (0-40 % CH$_3$CN in water) Yield = 0.1 g (20%) LCMS: R_T = 0.61 min., >98% @ 215 and 254 nm, m/z = 175.0 [M +

H]+. 1H NMR (500 MHz, DMSO-*d6*) δ 7.58 – 7.45 (m, 4H), 7.40 – 7.29 (m, 1H), 6.30 (s, 2H), 2.11

(s, 3H). 13C NMR (125 MHz, DMSO-d6) δ 157.91, 155.15, 137.87, 129.77, 126.97, 122.75, 14.35.
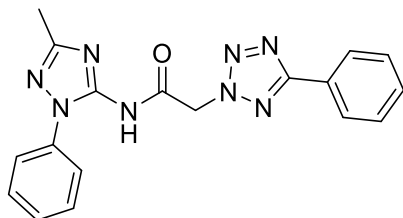
N-(3-methyl-1-phenyl-1H-1,2,4-triazol-5-yl)-2-(5-phenyl-2H-tetrazol-2-yl)acetamide (27r).

Yield = 22 mg, (26%, Off-white solid) LCMS: R$_T$ = 2.51 min., >98% @ 215 and 254 nm, *m/z* =

361.1 [M + H]+. 1H NMR (500 MHz, DMSO-*d6*) δ 11.29 (s, 1H), 8.08 (d, *J* = 6.4 Hz, 2H), 7.70 –

7.56 (m, 5H), 7.53 – 7.26 (m, 3H), 5.76 (s, 2H), 2.33 (s, 3H).
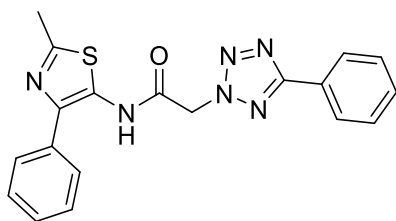
N-(2-methyl-4-phenylthiazol-5-yl)-2-(5-phenyl-2H-tetrazol-2-yl)acetamide (27s). Yield = 21

mg (35%, Off-white solid) LCMS: R$_T$ = 2.57 min., >98% @ 215 and 254 nm, *m/z* = 377.1 [M +

H]+. 1H NMR (500 MHz, DMSO-*d6*) δ 11.12 (s, 1H), 8.10 (dd, *J* = 7.7, 1.5 Hz, 2H), 7.80 (d, *J* =

7.3 Hz, 2H), 7.62 – 7.55 (m, 3H), 7.49 (t, *J* = 7.6 Hz, 2H), 7.39 (t, *J* = 7.4 Hz, 1H), 5.89 (s, 2H),

2.61 (s, 3H). 13C NMR (125 MHz, DMSO-*d6*) δ 164.78, 164.17, 159.85, 142.07, 134.18, 131.19,

129.82, 129.07, 128.54, 128.24, 127.20, 126.86, 55.22, 19.26.
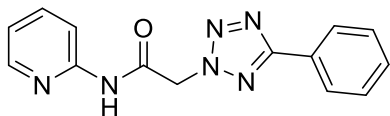
2-(5-phenyl-2*H*-tetrazol-2-yl)-*N*-(pyridin-2-yl)acetamide (27t). Yield = 40 mg (44%, White solid) LCMS: R_T = 2.31 min., >98% @ 215 and 254 nm, *m/z* = 281.1 [M + H]$^+$. ^{1}H NMR (500 MHz, DMSO-*d$_6$*) δ 11.17 (s, 1H), 8.42 – 8.37 (m, 1H), 8.13 – 8.07 (m, 2H), 7.99 (d, *J* = 6.3 Hz, 1H), 7.85 – 7.79 (m, 1H), 7.61 – 7.55 (m, 3H), 7.21 – 7.15 (m, 1H), 5.86 (s, 2H). ^{13}C NMR (125 MHz, DMSO-d$_6$) δ 164.71, 151.66, 148.70, 138.99, 131.14, 129.79, 127.22, 126.84, 120.60, 114.06, 55.69.
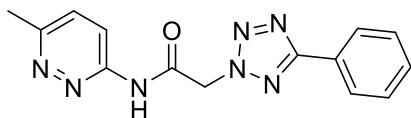
_N_-(6-methylpyridazin-3-yl)-2-(5-phenyl-2*H*-tetrazol-2-yl)acetamide (27u). Yield = 21 mg (42%, white solid) LCMS: R_T = 2.14 min., >98% @ 215 and 254 nm, *m/z* = 296.1 [M + H]$^+$. ^{1}H NMR (500 MHz, DMSO-*d$_6$*) δ 11.72 (s, 1H), 8.13 (d, *J* = 9.1 Hz, 1H), 8.09 (dd, *J* = 7.7, 1.7 Hz, 2H), 7.62 – 7.55 (m, 4H), 5.91 (s, 2H), 2.59 (s, 3H). ^{13}C NMR (125 MHz, DMSO-d$_6$) δ 165.04, 164.74, 157.45, 153.75, 131.16, 129.80, 129.49, 127.18, 126.85, 118.95, 55.64, 21.62.
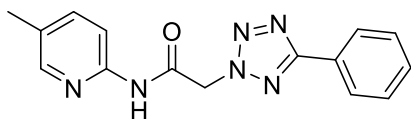
_N_-(5-methylpyridin-2-yl)-2-(5-phenyl-2*H*-tetrazol-2-yl)acetamide (27v). Yield = 19 mg (38%, White solid) LCMS: R_T = 2.38 min., >98% @ 215 and 254 nm, *m/z* = 295.1 [M + H]$^+$. ^{1}H NMR (500 MHz, DMSO-*d$_6$*) δ 11.08 (s, 1H), 8.22 (s, 1H), 8.09 (d, *J* = 7.6 Hz, 2H), 7.90 (d, *J* = 7.1 Hz, 1H), 7.64 (d, *J* = 8.4 Hz, 1H), 7.62 – 7.52 (m, *J* = 6.5 Hz, 3H), 5.84 (s, 2H), 2.27 (s, 3H). ^{13}C NMR

(125 MHz, DMSO-*d₆*) δ 164.72, 164.03, 149.51, 148.46, 139.28, 131.14, 129.79, 129.59, 127.24, 126.85, 113.61, 55.65, 17.76.
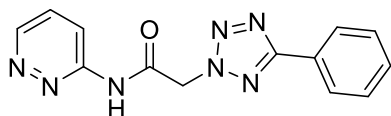
2-(5-phenyl-2*H*-tetrazol-2-yl)-*N*-(pyridazin-3-yl)acetamide (27w). Yield = 32 mg (35%, Light yellow solid) LCMS: R_T = 2.13 min., >98% @ 215 and 254 nm, *m/z* = 282.0 [M + H]⁺. ¹H NMR (500 MHz, DMSO-*d₆*) δ 11.80 (s, 1H), 9.03 (dd, *J* = 4.7, 1.3 Hz, 1H), 8.24 (d, *J* = 8.9 Hz, 1H), 8.10 (dd, *J* = 7.7, 1.7 Hz, 2H), 7.73 (dd, *J* = 9.0, 4.7 Hz, 1H), 7.61 – 7.54 (m, 3H), 5.94 (s, 2H). ¹³C NMR (125 MHz, DMSO-*d₆*) δ 165.31, 164.76, 155.44, 149.50, 131.18, 129.80, 129.30, 127.17, 126.85, 118.83, 55.69.

General Procedure C (Alkylation) for synthesis of tetrazole series

Reagents and Conditions: (a) TEA, DCM; (b) NaOEt, EtOH, MW, 90°C
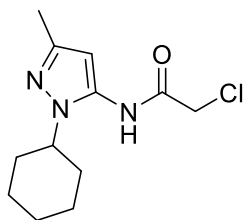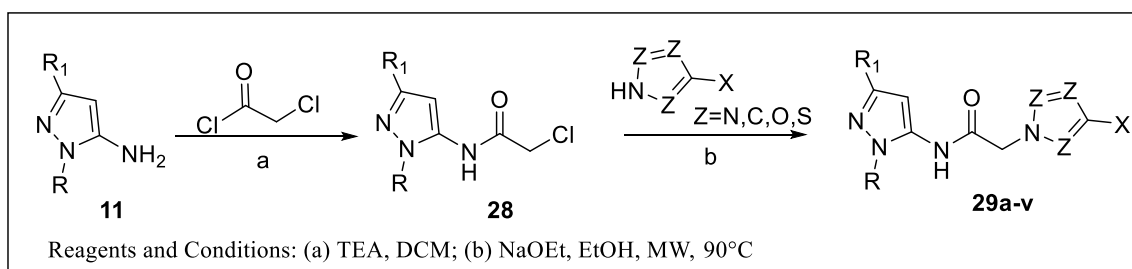
2-chloro-*N*-(1-cyclohexyl-3-methyl-1*H*-pyrazol-5-yl)acetamide. In a 50 mL RBF, to a solution of 1-cyclohexyl-3-methyl-1*H*-pyrazol-5-amine (0.65 g, 3.6 mmol), chloroacetyl chloride (0.31 mL,

3.9 mmol) in DCM (10 mL) at 0 ºC was added TEA (1.0 mL, 7.2 mmol). Reaction was stirred at RT for 2 h. 100 mL saturated NaHCO$_{3aq}$ was added to the crude and product was extracted with DCM (100 mL*2). Combined organic layer was washed with brine, dried over sodium sulphate, concentrated under vacuum and used as such. Yield = 0.78 g (85%) LCMS: R$_T$ = 2.17 min., >98% @ 215 and 254 nm, m/z = 256.0 [M + H]$^+$. ^{1}H NMR (500 MHz, DMSO-d_6) δ 10.12 (s, 1H), 5.97 (s, 1H), 4.32 (s, 2H), 4.01 – 3.94 (m, 1H), 2.11 (s, 3H), 1.82 – 1.71 (m, 6H), 1.65 (d, J = 12.8 Hz, 1H), 1.38 – 1.27 (m, 2H), 1.21 – 1.15 (m, 1H). ^{13}C NMR (125 MHz, DMSO-d_6) δ 165.49, 145.92, 134.82, 99.15, 55.55, 43.24, 32.91, 25.60, 25.37, 14.39.
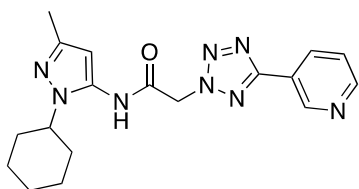
N-(1-cyclohexyl-3-methyl-1H-pyrazol-5-yl)-2-(5-(pyridin-3-yl)-2H-tetrazol-2-yl)acetamide (29a). In a 10 mL Microwave vial, 2-chloro-N-(1-cyclohexyl-3-methyl-1H-pyrazol-5-yl)acetamide (0.050 mg, 0.19 mmol), 3-(2H-tetrazol-5-yl)pyridine (28 mg, 0.19 mmol) and NaOEt (15 mg, 0.23 mmol) in ethanol (1.5 mL) was subjected to microwave irradiation at 90 ºC for 2 h. Crude was partitioned between brine (20 mL) and ethyl acetate (25 mL*2), combined organic layer was dried over sodium sulphate, concentrated and purified by Preparative HPLC (0-100% CH$_3$CN in water). Yield = 24 mg (76%, White solid) LCMS: R$_T$ = 2.10 min., >98% @ 215 and 254 nm, m/z = 367.1 [M + H]$^+$. ^{1}H NMR (500 MHz, DMSO-d_6) δ 10.46 (s, 1H), 9.26 (s, 1H), 8.77 (d, J = 3.6 Hz, 1H), 8.44 (d, J = 8.0 Hz, 1H), 7.64 (dd, J = 7.4, 5.0 Hz, 1H), 6.00 (s, 1H), 5.89 (d, J = 9.3 Hz, 2H), 4.06 (t, J = 10.6 Hz, 2H), 2.10 (s, 3H), 1.85 – 1.70 (m, 6H), 1.66 (d, J = 12.1 Hz, 1H), 1.35 (dd, J = 25.2, 12.7 Hz, 2H), 1.22 – 1.16 (m, 1H). ^{13}C NMR (125 MHz, DMSO-d_6) δ 163.66, 162.65, 152.05, 147.62, 146.05, 134.45, 124.89, 123.39, 98.96, 55.65, 55.53, 32.95, 25.63, 25.37, 14.39.
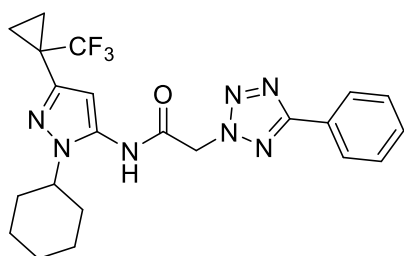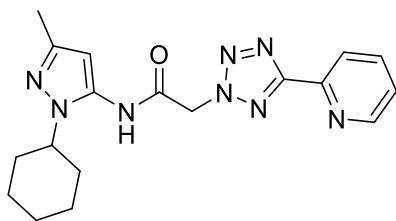
N-(1-cyclohexyl-3-methyl-1H-pyrazol-5-yl)-2-(5-(pyridin-2-yl)-2H-tetrazol-2-yl)acetamide

(29b). Yield = 18 mg (35%, White solid) LCMS: R_T = 2.17 min., >98% @ 215 and 254 nm, m/z = 367.1 [M + H]$^+$. ^{1}H NMR (500 MHz, DMSO-d_6) δ 10.46 (s, 1H), 8.77 (d, J = 4.0 Hz, 1H), 8.18 (d, J = 7.8 Hz, 1H), 8.04 (t, J = 7.7 Hz, 1H), 7.61 – 7.55 (m, 1H), 6.00 (s, 1H), 5.87 (s, 2H), 4.07 (t, J = 10.3 Hz, 1H), 2.11 (s, 3H), 1.86 – 1.71 (m, J = 24.3, 11.4 Hz, 6H), 1.65 (d, J = 12.1 Hz, 1H), 1.37 (dd, J = 24.4, 12.1 Hz, 2H), 1.23 – 1.17 (m, 1H). ^{13}C NMR (125 MHz, DMSO-d_6) δ 164.75, 163.71, 150.70, 146.53, 146.04, 138.15, 134.46, 125.83, 122.90, 98.98, 55.58, 55.53, 32.96, 25.58, 25.39, 14.40.
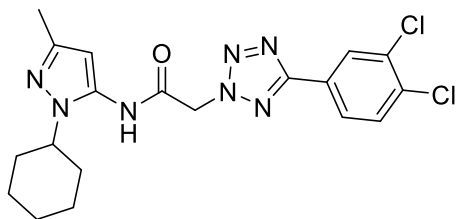
N-(1-cyclohexyl-3-methyl-1H-pyrazol-5-yl)-2-(5-(3,4-dichlorophenyl)-2H-tetrazol-2-yl)acetamide (29c). Yield = 25 mg (20%, White solid) LCMS: R_T = 2.94 min., >98% @ 215 and 254 nm, m/z = 434.1 [M + H]$^+$. ^{1}H NMR (500 MHz, DMSO-d_6) δ 10.45 (s, 1H), 8.24 (d, J = 1.6 Hz, 1H), 8.06 (dd, J = 8.4, 1.7 Hz, 1H), 7.88 (d, J = 8.4 Hz, 1H), 5.99 (s, 1H), 5.86 (s, 2H), 4.10 – 4.02 (m, 1H), 2.10 (s, 3H), 1.86 – 1.71 (m, 6H), 1.66 (d, J = 12.5 Hz, 1H), 1.35 (dd, J = 25.0, 12.6 Hz, 2H), 1.19 (dd, J = 25.6, 12.7 Hz, 1H). ^{13}C NMR (125 MHz, DMSO-d_6) δ 163.62, 162.86, 146.06, 134.42, 133.89, 132.71, 132.32, 128.40, 127.66, 126.94, 98.99, 55.6, 32.94, 25.64, 25.37, 14.39.
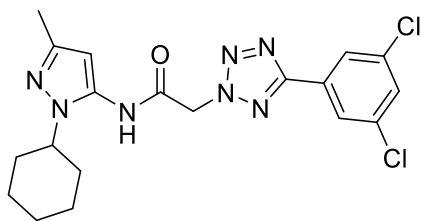
N-(1-cyclohexyl-3-methyl-1H-pyrazol-5-yl)-2-(5-(3,5-dichlorophenyl)-2H-tetrazol-2-yl)acetamide (29d). Yield = 28 mg (23%, pink solid) LCMS: R_T = 3.0 min., >98% @ 215 and 254 nm, m/z = 434.1 [M + H]$^+$. ^{1}H NMR (500 MHz, DMSO-d_6) δ 10.45 (s, 1H), 8.04 (d, J = 1.6 Hz, 2H), 7.87 (s, 1H), 5.99 (s, 1H), 5.87 (s, 2H), 4.10 – 4.02 (m, 1H), 2.11 (s, 3H), 1.85 – 1.72 (m, 6H), 1.66 (d, J = 12.5 Hz, 1H), 1.35 (dd, J = 25.0, 12.6 Hz, 2H), 1.19 (dd, J = 25.7, 12.8 Hz, 1H). ^{13}C NMR (125 MHz, DMSO-d_6) δ 163.59, 162.53, 146.06, 135.70, 134.38, 130.71, 130.34, 125.27, 99.05, 55.64, 32.94, 25.65, 25.37, 14.39.

N-(1-cyclohexyl-3-methyl-1H-pyrazol-5-yl)-2-(5-(3,4-difluorophenyl)-2H-tetrazol-2-yl)acetamide (29e). Yield = 19 mg (28%, clear oil) LCMS: R_T = 2.65 min., >98% @ 215 and 254 nm, m/z = 402.1 [M + H]$^+$. ^{1}H NMR (500 MHz, DMSO-d_6) δ 10.45 (s, 1H), 8.11 – 8.02 (m, 1H), 7.95 (d, J = 4.8 Hz, 1H), 7.68 (dd, J = 18.9, 8.5 Hz, 1H), 6.00 (s, 1H), 5.85 (s, 2H), 4.11 – 4.01 (m, 1H), 2.10 (s, 3H), 1.85 – 1.72 (m, 6H), 1.66 (d, J = 12.5 Hz, 1H), 1.36 (dd, J = 25.1, 12.6 Hz, 2H), 1.19 (dd, J = 25.6, 13.0 Hz, 1H). ^{13}C NMR (125 MHz, DMSO-d_6) δ 163.65, 163.13, 146.07, 134.45, 124.72, 124.67, 124.24, 124.21, 124.18, 124.16, 119.45, 119.30, 116.16, 116.01, 98.95, 55.61, 55.51, 32.95, 25.63, 25.37, 14.39.
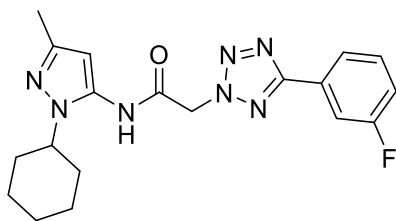
N-(1-cyclohexyl-3-methyl-1H-pyrazol-5-yl)-2-(5-(3-fluorophenyl)-2H-tetrazol-2-yl)acetamide (29f). Yield = 21 mg (21%, White solid) LCMS: R_T = 2.59 min., >98% @ 215 and 254 nm, m/z = 384.1 [M + H]$^+$. ^{1}H NMR (500 MHz, DMSO-d_6) δ 10.45 (s, 1H), 7.95 (d, J = 7.7 Hz, 1H), 7.83 (d, J = 9.5 Hz, 1H), 7.66 (dd, J = 14.0, 8.0 Hz, 1H), 7.43 (td, J = 8.7, 2.5 Hz, 1H), 6.00 (s, 1H), 5.85 (s, 2H), 4.11 – 4.02 (m, J = 15.0, 10.5, 4.2 Hz, 1H), 2.11 (s, 3H), 1.85 – 1.72 (m, 6H), 1.66 (d, J = 12.7 Hz, 1H), 1.41 – 1.31 (m, 2H), 1.24 – 1.16 (m, 1H). ^{13}C NMR (125 MHz, DMSO-d_6) δ 163.88, 163.68, 161.93, 146.05, 134.44, 132.24, 132.17, 129.36, 129.29, 123.04, 118.21, 118.04, 113.57, 113.38, 98.97, 55.60, 55.51, 32.95, 25.63, 25.37, 14.39.
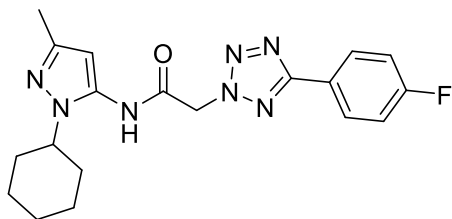
N-(1-cyclohexyl-3-methyl-1H-pyrazol-5-yl)-2-(5-(4-fluorophenyl)-2H-tetrazol-2-yl)acetamide (29g). Yield = 18.2 mg (24%, Light brown oil) LCMS: R_T = 2.61 min., >98% @ 215 and 254 nm, m/z = 384.1 [M + H]$^+$. ^{1}H NMR (500 MHz, DMSO-d_6) δ 10.44 (s, 1H), 8.14 (dd, J = 8.6, 5.5 Hz, 2H), 7.43 (t, J = 8.8 Hz, 2H), 6.00 (s, 1H), 5.83 (s, 2H), 4.10 – 4.02 (m, 1H), 2.10 (s, 3H), 1.84 – 1.73 (m, 6H), 1.66 (d, J = 12.2 Hz, 1H), 1.35 (dd, J = 23.3, 11.0 Hz, 2H), 1.21 – 1.16 (m, 1H). ^{13}C NMR (125 MHz, DMSO-d_6) δ 163.96, 163.73, 146.04, 134.46, 129.28, 129.21, 117.03, 116.86, 98.95, 55.60, 55.40, 32.95, 25.62, 25.37, 14.39.

N-(1-cyclohexyl-3-methyl-1H-pyrazol-5-yl)-2-(5-(2-fluorophenyl)-2H-tetrazol-2-yl)acetamide (29h). Yield = 23 mg (25%, White solid) LCMS: R_T = 2.59 min., >98% @ 215 and 254 nm, m/z = 384.1 [M + H]$^+$. ^{1}H NMR (500 MHz, DMSO-d_6) δ 10.45 (s, 1H), 8.11 (t, J = 6.9 Hz, 1H), 7.64 (dd, J = 12.5, 6.6 Hz, 1H), 7.52 – 7.40 (m, 2H), 6.00 (s, 1H), 5.87 (s, 2H), 4.12 – 4.02 (m, 1H), 2.11 (s, 3H), 1.84 – 1.71 (m, J = 23.7, 11.4 Hz, 6H), 1.65 (d, J = 12.5 Hz, 1H), 1.35 (dd, J = 23.2, 10.9 Hz, 2H), 1.18 (dd, J = 25.6, 12.9 Hz, 1H). ^{13}C NMR (125 MHz, DMSO-d_6) δ 163.73, 160.94, 160.77, 158.74, 146.05, 134.45, 133.29, 133.22, 130.20, 125.65, 117.46, 117.29, 115.17, 98.98, 55.59, 55.44, 32.95, 25.59, 25.37, 14.39.
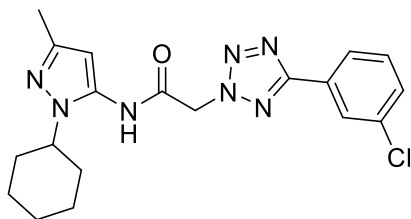
2-(5-(3-chlorophenyl)-2H-tetrazol-2-yl)-N-(1-cyclohexyl-3-methyl-1H-pyrazol-5-yl)acetamide (29i). Yield = 30 mg (19%, White solid) LCMS: R_T = 2.78 min., >98% @ 215 and 254 nm, m/z = 400.1 [M + H]$^+$. ^{1}H NMR (500 MHz, DMSO-d_6) δ 10.45 (s, 1H), 8.09 – 7.99 (m, 2H), 7.68 – 7.61 (m, 2H), 6.00 (s, 1H), 5.85 (s, 2H), 4.10 – 4.01 (m, 1H), 2.11 (s, 3H), 1.85 – 1.74 (m, J = 27.3, 15.3 Hz, 6H), 1.66 (d, J = 12.4 Hz, 1H), 1.35 (dd, J = 25.0, 12.5 Hz, 2H), 1.19 (dd, J = 25.5, 12.6 Hz, 1H). ^{13}C NMR (125 MHz, DMSO-d_6) δ 163.69, 163.55, 146.06, 134.48, 134.43, 131.93, 131.08, 129.13, 126.33, 125.48, 99.02, 55.62, 55.53, 32.94, 25.64, 25.37, 14.39.
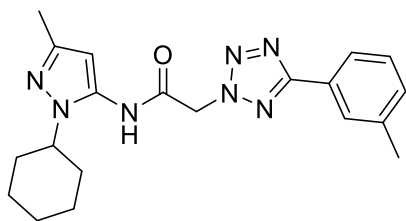
N-(1-cyclohexyl-3-methyl-1*H*-pyrazol-5-yl)-2-(5-(m-tolyl)-2*H*-tetrazol-2-yl)acetamide   (29j).

Yield = 12 mg (16%, white solid) LCMS: R_T = 2.71 min., >98% @ 215 and 254 nm, *m/z* = 380.1

[M + H]⁺. ¹H NMR (500 MHz, DMSO-*d₆*) δ 10.44 (s, 1H), 7.92 (s, 1H), 7.88 (d, *J* = 7.6 Hz, 1H),

7.47 (t, *J* = 7.6 Hz, 1H), 7.38 (d, *J* = 7.5 Hz, 1H), 6.00 (s, 1H), 5.82 (s, 2H), 4.17 – 3.98 (m, 1H),

2.42 (s, 3H), 2.11 (s, 3H), 1.85 – 1.72 (m, 6H), 1.66 (d, *J* = 12.2 Hz, 1H), 1.36 (dd, *J* = 25.1, 12.6

Hz, 2H), 1.23 – 1.15 (m, 1H). ¹³C NMR (125 MHz, DMSO-*d₆*) δ 164.81, 163.79, 146.05, 139.14,

134.46, 131.79, 129.70, 127.27, 127.13, 123.97, 99.01, 55.61, 55.38, 32.95, 25.63, 25.38, 21.39,

14.39.

N-(1-cyclohexyl-3-methyl-1*H*-pyrazol-5-yl)-2-(5-(p-tolyl)-2*H*-tetrazol-2-yl)acetamide   (29k).

Yield = 22 mg (44%, White solid) LCMS: R_T = 2.17 min., >98% @ 215 and 254 nm, *m/z* = 367.1

[M + H]⁺. ¹H NMR (500 MHz, DMSO-*d₆*) δ 10.44 (s, 1H), 7.98 (d, *J* = 7.6 Hz, 2H), 7.40 (d, *J* =

7.7 Hz, 2H), 6.00 (s, 1H), 5.81 (s, 2H), 4.06 (t, *J* = 10.3 Hz, 1H), 2.11 (s, 3H), 1.85 – 1.73 (m, 6H),

1.66 (d, *J* = 12.3 Hz, 1H), 1.36 (dd, *J* = 24.7, 12.3 Hz, 2H), 1.19 (dd, *J* = 25.3, 12.6 Hz, 1H). ¹³C

NMR (125 MHz, DMSO-*d₆*) δ 164.80, 163.82, 146.05, 140.94, 134.50, 130.34, 126.77, 124.48,

98.97, 55.60, 55.34, 32.95, 25.63, 25.38, 21.49, 14.39.
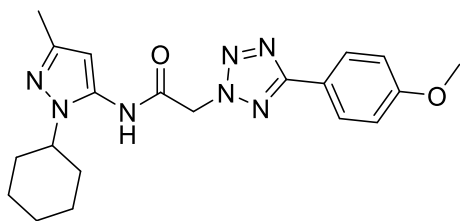
N-(1-cyclohexyl-3-methyl-1H-pyrazol-5-yl)-2-(5-(4-methoxyphenyl)-2H-tetrazol-2-yl)acetamide (29l). Yield = 16.5 mg (21%, White solid) LCMS: R_T = 2.52 min., >98% @ 215 and 254 nm, m/z = 396.1 [M + H]$^+$. ^{1}H NMR (500 MHz, DMSO-d_6) δ 10.43 (s, 1H), 8.02 (d, J = 8.8 Hz, 2H), 7.13 (d, J = 8.8 Hz, 2H), 6.00 (s, 1H), 5.79 (s, 2H), 4.06 (ddd, J = 15.0, 10.5, 4.1 Hz, 1H), 2.11 (s, 3H), 1.84 – 1.73 (m, 6H), 1.66 (d, J = 12.6 Hz, 1H), 1.41 – 1.29 (m, 2H), 1.23 – 1.15 (m, 1H). ^{13}C NMR (125 MHz, DMSO-d_6) δ 164.65, 163.82, 161.49, 146.03, 134.49, 128.40, 119.63, 115.17, 98.95, 55.81, 55.59, 55.28, 32.95, 25.62, 25.37, 14.39.
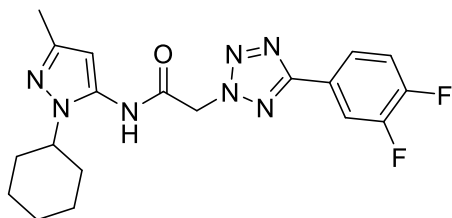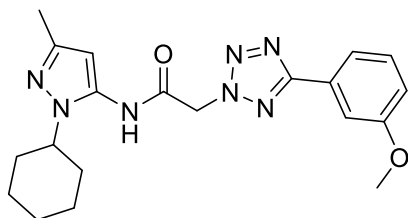

N-(1-cyclohexyl-3-methyl-1H-pyrazol-5-yl)-2-(5-(3-methoxyphenyl)-2H-tetrazol-2-yl)acetamide (29m). Yield = 16 mg (27%, Clear oil) LCMS: R_T = 2.55 min., >98% @ 215 and 254 nm, m/z = 396.1 [M + H]$^+$. ^{1}H NMR (500 MHz, DMSO-d_6) δ 10.45 (s, 1H), 7.68 (d, J = 7.6 Hz, 1H), 7.59 (s, 1H), 7.51 (t, J = 8.0 Hz, 1H), 7.14 (dd, J = 8.0, 2.1 Hz, 1H), 6.00 (s, 1H), 5.83 (s, 2H), 4.11 – 4.03 (m, 1H), 2.11 (s, 3H), 1.85 – 1.72 (m, 6H), 1.66 (d, J = 12.4 Hz, 1H), 1.41 – 1.31 (m, 2H), 1.19 (dd, J = 25.6, 12.7 Hz, 1H). ^{13}C NMR (125 MHz, DMSO-d_6) δ 164.60, 163.77, 160.21, 146.05, 134.46, 131.08, 128.45, 119.10, 117.09, 111.65, 98.97, 55.75, 55.60, 55.40, 32.95, 25.63, 25.37, 14.39.

2-(5-(4-chloro-3-methylphenyl)-2*H*-tetrazol-2-yl)-*N*-(1-cyclohexyl-3-methyl-1*H*-pyrazol-5-yl)acetamide (29n). Yield = 14 mg (22%, White solid) LCMS: R_T = 2.88 min., >98% @ 215 and 254 nm, *m/z* = 414.1 [M + H]$^+$. ^{1}H NMR (500 MHz, CD$_3$OD) δ 8.10 (s, 1H), 7.96 (d, *J* = 8.2 Hz, 1H), 7.54 (d, *J* = 8.3 Hz, 1H), 6.08 (s, 1H), 5.75 (d, *J* = 7.4 Hz, 2H), 4.10 – 4.03 (m, 1H), 2.48 (s, 3H), 2.22 (s, 3H), 1.88 (d, *J* = 6.4 Hz, 6H), 1.77 – 1.70 (m, 1H), 1.51 – 1.39 (m, 2H), 1.31 (t, *J* = 12.9 Hz, 1H). ^{13}C NMR (125 MHz, CD$_3$OD) δ 164.47, 147.36, 136.80, 136.32, 134.23, 129.44, 128.84, 125.84, 125.34, 99.44, 56.39, 54.50, 32.33, 25.36, 24.95, 18.71, 12.30.
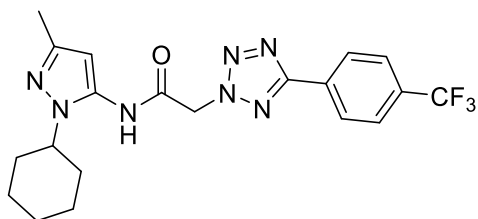
_N_-(1-cyclohexyl-3-methyl-1*H*-pyrazol-5-yl)-2-(5-(4-(trifluoromethyl)phenyl)-2*H*-tetrazol-2-yl)acetamide (29o). Yield = 30 mg (35%, Off-white solid) LCMS: R_T = 2.81 min., >98% @ 215 and 254 nm, *m/z* = 434.1 [M + H]$^+$. ^{1}H NMR (500 MHz, DMSO-*d$_6$*) δ 10.50 – 10.45 (m, 1H), 8.31 (d, *J* = 8.1 Hz, 2H), 7.97 (d, *J* = 8.3 Hz, 2H), 6.00 (s, 1H), 5.88 (s, 2H), 4.11 – 4.04 (m, 1H), 2.11 (s, 3H), 1.84 – 1.75 (m, 6H), 1.66 (d, *J* = 12.4 Hz, 1H), 1.42 – 1.31 (m, 2H), 1.25 – 1.15 (m, 1H). ^{13}C NMR (125 MHz, DMSO-*d$_6$*) δ 163.64, 163.55, 146.05, 134.45, 131.22, 131.00, 127.65, 126.86, 126.83, 125.47, 98.93, 55.60, 32.95, 25.62, 25.37, 14.39.
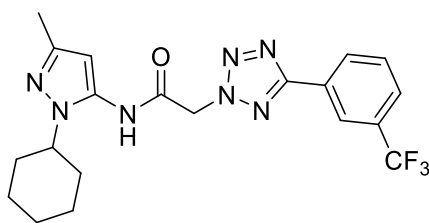
N-(1-cyclohexyl-3-methyl-1H-pyrazol-5-yl)-2-(5-(3-(trifluoromethyl)phenyl)-2H-tetrazol-2-yl)acetamide (29p). Yield = 23 mg (27%, Off-white solid) LCMS: R_T = 2.79 min., >98% @ 215 and 254 nm, m/z = 434.1 [M + H]$^+$. ^{1}H NMR (500 MHz, DMSO-d_6) δ 10.46 (s, 1H), 8.40 (d, J = 7.8 Hz, 1H), 8.32 (s, 1H), 7.97 (d, J = 7.8 Hz, 1H), 7.86 (t, J = 7.8 Hz, 1H), 6.00 (s, 1H), 5.88 (s, 2H), 4.11 – 4.02 (m, 1H), 2.11 (s, 3H), 1.84 – 1.73 (m, 6H), 1.65 (d, J = 12.4 Hz, 1H), 1.40 – 1.30 (m, 2H), 1.24 – 1.15 (m, J = 24.0, 11.2 Hz, 1H). ^{13}C NMR (125 MHz, DMSO-d_6) δ 163.69, 163.53, 146.06, 134.41, 131.33, 130.79, 130.68, 130.42, 128.18, 127.83, 127.80, 123.02, 99.05, 55.63, 55.58, 32.94, 25.63, 25.36, 14.38.
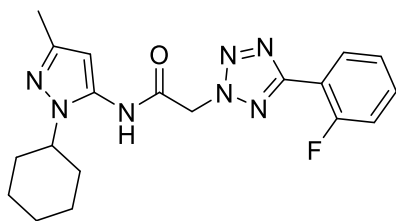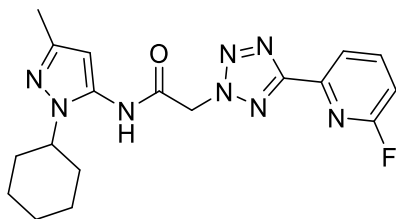

N-(1-cyclohexyl-3-methyl-1H-pyrazol-5-yl)-2-(5-(6-fluoropyridin-2-yl)-2H-tetrazol-2-yl)acetamide (29q). Yield = 12 mg (15%, clear oil) LCMS: R_T = 2.22 min., >98% @ 215 and 254 nm, m/z = 384.1 [M + H]$^+$. ^{1}H NMR (500 MHz, DMSO-d_6) δ 10.47 (s, 1H), 8.24 (dd, J = 15.8, 8.0 Hz, 1H), 8.15 (d, J = 7.3 Hz, 1H), 7.41 (d, J = 8.1 Hz, 1H), 6.00 (s, 1H), 5.88 (s, 2H), 4.07 (dd, J = 12.5, 8.7 Hz, 1H), 2.11 (s, 3H), 1.74 (dd, J = 24.2, 12.2 Hz, 6H), 1.66 (d, J = 12.4 Hz, 1H), 1.37 (dd, J = 23.0, 10.7 Hz, 2H), 1.19 (dd, J = 25.2, 12.5 Hz, 1H). ^{13}C NMR (125 MHz, DMSO-d_6) δ 163.65, 163.49, 146.07, 146.05, 144.62, 144.58, 144.38, 144.31, 134.42, 120.81, 112.22, 111.93, 99.01, 55.63, 32.96, 25.58, 25.38, 14.39.
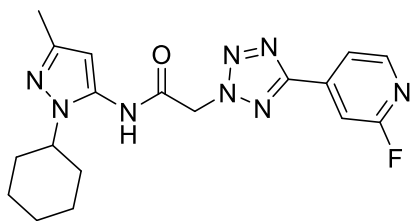
N-(1-cyclohexyl-3-methyl-1H-pyrazol-5-yl)-2-(5-(2-fluoropyridin-4-yl)-2H-tetrazol-2-yl)acetamide (29r). Yield = 14 mg, 18%, clear oil) LCMS: R_T = 2.44 min., >98% @ 215 and 254 nm, m/z = 385.1 [M + H]$^+$. ^{1}H NMR (500 MHz, DMSO-d_6) δ 10.48 (s, 1H), 8.50 (d, J = 5.1 Hz, 1H), 8.00 (d, J = 4.9 Hz, 1H), 7.77 (s, 1H), 6.00 (s, 1H), 5.92 (s, 2H), 4.12 – 4.02 (m, 1H), 2.10 (s, 3H), 1.86 – 1.70 (m, 6H), 1.67 (d, J = 12.3 Hz, 1H), 1.36 (dd, J = 25.0, 12.5 Hz, 2H), 1.19 (dd, J = 25.7, 12.8 Hz, 1H). ^{13}C NMR (125 MHz, DMSO-d_6) δ 165.13, 163.49, 163.25, 162.05, 149.94, 149.81, 146.07, 139.97, 134.41, 119.48, 107.13, 106.81, 98.92, 55.75, 55.61, 32.95, 25.63, 25.37, 14.38.
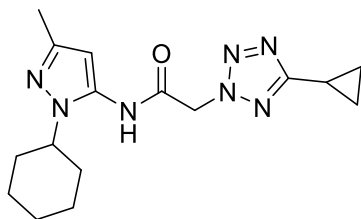
N-(1-cyclohexyl-3-methyl-1H-pyrazol-5-yl)-2-(5-cyclopropyl-2H-tetrazol-2-yl)acetamide (29s). Yield = 11 mg (17%, clear oil) LCMS: R_T = 2.32 min., >98% @ 215 and 254 nm, m/z = 330.1 [M + H]$^+$. ^{1}H NMR (500 MHz, CD$_3$OD) δ 6.06 (s, 1H), 5.60 (s, 2H), 4.04 (ddd, J = 15.4, 10.2, 5.0 Hz, 1H), 2.28 – 2.23 (m, 1H), 2.21 (s, 3H), 1.92 – 1.83 (m, 6H), 1.75 (d, J = 12.7 Hz, 1H), 1.52 – 1.42 (m, 2H), 1.31 (dd, J = 17.8, 8.1 Hz, 1H), 1.18 – 1.12 (m, 2H), 1.07 – 1.02 (m, 2H). ^{13}C NMR (125 MHz, CD$_3$OD) δ 169.06, 164.49, 147.39, 134.20, 99.46, 56.39, 54.20, 32.33, 25.36, 24.94, 12.32, 7.65, 5.81.
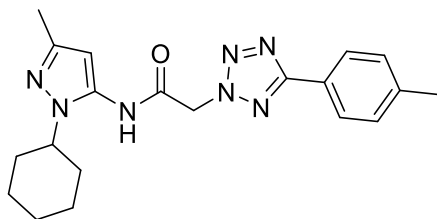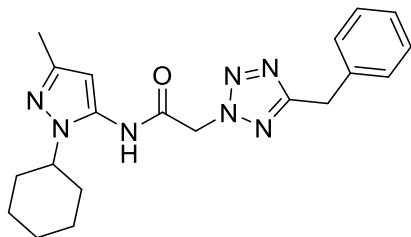
2-(5-benzyl-2H-tetrazol-2-yl)-N-(1-cyclohexyl-3-methyl-1H-pyrazol-5-yl)acetamide (29t): Yield = 11.0 mg (30.1%, white solid) LCMS: R_T = 2.56 min., >98% @ 215 and 254 nm, m/z = 366.1 [M + H]$^+$. ^{1}H NMR (500 MHz, DMSO-d_6) δ 10.87 (s, 1H), 7.52 – 7.35 (m, J = 14.8, 6.4 Hz, 5H), 6.08 (s, 2H), 5.97 (s, 1H), 3.97 (t, J = 11.0 Hz, 1H), 2.14 (s, 3H), 1.86 – 1.68 (m, 6H), 1.61 (d, J = 12.3 Hz, 1H), 1.35 – 1.22 (m, 2H), 1.22 – 1.13 (m, 1H). ^{13}C NMR (125 MHz, DMSO-d_6) δ 159.81, 156.20, 146.00, 134.00, 129.42, 129.31, 129.11, 101.01, 57.12, 55.87, 32.92, 25.54, 25.39, 14.42.
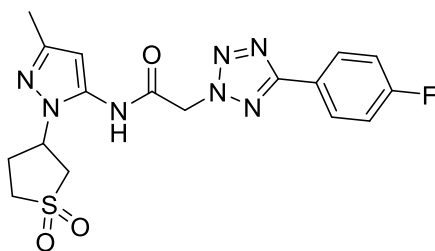
N-(1-(1,1-dioxidotetrahydrothiophen-3-yl)-3-methyl-1H-pyrazol-5-yl)-2-(5-(4-fluorophenyl)-2H-tetrazol-2-yl)acetamide (29u). Yield = 15.5 mg (21%, clear oil) LCMS: R_T = 2.37 min., >98% @ 215 and 254 nm, m/z = 420.1 [M + H]$^+$. ^{1}H NMR (500 MHz, DMSO-d_6) δ 10.64 (s, 1H), 8.14 (dd, J = 8.6, 5.5 Hz, 2H), 7.43 (t, J = 8.8 Hz, 2H), 6.08 (s, 1H), 5.84 (s, 2H), 5.25 – 5.16 (m, 1H), 3.62 (dd, J = 13.4, 8.3 Hz, 1H), 3.56 – 3.46 (m, 1H), 3.32 – 3.26 (m, 2H), 3.25 – 3.16 (m, 1H), 2.49 – 2.42 (m, J = 13.4 Hz, 1H), 2.15 (s, 3H). ^{13}C NMR (125 MHz, DMSO-d_6) δ 164.06, 163.97, 162.92, 148.02, 135.87, 129.31, 129.24, 123.79, 117.06, 116.88, 99.91, 55.33, 54.95, 52.15, 51.56, 29.56, 14.43.
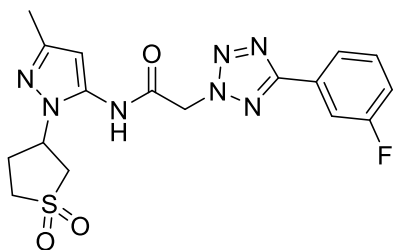
N-(1-(1,1-dioxidotetrahydrothiophen-3-yl)-3-methyl-1H-pyrazol-5-yl)-2-(5-(3-fluorophenyl)-2H-tetrazol-2-yl)acetamide (29v): Yield = 24.0 mg (33%, light yellow solid) LCMS: R_T = 2.4 min., >98% @ 215 and 254 nm, m/z = 420.1 [M + H]$^+$. ^{1}H NMR (500 MHz, DMSO-d_6) δ 10.65 (s, 1H), 7.95 (d, J = 7.7 Hz, 1H), 7.84 (d, J = 9.3 Hz, 1H), 7.66 (dd, J = 14.0, 8.0 Hz, 1H), 7.43 (td, J = 8.6, 2.3 Hz, 1H), 6.08 (s, 1H), 5.87 (s, 2H), 5.26 – 5.17 (m, 1H), 3.63 (dd, J = 13.4, 8.4 Hz, 1H), 3.57 – 3.48 (m, 1H), 3.32 – 3.27 (m, 1H), 3.20 (dt, J = 13.1, 8.6 Hz, 1H), 2.48 – 2.42 (m, 1H), 2.15 (s, 3H). ^{13}C NMR (125 MHz, DMSO-d_6) δ 164.01, 163.76, 161.95, 148.02, 135.86, 132.26, 132.19, 129.28, 123.05, 118.23, 118.07, 113.60, 113.41, 99.91, 55.43, 54.95, 52.15, 51.56.
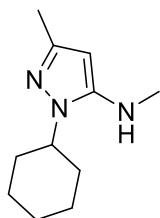
1-cyclohexyl-N,3-dimethyl-1H-pyrazol-5-amine. In a 10 mL RBF, formaldehyde (37% w/w, 45 µL, 0.56 mmol) was added dropwise to a solution of 1-cyclohexyl-3-methyl-1H-pyrazol-5-amine (0.10 g. 0.56 mmol) in MeOH (5 mL). Reaction was stirred for 30 min at RT followed by addition of acetic acid (33 µL, 0.56 mmol) and NaCNBH$_4$ (52 mg, 0.84 mmol) at 0 °C. The reaction was stirred at RT for 6 h. Crude was basified with 2 N NaOH$_{aq}$. Product was extracted with ethyl acetate (30 mL*2). Combined organic layer was washed with brine, dried over sodium sulphate and loaded on flash chromatography to afford product at 35% ethyl acetate in hexane. Yield = 18 mg (16%). LCMS: R_T = 1.73 min., >98% @ 215 and 254 nm, m/z = 194.1 [M + H]$^+$. ^{1}H NMR (500 MHz, DMSO-d_6) δ 5.24 (dd, J =

9.7, 4.7 Hz, 1H), 5.07 (s, 1H), 3.80 (m, *J* = 11.1, 4.1 Hz, 1H), 2.61 (d, *J* = 4.6 Hz, 3H), 2.00

(s, 3H), 1.80 – 1.69 (m, 4H), 1.68 – 1.60 (m, 3H), 1.37 – 1.27 (m, 2H), 1.16 (tt, *J* = 13.0,
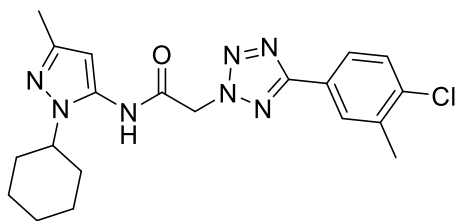
3.4 Hz, 1H).
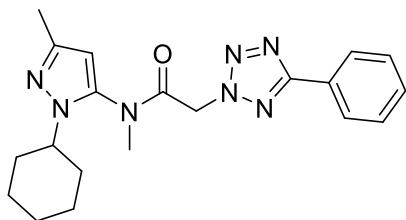
N-(1-cyclohexyl-3-methyl-1H-pyrazol-5-yl)-N-methyl-2-(5-phenyl-2H-tetrazol-2-

yl)acetamide (30a): Yield = 15.0 mg (48%, white solid) LCMS: R_T = 2.82 min., >98% @ 215 and

254 nm, *m/z* = 380.2 [M + H]$^+$. ^{1}H NMR (500 MHz, DMSO-d_6) δ 8.06 (dd, *J* = 10.7, 9.1 Hz, 2H),

7.63 – 7.53 (m, 3H), 6.31 (s, 1H), 5.67 (d, *J* = 16.6 Hz, 1H), 5.20 (d, *J* = 16.6 Hz, 1H), 4.02 (t, *J* =

11.2 Hz, 1H), 3.16 (s, 3H), 2.20 (s, 3H), 2.01 (d, *J* = 11.0 Hz, 1H), 1.94 – 1.62 (m, 6H), 1.56 – 1.42

(m, 2H), 1.23 (dd, *J* = 25.7, 12.9 Hz, 1H). ^{13}C NMR (125 MHz, DMSO-d_6) δ 165.58, 164.59,

147.24, 138.43, 131.16, 129.82, 127.18, 126.76, 102.83, 55.91, 54.12, 37.32, 33.58, 33.08, 25.44,

25.34, 14.56.
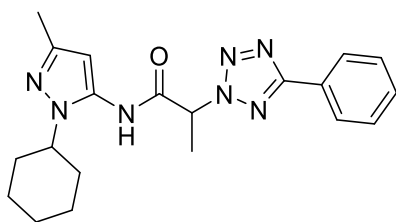
N-(1-cyclohexyl-3-methyl-1H-pyrazol-5-yl)-2-(5-phenyl-2H-tetrazol-2-yl)propenamide

(30b): Yield = 13 mg, 18%) LCMS: R_T = 2.62 min., >98% @ 215 and 254 nm, *m/z* = 380.2 [M +

H]$^+$. ^{1}H NMR (500 MHz, CDCl$_3$) δ 8.21 (d, *J* = 3.3 Hz, 2H), 7.55 (s, 3H), 6.16 (s, 1H), 5.84 (q, *J* =

7.1 Hz, 1H), 3.69 – 3.59 (m, 1H), 2.25 (s, 3H), 2.12 (d, *J* = 7.2 Hz, 3H), 1.87 – 1.73 (m, 7H), 1.57

(s, 1H), 1.18 (d, J = 6.4 Hz, 3H). ^{13}C NMR (125 MHz, CDCl$_3$) δ 166.10, 164.72, 147.33, 131.12, 129.11, 127.02, 126.40, 99.46, 63.09, 57.40, 32.48, 25.52, 25.48, 24.95, 17.92, 13.95.
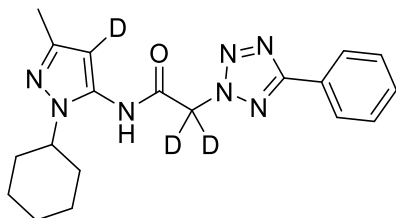
N-(1-cyclohexyl-3-methyl-1H-pyrazol-5-yl-4-d)-2-(5-phenyl-2H-tetrazol-2-yl)acetamide-2,2-d_2 (30c): 27a was refluxed in D$_2$O at 120º C under N$_2$ for 3 days. But the compound decays over time. LCMS: R$_T$ = 2.53 min., >98% @ 215 and 254 nm, m/z = 368.2 [M + H]$^+$. ^{1}H NMR (500 MHz, DMSO-d_6) δ 10.45 (s, 1H), 8.18 – 8.00 (m, 2H), 7.61 – 7.55 (m, 3H), 4.10 – 4.02 (m, 1H), 2.11 (s, 3H), 1.84 – 1.72 (m, 6H), 1.66 (d, J = 12.4 Hz, 1H), 1.42 – 1.30 (m, 2H), 1.19 (dd, J = 25.6, 12.8 Hz, 1H). ^{13}C NMR (125 MHz, DMSO-d_6) δ 164.73, 163.72, 145.96, 134.42, 131.17, 129.80, 127.20, 126.82, 55.59, 32.95, 25.62, 25.37, 14.37.
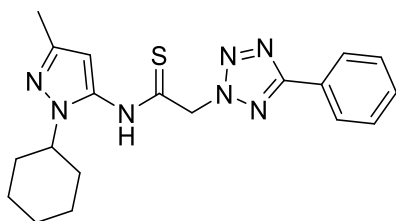
N-(1-cyclohexyl-3-methyl-1H-pyrazol-5-yl)-2-(5-phenyl-2H-tetrazol-2-yl)ethanethioamide (30d): 27a was refluxed with Lawesson's reagent in O-xylene:THF (5:1) at 75º C under N$_2$ for 12 hours. Yield = 8.0 mg (26 %, off-white solid) LCMS: R$_T$ = 2.73 min., >98% @ 215 and 254 nm, m/z = 382.1 [M + H]$^+$. ^{1}H NMR (500 MHz, CDCl$_3$) δ 9.21 (s, 1H), 8.20 (dd, J = 6.6, 2.9 Hz, 2H), 7.57 – 7.52 (m, 4H), 6.35 (s, 1H), 5.96 (s, 2H), 3.64 – 3.56 (m, 1H), 2.28 (s, 4H), 1.84 – 1.74 (m, J = 7.8 Hz, 7H), 1.61 (d, J = 22.4 Hz, 3H). ^{13}C NMR (125 MHz, CDCl$_3$) δ 190.58, 166.38, 147.37, 134.08, 131.22, 129.16, 127.07, 126.21, 100.67, 62.70, 57.54, 32.60, 25.46, 24.95, 14.15.
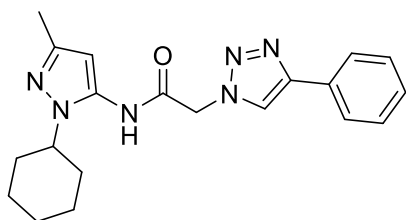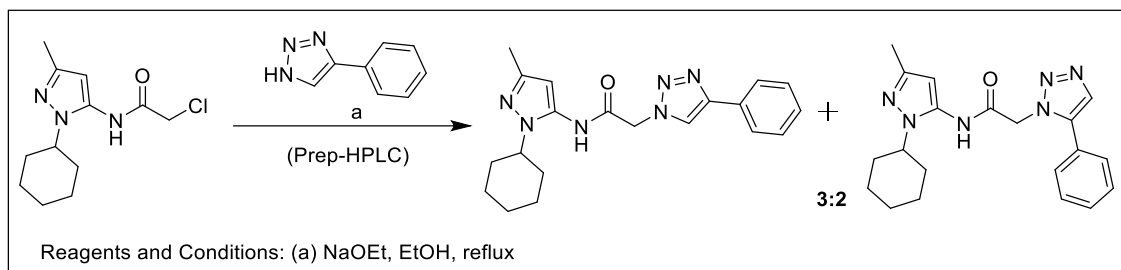
N-(1-cyclohexyl-3-methyl-1H-pyrazol-5-yl)-2-(4-phenyl-1H-1,2,3-triazol-1-yl)acetamide

(30e). Yield = 44 mg (30% collective yield of isomers, white solid) LCMS: R_T = 2.39 min., >98% @ 215 and 254 nm, m/z = 366.1 [M + H]$^+$. ^{1}H NMR (500 MHz, DMSO-d_6) δ 10.32 (s, 1H), 8.60 (s, 1H), 7.88 (d, J = 7.5 Hz, 2H), 7.47 (t, J = 7.5 Hz, 2H), 7.35 (t, J = 7.3 Hz, 1H), 6.00 (s, 1H), 5.46 (s, 2H), 4.11 – 4.01 (m, 1H), 2.11 (s, 3H), 1.85 – 1.72 (m, 6H), 1.66 (d, J = 12.1 Hz, 1H), 1.42 – 1.31 (m, 2H), 1.25 – 1.16 (m, 1H). ^{13}C NMR (125 MHz, DMSO-d_6) δ 164.93, 146.75, 146.21, 134.60, 130.95, 129.46, 128.47, 125.62, 123.52, 98.92, 55.64, 52.27, 32.91, 25.55, 25.32, 14.27. Isomers confirmed by HSQC.
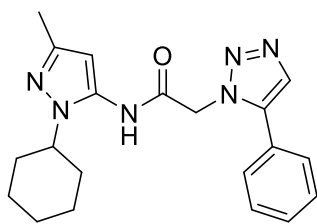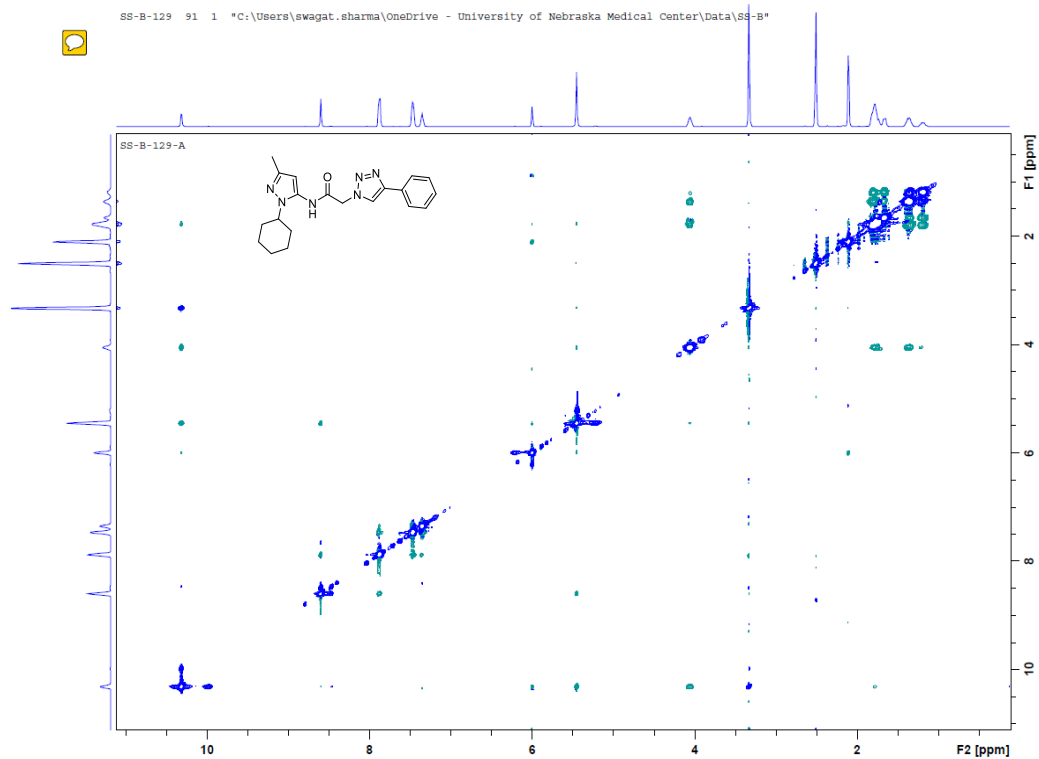
N-(1-cyclohexyl-3-methyl-1H-pyrazol-5-yl)-2-(5-phenyl-1H-1,2,3-triazol-1-yl)acetamide

(30f). Yield = 44 mg (30% collective yield of isomers, off-white solid) LCMS: R_T = 2.54 min., >98% @ 215 and 254 nm, m/z = 366.1 [M + H]$^+$. ^{1}H NMR (500 MHz, DMSO-d_6) δ 10.26 (s, 1H), 8.34 (s, 1H), 7.87 (d, J = 7.4 Hz, 2H), 7.48 (t, J = 7.4 Hz, 2H), 7.40 (t, J = 7.2 Hz, 1H), 5.98 (s, 1H), 5.46 (s, 2H), 4.05 (t, J = 10.3 Hz, 1H), 2.11 (s, 3H), 1.85 – 1.72 (m, 6H), 1.65 (d, J = 12.0 Hz, 1H), 1.41 – 1.30 (m, 2H), 1.22 – 1.15 (m, 1H). ^{13}C NMR (125 MHz, DMSO-d_6) δ 165.02, 147.90, 145.98, 134.73, 132.54, 130.35, 129.48, 129.03, 126.07, 99.00, 57.28, 55.55, 32.94, 25.61, 25.39, 14.41.

Reagents and conditions: (a) TEA, DCM, rt, 6 h (b) POCl$_3$, 110 °C, 4 h (c) LiOH, THF, water, MeOH, rt, 24 h (d) T3P
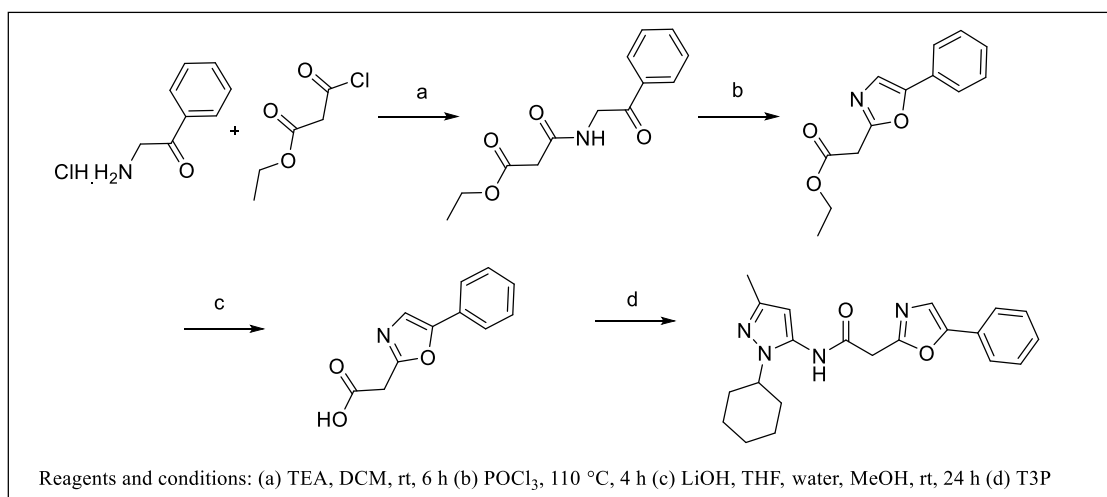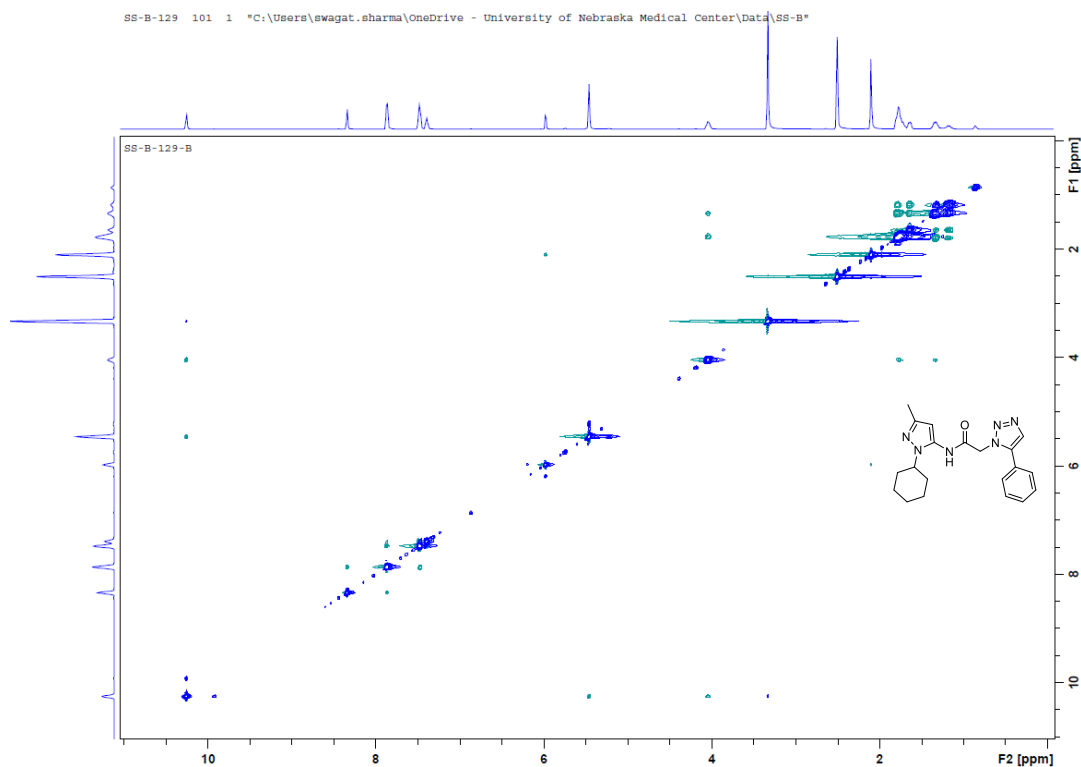
Ethyl 3-oxo-3-((2-oxo-2-phenylethyl)amino)propanoate. To a solution of 2-amino-1-phenylethan-1-one hydrochloride (1.0 g, 5.8 mmol) and ethyl 3-chloro-3-oxopropanoate (1.05 g, 7.01 mmol) in DCM (5 mL) at 0 °C was added TEA (2.40 mL, 17.5 mmol). The reaction was stirred at RT for 6 h. Product was partitioned between water (100 mL) and DCM (100 mL*2), organic

layer was washed with brine, dried over sodium sulphate and concentrated. Product obtained was used as such. Yield = 1.7 g (crude) LCMS: R_T = 2.03 min., >80% @ 215 and 254 nm, m/z = 250.0 [M + H]$^+$.

Ethyl 2-(5-phenyloxazol-2-yl)acetate. Ethyl-3-oxo-3-((2-oxphenylethyl)amino) propanoate (1.7 g, crude) was refluxed in POCl$_3$ (15 mL) at 110 °C for 4 h. Reaction was allowed to cool down, and was drop by drop added to a slurry of solid NaHCO$_3$ and ice. The mixture was stirred until effervesces seized and pH was slightly basic. Product was xtracted with ethyl acetate, washed with brine, dired over sodium sulphate, concentrated and used as such. LCMS: R_T = 2.46 min., >80% @ 215 and 254 nm, m/z = 232.1 [M + H]$^+$.

2-(5-phenyloxazol-2-yl)acetic acid. To a solution of ethyl 2-(5-phenyloxazol-2-yl)acetate (0.20 g, 0.86 mmol,) in THF (6 mL) and MeOH (1 mL) was added LiOH (59 mg, 2.6 mmol) dissolved in water. Reaction was stirred at rt for 24 h. Crude was diluted with water and impurities were washed with ethyl acetate (30 mL*2). Water layer was acidified upto pH-3 and product was extracted with ethyl acetate (30 mL *2). Organic layer was washed with brine, dired over sodium sulphate, concentrated and used as such. Yield = 60 mg (34 %). LCMS: R_T = 2.01 min., >95% @ 215 and 254 nm, m/z = 204.0 [M + H]$^+$.
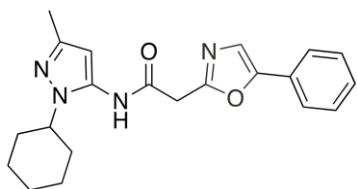
N-(1-cyclohexyl-3-methyl-1H-pyrazol-5-yl)-2-(5-phenyloxazol-2-yl)acetamide (30g). Yield = 25 mg (40%, yellow oil LCMS: R_T = 2.49 min., >98% @ 215 and 254 nm, m/z = 365.1 [M + H]$^+$. ^{1}H NMR (500 MHz, CD$_3$OD) δ 7.73 (d, J = 7.5 Hz, 2H), 7.50 (s, 1H), 7.47 (t, J = 7.6 Hz, 2H), 7.38 (t, J = 7.4 Hz, 1H), 6.06 (s, 1H), 4.08 (s, 2H), 4.07 – 4.00 (m, 1H), 2.22 (s, 3H), 1.92 – 1.80 (m, J

= 20.4, 12.1 Hz, 6H), 1.69 (d, J = 12.5 Hz, 1H), 1.47 – 1.34 (m, 2H), 1.33 – 1.23 (m, 1H). ^{13}C NMR (125 MHz, CD$_3$OD) δ 166.60, 158.32, 152.48, 147.26, 134.73, 128.69, 128.45, 127.54, 123.89, 121.45, 99.61, 56.35, 35.23, 32.29, 25.34, 24.94, 12.30.
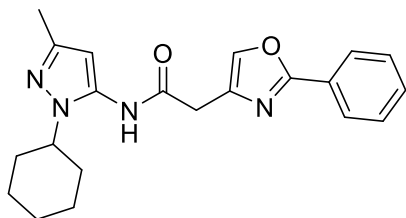
N-(1-cyclohexyl-3-methyl-1H-pyrazol-5-yl)-2-(2-phenyloxazol-4-yl)acetamide (30h). Yield = 25 mg (30%, off-white solid) LCMS: R$_T$ = 2.58 min., >98% @ 215 and 254 nm, *m/z* = 365.1 [M + H][+]. ^{1}H NMR (500 MHz, DMSO-*d₆*) δ 9.95 (s, 1H), 8.08 (s, 1H), 8.01 – 7.96 (m, 2H), 7.58 – 7.50 (m, 3H), 5.95 (s, 1H), 4.04 – 3.96 (m, 1H), 3.71 (s, 2H), 2.10 (s, 3H), 1.80 – 1.67 (m, 6H), 1.57 (d, J = 12.1 Hz, 1H), 1.33 – 1.21 (m, 2H), 1.15 (t, J = 12.7 Hz, 1H). ^{13}C NMR (125 MHz, DMSO-*d₆*) δ 168.29, 160.84, 145.78, 137.57, 136.54, 135.38, 131.07, 129.59, 127.33, 126.28, 99.28, 55.48, 34.03, 32.89, 25.58, 25.37, 14.41.
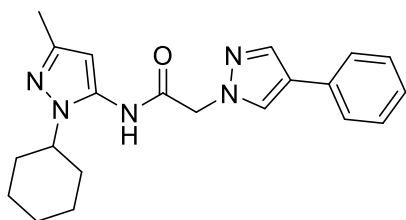
N-(1-cyclohexyl-3-methyl-1H-pyrazol-5-yl)-2-(4-phenyl-1H-pyrazol-1-yl)acetamide (30i). Yield = 12 mg (12%, off-white solid) LCMS: R$_T$ = 2.53 min., >98% @ 215 and 254 nm, *m/z* = 364.1 [M + H][+]. ^{1}H NMR (500 MHz, DMSO-*d₆*) δ 10.14 (s, 1H), 8.21 (s, 1H), 7.95 (s, 1H), 7.60 (d, J = 7.4 Hz, 2H), 7.37 (t, J = 7.7 Hz, 2H), 7.21 (t, J = 7.4 Hz, 1H), 5.98 (s, 1H), 5.09 (s, 2H), 4.07 – 3.99 (m, 1H), 2.10 (s, 3H), 1.85 – 1.71 (m, 6H), 1.65 (d, J = 12.2 Hz, 1H), 1.40 – 1.29 (m, 2H), 1.24 – 1.14 (m, 1H). ^{13}C NMR (125 MHz, DMSO-*d₆*) δ 166.05, 145.91, 137.24, 134.94, 132.88, 129.32, 129.23, 126.54, 125.44, 122.50, 98.82, 55.50, 54.64, 32.93, 25.61, 25.39, 14.41.
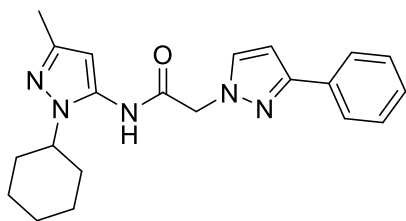
N-(1-cyclohexyl-3-methyl-1H-pyrazol-5-yl)-2-(3-phenyl-1H-pyrazol-1-yl)acetamide   (30j).
Yield =17 mg (71%, white solid) LCMS: R_T = 2.52 min., >98% @ 215 and 254 nm, *m/z* = 364.2
[M + H]⁺. ¹H NMR (500 MHz, CDCl₃) δ 9.00 (s, 1H), 7.86 (d, *J* = 7.2 Hz, 2H), 7.60 (d, *J* = 2.2 Hz,
1H), 7.46 (t, *J* = 7.5 Hz, 2H), 7.39 (t, *J* = 7.4 Hz, 1H), 6.73 (d, *J* = 2.3 Hz, 1H), 6.26 (s, 1H), 5.01
(s, 2H), 3.58 – 3.47 (m, 1H), 2.24 (s, 3H), 1.75 (dd, *J* = 18.0, 5.1 Hz, 4H), 1.62 (d, *J* = 13.4 Hz,
2H), 1.44 (d, *J* = 12.9 Hz, 1H), 1.15 – 1.03 (m, 1H), 0.98 – 0.87 (m, 2H). ¹³C NMR (125 MHz,
CDCl₃) δ 163.99, 154.36, 147.28, 133.28, 132.22, 128.89, 128.63, 125.76, 104.13, 97.74, 57.07,
55.20, 32.40, 25.13, 24.86, 13.98.
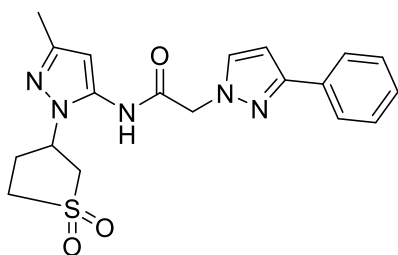
**N-(1-(1,1-dioxidotetrahydrothiophen-3-yl)-3-methyl-1H-pyrazol-5-yl)-2-(3-phenyl-1H-
pyrazol-1-yl)acetamide (30k).** Yield = 45 mg (66%, light yellow oil) LCMS: R_T = 2.30 min.,
>98% @ 215 and 254 nm, *m/z* = 400.1 [M + H]⁺. ¹H NMR (500 MHz, DMSO-*d₆*) δ 10.35 (s, 1H),
7.84 (d, *J* = 2.1 Hz, 1H), 7.80 (d, *J* = 7.4 Hz, 2H), 7.41 (t, *J* = 7.6 Hz, 2H), 7.30 (t, *J* = 7.3 Hz, 1H),
6.77 (d, *J* = 2.2 Hz, 1H), 6.07 (s, 1H), 5.23 – 5.16 (m, 1H), 5.14 (s, 2H), 3.62 (dd, *J* = 13.4, 8.4 Hz,
1H), 3.55 – 3.47 (m, 1H), 3.35 – 3.27 (m, 2H), 3.18 (dt, *J* = 13.1, 8.5 Hz, 1H), 2.48 – 2.40 (m, 1H),
2.14 (s, 3H). ¹³C NMR (125 MHz, DMSO-*d₆*) δ 166.50, 150.96, 147.90, 136.40, 133.99, 133.69,
129.12, 127.98, 125.57, 103.40, 99.65, 54.97, 54.55, 52.14, 51.54, 29.57, 14.44.
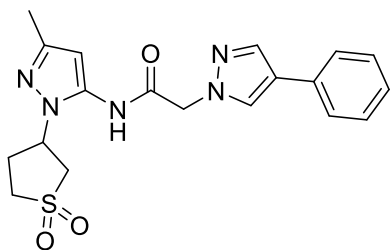
N-(1-(1,1-dioxidotetrahydrothiophen-3-yl)-3-methyl-1*H*-pyrazol-5-yl)-2-(4-phenyl-1*H*-pyrazol-1-yl)acetamide (30l). Yield = 40 mg (40%, clear oil) LCMS: R_T = 2.28 min., >98% @ 215 and 254 nm, *m/z* = 400.1 [M + H]⁺. ¹H NMR (500 MHz, DMSO-*d₆*) δ 10.34 (s, 1H), 8.21 (s, 1H), 7.94 (s, 1H), 7.59 (t, *J* = 7.4 Hz, 2H), 7.37 (t, *J* = 7.6 Hz, 2H), 7.21 (t, *J* = 7.4 Hz, 1H), 6.06 (s, 1H), 5.16 (dd, *J* = 15.5, 8.1 Hz, 1H), 5.11 (s, 2H), 3.62 (dd, *J* = 13.4, 8.3 Hz, 1H), 3.55 – 3.47 (m, 1H), 3.32 – 3.26 (m, 2H), 3.25 – 3.17 (m, 1H), 2.46 – 2.40 (m, 1H), 2.14 (s, 3H).
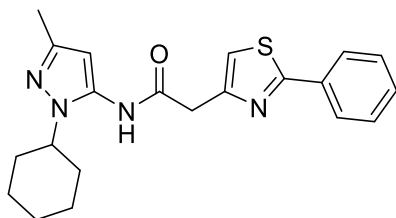
N-(1-cyclohexyl-3-methyl-1*H*-pyrazol-5-yl)-2-(2-phenylthiazol-4-yl)acetamide (30m). Yield = 30 mg (28%, off-white solid) LCMS: R_T = 2.60 min., >98% @ 215 and 254 nm, *m/z* = 381.1 [M + H]⁺. ¹H NMR (500 MHz, CDCl₃) δ 9.34 (s, 1H), 7.97 (dd, *J* = 6.5, 2.9 Hz, 2H), 7.52 – 7.47 (m, 3H), 7.20 (s, 1H), 6.20 (s, 1H), 3.98 (d, *J* = 16.9 Hz, 2H), 3.73 – 3.63 (m, *J* = 15.2, 10.4, 5.1 Hz, 1H), 2.24 (d, *J* = 9.5 Hz, 3H), 1.82 – 1.75 (m, *J* = 9.5 Hz, 4H), 1.66 (d, *J* = 13.2 Hz, 2H), 1.48 (d, *J* = 13.0 Hz, 1H), 1.17 – 1.08 (m, 1H), 1.01 – 0.90 (m, 2H). ¹³C NMR (125 MHz, CDCl₃) δ 169.78, 166.46, 149.92, 147.24, 134.47, 132.86, 130.79, 129.24, 126.58, 116.56, 98.46, 56.84, 39.32, 32.47, 25.30, 24.94, 14.05.

Reagents and condition: (a) diethyl malonate, picolinic acid, CuI, Cs₂CO₃, 1,4-dioxane, 90 °C, 48 h (b) K₂CO₃, EtOH, water, 85 °C, 8 h (c) T3P, TEA, DCM, rt, 1 h
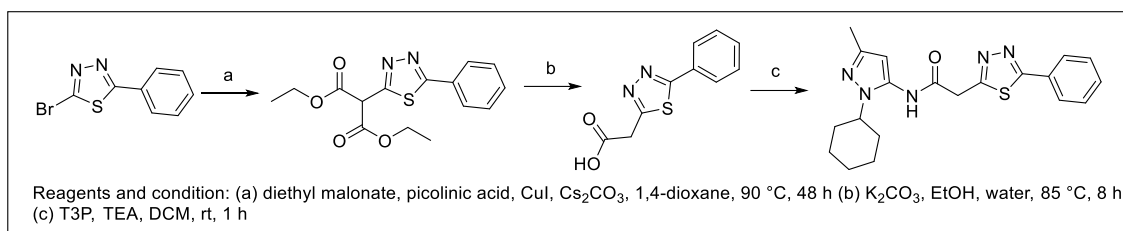
Diethyl 2-(5-phenyl-1,3,4-thiadiazol-2-yl)malonate. In an oven dried seal tube, 2-bromo-5-phenyl-1,3,4-thiadiazole (150 mg, 0.62 mmol), diethyl malonate Yield = 198 mg, 1.24 mmol), picolinic acid (15.2 mg, 0.124 mmol), CuI (11.8 g, 0.062 mmol), Cs₂CO₃ (604 mg, 1.86 mmol) in anhydrous 1,4-dioxane (1 mL) under inert atmosphere were reacted at 90 ℃ for 48 h. Crude was directly loaded on flash chromatography, product eluted out in 0-25 % ethyl acetate in hexane. Yield = 80 mg (40%) LCMS: R_T = 3.0 min., >98% @ 215 and 254 nm, m/z = 321.0 [M + H]⁺. ¹H NMR (500 MHz, CDCl₃) δ 13.50 (s, 1H), 7.86 (dd, J = 7.5, 1.9 Hz, 2H), 7.54 – 7.48 (m, 3H), 4.34 (qd, J = 7.1, 2.5 Hz, 4H), 1.40 (tt, J = 9.8, 4.9 Hz, 6H).

2-(5-phenyl-1,3,4-thiadiazol-2-yl)acetic acid. Diethyl 2-(5-phenyl-1,3,4-thiadiazol-2-yl)malonate (0.080 g, 0.25 mmo) and K₂CO₃ (65 mg, 0.50 mmol) in ethanol (1.4 mL) and water (0.6 mL) were stirred at 85 ℃ for 8 h. Crude was evaporated, add water (30 mL), acidified up to pH-3 and product extracted with ethyl acetate (25 mL*2). Combine organic layer was washed with brine, dried over sodium sulphate, evaporated and used as such. Yield = 20 mg (36%) LCMS: R_T = 1.96 min., >98% @ 215 and 254 nm, m/z = 221.0 [M + H]⁺. ¹H NMR (500 MHz, DMSO-d_6) δ 7.98 – 7.91 (m, 2H), 7.62 – 7.53 (m, 3H), 2.78 (s, 2H). ¹³C NMR (125 MHz, DMSO-d_6) δ 169.29, 168.54, 165.73, 131.58, 130.24, 129.90, 127.99, 127.97, 15.77.

***N*-(1-cyclohexyl-3-methyl-1*H*-pyrazol-5-yl)-2-(5-phenyl-1,3,4-thiadiazol-2-yl)acetamide**
(30n): Yield = 9 mg (31%) LCMS: R_T = 2.47 min., >98% @ 215 and 254 nm, m/z = 382.1 [M + H]⁺. ¹H NMR (500 MHz, CD₃OD) δ 8.01 – 7.98 (m, J = 7.4, 1.5 Hz, 2H), 7.60 – 7.53 (m, 3H), 6.08 (s, 1H), 4.85 (s, 2H), 4.09 – 4.00 (m, 1H), 2.23 (s, 3H), 1.93 – 1.82 (m, J = 21.7, 9.0 Hz, 6H), 1.71 (d, J = 12.6 Hz, 1H), 1.48 – 1.37 (m, J = 9.8, 3.4 Hz, 2H), 1.34 – 1.25 (m, J = 24.3, 11.3 Hz, 1H).

¹³C NMR (125 MHz, CD₃OD) δ 170.37, 167.35, 163.51, 147.28, 134.71, 131.18, 129.70, 129.10, 127.41, 99.50, 56.31, 32.33, 25.35, 24.95, 12.31.
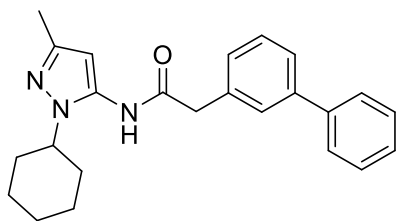
2-([1,1'-biphenyl]-3-yl)-*N*-(1-cyclohexyl-3-methyl-1*H*-pyrazol-5-yl)acetamide (30o): Yield = 31 mg (50%, off-white solid) LCMS: R_T = 2.82 min., >98% @ 215 and 254 nm, *m/z* = 374.1 [M + H]⁺. ¹H NMR (500 MHz, CDCl₃) δ 7.65 – 7.58 (m, 4H), 7.53 (t, *J* = 7.6 Hz, 1H), 7.48 (t, *J* = 7.5 Hz, 2H), 7.40 (t, *J* = 7.3 Hz, 1H), 7.35 (d, *J* = 7.4 Hz, 1H), 6.09 (s, 1H), 3.86 (s, 2H), 3.51 – 3.44 (m, 1H), 2.23 (s, 3H), 1.77 – 1.68 (m, 6H), 1.55 (d, *J* = 8.9 Hz, 1H), 1.14 – 1.04 (m, 3H). ¹³C NMR (125 MHz, CDCl₃) δ 168.92, 147.14, 142.62, 140.19, 134.77, 133.75, 129.94, 128.95, 128.24, 128.21, 127.85, 127.09, 126.78, 99.33, 57.21, 44.09, 32.42, 25.58, 24.99, 14.01.
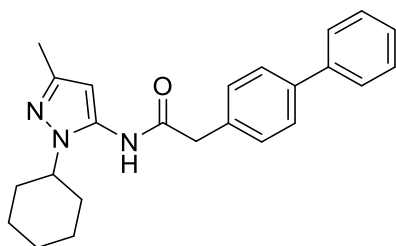
2-([1,1'-biphenyl]-4-yl)-*N*-(1-cyclohexyl-3-methyl-1*H*-pyrazol-5-yl)acetamide (30p): Yield = 24 mg (29%, white solid) LCMS: R_T = 2.96 min., >98% @ 215 and 254 nm, *m/z* = 374.1 [M + H]⁺. ¹H NMR (500 MHz, DMSO-*d₆*) δ 9.93 (s, 1H), 7.65 (dd, *J* = 7.8, 2.7 Hz, 4H), 7.46 (dd, *J* = 14.8, 7.7 Hz, 4H), 7.36 (t, *J* = 7.3 Hz, 1H), 3.86 – 3.77 (m, 1H), 3.70 (s, 2H), 2.10 (s, 3H), 1.77 – 1.64 (m, 6H), 1.57 (d, *J* = 10.6 Hz, 1H), 1.23 – 1.09 (m, 3H). ¹³C NMR (125 MHz, DMSO-*d₆*) δ 169.97, 145.75, 140.43, 139.12, 135.53, 135.37, 130.08, 129.39, 127.80, 127.18, 127.02, 99.56, 55.48, 42.47, 32.82, 25.57, 25.36, 14.41.
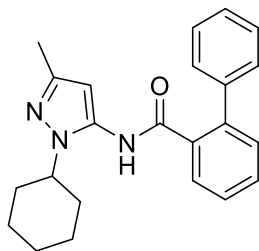
N-(1-cyclohexyl-3-methyl-1H-pyrazol-5-yl)-[1,1'-biphenyl]-2-carboxamide (30q): Yield = 7 mg (35%, white solid) LCMS: R_T = 2.68 min., >98% @ 215 and 254 nm, m/z = 360.1 [M + H]$^+$.

Reagents and condition: (a) T3P, TEA, DCM, rt, 1 h (b) Phenyl boronic acid, PdCl$_2$.dppf.DCM, Cs$_2$CO$_3$, 1,4-dioxane, MW, 120 °C, 30 min
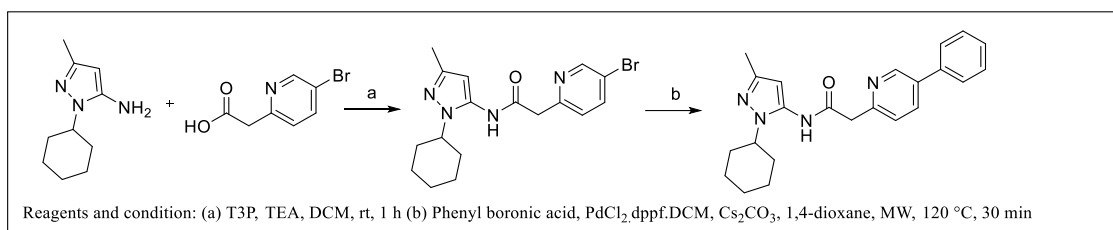
2-(5-bromopyridin-2-yl)-N-(1-cyclohexyl-3-methyl-1H-pyrazol-5-yl)acetamide. Prepared according to general procedure using T3P. Yield = 220 mg (84%) LCMS: R_T = 2.37 min., >98% @ 215 and 254 nm, m/z = 377.1, 379.0 [M + H]$^+$, [M + H+2]$^+$. ^{1}H NMR (500 MHz, DMSO-d_6) δ 10.02 (s, 1H), 8.65 (d, J = 2.3 Hz, 1H), 8.04 (dd, J = 8.3, 2.5 Hz, 1H), 7.41 (d, J = 8.3 Hz, 1H), 5.92 (s, 1H), 4.00 – 3.91 (m, 1H), 3.87 (s, 2H), 2.09 (s, 3H), 1.81 – 1.63 (m, 7H), 1.31 – 1.21 (m, 2H), 1.20 – 1.11 (m, 1H). ^{13}C NMR (125 MHz, DMSO-d_6) δ 168.47, 155.34, 150.09, 145.75, 139.68, 135.36, 126.43, 118.95, 99.21, 55.44, 44.53, 32.87, 25.65, 25.41, 14.41.

N-(1-cyclohexyl-3-methyl-1H-pyrazol-5-yl)-2-(5-phenylpyridin-2-yl)acetamide (30r). In a 10 mL microwave vial, 2-(5-bromopyridin-2-yl)-N-(1-cyclohexyl-3-methyl-1H-pyrazol-5-yl)acetamide (0.060 g, 0.16 mmol,), phenyl boronic acid (29 mg, 0.29 mmol) and Cs$_2$CO$_3$ in 1,4-dioxane (1 mL) were degassed with nitrogen for 5 mins, PdCl$_2$.dppf.DCM (11.6 mg, 0.016 mmol) was added to it and reaction was subjected to microwave at 120 °C for 30 min. Crude was filtered over celite, concentrated and loaded on flash chromatography. Product elutes out at 0-40% ethyl acetate in hexane. (33 mg, 66%, yellow oil) LCMS: R_T = 2.47 min., >98% @ 215 and 254 nm, m/z =

375.2 [M + H]$^+$. ^{1}H NMR (500 MHz, DMSO-d_6) δ 10.05 (s, 1H), 8.80 (d, J = 34.5 Hz, 1H), 8.08 (d, J = 7.7 Hz, 1H), 7.72 (d, J = 7.5 Hz, 2H), 7.54 – 7.48 (m, J = 12.9, 5.8 Hz, 3H), 7.43 (t, J = 7.2 Hz, 1H), 5.95 (s, 1H), 4.05 – 3.95 (m, J = 10.6 Hz, 1H), 3.93 (s, 2H), 2.10 (s, 3H), 1.81 – 1.68 (m, 6H), 1.62 (d, J = 12.0 Hz, 1H), 1.24 (dd, J = 24.8, 15.0 Hz, 2H), 1.20 – 1.12 (m, 1H). ^{13}C NMR (125 MHz, DMSO-d_6) δ 168.86, 155.36, 147.45, 145.77, 137.43, 135.48, 135.20, 134.32, 129.63, 128.52, 127.24, 124.46, 99.24, 55.45, 44.94, 32.88, 25.65, 25.41, 14.42.
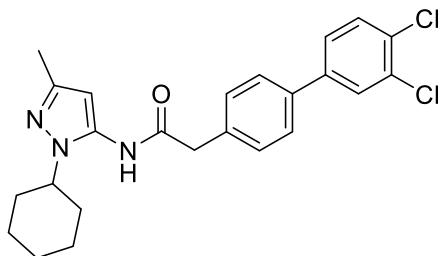
N-(1-cyclohexyl-3-methyl-1H-pyrazol-5-yl)-2-(3',4'-dichloro-[1,1'-biphenyl]-4-yl)acetamide

(30s): Yield = 35 mg (35%, white solid) LCMS: R$_T$ = 2.47 min., >98% @ 215 and 254 nm, m/z = 442.1 [M + H]$^+$. ^{1}H NMR (500 MHz, DMSO-d_6) δ 9.94 (s, 1H), 7.92 (d, J = 1.6 Hz, 1H), 7.71 (dd, J = 8.1, 3.2 Hz, 3H), 7.66 (dd, J = 8.4, 1.7 Hz, 1H), 7.46 (d, J = 8.0 Hz, 2H), 5.92 (s, 1H), 3.81 (tt, J = 9.8, 4.8 Hz, 1H), 3.71 (s, 2H), 2.09 (s, 3H), 1.77 – 1.64 (m, J = 29.5, 15.9 Hz, 6H), 1.57 (d, J = 10.4 Hz, 1H), 1.21 – 1.09 (m, 3H). ^{13}C NMR (125 MHz, DMSO-d_6) δ 169.79, 145.76, 141.00, 136.59, 136.40, 135.35, 132.17, 131.47, 130.53, 130.25, 128.76, 127.29, 127.20, 99.50, 55.49, 42.43, 32.82, 25.58, 25.36, 14.41.

General Procedure D for synthesis of ether series (Class-III)

Reagents and Conditions: (a) K$_2$CO$_3$, DMF; (b) LiOH
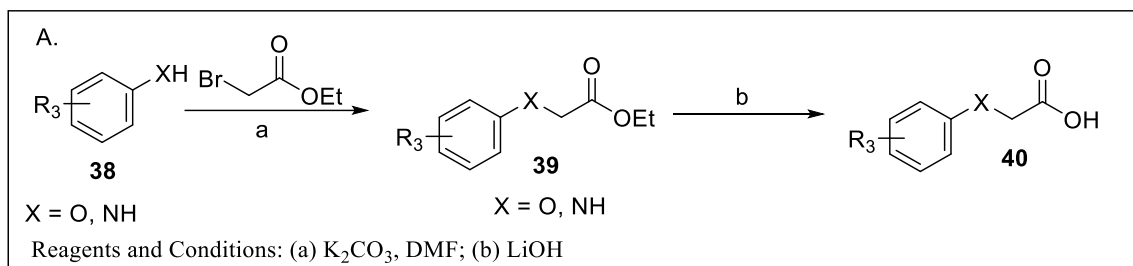
Step-1 (39): In a vial, the substituted phenol or aniline (3.89 mmol) and potassium carbonate (1.49 g, 10.8 mmol) were dissolved in DMF (3.0 mL), followed by the addition of ethyl 2-bromoacetate (520 µL, 4.6 mmol). The reaction was stirred at 60 ˚C overnight, then diluted with ethyl acetate and washed with saturated sodium bicarbonate, dried over anhydrous sodium sulfate, filtered, and concentrated under vacuum. The crude product was used without further purification.
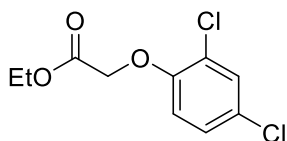
ethyl 2-(2,4-dichlorophenoxy)acetate: Yield = 0.4 g (87%) ^{1}H NMR (500 MHz, DMSO-d_6) δ 7.60 (d, J = 2.5 Hz, 1H), 7.36 (dd, J = 8.9, 2.5 Hz, 1H), 7.10 (d, J = 8.9 Hz, 1H), 4.94 (s, 2H), 4.17 (q, J = 7.1 Hz, 2H), 1.21 (t, J = 7.1 Hz, 3H).

Step-2 (40): In a vial, the substituted ethyl 2-phenoxyacetate or ethyl 2-phenylglycinate (3.33 mmol) and lithium hydroxide (120 mg, 5.0 mmol) were dissolved in 12.0 mL of a 3:1.5:7.5 mixture of H$_2$O, methanol, and tetrahydrofuran, respectively. The reaction was stirred overnight at room temperature, then diluted with water and washed with ethyl acetate, the aqueous layer was acidified and precipitated product was extracted again with ethyl acetate. Organic layer washed with brine, dried over anhydrous sodium sulfate, filtered, and concentrated under vacuum. Product used as such.
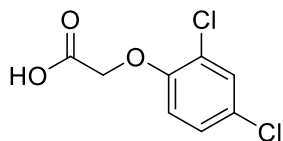
2-(2,4-dichlorophenoxy)acetic acid: Yield = 0.28 g (78.8%) ^{1}H NMR (500 MHz, DMSO-d_6) δ

13.16 (s, 1H), 7.59 (d, J = 2.6 Hz, 1H), 7.35 (dd, J = 8.9, 2.6 Hz, 1H), 7.07 (d, J = 8.9 Hz, 1H),

4.84 (s, 2H). ^{13}C NMR (125 MHz, DMSO-d_6) δ 169.96, 152.81, 129.83, 128.37, 125.27, 122.70,

115.38, 65.65.
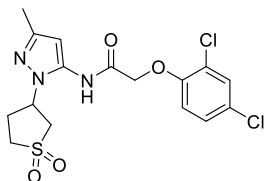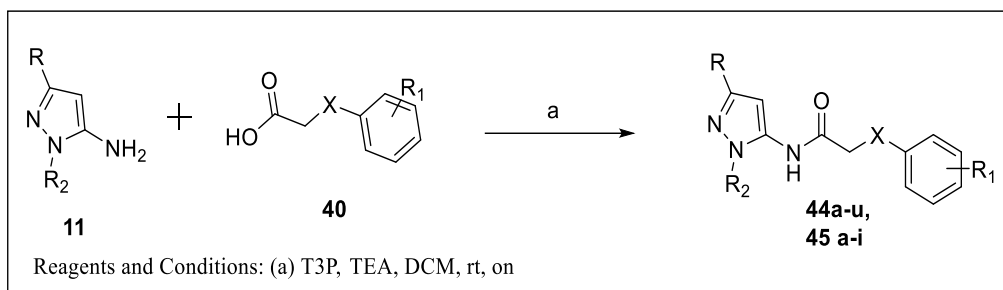
2-(2,4-dichlorophenoxy)-*N*-(1-(1,1-dioxidotetrahydrothiophen-3-yl)-3-methyl-1*H*-pyrazol-5-yl)acetamide (44a) In a 1 dram vial, to a stirred solution of 3-(5-amino-3-methyl-1H-pyrazol-1-yl)tetrahydrothiophene 1,1-dioxide (50.0 mg, 0.230 mmol), 2-(2,4-dichlorophenoxy)acetic acid (51 mg, 0.23 mmol) and TEA (96 µL, 0.69 mmol) in DCM (1.0 mL) was dropwise added propylphosphonic anhydride solution ≥50 wt. % in ethyl acetate (171 µL, 0.270 mmol). The reaction was stirred at RT overnight. The product was partitioned between ethyl acetate (15 mL * 2) and water (15 mL). Organic layers were combined, washed with brine, dried over sodium sulphate, concentrated and purified by reverse phase preparative chromatography (0-100% CH_3CN in water). Yield = 77.9 mg (80%, white solid) LCMS: R_T = 2.5 min., >95% @ 215 and 254 nm, *m/z* = 420.0 [M + H]$^+$. ^{1}H NMR (500 MHz, DMSO-*d6*) δ 10.18 (s, 1H), 7.62 (d, *J* = 2.5 Hz, 1H), 7.39 (dd, *J* = 8.9, 2.5 Hz, 1H), 7.13 (d, *J* = 8.9 Hz, 1H), 6.04 (s, 1H), 5.11 (p, *J* = 8.0 Hz, 1H), 4.93 (s, 2H), 3.58 (dd, *J* = 13.4, 8.4 Hz, 1H), 3.49 (dt, *J* = 12.8, 6.3 Hz, 1H), 3.29 (dd, *J* = 13.4, 8.5 Hz, 1H), 3.18 (dt, *J* = 12.7, 8.5 Hz, 1H), 2.46 (dd, *J* = 11.2, 4.5 Hz, 2H), 2.15 (s, 3H). ^{13}C NMR (125 MHz, DMSO-*d6*) δ 166.89, 152.97, 147.87, 136.05, 129.93, 128.49, 125.62, 122.95, 115.77, 100.14, 67.84, 54.95, 52.13, 51.56, 29.53, 14.43.
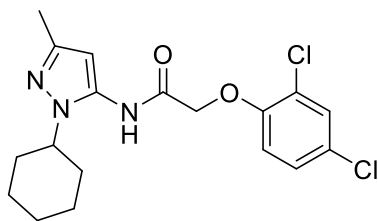
N-(1-cyclohexyl-3-methyl-1H-pyrazol-5-yl)-2-(2,4-dichlorophenoxy)acetamide. (44b). Yield =26.0 mg (43.3%, white solid) LCMS: R_T = 2.88 min., >95% @ 215 and 254 nm, *m/z* = 382.0 [M+H]$^+$. ^{1}H NMR (500 MHz, DMSO-*d$_6$*) δ 9.97 (s, 1H), 7.63 (d, *J* = 2.4 Hz, 1H), 7.40 (dd, *J* = 8.9, 2.4 Hz, 1H), 7.11 (d, *J* = 8.9 Hz, 1H), 5.97 (s, 1H), 3.93 (dt, *J* = 9.8, 5.3 Hz, 1H), 2.11 (s, 1H), 1.82 – 1.68 (m, 3H), 1.64 (d, *J* = 12.5 Hz, 1H), 1.28 (dd, *J* = 25.0, 12.5 Hz, 1H), 1.16 (dd, *J* = 24.8, 12.1 Hz, 1H). ^{13}C NMR (125 MHz, DMSO-*d$_6$*) δ 166.47, 152.91, 145.89, 134.59, 129.93, 128.47, 125.58, 122.95, 115.59, 99.13, 68.01, 55.54, 32.88, 25.60, 25.39, 14.39.
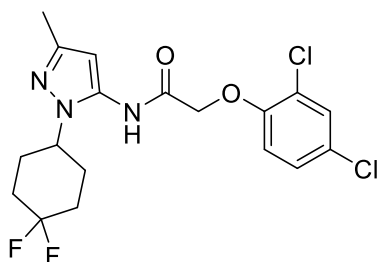
2-(2,4-dichlorophenoxy)-N-(1-(4,4-difluorocyclohexyl)-3-methyl-1H-pyrazol-5-yl)acetamide (44c) Yield =36 mg (62.0%, white solid) LCMS: R_T = 2.78 min., >95% @ 215 and 254 nm, *m/z* = 418.0 [M+H]$^+$. ^{1}H NMR (500 MHz, DMSO-*d$_6$*) δ 10.02 (s, 1H), 7.63 (d, *J* = 2.4 Hz, 1H), 7.41 (dd, *J* = 8.9, 2.4 Hz, 1H), 7.13 (d, *J* = 8.9 Hz, 1H), 5.98 (s, 1H), 4.92 (s, 2H), 4.16 (t, *J* = 10.0 Hz, 1H), 2.13 (d, *J* = 5.3 Hz, 2H), 2.12 (s, 3H), 2.04 – 1.92 (m, 3H), 1.86 (s, 3H). ^{13}C NMR (125 MHz, DMSO-*d$_6$*) δ 166.82, 152.95, 146.45, 135.02, 129.95, 128.48, 125.62, 122.97, 115.66, 99.77, 67.91, 52.78, 32.41, 28.66, 28.58, 14.39.
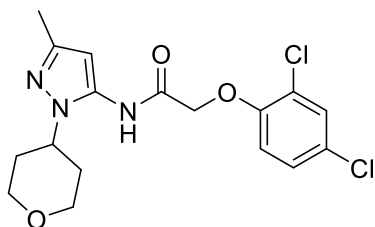
2-(2,4-dichlorophenoxy)-*N*-(3-methyl-1-(tetrahydro-2*H*-pyran-4-yl)-1*H*-pyrazol-5-yl)acetamide (44d). Yield = 40 mg (63.0 %, white solid) LCMS: R_T = 2.47 min., >95% @ 215 and 254 nm, *m/z* = 384.0 [M+H]⁺. ¹H NMR (500 MHz, DMSO-*d₆*) δ 10.04 (s, 1H), 7.63 (d, *J* = 2.4 Hz, 1H), 7.41 (dd, *J* = 8.9, 2.4 Hz, 1H), 7.12 (d, *J* = 8.9 Hz, 1H), 5.99 (s, 1H), 4.92 (s, 2H), 4.92 (s, 2H), 4.24 – 4.15 (m, 1H), 3.95 (dd, *J* = 11.3, 3.8 Hz, 2H), 3.41 – 3.34 (m, 2H), 2.12 (s, 3H), 2.01 – 1.92 (m, 2H), 1.69 (d, *J* = 10.7 Hz, 2H). ¹³C NMR (125 MHz, DMSO-*d₆*) δ 166.63, 152.93, 146.31, 134.87, 129.96, 128.50, 125.60, 122.96, 115.61, 99.49, 67.97, 66.74, 52.83, 32.91, 14.41.
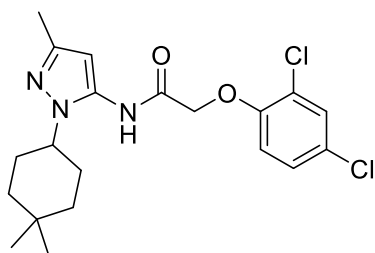
2-(2,4-dichlorophenoxy)-*N*-(1-(4,4-dimethylcyclohexyl)-3-methyl-1*H*-pyrazol-5-yl)acetamide (44e). Yield =29.0 mg (76.0%, off-white solid) LCMS: R_T = 3.15 min., >95% @ 215 and 254 nm, *m/z* = 410.1 [M+H]⁺. ¹H NMR (500 MHz, DMSO-*d₆*) δ 9.96 (s, 1H), 7.64 (d, *J* = 2.2 Hz, 1H), 7.39 (dd, *J* = 8.8, 2.2 Hz, 1H), 7.12 (d, *J* = 8.9 Hz, 1H), 5.96 (s, 1H), 4.90 (s, 2H), 3.84 (t, *J* = 11.6 Hz, 1H), 2.12 (s, 3H), 1.91 (dd, *J* = 24.1, 11.5 Hz, 2H), 1.56 (d, *J* = 11.4 Hz, 2H), 1.43 (d, *J* = 12.8 Hz, 2H), 1.24 (t, *J* = 12.2 Hz, 2H), 0.95 (d, *J* = 9.8 Hz, 6H). ¹³C NMR (125 MHz, DMSO-*d₆*) δ 166.56, 152.88, 145.96, 134.67, 129.96, 128.49, 125.58, 122.95, 115.52, 99.34, 68.00, 55.79, 38.31, 32.94, 29.67, 28.58, 24.30, 14.42.
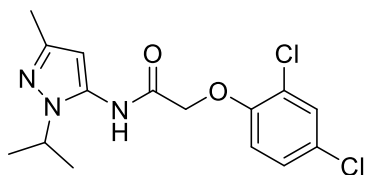
2-(2,4-dichlorophenoxy)-*N*-(1-isopropyl-3-methyl-1*H*-pyrazol-5-yl)acetamide (44f). Yield = 22.0 mg (47%, white solid) LCMS: R$_T$ = 2.61 min., >95% @ 215 and 254 nm, *m/z* = 342.0 [M+H]$^+$. ^{1}H NMR (500 MHz, DMSO-*d$_6$*) δ 9.99 (s, 1H), 7.62 (d, *J* = 2.5 Hz, 1H), 7.40 (dd, *J* = 8.9, 2.5 Hz, 1H), 7.10 (d, *J* = 8.9 Hz, 1H), 5.96 (s, 1H), 4.91 (s, 1H), 4.44 – 4.36 (m, 1H), 2.12 (s, 1H), 1.30 (d, *J* = 6.5 Hz, 1H). ^{13}C NMR (125 MHz, DMSO-*d$_6$*) δ 166.55, 152.97, 146.03, 134.55, 129.90, 128.46, 125.57, 122.96, 115.68, 99.32, 67.95, 48.20, 22.78, 14.43.
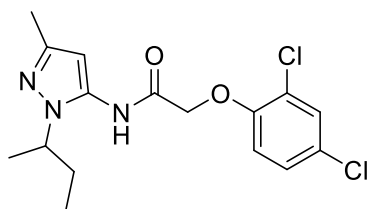
***N*-(1-(sec-butyl)-3-methyl-1*H*-pyrazol-5-yl)-2-(2,4-dichlorophenoxy)acetamide (44g).** Yield = 30.0 mg (65%, white solid) LCMS: R$_T$ = 2.71 min., >95% @ 215 and 254 nm, *m/z* = 356.0 [M+H]$^+$. ^{1}H NMR (500 MHz, CDCl$_3$) δ 8.42 (s, 1H), 7.47 (d, *J* = 2.4 Hz, 1H), 7.31 – 7.29 (m, 1H), 6.91 (d, *J* = 8.8 Hz, 1H), 6.24 (s, 1H), 4.69 (s, 2H), 4.07 – 3.97 (m, 1H), 2.28 (s, 3H), 2.03 – 1.93 (m, 1H), 1.83 – 1.73 (m, 1H), 1.49 (d, *J* = 6.7 Hz, 3H), 0.81 (t, *J* = 7.4 Hz, 3H). ^{13}C NMR (125 MHz, CDCl$_3$) δ 164.61, 151.06, 147.68, 133.54, 130.35, 128.27, 127.99, 123.53, 114.53, 98.62, 68.03, 55.24, 29.62, 20.52, 14.14, 10.99.
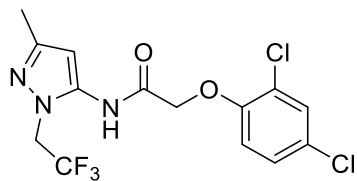
2-(2,4-dichlorophenoxy)-*N*-(3-methyl-1-(2,2,2-trifluoroethyl)-1*H*-pyrazol-5-yl)acetamide

(44h). Yield = 16.0 mg (47%, off-white solid) LCMS: R_T = 2.67 min., >95% @ 215 and 254 nm, *m/z* = 382.0 [M+H]$^+$. ^{1}H NMR (500 MHz, CDCl$_3$) δ 7.44 (d, *J* = 2.5 Hz, 1H), 7.25 (dd, *J* = 5.9, 3.0 Hz, 1H), 6.88 (d, *J* = 8.8 Hz, 1H), 6.36 (s, 1H), 4.73 – 4.66 (m, 4H), 2.28 (s, 3H). ^{13}C NMR (125 MHz, CDCl$_3$) δ 165.36, 151.00, 149.78, 130.43, 128.16, 128.10, 123.66, 121.77, 114.58, 100.94, 67.94, 13.64.
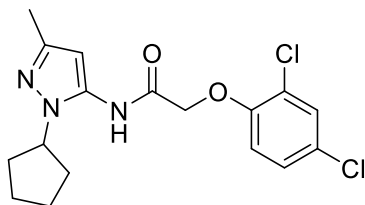
***N*-(1-cyclopentyl-3-methyl-1*H*-pyrazol-5-yl)-2-(2,4-dichlorophenoxy)acetamide (44i).** Yield = 30.0mg (68 %, white solid) LCMS: R_T = 2.82 min., >95% @ 215 and 254 nm, *m/z* = 368.0 [M+H]$^+$. ^{1}H NMR (500 MHz, CDCl$_3$) δ 8.48 (s, 1H), 7.47 (d, *J* = 2.4 Hz, 1H), 7.30 – 7.25 (m, 1H), 6.91 (d, *J* = 8.8 Hz, 1H), 6.26 (s, 1H), 4.69 (s, 2H), 4.42 (p, *J* = 7.7 Hz, 1H), 2.27 (s, 3H), 2.15 – 2.02 (m, 4H), 1.99 – 1.88 (m, 2H), 1.70 – 1.61 (m, 2H). ^{13}C NMR (125 MHz, CDCl$_3$) δ 164.50, 151.06, 147.34, 133.60, 130.35, 128.28, 127.97, 123.50, 114.50, 98.80, 68.00, 58.21, 32.18, 24.23, 14.15.
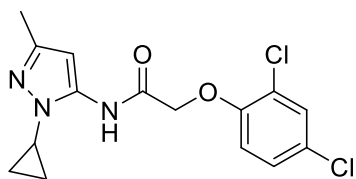
***N*-(1-cyclopropyl-3-methyl-1*H*-pyrazol-5-yl)-2-(2,4-dichlorophenoxy)acetamide (44j).** Yield = 12.0 mg (33%, white solid) LCMS: R_T = 2.59 min., >95% @ 215 and 254 nm, *m/z* = 340.0 [M+H]$^+$. ^{1}H NMR (500 MHz, CDCl$_3$) δ 8.94 (s, 1H), 7.48 (d, *J* = 2.5 Hz, 1H), 7.31 – 7.29 (m, 1H), 6.92 (d, *J* = 8.8 Hz, 1H), 6.43 (s, 1H), 4.71 (s, 2H), 3.26 – 3.20 (m, 1H), 2.25 (s, 3H), 1.19 – 1.11

(m, 4H). ^{13}C NMR (125 MHz, CDCl$_3$) δ 163.23, 151.00, 147.84, 136.72, 130.43, 128.24, 127.96, 123.45, 114.37, 96.65, 67.85, 27.61, 13.90.
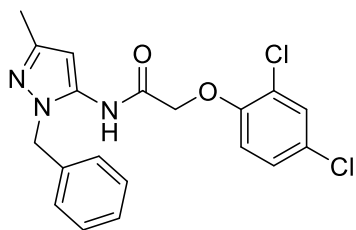
***N*-(1-benzyl-3-methyl-1*H*-pyrazol-5-yl)-2-(2,4-dichlorophenoxy)acetamide (44k).** Yield = 25.0 mg (48%, white solid) LCMS: R$_T$ = 2.76 min., >95% @ 215 and 254 nm, *m/z* = 390.0 [M+H]$^+$. ^{1}H NMR (500 MHz, DMSO-*d$_6$*) δ 10.20 (s, 1H), 7.60 (d, *J* = 2.4 Hz, 1H), 7.35 – 7.24 (m, 4H), 7.10 (d, *J* = 7.3 Hz, 2H), 7.01 (d, *J* = 8.9 Hz, 1H), 6.11 (s, 1H), 5.19 (s, 2H), 4.88 (s, 2H), 2.11 (s, 3H) ^{13}C NMR (125 MHz, DMSO-*d$_6$*) δ 166.23, 152.89, 146.94, 137.96, 136.26, 129.88, 128.84, 128.40, 127.70, 127.54, 125.56, 122.93, 115.57, 99.26, 67.93, 51.22, 14.22.
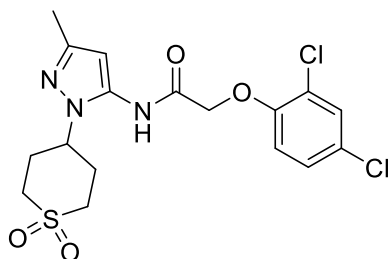
2-(2,4-dichlorophenoxy)-*N*-(1-(1,1-dioxidotetrahydro-2*H*-thiopyran-4-yl)-3-methyl-1*H*-pyrazol-5-yl)acetamide (44l) Yield = 15.0 mg (31.9%, brown solid) LCMS: R$_T$ = 2.43 min., >95% @ 215 and 254 nm, *m/z* = 432.0 [M+H]$^+$. ^{1}H NMR (500 MHz, DMSOv) δ 10.50 (s, 1H), 8.09 (dd, *J* = 7.7, 1.8 Hz, 1H), 7.64 – 7.54 (m, 2H), 6.03 (s, 1H), 5.83 (s, 1H), 4.52 – 4.46 (m, 1H), 3.30 (d, *J* = 7.2 Hz, 2H), 2.48 – 2.37 (m, 1H), 2.14 (s, 1H), 2.12 (s, 1H), 1.31 – 1.19 (m, 1H). ^{13}C NMR (125 MHz, DMSO-*d$_6$*) δ 164.71, 164.37, 147.07, 134.83, 131.18, 129.82, 126.83, 100.12, 55.27, 51.40, 49.60, 30.24, 22.21, 14.40.
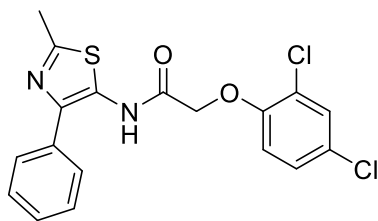
2-(2,4-dichlorophenoxy)-*N*-(2-methyl-4-phenylthiazol-5-yl)acetamide (44m) Yield = 15.0 mg (24.0%, off- white solid) LCMS: R_T = 2.98 min., >95% @ 215 and 254 nm, *m/z* = 393.0 [M+H]$^+$. ^{1}H NMR (500 MHz, DMSO-*d$_6$*) δ 10.51 (s, 1H), 7.74 (d, *J* = 7.3 Hz, 2H), 7.63 (d, *J* = 2.5 Hz, 1H), 7.45 (t, *J* = 7.6 Hz, 2H), 7.39 (dt, *J* = 11.2, 5.0 Hz, 2H), 7.13 (d, *J* = 8.9 Hz, 1H), 4.96 (s, 2H), 2.61 (s, 3H). ^{13}C NMR (125 MHz, DMSO-*d$_6$*) δ 166.45, 159.36, 152.72, 141.40, 134.33, 129.90, 129.11, 128.53, 128.32, 128.12, 127.85, 125.66, 122.87, 115.59, 67.80, 19.17.
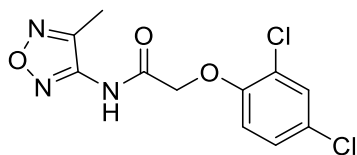
2-(2,4-dichlorophenoxy)-*N*-(4-methyl-1,2,5-oxadiazol-3-yl)acetamide (44n) Yield = 29.0 mg (67.3%, white solid) LCMS: R_T = 2.60 min., >95% @ 215 and 254 nm, *m/z* = 302.0 [M+H]$^+$. ^{1}H NMR (500 MHz, DMSO-*d$_6$*) δ 11.02 (s, 1H), 7.62 (d, *J* = 2.5 Hz, 1H), 7.39 (dd, *J* = 8.9, 2.5 Hz, 1H), 7.13 (d, *J* = 8.9 Hz, 1H), 5.03 (s, 2H), 2.32 (s, 3H). ^{13}C NMR (125 MHz, DMSO-*d$_6$*) δ 167.25, 152.86, 150.75, 148.73, 129.93, 128.48, 125.66, 122.92, 115.71, 67.56, 8.89.
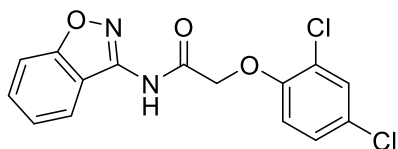
***N*-(benzo[*d*]isoxazol-3-yl)-2-(2,4-dichlorophenoxy)acetamide (44o).** Yield = 29.0 mg (67.3%, light yellow solid) LCMS: R_T = 2.60 min., >95% @ 215 and 254 nm, *m/z* = 302.0 [M+H]$^+$. ^{1}H

NMR (500 MHz, DMSO-d_6) δ 11.41 (s, 1H), 8.02 (d, J = 8.0 Hz, 1H), 7.73 – 7.65 (m, 2H), 7.63

(d, J = 2.5 Hz, 1H), 7.39 (dt, J = 7.1, 4.3 Hz, 2H), 7.17 (d, J = 8.9 Hz, 1H), 5.10 (s, 2H). ^{13}C NMR

(125 MHz, DMSO-d_6) δ 163.44, 153.45, 152.99, 131.36, 129.90, 128.50, 125.52, 123.90, 122.86,

116.33, 115.67, 110.40, 67.65.

Reagents and Conditions: (a) TEA, Dioxane
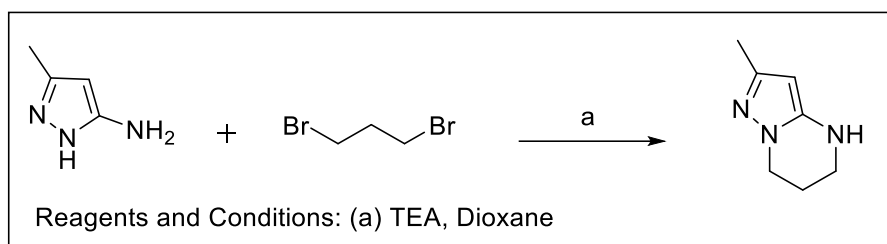
2-methyl-4,5,6,7-tetrahydropyrazolo[1,5-a]pyrimidine. A mixture of 3-methyl-1H-pyrazol-5-

amine Yield = 0.67 g, 6.9 mmol), dibromo propane (0.76 mL, 7.6 mmol) and TEA (2.90 mL, 20.8

mmol) in Dioxane (5.0 mL) was stirred at 80 °C for 12 hours. Volatiles were evaporated under

vacuum and loaded on silica gel. Product was eluted out by flash chromatography at 50% Ethyl

acetate in hexane. Yield = 0.48 g (50%, light brown solid). LCMS: R_T = 1.50 min., >90% @ 215

and 254 nm, m/z = 138.0 [M + H]$^+$. ^{1}H NMR ^{1}H NMR (500 MHz, CD$_3$CN) δ 5.10 (s, 1H), 3.92 (t,

J = 6.2 Hz, 2H), 3.21 – 3.17 (m, 2H), 2.05 (s, 3H), 2.04 – 2.00 (m, 2H). ^{13}C NMR (125 MHz,

CD$_3$CN) δ 146.70, 146.33, 85.76, 44.53, 39.35, 22.28, 12.87.
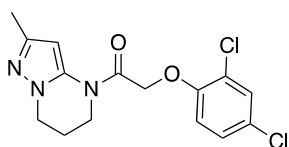
2-(2,4-dichlorophenoxy)-1-(2-methyl-6,7-dihydropyrazolo[1,5-a]pyrimidin-4(5H)-yl)ethan-

1-one (44p). Yield =10 mg (8.0%, light brown solid). LCMS: R_T = 2.63 min., >95% @ 215 and

254 nm, m/z = 340.0 [M + H]$^+$. ^{1}H NMR (500 MHz, DMSO-d_6) δ 7.59 (d, J = 2.5 Hz, 1H), 7.33

(dd, J = 8.9, 2.4 Hz, 1H), 7.14 (d, J = 8.6 Hz, 1H), 6.34 (s, 1H), 5.24 (s, 2H), 2.14 (s, 2H), 2.09 (s,

3H). ^{13}C NMR (125 MHz, DMSO-d_6) δ 164.41, 153.04, 129.70, 128.21, 125.12, 122.59, 115.80, 85.53, 67.07, 44.81, 39.33, 21.89, 14.03.
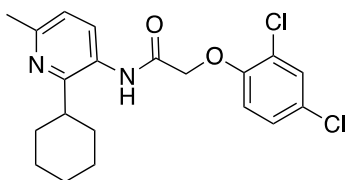
N-(2-cyclohexyl-6-methylpyridin-3-yl)-2-(2,4-dichlorophenoxy)acetamide (44q). Yield = 20 mg (20%, off-white solid). LCMS: R_T = 2.86 min., >95% @ 215 and 254 nm, m/z = 393.0 [M + H]$^+$. ^{1}H NMR (500 MHz, CDCl$_3$) δ 8.79 (s, 1H), 8.59 (s, 1H), 7.47 (d, J = 2.5 Hz, 1H), 7.27 (dd, J = 8.8, 2.5 Hz, 1H), 7.09 (d, J = 8.2 Hz, 1H), 6.91 (d, J = 8.8 Hz, 1H), 5.90 (s, 1H), 4.66 (s, 2H), 2.55 (d, J = 12.5 Hz, 3H), 2.36 (d, J = 1.8 Hz, 2H), 2.15 (dd, J = 6.0, 2.6 Hz, 2H), 1.81 – 1.75 (m, 2H), 1.71 – 1.65 (m, 2H). ^{13}C NMR (125 MHz, CDCl$_3$) δ 165.54, 151.55, 151.03, 130.45, 128.11, 128.04, 124.03, 115.08, 68.95, 28.11, 25.26, 22.47, 21.62.
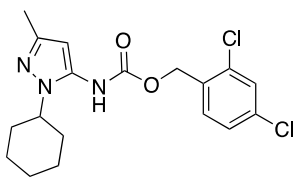
2,4-dichlorobenzyl (1-cyclohexyl-3-methyl-1H-pyrazol-5-yl)carbamate (44s). Yield = 20 mg (9.0%, white solid). LCMS: R_T = 2.93 min., >95% @ 215 and 254 nm, m/z = 382.0 [M + H]$^+$. ^{1}H NMR (500 MHz, CDCl$_3$) δ 7.43 (s, 1H), 7.26 (d, J = 7.8 Hz, 1H), 6.80 (s, 1H), 5.96 (s, 1H), 5.27 (s, 2H), 3.88 (m, 1H), 2.24 (s, 3H), 1.87 (m, 5H), 1.68 (m, 1H), 1.36 – 1.21 (m, 4H). ^{13}C NMR (125 MHz, CDCl$_3$) δ 153.71, 147.16, 135.05, 133.74, 132.01, 129.50, 127.28, 64.36, 56.47, 32.67, 25.72, 25.08, 14.06.
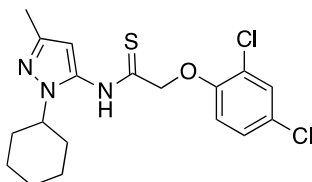
***N*-(1-cyclohexyl-3-methyl-1*H*-pyrazol-5-yl)-2-(2,4-dichlorophenoxy)ethanethioamide (44t).**

Yield = 10 mg (18%, light brown oil). LCMS: R_T = 4.55 min. (8 min method), >95% @ 215 and 254 nm, m/z = 398.0 [M + H]$^+$. ^{1}H NMR (500 MHz, CD$_3$OD) δ 7.53 (d, J = 2.4 Hz, 1H), 7.34 (dd, J = 8.8, 2.4 Hz, 1H), 7.17 (d, J = 8.9 Hz, 1H), 6.14 (s, 1H), 5.13 (s, 2H), 3.78 – 3.70 (m, 1H), 2.25 (s, 3H), 1.80 (d, J = 22.0 Hz, 6H), 1.68 (s, 1H), 1.23 (s, 3H). ^{13}C NMR (125 MHz, CD$_3$OD) δ 152.22, 147.22, 129.83, 127.78, 126.90, 123.69, 115.37, 100.91, 75.56, 56.66, 32.20, 25.32, 24.91, 12.40.
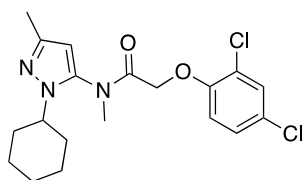
***N*-(1-cyclohexyl-3-methyl-1*H*-pyrazol-5-yl)-2-(2,4-dichlorophenoxy)-*N*-methylacetamide (44u).** Yield = 9.4 mg (29%, light yellow oil). LCMS: R_T = 3.08 min., >95% @ 215 and 254 nm, m/z = 396.1 [M + H]$^+$. ^{1}H NMR (500 MHz, CDCl$_3$) δ 7.38 (d, J = 2.3 Hz, 1H), 7.15 (dd, J = 8.8, 2.3 Hz, 1H), 6.72 (d, J = 8.8 Hz, 1H), 5.94 (s, 1H), 4.61 (d, J = 15.1 Hz, 1H), 4.34 (d, J = 15.1 Hz, 1H), 3.87 – 3.78 (m, 1H), 3.23 (s, 3H), 2.29 (s, 3H), 2.14 – 2.04 (m, 1H), 2.00 – 1.89 (m, 3H), 1.82 (s, 2H), 1.75 (d, J = 11.0 Hz, 1H), 1.41 – 1.41 (m, 1H), 1.42 – 1.27 (m, 3H). ^{13}C NMR (125 MHz, CDCl$_3$) δ 167.80, 152.71, 148.22, 137.98, 130.30, 127.50, 127.16, 124.53, 115.38, 101.69, 66.99, 56.45, 36.87, 33.72, 32.76, 25.69, 25.65, 24.93, 14.21.
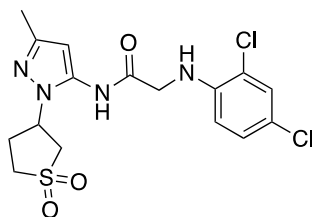
2-((2,4-dichlorophenyl)amino)-*N*-(1-(1,1-dioxidotetrahydrothiophen-3-yl)-3-methyl-1*H*-pyrazol-5-yl)acetamide (45d). Yield = 13 mg (13%, clear oil). LCMS: R_T = 2.51 min., >95% @ 215 and 254 nm, m/z = 417.0 [M + H]$^+$. ^{1}H NMR (500 MHz, DMSO-d_6) δ 10.09 (s, 1H), 7.41 (d, J

= 2.3 Hz, 1H), 7.22 (dd, *J* = 8.7, 2.2 Hz, 1H), 6.62 (d, *J* = 8.8 Hz, 1H), 6.00 (s, 1H), 5.93 (t, *J* = 5.8

Hz, 1H), 5.11 – 5.03 (m, 1H), 4.06 (d, *J* = 5.8 Hz, 1H), 3.56 (dd, *J* = 13.4, 8.4 Hz, 1H), 3.49 (dt, *J*

= 12.8, 6.3 Hz, 1H), 3.28 (dd, *J* = 13.4, 8.4 Hz, 1H), 3.16 (dt, *J* = 13.1, 8.5 Hz, 1H), 2.45 (dd, *J* =

14.8, 7.6 Hz, 2H), 2.14 (s, 3H). ^{13}C NMR (125 MHz, DMSO-d_6) δ 169.42, 147.80, 143.40, 136.56,

128.74, 128.30, 120.15, 118.99, 112.86, 99.98, 54.95, 52.11, 51.53, 46.52, 29.52, 14.44.
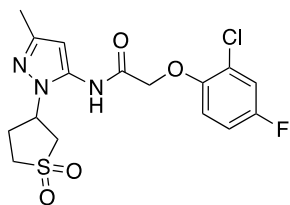
2-(2-chloro-4-fluorophenoxy)-*N*-(1-(1,1-dioxidotetrahydrothiophen-3-yl)-3-methyl-1*H*-

pyrazol-5-yl)acetamide (45h).. Yield = 0.29 g (81%, yellow solid). LCMS: R_T = 2.460 min., >95%

@ 215 and 254 nm, *m/z* = 402.0 [M + H]$^+$. ^{1}H NMR (500 MHz, DMSO-d_6) δ 10.16 (s, 1H), 7.48

(dd, *J* = 8.3, 3.0 Hz, 1H), 7.20 (td, *J* = 8.6, 3.0 Hz, 1H), 7.14 (dd, *J* = 9.2, 4.9 Hz, 1H), 6.04 (s, 1H),

5.11 (p, *J* = 8.0 Hz, 1H), 3.58 (dd, *J* = 13.4, 8.4 Hz, 1H), 3.49 (dt, *J* = 12.9, 6.3 Hz, 1H), 3.29 (dd,

J = 13.4, 8.4 Hz, 2H), 3.18 (dt, *J* = 13.1, 8.6 Hz, 1H), 2.47 (dd, *J* = 15.4, 8.3 Hz, 3H), 2.15 (s, 3H).

^{13}C NMR (125 MHz, DMSO-d_6) δ 167.09, 150.63, 147.85, 136.08, 117.86, 115.58, 115.15, 114.97,

100.18, 68.23, 54.95, 52.12, 51.55, 29.53, 14.43.

General Procedure E for synthesis of ether series (Class-III)

Reagents and Conditions: (a) TEA, DCM; (b) K$_2$CO$_3$, DMF
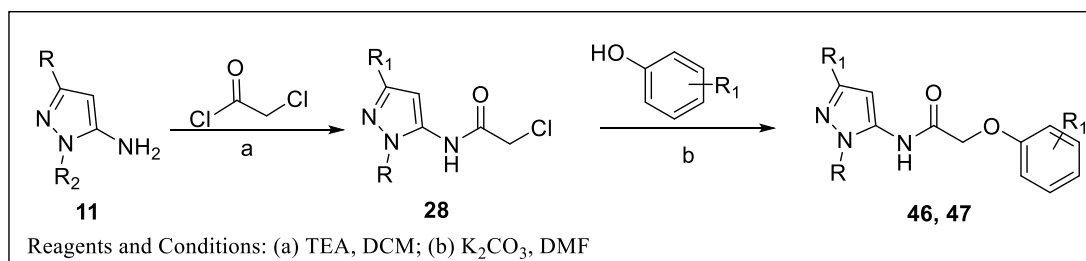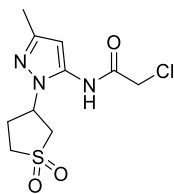
Step-1:2-chloro-*N*-(1-(1,1-dioxidotetrahydrothiophen-3-yl)-3-methyl-1*H*-pyrazol-5

yl)acetamide. To a stirred solution of 3-(5-amino-3-methyl-1*H*-pyrazol-1-yl)tetrahydrothiophene

1,1-dioxide (0.50 g, 2.3 mmol) and chloroacetyl chloride (280 mg, 2.55 mmol) in DCM (7 ml)

under nitrogen, was added TEA (0.97 mL. 6.9 mmol). The reaction was stirred at rt for 2 hours.

After checking completion on TLC. The reaction was quenched with saturated NahCO₃ solution

(15 ml) and product was extracted with ethyl acetate (30 ml *2). Combined organic layer was

washed with brine, dried over sodium sulfate, concentrated and used as such. Yield = 0.55 g (81%).

LCMS: R_T = 2.407 min., >90% @ 215 and 254 nm, *m/z* = 292.0. ¹H NMR (500 MHz, DMSO-*d₆*)

δ 6.05 (s, 1H), 5.19 – 5.12 (m, 1H), 4.36 (s, 2H), 3.62 – 3.58 (m, 1H), 3.48 (dd, *J* = 12.7, 6.0 Hz,

1H), 3.28 (dd, *J* = 13.4, 8.3 Hz, 1H), 3.23 – 3.15 (m, 1H), 3.08 (tt, *J* = 12.1, 6.1 Hz, 1H), 2.48 –

2.42 (m, 2H), 2.15 (s, 3H).

Step-2: Respective chloro acetamide (1 equiv., 0.1 mmol), phenol (1 equiv.) and K₂CO₃ (2 equiv.)

in DMF (0.5 ml) are stirred at 60 ºC for 6h. After completion of reaction by TLC. Product is

separated between water and ethyl acetate. Organic layer is purified using Prep-HPLC (Reverse

phase).
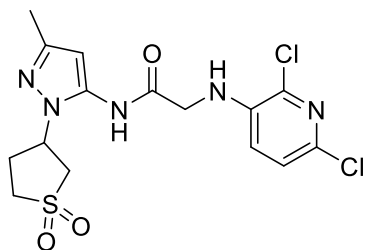
2-((2,6-dichloropyridin-3-yl)amino)-*N*-(1-(1,1-dioxidotetrahydrothiophen-3-yl)-3-methyl-

1*H*-pyrazol-5-yl)acetamide (46c): Yield = 8.0 mg (5.6%, clear oil). LCMS: R_T = 2.97 min., >95%

@ 215 and 254 nm, *m/z* = 418.0 [M + H]⁺. ¹H NMR (500 MHz, CD₃CN) δ 8.45 (s, 1H), 7.28 (d, *J*

= 8.4 Hz, 1H), 7.05 (d, *J* = 8.4 Hz, 1H), 5.95 (s, 1H), 5.50 (s, 1H), 4.94 – 4.85 (m, 1H), 4.06 (d, *J*

= 5.9 Hz, 2H), 3.46 (dt, *J* = 13.8, 7.0 Hz, 2H), 3.35 (dd, *J* = 13.6, 7.9 Hz, 1H), 3.10 (dt, *J* = 13.2,

8.2 Hz, 1H), 2.59 – 2.48 (m, 2H), 2.19 (d, *J* = 3.6 Hz, 3H). ¹³C NMR (125 MHz, CD₃CN) δ 169.26,

148.37, 139.95, 135.68, 135.26, 123.82, 121.35, 100.91, 54.66, 52.16, 51.06, 46.41, 29.16, 13.21.
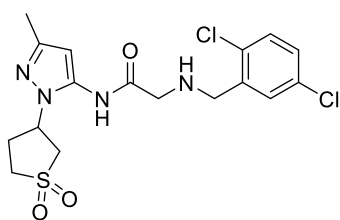
2-((2,5-dichlorobenzyl)amino)-*N*-(1-(1,1-dioxidotetrahydrothiophen-3-yl)-3-methyl-1*H*-

pyrazol-5-yl)acetamide (46d): Yield =14.0 mg (19%,). LCMS: R_T = 1.9 min., >95% @ 215 and

254 nm, *m/z* = 431.0 [M + H]⁺. Product degrades overtime.
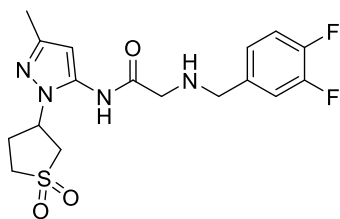
2-((3,4-difluorobenzyl)amino)-*N*-(1-(1,1-dioxidotetrahydrothiophen-3-yl)-3-methyl-1*H*-

pyrazol-5-yl)acetamide (46e): Yield = 9.0 mg, (26.4%). LCMS: R_T = 2.460 min., >95% @ 215

and 254 nm, *m/z* = 399.1 [M + H]⁺. Product degrades overtime.
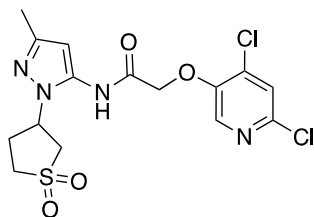
2-((4,6-dichloropyridin-3-yl)oxy)-*N*-(1-(1,1-dioxidotetrahydrothiophen-3-yl)-3-methyl-1*H*-pyrazol-5-yl)acetamide (46f). Yield = 14 mg (33%, white solid). LCMS: R_T = 2.28 min., >95% @ 215 and 254 nm, *m/z* = 419.0 [M + H]$^+$. ^{1}H NMR (500 MHz, CD$_3$CN) δ 8.19 (s, 1H), 7.59 (s, 1H), 6.04 (s, 1H), 5.04 – 4.97 (m, 1H), 4.89 (s, 2H), 3.48 (ddd, *J* = 15.5, 13.7, 7.6 Hz, 2H), 3.39 (dd, *J* = 13.6, 7.9 Hz, 1H), 3.12 (dt, *J* = 13.2, 8.2 Hz, 1H), 2.61 – 2.52 (m, 2H), 2.22 (s, 3H). ^{13}C NMR (125 MHz, CD$_3$CN) δ 166.71, 150.00, 148.53, 143.56, 135.73, 134.65, 134.54, 125.15, 101.07, 68.56, 54.64, 52.20, 51.06, 29.20, 13.20.
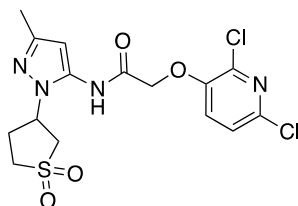
2-((2,6-dichloropyridin-3-yl)oxy)-*N*-(1-(1,1-dioxidotetrahydrothiophen-3-yl)-3-methyl-1*H*-pyrazol-5-yl)acetamide (46g). Yield = 22 mg (15%, clear oil). LCMS: R_T = 2.30 min., >95% @ 215 and 254 nm, *m/z* = 419.0 [M + H]$^+$. ^{1}H NMR (500 MHz, CD$_3$CN) δ 7.50 (d, *J* = 8.5 Hz, 1H), 7.41 (d, *J* = 8.5 Hz, 1H), 6.03 (s, 1H), 4.99 (dt, *J* = 15.4, 7.8 Hz, 1H), 4.85 (d, *J* = 15.3 Hz, 2H), 3.52 – 3.43 (m, 2H), 3.38 (dd, *J* = 13.6, 7.9 Hz, 1H), 3.12 (dt, *J* = 13.2, 8.2 Hz, 1H), 2.61 – 2.52 (m, 2H), 2.21 (s, 3H). ^{13}C NMR (125 MHz, CD$_3$CN) δ 166.75, 149.68, 148.51, 140.70, 138.92, 134.61, 125.04, 124.04, 101.08, 68.20, 54.64, 52.20, 51.05, 29.17, 13.20.
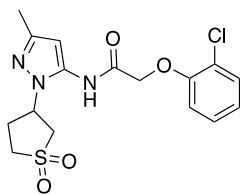
2-(2-chlorophenoxy)-*N*-(1-(1,1-dioxidotetrahydrothiophen-3-yl)-3-methyl-1*H*-pyrazol-5-yl)acetamide (46h). Yield = 30 mg (78%, white solid). LCMS: R_T = 2.407 min., >98% @ 215 and 254 nm, *m/z* = 384.0 [M + H]$^+$. ^{1}H NMR (500 MHz, DMSO-d_6) δ 10.16 (s, 1H), 7.50 – 7.44 (m, 1H), 7.32 (dd, *J* = 11.5, 4.2 Hz, 1H), 7.10 (d, *J* = 8.2 Hz, 1H), 7.01 (t, *J* = 7.4 Hz, 1H), 6.05 (s, 1H), 5.11 (p, *J* = 8.1 Hz, 1H), 4.90 (s, 2H), 3.58 (dd, *J* = 13.4, 8.4 Hz, 1H), 3.49 (dt, *J* = 12.9, 6.3 Hz, 1H), 3.32 – 3.25 (m, 1H), 3.17 (dt, *J* = 13.1, 8.5 Hz, 1H), 2.46 (dd, *J* = 15.1, 8.1 Hz, 2H), 2.15 (s, 3H). ^{13}C NMR (125 MHz, DMSO-d_6) δ 167.61, 154.21, 148.31, 136.57, 131.07, 129.17, 123.17, 122.36, 114.97, 100.61, 68.14, 55.41, 52.59, 52.01, 29.99, 14.89.

2-(4-chlorophenoxy)-*N*-(1-(1,1-dioxidotetrahydrothiophen-3-yl)-3-methyl-1*H*-pyrazol-5-yl)acetamide (46i). Yield = 8.5 mg (22%, white solid). LCMS: R_T = 2.444 min., >98% @ 215 and 254 nm, *m/z* = 384.0 [M + H]$^+$. ^{1}H NMR (500 MHz, 500 MHz, DMSO-d_6) δ 10.16 (s, 1H), 7.38 (d, *J* = 8.9 Hz, 2H), 7.04 (d, *J* = 8.9 Hz, 2H), 6.01 (s, 1H), 5.12 – 4.99 (m, 1H), 4.78 (s, 2H), 3.55 (dd, *J* = 13.4, 8.4 Hz, 1H), 3.48 (dt, *J* = 12.8, 6.2 Hz, 1H), 3.27 (dd, *J* = 13.6, 8.4 Hz, 1H), 3.17 (dt, *J* = 13.2, 8.6 Hz, 1H), 2.47 – 2.42 (m, 2H), 2.15 (s, 2H). ^{13}C NMR (125 MHz, DMSO-d_6) δ 167.71, 156.98, 147.83, 136.03, 129.76, 125.49, 116.97, 100.68, 67.37, 54.97, 52.13, 51.51, 29.56, 14.44.
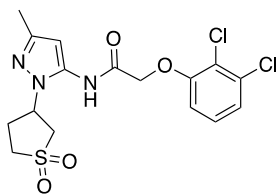
2-(2,3-dichlorophenoxy)-*N*-(1-(1,1-dioxidotetrahydrothiophen-3-yl)-3-methyl-1*H*-pyrazol-5-yl)acetamide (46j). Yield = 19 mg (46%, white solid). LCMS: R_T = 2.553 min., >98% @ 215 and 254 nm, m/z = 418.0 [M + H]$^+$. ^{1}H NMR (500 MHz, 500 MHz, DMSO-d_6) δ 10.18 (s, 1H), 7.34 (t, *J* = 8.2 Hz, 1H), 7.27 (d, *J* = 7.4 Hz, 1H), 7.10 (d, *J* = 8.2 Hz, 1H), 6.04 (s, 1H), 5.11 (p, *J* = 8.0 Hz, 1H), 4.96 (s, 2H), 3.58 (dd, *J* = 13.4, 8.4 Hz, 1H), 3.49 (dt, *J* = 12.9, 6.3 Hz, 1H), 3.29 (dd, *J* = 13.4, 8.4 Hz, 1H), 3.18 (dt, *J* = 12.2, 8.6 Hz, 1H), 2.46 (dd, *J* = 15.3, 8.1 Hz, 2H), 2.14 (s, 3H). ^{13}C NMR (125 MHz, DMSO-d_6) δ 166.84, 155.33, 147.85, 136.09, 132.91, 128.87, 123.13, 120.67, 112.93, 100.13, 67.95, 54.94, 52.12, 51.55, 29.52, 14.43.

2-(2,5-dichlorophenoxy)-*N*-(1-(1,1-dioxidotetrahydrothiophen-3-yl)-3-methyl-1*H*-pyrazol-5-yl)acetamide (46k) Yield = 0.30 g (80%, white solid). LCMS: R_T = 2.556 min., >98% @ 215 and 254 nm, m/z = 418.0 [M + H]$^+$. ^{1}H NMR (500 MHz, DMSO-d_6) δ 10.17 (s, 1H), 7.50 (d, *J* = 8.5 Hz, 1H), 7.24 (d, *J* = 2.1 Hz, 1H), 7.09 (dd, *J* = 8.5, 2.2 Hz, 1H), 6.05 (s, 1H), 5.20 – 5.10 (m, 1H), 4.98 (s, 2H), 3.59 (dd, *J* = 13.5, 8.4 Hz, 1H), 3.54 – 3.45 (m, 1H), 3.29 (d, *J* = 8.4 Hz, 1H), 3.21 – 3.12 (m, 1H), 2.50 – 2.44 (m, 2H), 2.15 (s, 3H). ^{13}C NMR (125 MHz, DMSO-d_6) δ 166.71, 154.49, 147.88, 136.06, 132.67, 131.57, 122.43, 120.83, 114.88, 100.06, 67.79, 54.94, 52.12, 51.55, 29.56, 14.43.

2-(4-bromo-2-chlorophenoxy)-*N*-(1-(1,1-dioxidotetrahydrothiophen-3-yl)-3-methyl-1*H*-

pyrazol-5-yl)acetamide (46l). Yield = 0.47 g (74%, white solid). LCMS: R_T = 2.60 min., >95%

@ 215 and 254 nm, m/z = 461.9 [M + H]$^+$. ^{1}H NMR (500 MHz, DMSO-d_6) δ 10.23 (s, 1H), 7.72

(d, J = 2.3 Hz, 1H), 7.51 (dd, J = 8.8, 2.3 Hz, 1H), 7.07 (d, J = 8.9 Hz, 1H), 6.04 (s, 1H), 5.16 –

5.08 (m, 1H), 4.93 (s, 2H), 3.58 (dd, J = 13.4, 8.4 Hz, 1H), 3.53 – 3.46 (m, 2H), 3.29 – 3.26 (m,

1H), 3.18 (dt, J = 13.2, 8.6 Hz, 1H), 2.46 (M, 2H), 2.14 (s, 3H). ^{13}C NMR (125 MHz, DMSO-d_6) δ

166.84, 153.39, 147.87, 136.06, 132.56, 131.40, 123.26, 116.25, 112.96, 100.09, 67.75, 54.95,

52.14, 51.56, 29.54, 14.43.

2-(4-chloro-2-fluorophenoxy)-*N*-(1-(1,1-dioxidotetrahydrothiophen-3-yl)-3-methyl-1*H*-

pyrazol-5-yl)acetamide (46m). Yield = 25 mg (36%, white solid). LCMS: R_T = 2.43 min., >95%

@ 215 and 254 nm, m/z = 402.0 [M + H]$^+$. ^{1}H NMR (500 MHz, CDCl$_3$) δ 8.26 (s, 1H), 7.23 (dd, J

= 10.7, 2.2 Hz, 1H), 7.17 (d, J = 8.8 Hz, 1H), 7.00 (t, J = 8.8 Hz, 1H), 6.03 (s, 1H), 4.93 – 4.84 (m,

1H), 4.72 (s, 2H), 3.61 (ddd, J = 14.2, 11.1, 7.7 Hz, 2H), 3.51 (dd, J = 13.4, 7.9 Hz, 1H), 3.21 –

3.12 (m, 1H), 2.78 (dq, J = 16.2, 8.1 Hz, 1H), 2.66 (td, J = 13.8, 6.9 Hz, 1H), 2.27 (s, 3H). ^{13}C

NMR (125 MHz, CDCl$_3$) δ 167.06, 153.37, 151.38, 149.36, 143.81, 143.72, 133.62, 128.35,

125.02, 124.99, 117.78, 117.61, 116.84, 101.59, 68.97, 54.66, 52.37, 50.97, 29.06, 14.10.

2-(2,4-dibromophenoxy)-*N*-(1-(1,1-dioxidotetrahydrothiophen-3-yl)-3-methyl-1*H*-pyrazol-5-

yl)acetamide (46n). Yield = 43 mg (50%, off-white solid). LCMS: R_T = 2.62 min., >95% @ 215

and 254 nm, m/z = 505.9 [M + H]$^+$. ^{1}H NMR (500 MHz, DMSO-d_6) δ 10.17 (s, 1H), 7.84 (d, J = 2.1 Hz, 1H), 7.55 (dd, J = 8.8, 2.1 Hz, 1H), 7.04 (d, J = 8.8 Hz, 1H), 6.05 (s, 1H), 5.16 – 5.08 (m, 1H), 4.92 (s, 2H), 3.58 (dd, J = 13.4, 8.3 Hz, 1H), 3.49 (M, 1H), 3.30 – 3.25 (m, 1H), 3.18 (dt, J = 13.0, 8.5 Hz, 1H), 2.14 (s, 3H). ^{13}C NMR (125 MHz, DMSO-d_6) δ 166.77, 154.30, 147.87, 136.04, 135.27, 131.97, 116.10, 113.37, 112.66, 100.06, 67.93, 54.95, 52.13, 51.56, 29.53, 14.42
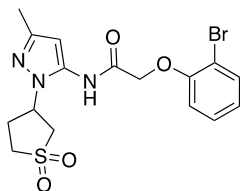
2-(2-bromophenoxy)-N-(1-(1,1-dioxidotetrahydrothiophen-3-yl)-3-methyl-1H-pyrazol-5-yl)acetamide (46o). Yield = 4.7 mg (11%, white solid). LCMS: R_T = 2.452 min., >95% @ 215 and 254 nm, m/z = 428.0 [M + H]$^+$. ^{1}H NMR (500 MHz, DMSO-d_6) δ 10.16 (s, 1H), 7.62 (d, J = 7.9 Hz, 1H), 7.36 (t, J = 7.8 Hz, 1H), 7.07 (d, J = 8.1 Hz, 1H), 6.95 (t, J = 7.6 Hz, 1H), 5.17 – 5.08 (m, 1H), 4.89 (s, 1H), 3.58 (dd, J = 13.4, 8.4 Hz, 1H), 3.49 (dt, J = 12.8, 6.3 Hz, 1H), 3.27 (dd, J = 16.4, 7.7 Hz, 1H), 3.17 (dt, J = 13.6, 8.7 Hz, 1H), 2.49 – 2.44 (m, 1H), 2.14 (s, 1H). ^{13}C NMR (125 MHz, DMSO-d_6) δ 166.58, 154.15, 147.37, 135.64, 133.15, 128.90, 122.74, 113.96, 111.01, 99.60, 67.38, 54.47, 51.65, 51.08, 29.04, 13.94
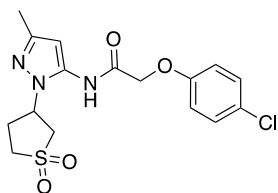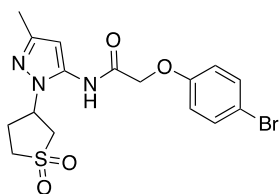

2-(4-bromophenoxy)-N-(1-(1,1-dioxidotetrahydrothiophen-3-yl)-3-methyl-1H-pyrazol-5-yl)acetamide (46p). Yield = 10 mg (24%, white solid). LCMS: R_T = 2.485 min., >98% @ 215 and 254 nm, m/z = 428.0 [M + H]$^+$. ^{1}H NMR (500 MHz, DMSO-d_6) δ 10.15 (s, 1H), 7.50 (d, J = 8.9 Hz, 2H), 6.99 (d, J = 8.9 Hz, 2H), 6.01 (s, 1H), 5.10 – 5.01 (m, 1H), 4.77 (s, 2H), 3.55 (dd, J =

13.4, 8.4 Hz, 1H), 3.48 (dt, *J* = 12.8, 6.3 Hz, 1H), 3.27 (dd, *J* = 13.6, 8.5 Hz, 2H), 3.17 (dt, *J* = 13.1,

8.6 Hz, 1H), 2.47 – 2.41 (m, 3H), 2.15 (s, 4H). ^{13}C NMR (125 MHz, DMSO-d_6) δ 167.69, 157.45,

147.81, 132.65, 117.49, 113.21, 100.65, 67.32, 54.96, 52.11, 51.51, 29.56, 14.44.
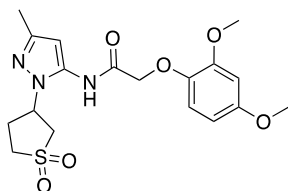
**2-(2,4-dimethoxyphenoxy)-*N*-(1-(1,1-dioxidotetrahydrothiophen-3-yl)-3-methyl-1*H*-pyrazol-
5-yl)acetamide (46q).** Yield = 26 mg (37%, yellow solid). LCMS: R_T = 2.90 min., >95% @ 215

and 254 nm, *m/z* = 410.1 [M + H]$^+$. ^{1}H NMR (500 MHz, CDCl$_3$) δ 8.83 (s, 1H), 6.96 (d, *J* = 8.8 Hz,

1H), 6.58 (t, *J* = 6.0 Hz, 1H), 6.48 (dd, *J* = 8.7, 2.6 Hz, 1H), 6.00 (s, 1H), 4.90 – 4.82 (m, 1H), 4.66

(s, 2H), 3.90 (s, 3H), 3.82 (s, 3H), 3.66 – 3.56 (m, 2H), 3.48 (dd, *J* = 13.4, 7.9 Hz, 1H), 3.17 – 3.09

(m, 1H), 2.78 (td, *J* = 16.1, 8.0 Hz, 1H), 2.64 (td, *J* = 13.8, 6.9 Hz, 1H), 2.27 (s, 3H). (10-15%

rotamers observed). ^{13}C NMR (125 MHz, CDCl$_3$) δ 168.88, 156.54, 150.66, 149.27, 141.15,

134.50, 117.78, 104.17, 101.01, 100.76, 71.04, 56.17, 55.73, 54.64, 52.33, 50.98, 29.03, 14.05.
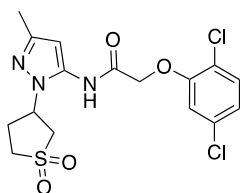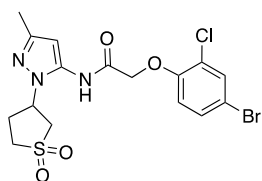

**2-(2,4-dimethylphenoxy)-*N*-(1-(1,1-dioxidotetrahydrothiophen-3-yl)-3-methyl-1*H*-pyrazol-5-
yl)acetamide (46r).** Yield = 25 mg (48%, off-white solid). LCMS: R_T = 2.49 min., >95% @ 215

and 254 nm, *m/z* = 378.1 [M + H]$^+$. ^{1}H NMR (500 MHz, DMSO-d_6) δ 10.00 (s, 1H), 6.98 (d, *J* =

9.7 Hz, 1H), 6.96 (d, *J* = 8.2 Hz, 1H), 6.77 (d, *J* = 8.2 Hz, 1H), 6.02 (s, 1H), 5.06 – 4.97 (m, 1H),

4.72 (s, 2H), 3.56 – 3.49 (m, 1H), 3.46 (dd, *J* = 12.9, 6.4 Hz, 1H), 3.27 (dd, *J* = 13.4, 8.3 Hz, 1H),

3.14 (dt, *J* = 13.1, 8.6 Hz, 1H), 2.43 (dd, *J* = 16.0, 8.3 Hz, 2H), 2.22 (d, *J* = 5.1 Hz, 6H), 2.15 (s,

3H). ¹³C NMR (125 MHz, DMSO) δ 168.22, 154.23, 147.80, 136.11, 131.88, 130.21, 127.46,

126.44, 111.92, 100.66, 67.65, 54.93, 52.12, 51.49, 29.51, 20.53, 16.55, 14.43.
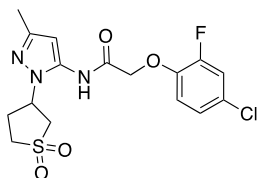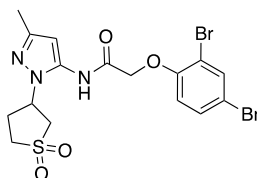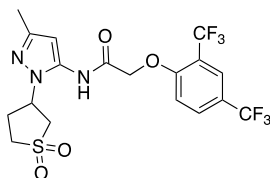

2-(2,4-bis(trifluoromethyl)phenoxy)-*N*-(1-(1,1-dioxidotetrahydrothiophen-3-yl)-3-methyl-

1*H*-pyrazol-5-yl)acetamide (46s). Yield = 22 mg (17%, white solid). LCMS: R$_T$ = 2.70 min.,

>95% @ 215 and 254 nm, *m/z* = 486.1 [M + H]⁺. ¹H NMR (500 MHz, CDCl₃) δ 8.15 (s, 1H), 7.96

(s, 1H), 7.93 (d, *J* = 8.7 Hz, 1H), 7.17 (d, *J* = 8.6 Hz, 1H), 6.10 (s, 1H), 4.88 (d, *J* = 7.0 Hz, 1H),

4.85 (s, 2H), 3.70 – 3.57 (m, 3H), 3.51 (dd, *J* = 13.5, 7.8 Hz, 1H), 3.21 – 3.12 (m, 1H), 2.78 (td, *J*

= 16.1, 8.0 Hz, 1H), 2.67 (td, *J* = 13.8, 6.9 Hz, 1H), 2.28 (s, 3H). ¹³C NMR (125 MHz, CDCl₃) δ

165.43, 156.41, 149.47, 133.48, 131.55, 125.39, 124.86, 124.07, 121.89, 119.46, 113.30, 101.15,

67.44, 54.61, 52.33, 50.93, 29.13, 14.08.
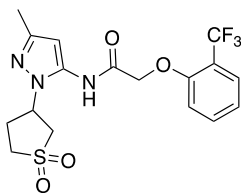
***N*-(1-(1,1-dioxidotetrahydrothiophen-3-yl)-3-methyl-1H-pyrazol-5-yl)-2-(2-**

(trifluoromethyl)phenoxy)acetamide (46t). Yield = 16 mg (38%, white solid). LCMS: R$_T$ =

2.513 min., >98% @ 215 and 254 nm, *m/z* = 418.0 [M + H]⁺. ¹H NMR (500 MHz, DMSO-*d₆*) δ

10.18 (s, 1H), 7.68 – 7.60 (m, 2H), 7.20 (d, *J* = 8.3 Hz, 1H), 7.15 (t, *J* = 7.6 Hz, 1H), 6.06 (s, 1H),

5.13 (p, *J* = 8.1 Hz, 1H), 4.97 (s, 2H), 3.58 (dd, *J* = 13.4, 8.4 Hz, 1H), 3.50 (dt, *J* = 12.9, 6.3 Hz,

1H), 3.31 – 3.27 (m, 1H), 3.17 (dt, *J* = 13.1, 8.5 Hz, 1H), 2.46 (dd, *J* = 11.2, 5.0 Hz, 2H), 2.14 (s,

3H). ¹³C NMR (125 MHz, DMSO-d_6) δ 166.73, 156.26, 147.87, 136.19, 136.03, 134.59, 127.34, 121.41, 114.23, 99.87, 67.39, 54.93, 52.09, 51.55, 29.54, 14.42.
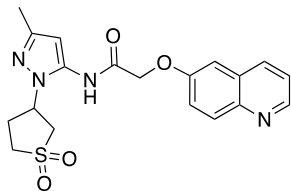
N-(1-(1,1-dioxidotetrahydrothiophen-3-yl)-3-methyl-1H-pyrazol-5-yl)-2-(quinolin-6-yloxy)acetamide (46u). Yield = 16 mg (19%, clear oil). LCMS: R_T = 1.71 min., >95% @ 215 and 254 nm, m/z = 401.1 [M + H]⁺. ¹H NMR (500 MHz, CD₃CN) δ 8.81 (d, J = 3.5 Hz, 1H), 8.79 (s, 1H), 8.32 (d, J = 8.2 Hz, 1H), 8.14 (d, J = 9.2 Hz, 1H), 7.63 (dd, J = 9.2, 2.7 Hz, 1H), 7.54 (dd, J = 8.3, 4.3 Hz, 1H), 7.42 (d, J = 2.7 Hz, 1H), 6.01 (s, 1H), 5.04 – 4.95 (m, 1H), 4.85 (s, 2H), 3.49 – 3.40 (m, 2H), 3.36 (dd, J = 13.7, 7.8 Hz, 1H), 3.08 – 3.00 (m, 1H), 2.56 (dd, J = 8.3, 5.2 Hz, 1H), 2.52 – 2.47 (m, 1H), 2.22 (s, 3H). ¹³C NMR (125 MHz, CD₃CN) δ 167.83, 155.71, 148.45, 147.65, 136.29, 134.85, 129.89, 129.37, 122.65, 121.92, 107.17, 101.39, 67.33, 54.69, 52.18, 51.04, 29.26, 13.24.
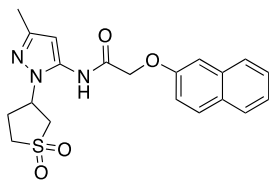
N-(1-(1,1-dioxidotetrahydrothiophen-3-yl)-3-methyl-1H-pyrazol-5-yl)-2-(naphthalen-2-yloxy)acetamide (46v). Yield = 17 mg (21%, yellow oil). LCMS: R_T = 2.45 min., >95% @ 215 and 254 nm, m/z = 400.1 [M + H]⁺. ¹H NMR (500 MHz, DMSO-d_6) δ 10.20 (s, 1H), 7.91 – 7.80 (m, 1H), 7.52 – 7.46 (m, 1H), 7.40 – 7.35 (m, 1H), 7.32 (dd, J = 8.9, 2.5 Hz, 1H), 6.03 (s, 1H), 5.10 – 5.04 (m, 1H), 4.89 (s, 1H), 3.55 (dd, J = 13.4, 8.5 Hz, 1H), 3.48 – 3.41 (m, 1H), 3.31 – 3.25 (m, 1H), 3.10 (dt, J = 13.1, 8.7 Hz, 1H), 2.46 – 2.38 (m, 1H), 2.15 (s, 1H). ¹³C NMR (125 MHz, DMSO-

d_6) δ 167.91, 155.97, 147.83, 136.06, 134.46, 129.93, 129.26, 128.03, 127.23, 127.04, 124.45, 119.07, 107.70, 100.81, 67.29, 54.96, 52.15, 51.45, 29.58, 14.44.
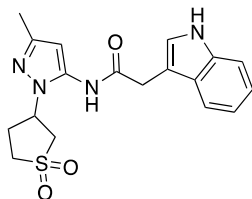
N-(1-(1,1-dioxidotetrahydrothiophen-3-yl)-3-methyl-1H-pyrazol-5-yl)-2-(1H-indol-3-yl)acetamide (46y). Prepared using general procedure A. Yield = 12 mg (23%, clear oil). LCMS: R_T = 2.47 min., >95% @ 215 and 254 nm, *m/z* = 373.1 [M + H]⁺. ¹H NMR (500 MHz, CD₃CN) δ 9.44 (s, 1H), 7.63 (d, *J* = 7.9 Hz, 2H), 7.44 (t, *J* = 11.3 Hz, 2H), 7.29 (s, 2H), 7.20 (t, *J* = 7.5 Hz, 2H), 7.12 (t, *J* = 7.4 Hz, 2H), 5.90 (s, 2H), 4.82 – 4.74 (m, 2H), 3.84 (s, 4H), 3.42 – 3.29 (m, 5H), 2.95 (ddd, *J* = 13.2, 9.0, 7.6 Hz, 2H), 2.50 – 2.44 (m, 2H), 2.38 (dd, *J* = 13.6, 7.0 Hz, 2H), 2.17 (s, 5H). ¹³C NMR (125 MHz, CD₃CN) δ 171.43, 148.24, 135.99, 127.26, 124.47, 124.31, 121.82, 119.28, 118.42, 111.57, 111.52, 100.79, 100.76, 54.54, 52.07, 51.01, 32.88, 29.13, 13.20.
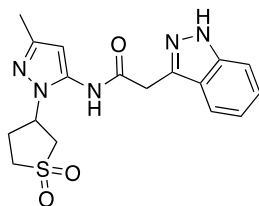
N-(1-(1,1-dioxidotetrahydrothiophen-3-yl)-3-methyl-1H-pyrazol-5-yl)-2-(1H-indazol-3-yl)acetamide (46z). Yield = 21 mg (16%, clear oil). LCMS: R_T = 2.04 min., >95% @ 215 and 254 nm, *m/z* = 374.1 [M + H]⁺. ¹H NMR (500 MHz, CD₃CN) δ 8.64 (s, 1H), 7.79 (d, *J* = 8.2 Hz, 1H), 7.56 (d, *J* = 8.4 Hz, 1H), 7.42 (t, *J* = 7.6 Hz, 1H), 7.20 (t, *J* = 7.5 Hz, 1H), 5.97 (s, 1H), 5.05 – 4.97 (m, 1H), 4.10 (s, 2H), 3.43 (td, *J* = 13.6, 7.7 Hz, 2H), 3.38 – 3.30 (m, 1H), 3.05 (dt, *J* = 13.2, 8.2 Hz, 1H), 2.55 – 2.45 (m, 3H), 2.18 (s, 3H). ¹³C NMR (125 MHz, CD₃CN) δ 169.26, 148.28, 141.24,

139.97, 135.94, 126.70, 122.16, 120.59, 119.96, 110.29, 100.60, 54.65, 52.17, 51.09, 34.63, 29.13, 13.24.
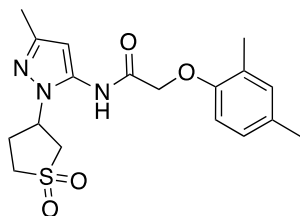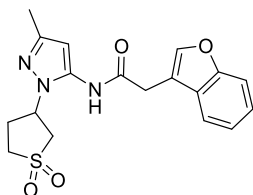

2-(benzofuran-3-yl)-*N*-(1-(1,1-dioxidotetrahydrothiophen-3-yl)-3-methyl-1*H*-pyrazol-5-yl)acetamide (47a) Yield = 16 mg (12.7%, yellow solid). LCMS: R_T = 2.32 min., >95% @ 215 and 254 nm, *m/z* = 374.1 [M + H]$^+$. ^{1}H NMR (500 MHz, CDCl$_3$) δ 7.75 (s, 1H), 7.65 – 7.54 (m, 2H), 7.38 (dt, *J* = 22.7, 7.3 Hz, 2H), 5.92 (s, 1H), 4.86 – 4.78 (m, 1H), 3.89 (s, 2H), 3.58 – 3.47 (m, 2H), 3.44 – 3.37 (m, 1H), 3.10 – 3.01 (m, 1H), 2.71 – 2.62 (m, 1H), 2.53 (td, *J* = 13.6, 6.7 Hz, 1H), 2.21 (s, 3H). ^{13}C NMR (125 MHz, CDCl$_3$) δ 169.56, 155.55, 149.04, 143.57, 126.88, 125.38, 123.45, 119.25, 113.06, 112.10, 101.38, 54.46, 52.31, 51.02, 31.86, 28.89, 13.92.
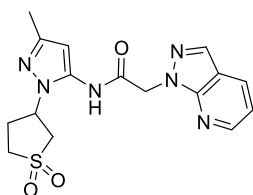
***N*-(1-(1,1-dioxidotetrahydrothiophen-3-yl)-3-methyl-1*H*-pyrazol-5-yl)-2-(1*H*-pyrazolo[3,4-b]pyridin-1-yl)acetamide (47b):** Yield = 16 mg (12.7%, off-white solid). LCMS: R_T = 2.15 min., >95% @ 215 and 254 nm, *m/z* = 375.1 [M + H]$^+$. ^{1}H NMR (500 MHz, CD$_3$CN) δ 8.61 (dd, *J* = 4.5, 1.2 Hz, 1H), 8.46 (s, 1H), 8.25 (dd, *J* = 8.0, 1.3 Hz, 1H), 8.17 (s, 1H), 7.27 (dd, *J* = 8.0, 4.5 Hz, 1H), 5.98 (s, 1H), 5.36 (s, 2H), 5.08 – 5.00 (m, 1H), 3.45 (dt, *J* = 13.4, 6.7 Hz, 2H), 3.37 – 3.30 (m, 1H), 3.11 (dt, *J* = 13.2, 8.2 Hz, 1H), 2.58 – 2.51 (m, 2H), 2.18 (s, 3H). ^{13}C NMR (125 MHz, CD$_3$CN) δ 167.06, 150.86, 149.20, 148.38, 135.16, 133.47, 130.64, 115.81, 100.76, 54.67, 52.16, 51.09, 49.92, 29.14, 13.21.
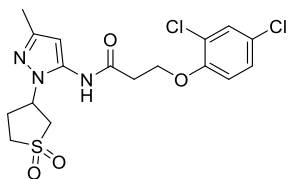
3-(2,4-dichlorophenoxy)-*N*-(1-(1,1-dioxidotetrahydrothiophen-3-yl)-3-methyl-1*H*-pyrazol-5-yl)propenamide (47c) Yield = 13 mg (21.7%, white solid). LCMS: R_T = 2.56 min., >95% @ 215 and 254 nm, m/z = 432.1 [M + H]$^+$. ^{1}H NMR (500 MHz, CD$_3$CN) δ 8.30 (s, 1H), 7.48 (t, J = 3.6 Hz, 1H), 7.32 (td, J = 9.0, 2.6 Hz, 1H), 7.11 (d, J = 8.9 Hz, 1H), 5.98 (s, 2H), 4.98 (dq, J = 15.2, 7.6 Hz, 1H), 4.39 (t, J = 5.9 Hz, 2H), 3.50 – 3.42 (m, 2H), 3.35 (dd, J = 13.5, 7.6 Hz, 1H), 3.06 (dt, J = 13.2, 8.0 Hz, 1H), 2.86 (t, J = 5.9 Hz, 2H), 2.54 (dt, J = 6.9, 6.1 Hz, 2H), 2.20 (s, 3H). Rotamers observed in the ration of 80:20, spectra of major rotamer reported. ^{13}C NMR (125 MHz, CD$_3$CN) δ 169.79, 153.12, 148.33, 135.84, 129.62, 128.01, 125.43, 114.91, 100.34, 65.45, 54.71, 52.16, 51.02, 35.60, 29.21, 13.21.

Reagents and conditions: (a) aryl bromide, PdCl$_2$.dppf.DCM, Cs$_2$CO$_3$, ACN, Water, MW, 120 °C, 1h (b) HBr in AcOH, 100 °C, 12h (c) **28,** Cs$_2$CO$_3$, DMF, 60 °C, 6h
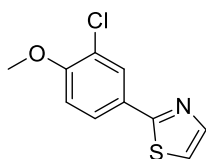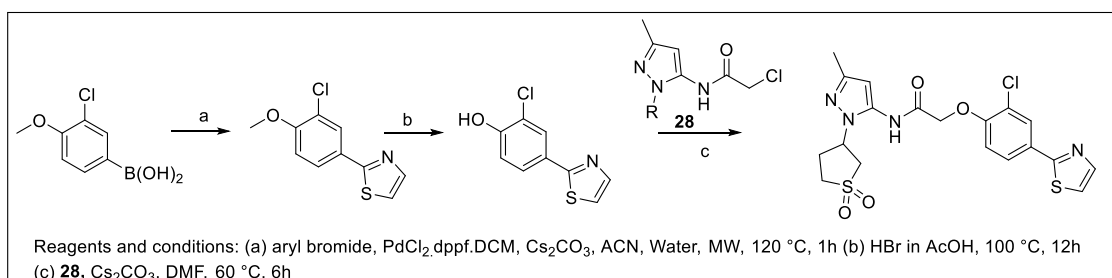
2-(3-chloro-4-methoxyphenyl)thiazole

In a 10 mL microwave vial, (3-chloro-4-methoxyphenyl)boronic acid (0.269 g, 1.45 mmol), 2-bromothiazole (0.20 g, 1.2 mmol) and Cs$_2$CO$_3$ (0.78 g, 2.0 mmol) were dissolved in CH$_3$CN:water (4:1, 5.0 mL). The mixture was degassed with N$_2$ for 10 minutes. To the mixture was added PdCl$_2$.dppf.DCM (87.0 mg, 0.12 mmol) and subjected to microwave

irradiation at 120 ℃ for 1 hour. After confirming the product formation by LCMS, the crude was filtered over celite and purified by flash chromatography to yield the product. Yield = 120.0 mg (44.1 %). LCMS: R_T = 2.70 min., >95% @ 215 and 254 nm, m/z = 225.9 [M + H]⁺. ¹H NMR (500 MHz, DMSO) δ 7.98 (d, J = 2.2 Hz, 1H), 7.90 (dd, J = 6.9, 2.7 Hz, 2H), 7.77 (d, J = 3.2 Hz, 1H), 3.94 (s, 3H). ¹³C NMR (125 MHz, DMSO) δ 165.94, 156.33, 144.16, 127.64, 127.16, 126.96, 122.26, 120.71, 113.81, 56.89.
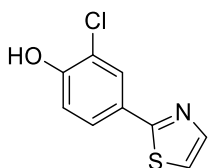
2-chloro-4-(thiazol-2-yl)phenol

2-(3-chloro-4-methoxyphenyl)thiazole (120.0 mg) was dissolved in HBr in AcOH (2.0 mL) and refluxed at 100 ℃ for 12 h. The crude was evaporated under vacuum, washed with NaHCO₃ aqueous solution and the product was extracted in ethyl acetate and used as such. Yield = 100.0 mg (89.3%). LCMS: R_T = 2.34 min., >95% @ 215 and 254 nm, m/z = 211.9 [M + H]⁺. ¹H NMR (500 MHz, DMSO) δ 10.79 (s, 1H), 7.90 (d, J = 2.2 Hz, 1H), 7.86 (d, J = 3.2 Hz, 1H), 7.76 – 7.73 (m, 1H), 7.71 (d, J = 3.2 Hz, 1H). ¹³C NMR (125 MHz, DMSO) δ 166.36, 155.31, 144.01, 127.82, 126.84, 125.99, 120.88, 120.18, 117.58.
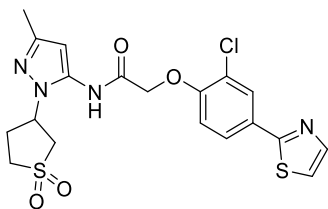
2-(2-chloro-4-(thiazol-2-yl)phenoxy)-*N*-(1-(1,1-dioxidotetrahydrothiophen-3-yl)-3-methyl-1*H*-pyrazol-5-yl)acetamide (47d)

Yield = 35.0 mg (22.1%,, white solid). LCMS: R_T = 2.46 min., >95% @ 215 and 254 nm, m/z = 467.0 [M + H]⁺.¹H NMR (500 MHz, CD₃CN) δ 9.67 (s, 1H), 7.46 (d, J = 2.1 Hz, 1H), 7.34 (dd, J

= 10.8, 2.7 Hz, 2H), 7.22 (d, J = 3.2 Hz, 1H), 6.66 (d, J = 8.7 Hz, 1H), 5.50 (s, 1H), 4.62 – 4.53 (m, 1H), 4.45 (s, 2H), 3.03 (dd, J = 13.4, 8.4 Hz, 1H), 2.94 (dt, J = 12.9, 6.4 Hz, 1H), 2.75 – 2.71 (m, 1H), 2.62 (dt, J = 13.1, 8.6 Hz, 1H), 1.91 (dd, J = 11.0, 6.0 Hz, 2H), 1.59 (s, 3H). ^{13}C NMR (125 MHz, CD$_3$CN) δ 166.28, 165.23, 154.54, 147.33, 143.67, 135.50, 127.30, 126.23, 122.09, 120.37, 114.35, 99.60, 67.16, 54.40, 51.59, 51.00, 28.98, 13.87.
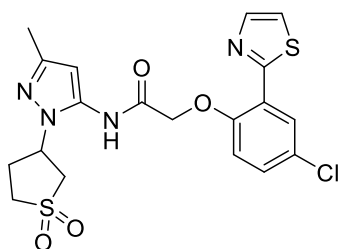
2-(4-chloro-2-(thiazol-2-yl)phenoxy)-*N*-(1-(1,1-dioxidotetrahydrothiophen-3-yl)-3-methyl-1*H*-pyrazol-5-yl)acetamide (47e)

Yield = 15.0 mg (15.1%, white solid). LCMS: R_T = 2.38 min., >95% @ 215 and 254 nm, *m/z* = 467.0 [M + H]$^+$. ^{1}H NMR (500 MHz, DMSO-*d$_6$*) δ 10.34 (s, 1H), 8.28 (d, J = 2.7 Hz, 1H), 8.00 (d, J = 3.2 Hz, 1H), 7.89 (d, J = 3.2 Hz, 1H), 7.52 (dd, J = 8.9, 2.7 Hz, 1H), 7.26 (d, J = 8.9 Hz, 1H), 6.07 (s, 1H), 5.13 (dd, J = 15.8, 7.8 Hz, 1H), 5.08 (s, 2H), 3.59 (dd, J = 13.4, 8.4 Hz, 1H), 3.50 (dt, J = 12.5, 6.2 Hz, 1H), 3.32 – 3.27 (m, 1H), 3.17 (dt, J = 13.1, 8.5 Hz, 1H), 2.49 – 2.45 (m, 2H), 2.15 (s, 3H). ^{13}C NMR (125 MHz, DMSO-*d$_6$*) δ 166.71, 160.09, 153.83, 147.96, 142.68, 136.10, 130.56, 127.29, 126.09, 123.93, 122.64, 115.80, 100.06, 68.08, 54.97, 52.17, 51.55, 29.56, 14.43.
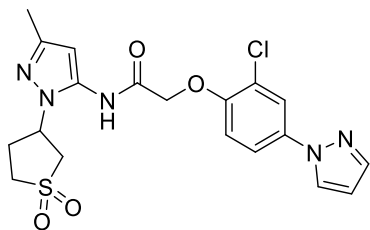
2-(2-chloro-4-(1*H*-pyrazol-1-yl)phenoxy)-*N*-(1-(1,1-dioxidotetrahydrothiophen-3-yl)-3-methyl-1*H*-pyrazol-5-yl)acetamide (47f)

Yield = 14.0 mg (18.4%,). LCMS: R_T = 2.39 min., >95% @ 215 and 254 nm, m/z = 450.0 [M + H]$^+$. ^{1}H NMR (500 MHz, CDCl$_3$) δ 7.88 (d, J = 2.0 Hz, 1H), 7.84 (d, J = 2.1 Hz, 1H), 7.72 (s, 1H), 7.61 (d, J = 6.9 Hz, 1H), 7.07 (d, J = 8.7 Hz, 1H), 6.49 (s, 1H), 4.97 – 4.86 (m, 1H), 4.77 (s, 2H), 3.64 – 3.53 (m, 2H), 3.49 (dd, J = 13.1, 7.4 Hz, 1H), 3.19 – 3.09 (m, 1H), 2.75 (dt, J = 15.8, 7.8 Hz, 1H), 2.68 – 2.59 (m, 1H), 2.25 (s, 3H). ^{13}C NMR (125 MHz, CDCl$_3$) δ 166.99, 150.82, 149.34, 141.47, 135.71, 134.06, 127.07, 123.77, 121.89, 118.88, 114.69, 108.15, 68.42, 54.53, 52.33, 50.97, 28.95, 13.93.
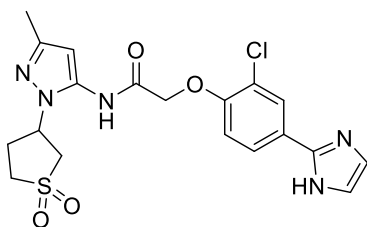
2-(2-chloro-4-(1*H*-imidazol-2-yl)phenoxy)-*N*-(1-(1,1-dioxidotetrahydrothiophen-3-yl)-3-methyl-1*H*-pyrazol-5-yl)acetamide (47g)

Yield = 4.0 mg (23.5%, yellow solid). LCMS: R_T = 2.28 min., >95% @ 215 and 254 nm, m/z = 450.0 [M + H]$^+$. ^{1}H NMR (500 MHz, CDCl$_3$) δ 7.95 (d, J = 6.0 Hz, 1H), 7.79 (d, J = 8.2 Hz, 1H), 7.16 (d, J = 8.7 Hz, 2H), 6.97 – 6.93 (m, 1H), 6.07 (s, 1H), 4.98 – 4.89 (m, 1H), 4.79 (s, 2H), 3.57 – 3.50 (m, 3H), 3.46 (dd, J = 13.5, 8.0 Hz, 1H), 3.17 – 3.10 (m, 2H), 2.23 (s, 3H). ^{13}C NMR (125 MHz, CDCl$_3$) δ 153.46, 149.42, 128.06, 125.96, 124.44, 123.45, 122.02, 116.24, 113.97, 101.05, 67.97, 54.64, 52.21, 40.65, 29.00, 28.44, 14.05.
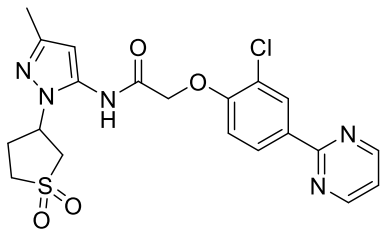

2-(2-chloro-4-(pyrimidin-2-yl)phenoxy)-*N*-(1-(1,1-dioxidotetrahydrothiophen-3-yl)-3-methyl-1*H*-pyrazol-5-yl)acetamide (47h)

Yield = 17.0 mg (15.3%, yellow solid). LCMS: R_T = 2.38 min., >95% @ 215 and 254 nm, m/z = 462.0 [M + H]$^+$. ^{1}H NMR (500 MHz, CD$_3$CN) δ 8.83 (d, J = 4.8 Hz, 2H), 8.54 (s, 1H), 8.52 (d, J = 2.0 Hz, 1H), 8.41 (dd, J = 8.7, 2.0 Hz, 1H), 7.32 (t, J = 4.8 Hz, 1H), 7.22 (d, J = 8.7 Hz, 1H), 6.05 (s, 1H), 5.04 – 4.96 (m, 1H), 4.88 (s, 2H), 3.52 – 3.42 (m, 2H), 3.38 (dd, J = 13.7, 7.8 Hz, 1H), 3.10 (dt, J = 13.2, 8.2 Hz, 1H), 2.59 – 2.52 (m, 2H), 2.22 (s, 3H). ^{13}C NMR (125 MHz, CD$_3$CN) δ 167.26, 162.50, 157.55, 155.01, 148.43, 134.76, 132.63, 129.71, 127.96, 122.70, 119.56, 113.89, 101.09, 68.02, 54.66, 52.19, 51.04, 29.22, 13.24.
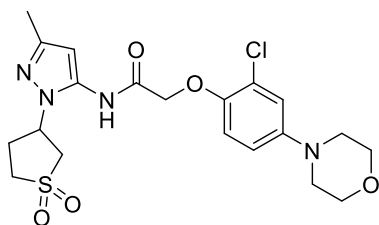
2-(2-chloro-4-morpholinophenoxy)-N-(1-(1,1-dioxidotetrahydrothiophen-3-yl)-3-methyl-1H-pyrazol-5-yl)acetamide (47i) Yield = 18.0mg (23.8%, clear oil). LCMS: R_T = 2.25 min., >95% @ 215 and 254 nm, m/z = 469.0 [M + H]$^+$.]$^+$.^{1}H NMR (500 MHz, CD$_3$CN) δ 9.67 (s, 1H), 7.42 (d, J = 2.1 Hz, 1H), 7.32 (d, J = 8.5,Hz, 1H), 7.2 (d, J = 8.7 Hz, 1H), 5.50 (s, 1H), 4.62 – 4.53 (m, 1H), 4.45 (s, 2H), 3.7 (m, 4H), 3.03 (dd, J = 13.4, 8.4 Hz, 1H), 2.94 (dt, J = 12.9, 6.4 Hz, 1H), 2.75 – 2.71 (m, 1H), 2.68 (m, 4H) 2.62 (dt, J = 13.1, 8.6 Hz, 1H), 1.91 (dd, J = 11.0, 6.0 Hz, 2H), 1.59 (s, 3H). ^{13}C NMR (125 MHz, CD$_3$CN) δ 166.89, 152.97, 147.87, 136.05, 129.93, 128.49, 125.62, 122.95, 115.77, 100.14, 68.6, 67.84, 54.95, 52.13, 51.56, 49.2, 29.53, 14.43.

1.7. References

1.   Hille, B. Potassium channels in myelinated nerve: selective permeability to small cations. *J.Gen.Physiol.* **1973,** 61, 669-686.

2.   Clare, J. J. Targeting ion channels for drug discovery. *Discov. Med.* **2010,** 9, 253-260.

3.   Katz, B. Les constantes électriques de la membrane du muscle. *Arch. Sci. Physiol.* **1949,** 2, 285-299.

4.   Lüscher, C.; Slesinger, P. A. Emerging roles for G protein-gated inwardly rectifying potassium (GIRK) channels in health and disease. *Nat. Rev. Neurosci.* **2010,** 11, 301-315.

5.   Wickenden, A.; Priest, B.; Erdemli, G. Ion channel drug discovery: challenges and future directions. *Future Med. Chem.* **2012,** 4, 661-679.

6.   Lüscher, C.; Slesinger, P. A. Emerging roles for G protein-gated inwardly rectifying potassium (GIRK) channels in health and disease. *Nat. Rev. Neurosci.* **2010,** 11, 301.

7.   Hibino, H.; Inanobe, A.; Furutani, K.; Murakami, S.; Findlay, I.; Kurachi, Y. Inwardly rectifying potassium channels: their structure, function, and physiological roles. *Physiol. Rev.* **2010,** 90, 291-366.

8.   Nishida, M.; Cadene, M.; Chait, B. T.; MacKinnon, R. Crystal structure of a Kir3. 1-prokaryotic Kir channel chimera. *The EMBO journal* **2007,** 26, 4005-4015.

9.   Pegan, S.; Arrabit, C.; Zhou, W.; Kwiatkowski, W.; Collins, A.; Slesinger, P. A.; Choe, S. Cytoplasmic domain structures of Kir2. 1 and Kir3. 1 show sites for modulating gating and rectification. *Nat. Neurosci.* **2005,** 8, 279-287.

10.   Ma, D.; Zerangue, N.; Raab-Graham, K.; Fried, S. R.; Jan, Y. N.; Jan, L. Y. Diverse trafficking patterns due to multiple traffic motifs in G protein-activated inwardly rectifying potassium channels from brain and heart. *Neuron* **2002,** 33, 715-729.

11.   Glaaser, I. W.; Slesinger, P. A. Structural insights into GIRK channel function. *Int. Rev. Neurobiol.* **2015,** 123, 117-160.

12. Whorton, M. R.; MacKinnon, R. Crystal structure of the mammalian GIRK2 K+ channel and gating regulation by G proteins, PIP2, and sodium. *Cell* **2011,** 147, 199-208.

13. Niu, Y.; Tao, X.; Touhara, K. K.; MacKinnon, R. Cryo-EM analysis of PIP2 regulation in mammalian GIRK channels. *Elife* **2020,** 9, e60552.

14. Mathiharan, Y. K.; Glaaser, I. W.; Zhao, Y.; Robertson, M. J.; Skiniotis, G.; Slesinger, P. A. Structural basis of GIRK2 channel modulation by cholesterol and PIP2. *BioRxiv* **2020**.

15. Marker, C. L.; Stoffel, M.; Wickman, K. Spinal G-protein-gated K+ channels formed by GIRK1 and GIRK2 subunits modulate thermal nociception and contribute to morphine analgesia. *J. Neurosci.* **2004,** 24, 2806-2812.

16. Kloukina, V.; Herzer, S.; Karlsson, N.; Perez, M.; Daraio, T.; Meister, B. G-protein-gated inwardly rectifying K+ channel 4 (GIRK4) immunoreactivity in chemically defined neurons of the hypothalamic arcuate nucleus that control body weight. *J. Chem. Neuroanat.* **2012,** 44, 14-23.

17. Wickman, K.; Pu, W. T.; Clapham, D. E. Structural characterization of the mouse Girk genes. *Gene* **2002,** 284, 241-250.

18. Wickman, K. D.; Iñiguez-Lluhi, J. A.; Davenport, P. A.; Taussig, R.; Krapivinsky, G. B.; Linder, M. E.; Gilman, A. G.; Clapham, D. E. Recombinant G-protein βγ-subunits activate the muscarinic-gated atrial potassium channel. *Nature* **1994,** 368, 255-257.

19. Kano, H.; Toyama, Y.; Imai, S.; Iwahashi, Y.; Mase, Y.; Yokogawa, M.; Osawa, M.; Shimada, I. Structural mechanism underlying G protein family-specific regulation of G protein-gated inwardly rectifying potassium channel. *Nat. Commun.* **2019,** 10, 1-13.

20. Ostrovskaya, O.; Xie, K.; Masuho, I.; Fajardo-Serrano, A.; Lujan, R.; Wickman, K.; Martemyanov, K. A. RGS7/Gβ5/R7BP complex regulates synaptic plasticity and memory by modulating hippocampal GABABR-GIRK signaling. *Elife* **2014,** 3, e02053.

21. Jeremic, D.; Sanchez-Rodriguez, I.; Jimenez-Diaz, L.; Navarro-Lopez, J. D. Therapeutic potential of targeting G protein-gated inwardly rectifying potassium (GIRK) channels in the central nervous system. *Pharmacol. Ther.* **2021**, 107808.

22.   Pravetoni, M.; Wickman, K. Behavioral characterization of mice lacking GIRK/Kir3 channel subunits. *Genes Brain Behav.* **2008,** 7, 523-531.

23.   Herman, M. A.; Sidhu, H.; Stouffer, D. G.; Kreifeldt, M.; Le, D.; Cates-Gatto, C.; Munoz, M. B.; Roberts, A. J.; Parsons, L. H.; Roberto, M. GIRK3 gates activation of the mesolimbic dopaminergic pathway by ethanol. *Proc. Natl. Acad. Sci. U.S.A.* **2015,** 112, 7091-7096.

24.   Kotecki, L.; Hearing, M.; McCall, N. M.; de Velasco, E. M. F.; Pravetoni, M.; Arora, D.; Victoria, N. C.; Munoz, M. B.; Xia, Z.; Slesinger, P. A. GIRK channels modulate opioid-induced motor activity in a cell type-and subunit-dependent manner. *J. Neurosci.* **2015,** 35, 7131-7142.

25.   Nagi, K.; Pineyro, G. Kir3 channel signaling complexes: focus on opioid receptor signaling. *Front. Cell. Neurosci.* **2014,** 8, 186.

26.   Ikekubo, Y.; Ide, S.; Hagino, Y.; Ikeda, K. Absence of methamphetamine-induced conditioned place preference in weaver mutant mice. *Neuropsychopharmacol. Rep.* **2020,** 40, 324-331.

27.   Abney, K. K.; Bubser, M.; Du, Y.; Kozek, K. A.; Bridges, T. M.; Lindsley, C. W.; Daniels, J. S.; Morrison, R. D.; Wickman, K.; Hopkins, C. R. Analgesic effects of the GIRK Activator, VU0466551, alone and in combination with morphine in acute and persistent pain models. *ACS chemical neuroscience* **2018,** 10, 1294-1299.

28.   Kimura, M.; Shiokawa, H.; Karashima, Y.; Sumie, M.; Hoka, S.; Yamaura, K. Antinociceptive effect of selective G protein-gated inwardly rectifying K+ channel agonist ML297 in the rat spinal cord. *Plos one* **2020,** 15, e0239094.

29.   Rifkin, R. A.; Moss, S. J.; Slesinger, P. A. G protein-gated potassium channels: A link to drug addiction. *Trends Pharmacol. Sci.* **2017,** 38, 378-392.

30.   Luján, R.; de Velasco, E. M. F.; Aguado, C.; Wickman, K. New insights into the therapeutic potential of Girk channels. *Trends Neurosci.* **2014,** 37, 20-29.

31.   Signorini, S.; Liao, Y. J.; Duncan, S. A.; Jan, L. Y.; Stoffel, M. Normal cerebellar development but susceptibility to seizures in mice lacking G protein-coupled, inwardly rectifying K+ channel GIRK2. *Proc. Natl. Acad. Sci. U.S.A.***1997,** 94, 923-927.

32.   Mazarati, A.; Lundström, L.; Sollenberg, U.; Shin, D.; Langel, Ü.; Sankar, R. Regulation of Kindling Epileptogenesis by Hippocampal Galanin Type 1 and Type 2 Receptors: The Effects of Subtype-Selective Agonists and the Role of G-Protein-Mediated Signaling. *J. Pharmacol. Exp. Ther.* **2006,** 318, 700-708.

33.   Mett, A.; Karbat, I.; Tsoory, M.; Fine, S.; Iwanir, S.; Reuveny, E. Reduced activity of GIRK1-containing heterotetramers is sufficient to affect neuronal functions, including synaptic plasticity and spatial learning and memory. *J Physiol* **2021,** 599, 521-545.

34.   Blednov, Y. A.; Stoffel, M.; Chang, S.; Harris, R. A. Potassium channels as targets for ethanol: studies of G-protein-coupled inwardly rectifying potassium channel 2 (GIRK2) null mutant mice. *J. Pharmacol. Exp. Ther.* **2001,** 298, 521-530.

35.   Llamosas, N.; Bruzos-Cidón, C.; Rodríguez, J. J.; Ugedo, L.; Torrecilla, M. Deletion of GIRK2 subunit of GIRK channels alters the 5-HT1A receptor-mediated signaling and results in a depression-resistant behavior. *Int. J. Neuropsychopharmacol.* **2015,** 18, pyv051.

36.   Marker, C. L.; Luján, R.; Loh, H. H.; Wickman, K. Spinal G-protein-gated potassium channels contribute in a dose-dependent manner to the analgesic effect of μ-and δ-but not κ-opioids. *J. Neurosci.* **2005,** 25, 3551-3559.

37.   Kozell, L. B.; Walter, N. A.; Milner, L. C.; Wickman, K.; Buck, K. J. Mapping a barbiturate withdrawal locus to a 0.44 Mb interval and analysis of a novel null mutant identify a role for Kcnj9 (GIRK3) in withdrawal from pentobarbital, zolpidem, and ethanol. *J. Neurosci.* **2009,** 29, 11662-11673.

38.   Kobayashi, T.; Ikeda, K. G protein-activated inwardly rectifying potassium channels as potential therapeutic targets. *Curr. Pharm. Des.* **2006,** 12, 4513-4523.

39. Aryal, P.; Dvir, H.; Choe, S.; Slesinger, P. A. A discrete alcohol pocket involved in GIRK channel activation. *Nat. Neurosci.* **2009,** 12, 988.

40. Glaaser, I. W.; Slesinger, P. A. Dual activation of neuronal G protein-gated inwardly rectifying potassium (GIRK) channels by cholesterol and alcohol. *Sci. Rep.* **2017,** 7, 1-11.

41. Yow, T. T.; Pera, E.; Absalom, N.; Heblinski, M.; Johnston, G. A.; Hanrahan, J. R.; Chebib, M. Naringin directly activates inwardly rectifying potassium channels at an overlapping binding site to tertiapin-Q. *Br. J. Pharmacol.* **2011,** 163, 1017-1033.

42. Chen, I. S.; Tateyama, M.; Fukata, Y.; Uesugi, M.; Kubo, Y. Ivermectin activates GIRK channels in a PIP2 -dependent, Gbetagamma -independent manner and an amino acid residue at the slide helix governs the activation. *J Physiol* **2017,** 595, 5895-5912.

43. Magyar, J.; Szabo, G. Effects of volatile anesthetics on the G protein-regulated muscarinic potassium channel. *Mol. Pharmacol.* **1996,** 50, 1520-1528.

44. Kollert, S.; Döring, F.; Gergs, U.; Wischmeyer, E. Chloroform is a potent activator of cardiac and neuronal Kir3 channels. *Naunyn-Schmiedeberg's Arch. Pharmacol.* **2020,** 393, 573-580.

45. Takigawa, T.; Alzheimer, C. G protein-activated inwardly rectifying K+ (GIRK) currents in dendrites of rat neocortical pyramidal cells. *J Physiol* **1999,** 517 (Pt 2), 385-390.

46. Weaver, C. D.; Harden, D.; Dworetzky, S. I.; Robertson, B.; Knox, R. J. A thallium-sensitive, fluorescence-based assay for detecting and characterizing potassium channel modulators in mammalian cells. *J Biomol Screen.* **2004,** 9, 671-677.

47. Ramos-Hunter, S. J.; Engers, D. W.; Kaufmann, K.; Du, Y.; Lindsley, C. W.; Weaver, C. D.; Sulikowski, G. A. Discovery and SAR of a novel series of GIRK1/2 and GIRK1/4 activators. *Bioorg. Med. Chem. Lett.* **2013,** 23, 5195-5198.

48. Wen, W.; Wu, W.; Romaine, I. M.; Kaufmann, K.; Du, Y.; Sulikowski, G. A.; Weaver, C. D.; Lindsley, C. W. Discovery of 'molecular switches' within a GIRK activator scaffold that afford selective GIRK inhibitors. *Bioorg. Med. Chem. Lett.* **2013,** 23, 4562-4566.

49.   Negus, S. S.; Banks, M. L. Pharmacokinetic-Pharmacodynamic (PKPD) Analysis with Drug Discrimination. *Curr Top Behav Neurosci* **2018,** 39, 245-259.

50.   Kaufmann, K.; Romaine, I.; Days, E.; Pascual, C.; Malik, A.; Yang, L.; Zou, B.; Du, Y.; Sliwoski, G.; Morrison, R. D. ML297 (VU0456810), the first potent and selective activator of the GIRK potassium channel, displays antiepileptic properties in mice. *ACS Chem. Neurosci.* **2013,** 4, 1278-1286.

51.   Wydeven, N.; De Velasco, E. M. F.; Du, Y.; Benneyworth, M. A.; Hearing, M. C.; Fischer, R. A.; Thomas, M. J.; Weaver, C. D.; Wickman, K. Mechanisms underlying the activation of G-protein–gated inwardly rectifying K+ (GIRK) channels by the novel anxiolytic drug, ML297. *ACS Chem. Neurosci.* **2014,** 111, 10755-10760.

52.   Kaufmann, K.; Romaine, I.; Days, E.; Pascual, C.; Malik, A.; Yang, L.; Zou, B.; Du, Y.; Sliwoski, G.; Morrison, R. D.; Denton, J.; Niswender, C. M.; Daniels, J. S.; Sulikowski, G. A.; Xie, X. S.; Lindsley, C. W.; Weaver, C. D. ML297 (VU0456810), the first potent and selective activator of the GIRK potassium channel, displays antiepileptic properties in mice. *ACS Chem. Neurosci.* **2013,** 4, 1278-86.

53.   Huang, Y.; Zhang, Y.; Kong, S.; Zang, K.; Jiang, S.; Wan, L.; Chen, L.; Wang, G.; Jiang, M.; Wang, X. GIRK1-mediated inwardly rectifying potassium current suppresses the epileptiform burst activities and the potential antiepileptic effect of ML297. *Biomed. Pharmacother.* **2018,** 101, 362-370.

54.   Zou, B.; Cao, W. S.; Guan, Z.; Xiao, K.; Pascual, C.; Xie, J.; Zhang, J.; Xie, J.; Kayser, F.; Lindsley, C. W. Direct activation of G-protein-gated inward rectifying K+ channels promotes nonrapid eye movement sleep. *Sleep* **2019,** 42, zsy244.

55.   Xu, Y.; Cantwell, L.; Molosh, A. I.; Plant, L. D.; Gazgalis, D.; Fitz, S. D.; Dustrude, E. T.; Yang, Y.; Kawano, T.; Garai, S. The small molecule GAT1508 activates brain-specific GIRK1/2 channel heteromers and facilitates conditioned fear extinction in rodents. *J. Biol. Chem.* **2020,** 295, 3614-3634.

56.   Zhao, Y.; Ung, P. M.-U.; Zahoránszky-Kőhalmi, G.; Zakharov, A. V.; Martinez, N. J.; Simeonov, A.; Glaaser, I. W.; Rai, G.; Schlessinger, A.; Marugan, J. J. Identification of a G-Protein-Independent Activator of GIRK Channels. *Cell reports* **2020,** 31, 107770.

57.   Wydeven, N. M. Molecular mechanisms of inhibitory signaling in the heart and brain. University of Minnesota, 2014.

58.   Dunetz, J. R.; Xiang, Y.; Baldwin, A.; Ringling, J. General and scalable amide bond formation with epimerization-prone substrates using T3P and pyridine. *Org. Lett.* **2011,** 13, 5048-5051.

59.   Bridges, T. M.; Morrison, R. D.; Byers, F. W.; Luo, S.; Scott Daniels, J. Use of a novel rapid and resource-efficient cassette dosing approach to determine the pharmacokinetics and CNS distribution of small molecule 7-transmembrane receptor allosteric modulators in rat. *Pharmacol. Res. Perspect.* **2014,** 2, e00077.

60.   Demko, Z. P.; Sharpless, K. B. Preparation of 5-substituted 1 H-tetrazoles from nitriles in water. *J. Org. Chem.* **2001,** 66, 7945-7950.

61.   Perez-Medrano, A.; Nelson, D.; Carroll, W.; Kort, M.; Gregg, R.; Voight, E.; Jarvis, M.; Kowaluk, E. Use of selective P2X7 receptor antagonists. In Google Patents: 2006.

62.   Koguro, K.; Oga, T.; Mitsui, S.; Orita, R. Novel synthesis of 5-substituted tetrazoles from nitriles. *Synthesis* **1998,** 1998, 910-914.

63.   Maxwell, J. R.; Wasdahl, D. A.; Wolfson, A. C.; Stenberg, V. I. Synthesis of 5-aryl-2H-tetrazoles, 5-aryl-2H-tetrazole-2-acetic acids, and [(4-phenyl-5-aryl-4H-1, 2, 4-triazol-3-yl) thio] acetic acids as possible superoxide scavengers and antiinflammatory agents. *J. Med. Chem.* **1984,** 27, 1565-1570.

64.   Sharma, S.; Lesiak, L.; Aretz, C. D.; Du, Y.; Kumar, S.; Gautam, N.; Alnouti, Y.; Dhuria, N. V.; Chhonker, Y. S.; Weaver, C. D. Discovery, synthesis and biological characterization of a series of N-(1-(1, 1-dioxidotetrahydrothiophen-3-yl)-3-methyl-1 H-pyrazol-5-yl) acetamide ethers as novel GIRK1/2 potassium channel activators. *RSC Med. Chem.* **2021**.

65.	Besnard, J.; Ruda, G. F.; Setola, V.; Abecassis, K.; Rodriguiz, R. M.; Huang, X.-P.; Norval, S.; Sassano, M. F.; Shin, A. I.; Webster, L. A.; Simeons, F. R. C.; Stojanovski, L.; Prat, A.; Seidah, N. G.; Constam, D. B.; Bickerton, G. R.; Read, K. D.; Wetsel, W. C.; Gilbert, I. H.; Roth, B. L.; Hopkins, A. L. Automated design of ligands to polypharmacological profiles. *Nature* **2012,** 492, 215-220.

Chapter 2. MrgX1 PAM

2.1 Introduction

Pain and need for new targets

Chronic pain is one of the most widespread debilitating and highly intricate medical conditions worldwide.[1] More than 30% of the American population suffers from some form of acute or chronic pain.[2] Accumulating evidence suggests a higher prevalence of adults with chronic pain, with opioids being the most commonly prescribed class of medication.[3, 4] Opioid analgesics exert their effect by binding to μ-opioid receptors which are densely found in central and peripheral nervous systems (CNS & PNS).[5] In the brain, opioid receptors are present in the regions associated with both regulating pain and reward mechanisms, leading to side effects including, but not limited to, nausea, respiratory depression, constipation and euphoria.[6] Over the years, numerous efforts have been made to shift the treatment paradigm from opioids to more safe, selective, and non-addictive pharmacotherapy. There is a huge demand for developing an alternate therapy considering the ever-increasing opioid epidemic.[7]

One of the main reasons most pain medicines produce an extensive array of side effects is the broad expression of drug targets (e.g., opioid receptors, cyclooxygenase-2 or COX-2, calcium channels, etc.) in the central and peripheral nervous system, immune pathways, cardiovascular system, etc.[8] Additionally, chronic pain is often primed with peripheral pathological conditions such as inflammation and nerve injury that sensitize nociceptors.[9] Identification of novel molecular targets and their small molecular probes on nociceptive sensory neurons in the trigeminal and dorsal root ganglia (DRG) imparts a great value towards effective and safe pain managment.[10]

Although the number of opioid prescriptions in 2019 (~153 million) have fallen approximately 40% from an all-time high in 2012 (~255 million), the death rates are at an all-time high, and the numbers are still increasing.[11] Even as the FDA and industries are trying innovative ways to stop opioid abuse such as abuse-deterrent formulations, there are numerous easily

accessible web-based resources providing information on "how to crack the code" (abuse drugs from new formulations) with the brand name and specifications. This epidemic demands a treatment that is safe to use chronically and one of the better ways is to target receptors that express exclusively inside the pain pathway and avoid targets with broad expression [8]. And since chronic pain is associated with peripheral pathological conditions such as inflammation or nerve injury, targeting pain through receptors present in nociceptive sensory neurons in PNS shall help in achieving nociception with fewer side-effects.[9, 12]

Mrg family in itch and pain

In mammals, pain sensation or nociception is initiated by a subset of primary sensory neurons known as nociceptors or pain-sensing neurons in the dorsal root ganglia (DRG), which is the part of the peripheral nervous system (PNS).[13] These neurons have both centrally and peripherally projecting axons, as shown in **Figure 2.1**. The peripherally projecting axons of nociceptors terminate in skin, muscles, visceral organs, and connective tissues, where they are activated by noxious stimuli. The centrally projecting axons of nociceptors terminate in the dorsal horn of the spinal cord, where they synapse with projection neurons which relay the information from these neurons to the higher-order brain centers.[14] Pathological conditions such as inflammation and nerve injury can sensitize DRG neurons which causes heightened pain sensitivity and often lead to chronic pain. Targeting localized nociceptors identified in DRG is of great significance as it can lead to newer analgesics with fewer side effects compared to opioids are they would be active in PNS and not CNS.[15]

One such potential target is the Mas-related G-protein–coupled receptor (Mrg), which is a family of orphan GPCRs consisting of many genes in humans, rats, and mice.[15] Many Mrgs, such as mouse MrgC11 and its human homologue MrgX1, are explicitlyexpressed in small-diameter afferent neurons (presumably nociceptive) in DRG but not detected in the CNS (i.e., the spinal cord and brain) or the rest of the body and have been reported to play essential roles in peripheral

sensation.[16-18] Activation of Mrgs by agonists in the peripheral nerve endings of DRG neurons in the skin evokes itch. Strikingly, this pro-itch effect is restricted to Mrg activation in the skin since intrathecal (spinal cord) injection of Mrg agonists did not induce any significant scratching. Activation of MrgC (rodent) with endogenous agonists such as bovine adrenal medulla peptide (**9**, BAM 8-22) and an agonist JHU58 (by intrathecal [i.t.] application) attenuates persistent pain in an MrgC-dependent manner in rodents.[17]
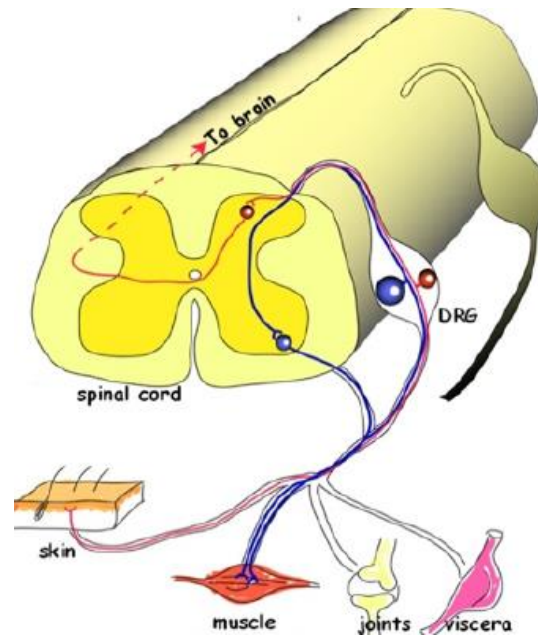
Figure 2.1. Schematic representation of pain circuit.

There are 31 pairs of DRG along the axis of the spinal cord each DRG contains numerous sensory neuron cell bodies. All primary sensory neurons, including small diameter nociceptors (red dots) and large diameter proprioceptors (blue dots), have peripherally and centrally projecting axons. The peripheral axons detect stimuli from skin, muscle, joints, and viscera organs this neuron then relays signals through their central axons to the dorsal horn of the spinal cord where have they synapse with projection neurons in the spinal cord. Mrgs exert their effect in this central terminal in the spinal cord.

Need for transgenic mice containing hMrgX1

Interestingly, Mrg-clusterΔ$^{-/-}$ mice (which have a deletion of 12 Mrgs, including MrgA3 and MrgC11) display enhanced spontaneous pain responses in the inflammatory phase of formalin-induced pain.[18] However, due to species differences across Mrgs, many drug candidates activate MrgX1 but not the rodent (MrgC). Further development of these drugs remained impeded due to the lack of a humanized animal model to test the anti-chronic pain effect *in vivo*. Our collaborators at Johns Hopkins (Dr. Xinzhong Dong's laboratory) were able to generate a transgenic mouse line in which human *MrgX1* gene is expressed in Mrg-expressing primary sensory DRG neurons.[19] The development of this humanized mouse model lead to a significant improvement in testing the potential of MrgX1 as a pain target and also the development of small molecular probes for MrgX1. Although few probes had been discovered for MrgX1 up until this point, the probes which were reported lacked conclusive results due to the inability of testing them *in vivo* in the absence of a transgenic animal model containing the human MrgX1.

Allosteric activators of MrgX1

Even though almost half of all modern drugs regulate the activity of GPCR in some or another way, the majority of GPCRs have not successfully been targeted by functional ligands yet. It is often challenging to develop ligands with high selectivity for specific GPCR subtypes as their orthosteric binding sites can be highly conserved across a GPCR subfamily. In addition, it is often infeasible to develop small molecule drugs for some GPCRs whose orthosteric binding sites are designed for peptides or proteins. Selective allosteric modulators, which bind to allosteric binding sites and either potentiate or inhibit the activation of the receptors by their endogenous orthosteric ligands is one of the favorable ways to circumvent this problem.[20]

Allosteric modulators can offer high selectivity as the orthosteric binding sites are often conserved across a GPCR subfamily. It also allows a better temporal and spatial control of modulating endogenous physiological signaling due to the requirement of endogenous orthosteric
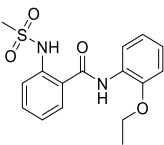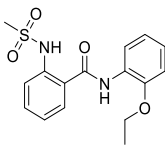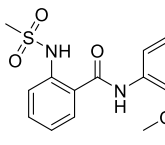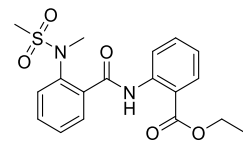
ligand binding. Allosteric ligands that bind at allosteric binding sites can provide better specificity than orthosteric ligands alone because they require colocalization of receptor and orthosteric ligand to function.[21]

Rodent MrgCs and MrgX1 have been reported for both analgesic and pruritogenic (itch) effects.[22, 23] To avoid inducing itch by the activation of peripherally expressed MrgX1,[24] the strategy of allosterically enhancing the endogenous activity of MrgX1 at the site where receptor and endogenous ligand coexist, i.e., at the central terminal, may be more beneficial over an orthosteric agonist. Mrg DRG neurons terminate both centrally at spinal cord lamina II and peripherally at the skin. If the endogenous orthosteric ligand of MrgX1 is restricted at the pain processing central terminal of DRG neurons, the allosteric drug would function only there even when it is administrated systemically. BAM22 peptide is an endogenous agonist of MrgX1. BAM22 immunoreactivity was found in several tissues, including brain and superficial spinal cord dorsal horn.[25, 26] Peripheral activation of MrgX1 receptor with exogenous agonist produces action potential and generates itch sensation. In persistent pain conditions, central activation of MrgX1 inhibits synaptic input into spinal cord dorsal horn neurons to attenuate persistent pain.

2.2. Discovery of ML382 as a positive allosteric agonist

A screen of the 307000 NIH Molecular Library Small Molecule Repository (MLSMR) compound collection was carried out using a triple addition protocol with BAM8–22 as the orthosteric ligand at the Johns Hopkins Ion Channel screening center. Combining the calcium mobilization functional assay activity and excellent selectivity profile as observed in the PubChem Assay and PubChem Hit rate (Assay ID: 588675), this series was chosen for further modification toward a novel positive allosteric agonist of MrgX1.[27] As shown in **Figure 2.2**. the numerical value associated with the Pubchem assay defines the number of times a particular structure appeared in various assays submitted into the PubChem database and hit rate shows how many times it was active (Hit) in those assays. After derivatizing the leads obtained from HTS **1-4** as shown in **Figure 2.2**, **5,** ML382 was discovered as a better allosteric agonist with potency and efficacy.[28]

Dose response studies showed that 5 μM of ML382 enhances the potency of BAM8–22 on MrgX1 by >7-fold (i.e., EC_{50} of BAM8–22 from 18.7 to 2.9 nM;); however, ML382 does not affect the E_{max} of BAM8–22. Furthermore, ML382 does not activate MrgX1 in the absence of BAM8–22, suggesting ML382 itself does not have agonistic activity toward MrgX1. Pharmacological and selectivity profiling of ML382 were performed against the closely related MrgX2 in HEK293 stable cell line expressing MrgX2 as a selectivity screen. The orthosteric agonist used was pro adrenomedullin amino-terminal 20 peptide, fragment 9-20 [PAMP(9-20)].[29] ML382 showed no significant effect on the activation of MrgX2 in the presence of the specific agonist peptide, PAMP.[19] The dose-dependent increase in BAM8–22 affinity demonstrates that ML382 is a positive allosteric modulator of MrgX1, as shown in **Figure 2.3**.[19]

SID	4258711	4262381	3665540	3607659
Compound	**1**	**2**	**3**	**4**
MrgX1 EC$_{50}$ (µM)	0.096	0.329	0.691	3.85
PubChem assays	758	761	765	754
PubChem hits	3	3	3	4

alkylation of the sulfonamide

alkyl, cycloalkyl, aryl

2-alkoxy and 2-thioalkyl

5,ML382

MrgX1 EC$_{50}$ - 123 nM
MrgX2 EC$_{50}$ > 30 µM
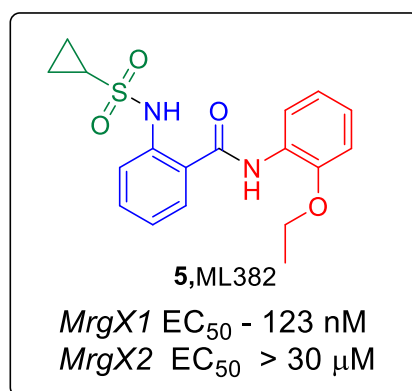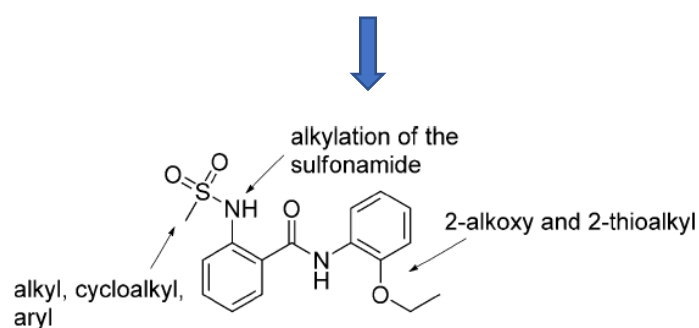
Figure 2.2. Development of ML382
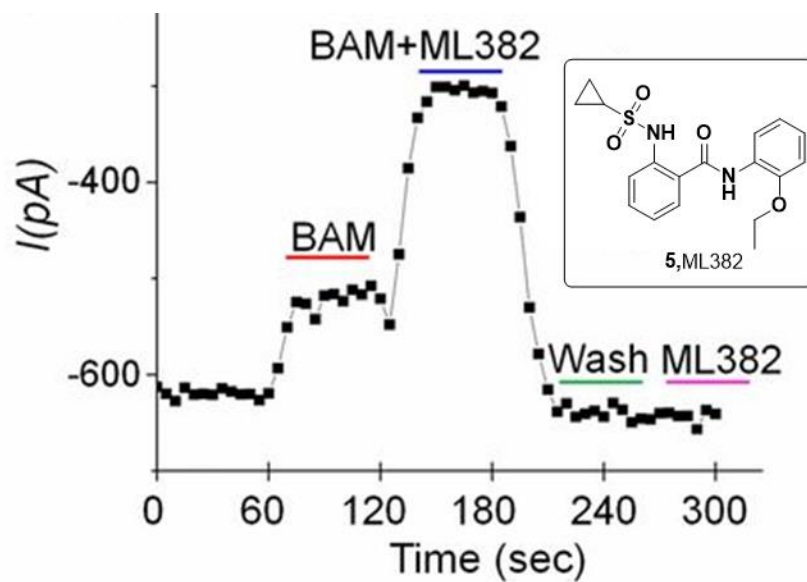
Figure 2.3. Representative time course of the drug effects on HVA ICa.

The enhancement of BAM8–22-induced inhibition of HVA I_{ca} by ML382 (5 μM) is rapid and reversible. (Inset) Chemical structure of ML382. But as such, ML382 has no effect on HVA I_{ca} currents.[19]

Mechanism of MrgX1 activator action

High voltage active (HVA) calcium (Ca^{2+}) channels play an essential role in controlling the release of neurotransmitter vesicles from nociceptive DRG neurons into spinal cord neurons.[30] However, because these channels are broadly expressed throughout the peripheral and central nervous systems and the cardiovascular system, channel blockers pose side effects such as nausea, anxiety, and sweating.[31] Many GPCRs, including μ and κ opioid receptors, mainly inhibit N-type HVA Ca^{2+} channels and mediate the reduction of Ca^{2+} dependent presynaptic neurotransmitter release to produce an analgesic effect. Since MrgX1 is more restricted to the pain pathway and can selectively modulate HVA Ca^{2+} channels to attenuate persistent pain, activation of MrgX1, rather than targeting Ca^{2+} channels directly, attenuates pain while avoiding most central and peripheral side effects. Inhibition of HVA ICa by BAM8–22 is partially mediated by Gi/o-sensitive Gβγ binding of HVA calcium channels and also involve a Gβγ-independent pathway as shown in **Figure 2.4**.[19]

Figure 2.4. Schematic model of MrgX1-mediated HVA ICa inhibition

Which is promoted, in part, by Gβγ binding and depends on the Gαi/o pathway. ML382 is a selective MrgX1 allosteric agonist that can boost BAM8–22-induced current inhibition by increasing its binding affinity (image taken from Li, Zhe, et al. Proc. Natl. Acad. Sci. 2017, 100, 1996-2005).[19]

ML382 Inhibits Nerve injury-induced chronic Pain in MrgX1 Mice

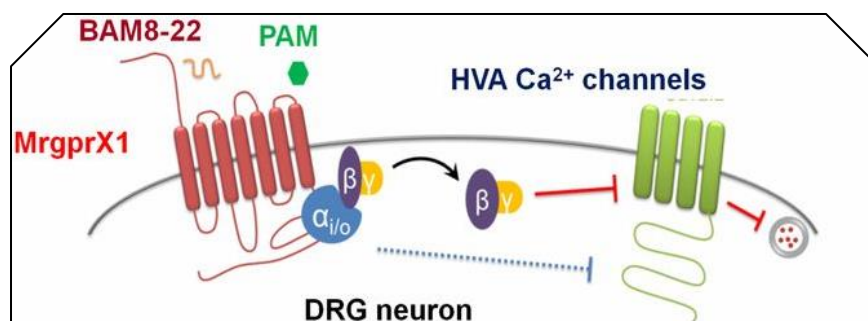When ML382 is injected (25 μM, 5μL, i.t.) half an hour before injecting formalin [2% (v/v) formaldehyde, 5 μL into the plantar aspect of the hind paw, the first phase of pain response (0–10 min post formalin) is not affected, but the later phase of inflammatory pain response (10–60 min post formalin) is significantly attenuated by ML382 in hMrgX1 containing mice compared with $Mrg^{-/-}$ mice. In models of Complete Freund's Adjuvant (CFA) induced inflammatory pain and chronic constriction injury (CCI) induced neuropathic pain, ML382 dose-dependently attenuated pain in MrgX1 mice, but not in $Mrg^{-/-}$ mice. In all these experiments, ML382 was able to induce antihyperalgesia effects without requiring exogenous BAM peptides, suggesting the endogenously released BAM22 upon injury is sufficient for ML382 to exert its analgesic effects.

ML382 did not induce conditional place preference (CPP), a widely used model to identify drug addiction in sham operated animals of either genotype. This suggests that ML382 does not activate innate reward circuitry in the absence of pain. ML382 at a much higher dose (250 μM, 5 μL, i.t.), did not affect locomotor function in either genotype. In addition, BAM8–22 can induce a significant increase in scratching behavior compared with saline; however, ML382 does not induce significant scratching when administered. The BAM22 peptide is a potent ligand for MrgX1 and MrgC, it also contains the characteristic Met-enkephalin YGGFM amino acid motif at the N-terminus that can activate classic opioid receptor subtypes (μ, δ). Thus, it cannot be used as such. However, MrgX1 receptor is insensitive to the classical opioid receptor antagonists and shows distinct structure-activity relationships and pharmacology with its known ligands.[32]

Previous Agonists

Human MrgX1 agonists **6** and **7**, as shown in **Figure 2.5**. reported by GSK[33] and ACADIA[34], respectively, were the first reported compounds that were not peptides. Even though they had very good efficacy with reported EC_{50} of around 30 nM for both against MrgX1, they were not active against MrgC11 and due to the lack of an *in vivo* model, they were not further characterized. These compounds have high molecular weight (MW > 500) which likely contributes to unfavorable CNS druglike molecular properties and solubility.[35] Indeed, compound **6** could not be tested *in vitro* at concentrations above 2 μM due to its limited solubility.[36]

**8**, JHU-58, as shown in **Figure 2.5**, an Arg-Phe-NH2 peptidomimetic with full agonist activity at mouse MRGC11 and rat MRGC, exhibits analgesic effects in rodent models of neuropathic pain. JHU-58, however, displayed negligible agonist activity at human MrgX1, hindering its ability to serve as a molecular template for further structural optimization efforts aimed at clinical translation.[10, 36]

By performing high throughput screening of Eisai's compound library in HEK293 cells stably transfected with human MrgX1 two submicromolar hits **10** and **11**, as shown in **Figure 2.5**. were identified as full agonists with EC_{50} values of 0.92 μM and 0.51 μM, respectively. Both the lead compounds had the presence of benzamidine moiety, which is known as a bioisostere of a guanidyl group of arginine, which is also present in the BAM8-22 peptide, indicating a common binding site. Even though some of the previous series had better activity, the fact that these new leads were low molecular weight compounds makes them more favorable for a CNS drug discovery effort. Eva *et al.* were successful in conversion of the benzamidine moiety of **10** and **11** into a 1-aminoisoquinoline moiety in **12** without loss of potency after performing SAR studies on the lead. **12** is a highly potent MrgX1 agonist devoid of positively charged amidinium group and with superior selectivity over opioid receptors. Although **12** has favorable distribution to the spinal cord, presumably due to the reduced pKa value for the 1-amino group of the aminoisoquinoline as compared to that of the benzamidine moiety, it showed a high degree of clearance.[37]
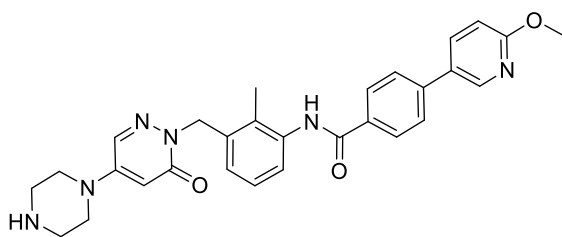
6. GSK
hMrgX1 (EC_{50}) = 0.03 μM
mMrgC11 (EC_{50}) = >2 μM
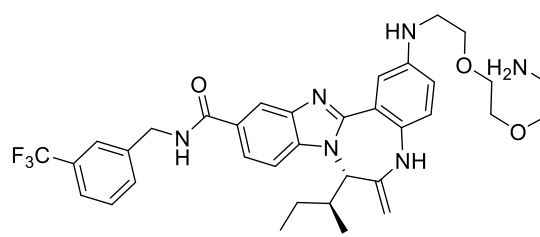
7. Acadia Pharmaceuticals
hMrgX1 (EC_{50}) = 0.3 μM
mMrgC11 (EC_{50}) = -
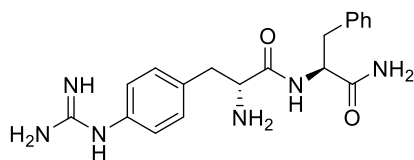
8. JHU-58
hMrgX1 (EC50) = >100μM
mMrgC11 (EC50) = 0.6 mM

Val-Gly-Arg-Pro-Glu-Trp-Trp-Met-
Asp-Tyr-Gln-Lys-Arg-Tyr-Glys

9. BAM8-22
hMrgX1 (EC50) = 0.05 μM
mMrgC11 (EC50) = 0.3 mM

10 (EC_{50} = 0.92 μM)

11 (EC_{50} = 0.51 μM)

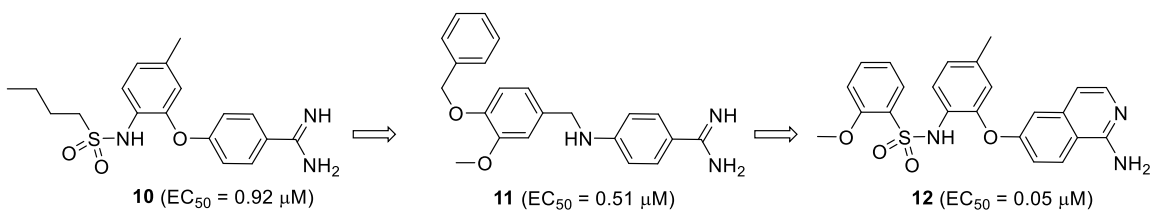**12** (EC_{50} = 0.05 μM)

Figure 2.5. Previous MrgX1 agonists

2.3. Design of new positive allosteric agonists based on ML382

Due to the complex neurochemistry and pharmacology of the GPCR receptors involved in nociception, direct targeting of such GPCR's can result in various unintended side effects. Positive allosteric activation of the MrgX1 in the dorsal root ganglion presents one such opportunity to target pain without activating the reward signal mechanism, which is the root cause for opioid addiction. The discovery and development of ML382 and its use to establish the pharmacology of MrgX1 using the humanized MrgX1 mouse instead of the rodent MrgC11 has helped in establishing the role of MrgX1 in nociception. Other small molecules identified and developed were direct agonists MrgX1 and were shown previously by our collaborators and many others to promote itch. ML382 was an active positive allosteric agonist of MrgX1, and had good physicochemical properties suited for a CNS drug.[35] A quick overview of the calculated physicochemical properties of ML382 using the QikProp module of Schrödinger as shown in **Table 2.1**, helps in determining if ML382 as a good candidate for lead optimization. ML382 has a lower molecular weight (MW = 360.4), the cLogP = 3.174 is in the acceptable range, the total polar surface area tPSA is less than 90. The QikProp produces a CNS activity score which is -1.4 for ML382 and falls in the CNS active range. The predicted apparent Caco-2 cell permeability used as a model for gut blood barrier is 1164, and the blood-brain barrier permeability parameter, QPlog BB, is in the active range. The predicted apparent MDCK cell permeability which is considered a good mimic of blood-brain barrier is 583, for CNS active molecule it should be greater than 500. Owing to such good physiochemical properties ML382 is well suited to be used as a lead for development of new better active allosteric agonist of MrgX1.

In vitro pharmacokinetic experiments suggest the ML382 is rapidly cleared in humans and rats and showed a free fraction %f_u of 0.4 in humans and 1.7 in rats. In a cassette and discrete *in vivo* experiment to measure the brain penetration ML382, it shows a brain to plasma (B:P) ratio of 0.5 in the cassette model and 0.6 in the discrete model with a dosage of 2 mg/kg. When the dose

was increased to 10 mg/kg the B:P ratio appears to be 0.37. Since ML382 was active and had acceptable physicochemical properties for a CNS drug but lacked the ideal pharmacokinetics, we decided to perform a metabolite identification study using mass derived identification of metabolites to identify the possible metabolically labile sites. In both human and mouse liver microsomal fractions (HLM and MLM), oxidation at two different places appears to be the primary mode of metabolism, as shown in **Table 2.2**. The *O*-dealkylation of the ethoxy group was one other metabolite to be identified. Since MetID studies are only predictive and not fully comprehensive, we considered amide hydrolysis to be one of the instability providers as clearance in rats was more than ten times faster than in humans and, as described earlier, proteolytic activity in rodents is higher than that of humans.

In addition, ML382 was evaluated using the Eurofins Lead Profiling Screen, a binding assay panel of 68 GPCRs, ion channels, and transporters screened at 10 μM. ML382 did not inhibit 67 of the 68 targets assayed (inhibition of radioligand binding >50% at 10 μM); the only target that was considered active was serotonin (5-hydroxytryptamine) $5HT_{2B}$, which showed 63% inhibition at 10 μM. Overall, ML382 displayed a very favorable selectivity profile.[28]

Table 2.1. Physicochemical and PKPD properties of ML382

QikProp Schrodinger		Results	CNS Range
MW		360.43	<400
cLogP		3.174	<3 – 4
QPLogS		-4.452	-6.5 – 0.5
PSA		83.61	<90
CNS		-1	-2 to +2
QPPCaco		1164.45	>25 poor >500 great
QPLogBB		-0.858	-3.0 – +1.2
QPPMDCK		583.2	<25 poor >500 great
Pharmacokinetics of ML382			
Human CL_{INT}	HCL_{HEP}	61.9	15.7
Rat CL_{INT}	CL_{HEP}	1065	65.7
Human PPB (%F_u)		0.4	
Rat PPB (%F_u)		1.7	
In vivo **PK (IP, 2 mg/kg, cassette)**			
Plasma (ng/mL)		151	
Brain (ng/g)		75.6	
B:P		0.5	
In vivo **PK (IP, 2 mg/kg, discrete)**			
Plasma (ng/mL)		419	
Brain (ng/g)		250	
B:P		0.6	
In vivo **PK (IP, 10 mg/kg, discrete)**			
Plasma (ng/mL)		2624	
Brain (ng/g)		976	
B:P		0.37	

Table 2.2. Metabolite identification of ML382

Peak ID	Tentative Metabolite Identification	Observed m/z	Retention Time (min)	Species/Matrix
ML382	Parent (P)	361.1211	7.66	MLM, HLM
M1	P + O	377.1148	5.84	MLM, HLM
M2	P + O	377.1175	5.94	MLM, HLM
M3	De-ethylation	333.0900	5.18	MLM, HLM
M4	P + O + O	393.1082	4.45	MLM, HLM
M5	P + O	377.1164	6.48	HLM

5, ML382, possible metabolites
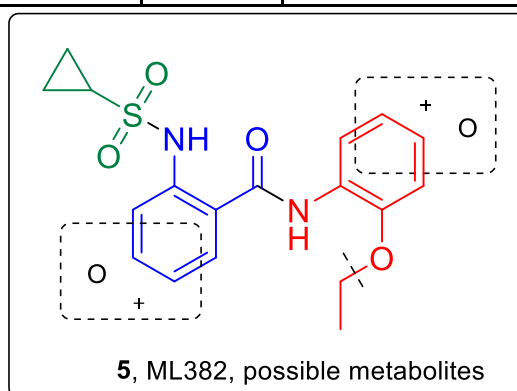
For the design of new analogs, we had two goals in mind to improve potency and metabolically stability. For imparting metabolic stability, we addressed the three phenomena which were responsible for rapid metabolism of the compound. Primarily, the breakage of the ethoxy group on the right-hand portion, amide bond hydrolysis and aromatic ring oxidations. As shown in **Figure 2.6**, a comprehensive study around ML382 was performed starting with a broad scan of different alkyl substitutions in the sulfonamide portion of the molecule as in class I compounds. Next, we substituted the sulfonamide with a carbonyl amide as in class II, which could help in decreasing the polarity of ML382 and improve CNS penetrantion. Class III compounds were made to prevent the breakage of the ethoxy moiety on the right-hand side and to identify ethoxy substituents which are active and stable. In Class IV, the molecule was cyclized to eliminate the free acidic NH on sulfonamide, which could hinder BBB penetration, and in doing so we also tried to address the amide hydrolysis problem. Class V compounds were made to address amide hydrolysis, which was not identified in the met ID study but could be one of the possible reasons for high clearance; we tried to understand the role and necessity of the amide bond and incorporated bio-isosteres to prevent metabolsim. In class VI and VII, we addressed the oxidation observed in the MetID study by inserting heterocycles into the aromatic ring, substituting with saturated rings, and halogenating the aromatic rings. This broad study allowed us to diversify the ML382 without drastically changing the core structure.
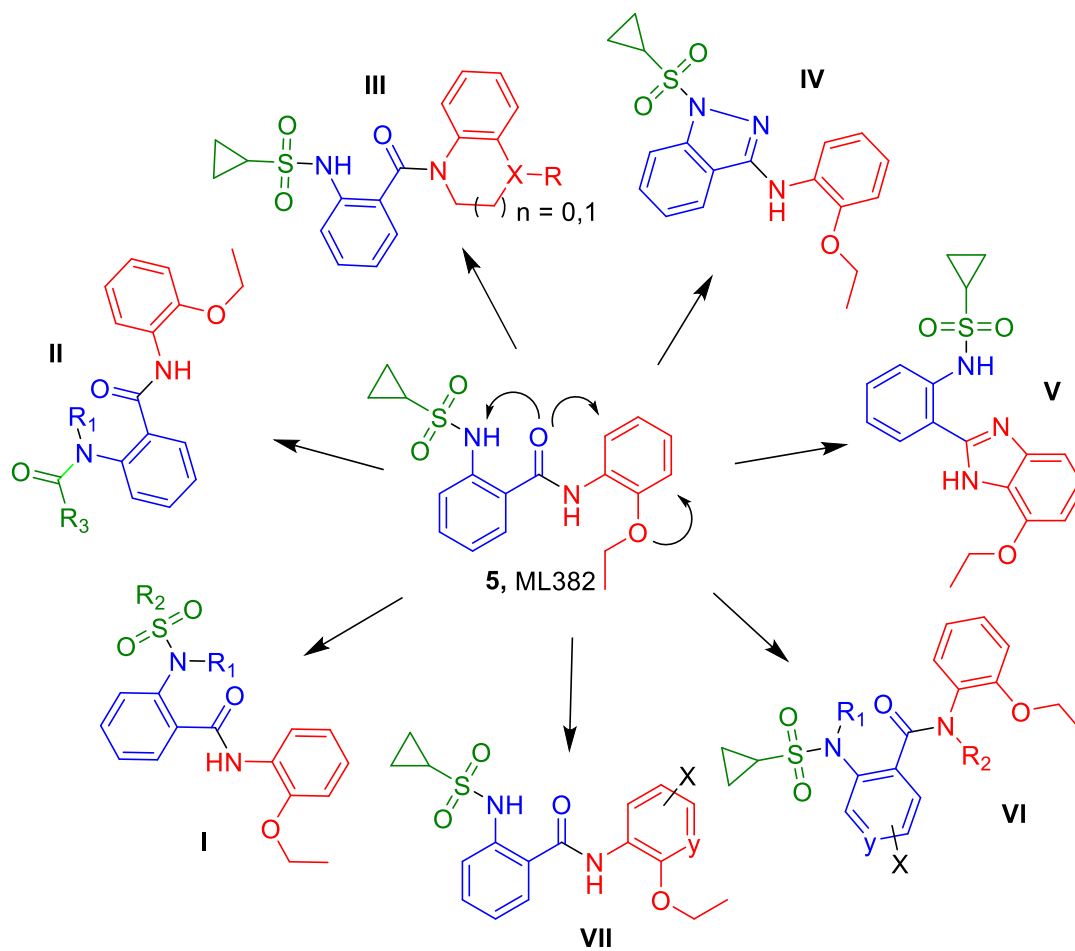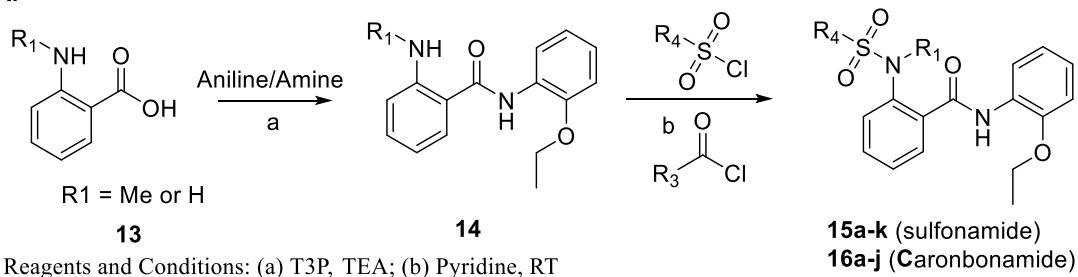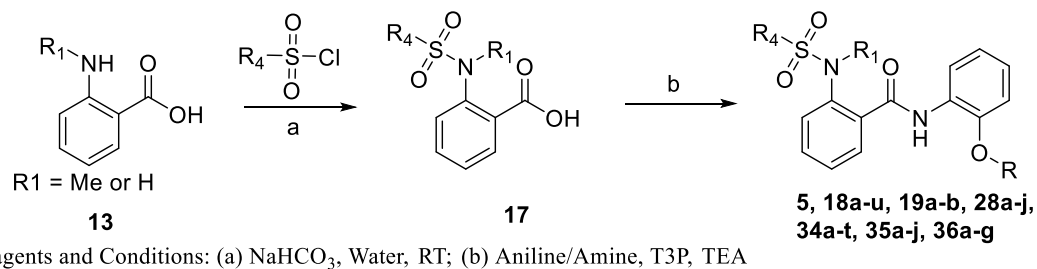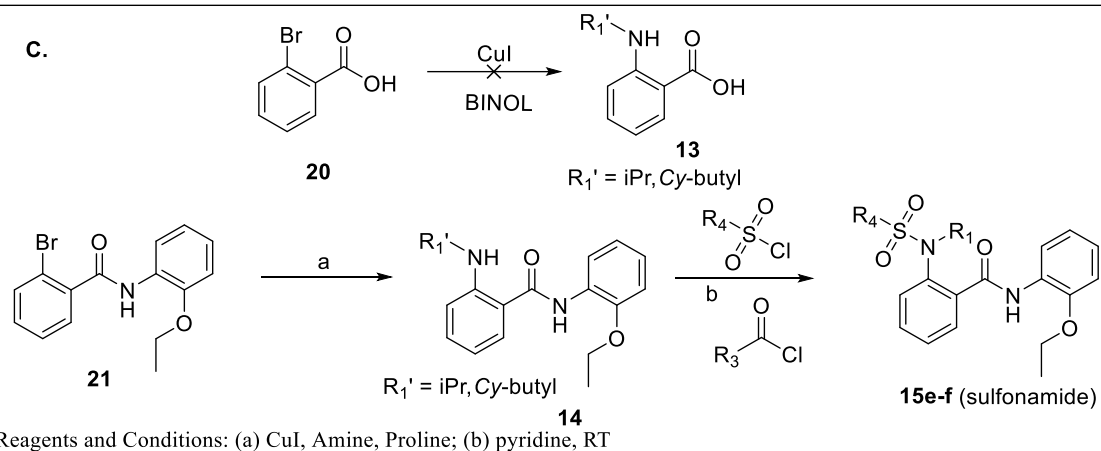
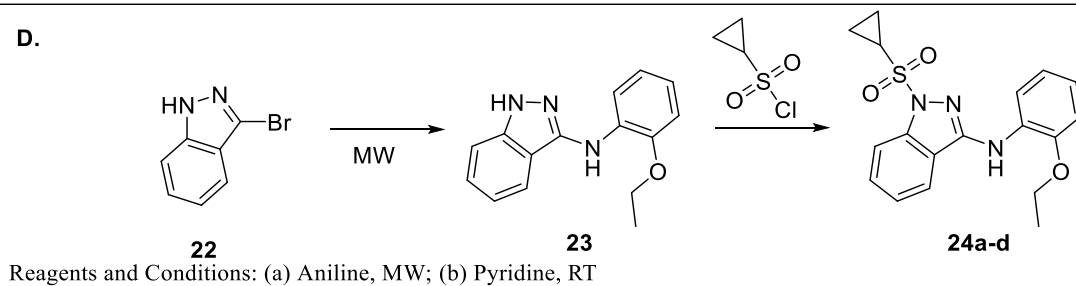**Figure 2.6. Designing of new MrgX1 allosteric agonists based on ML382**
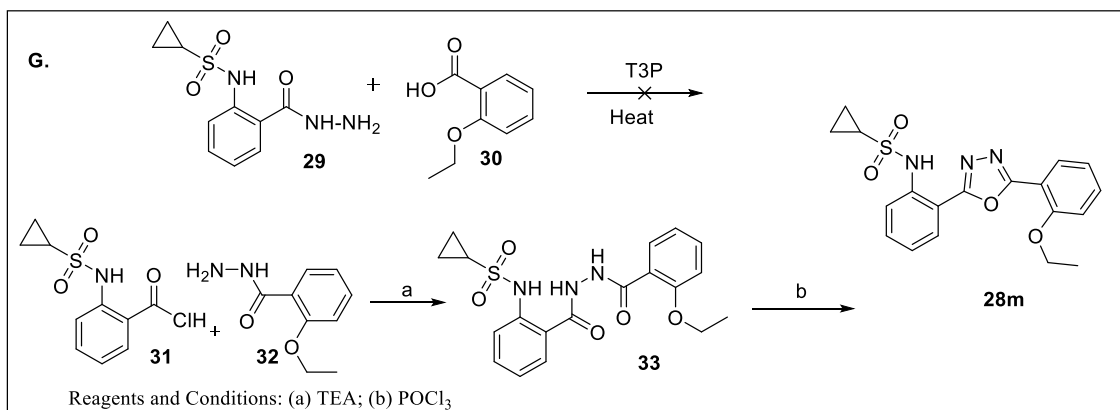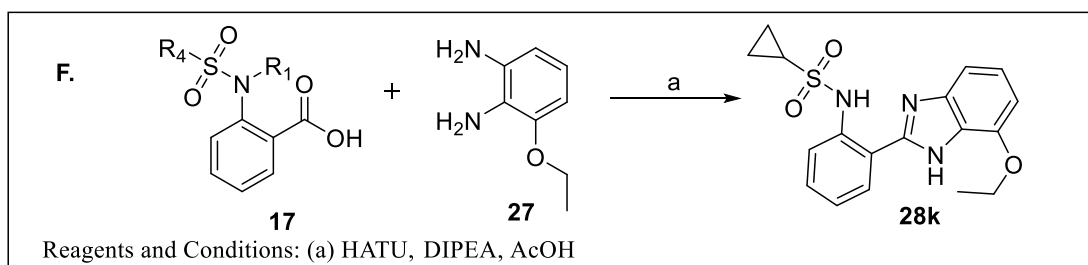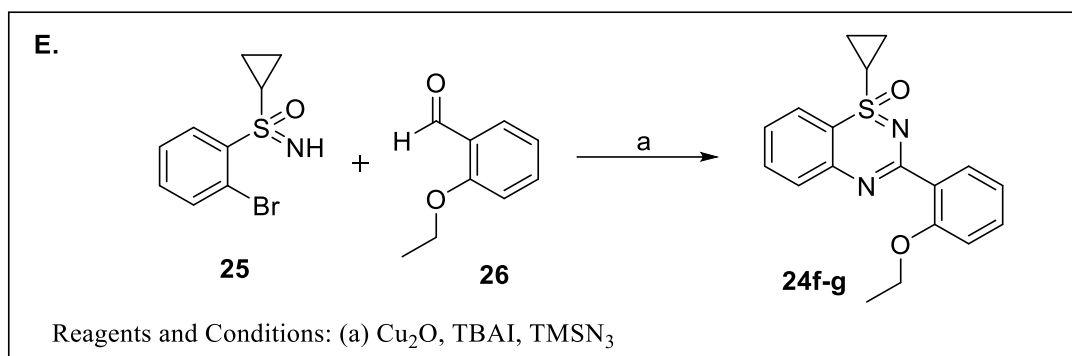
Synthesis of the new ML382 derivatives

The compounds containing main core, 2-(sulfonamido)-*N*-benzamide were all synthesized via a common scheme. As shown in **Scheme 2.1B**, the anthranilic acid derivative, **13** was coupled with an appropriate sulfonyl chloride under basic water conditions (NaHCO₃, H₂O) to yield the sulfonamide, **17**. This compound is then coupled with an aniline (or amine) using T3P to yield the final compounds**5, 18a-u, 19a-b, 28a-j**.[38] The T3P coupling works fairly well with most of the anilines/amine giving yields ranging from 20-90% within 1-12 hours of reaction, based upon the derivatives. Only in the case of cyclic amines to obtain derivatives like **18g** we had to utilize costly amide forming coupling agents like PyClU. This synthetic scheme was mainly used to make right-hand side changes using various aniline/amines. In a similar type of modular approach, the amide, **14** could be made first and then the sulfonamide as the final target **Scheme 2.1A**. This is helpful while trying to derivatize the left-hand side sulfonamide portion. This approach is limited to anthranilic acid and *N*-methyl anthranilic acid.

To make a diverse set of *N*-alkyl sulfonamide, we employed a copper catalyzed Buchwald-Hartwig type C-N bond coupling. A trial for amination of 2-bromobenzoic acid, **20** using a known protocol employing *rac*-BINOL as a ligand, was not successful and resulted in very low yields.[39] We then tried to make the amide, **21**, and then did the C-N coupling using CuI and L-proline as a ligand.[40] The reaction yielded the desired amide derivative, **13** which was rapidly converted into the sulfonamide/amide using sulfonyl/carbonyl chlorides as shown in **Scheme 2.1C**. To synthesize the indazole derivatives **24a-d**, as cyclic derivatives of ML382 lacking the free acidic -NH, initially we tried to make the left-hand side sulfonamide by condensing sulfonyl chloride with **22**, but the next step of C-N bond formation with *O*-phenetidine was very low yielding; thus, we shifted to alternate route, where a microwave assisted condensation of **22** with desired anilines/amines was carried out first followed by the formation of sulfonamide as shown in **Scheme 2.1D**.[41]

Another type of cyclic derivative **24f,g** was made using a recently developed one-pot benzo[*e*][1,2,4]thiadiazine oxide ring formation reaction between a sulfoximine, aldehyde, and

azide catalyzed by copper (I) oxide.[42, 43] The benzimidazole, **28k**, was synthesized by the coupling of the sulfonamide benzoic acid, **17**, with the 1,2-diaminophenyl, **27** via a two-step protocol. First, the amide was formed using HATU followed by ring closure under heat and acidic conditions to yield **28k**. A more conventional approach to directly condense the acid and diamine derivative under harsh acidic conditions failed to yield **28k**. Similarly, to make different types of bioisosteres, we had to try alternate approaches. Even though there are plenty of reports on the synthesis of heterocycles as bioisosteric amide replacements, an ideal condition to work in a given molecule has to be tried and optimized.[44, 45] As in the case of incorporating the oxadiazole ring to make bio-isostere, **28m** our primary approach to condense hydrazide **29** which can be easily made from **17,** with commercially available **30** failed. We then had to approach from the other side by making hydrazide on the right-hand side and conforming the initial condensation of hydrazide **32** with acid chloride **31** to form **33** and then cyclize in POCl$_3$ to achieve the desired product **28m**. Apart from the general synthesis shown in **A** and **B**, a broad emphasis on the yields of the reaction was not given. Our primary approach was to synthesize various primary leads using more straightforward and rapid chemistry to get the maximum number of leads in a given set of time. Once a lead molecule comes out to be active, we would place additional efforts to make the synthesis better yielding and modular. Molecules thus synthesized were sent in small batches to our collaborators Dr. Xinzhong Dong lab at Johns Hopkins University School of Medicine, Baltimore, MD. The efficacy of this compounds to activate MrgX1 stably expressed on heck 293 cell lines were tested. The enhanced activation of MrgX1 by the compounds in the presence of agonist BAM8-22 was monitored by a calcium imaging assay. One's a compound turns out to be active, then its EC$_{50}$ will be measured.

A.

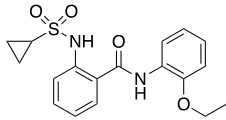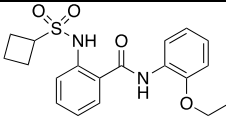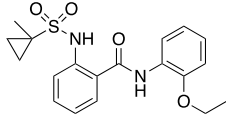R1 = Me or H
13

Reagents and Conditions: (a) T3P, TEA; (b) Pyridine, RT

14

15a-k (sulfonamide)
16a-j (Caronbonamide)

B.

R1 = Me or H
13

Reagents and Conditions: (a) NaHCO₃, Water, RT; (b) Aniline/Amine, T3P, TEA

17

**5, 18a-u, 19a-b, 28a-j,
34a-t, 35a-j, 36a-g**

C.

20

13
R₁' = iPr, *Cy*-butyl

21

R₁' = iPr, *Cy*-butyl
14

15e-f (sulfonamide)

Reagents and Conditions: (a) CuI, Amine, Proline; (b) pyridine, RT

D.

22

23

24a-d

Reagents and Conditions: (a) Aniline, MW; (b) Pyridine, RT

E.

25 + **26** → **24f-g**

Reagents and Conditions: (a) Cu₂O, TBAI, TMSN₃

F.

17 + **27** → **28k**

Reagents and Conditions: (a) HATU, DIPEA, AcOH

G.

29 + **30** —T3P / Heat (✗)→

31 + **32** —a→ **33** —b→ **28m**

Reagents and Conditions: (a) TEA; (b) POCl₃

Scheme 2.1. Synthesis of ML382 based derivatives

Results

Class I: Substituted sulfonamides

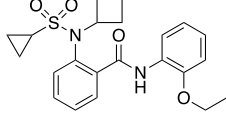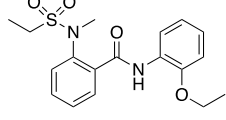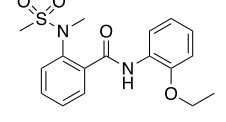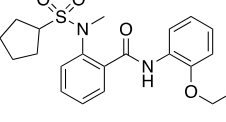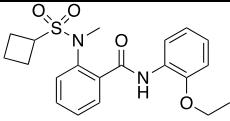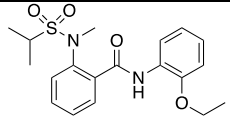Class I compounds were designed such that the cyclopropyl sulfonamide combination is the best going forward. We synthesized alkyl combinations which were not evaluated in the previous SAR studies leading to the identification of ML382. In this series, we replaced the cyclopropyl with cyclobutene, **15a**, 1-methyl cyclopropyl, **15b**, and cyclopentane **15c**. Even though **15a** and **15b** had very high E_{max}, those values did not into low EC_{50}, they had EC_{50} of 1.6 and 4.4 µM, respectively. Next, we varied the *N*-alkyl combinations starting from methyl, **15d**, propyl, **15e**, and cyclobutyl, **15f**. The best compound, *N*-methyl cyclopropyl sulfonamide, **15d**, had EC_{50} of 0.52 µM while the rest were not as active. Next, we tried to combine both the studies, making different alkyl-substituted *N*-methyl sulfonamide, out of which dimethyl combination **15h** was the best with EC_{50} of 0.55 µM. Derivatizing with bigger alkyl compared to cyclopropyl helped in identifying if there was any space in the MrgX1 binding site, which could be covered with a bulkier group. Still, cyclopropyl continues to be the best, with some toleration for ethyl and *N*-methyl. *N*-methyl sulfonamide helped in eliminating the acidic-*N*H and improve predicted solubility and BBB permeability.

Table 2.3. Class I sulfonamide modifications

Cmpd.	Structure	E_{max} (%)[a]	MrgX1 EC_{50} (μM)[a]
5		100	0.1237
15a		368.9 ± 27.2	1.634
15b		302.3 ± 28.7	4.44
15c		15.5 ± 16.5	ND
15d		65.7 ± 17.6	0.522
15e		34.0 ± 20.3	ND
15f		125.4 ± 22.6	ND
15g		343.5 ± 61.0	0.665
15h		202.5	0.551
15i		114.2 ± 41.0	ND

15j		296.5 ± 33.6	1.718
15k		226.0 ± 89.0	ND

[a]Assays were carried out in the presence of 10 nm BAM8-22; data are the mean ± SEM of n = 2 experiments; E_{max} values are normalized to the control compound ML382; ND/blanl: not determined, as E_{max} is too low.

Class II: Carbonylamide derivatives

   In this class of compounds, we tried to replace the sulfonamide with the carbonyl amide to see if the sulfonamide was necessary for potency. A carbonyl amide compound should, theoretically, have better brain penetrance, improve solubility, and also provide a more convenient handle for further derivatization. Firstly, we tried to replicate the cyclopropyl sulfonamide by making a similar cyclopropyl carbonyl amide, **16a**, which had an E_{max} of 53%. Later, we incorporated various cyclo alkyl substitutions, namely 1- and 2-methyl cyclopropyl, **16b** and **16c**, cyclobutane, **16d**, and cyclopentane **16e**. Unfortunately, none of these were active except **16d**. Our attempts to incorporate *N*-methyl with all of the same alkyl derivatives **16f**-**60i** resulted in no active compounds. Lastly, we tried to get rid of the carbonyl and made its corresponding alkylated amine **16j**, which led to complete loss of the activity compared to **16a**.

Table 2.4. Class-II carbonamide modifications

Cmpd.	Structure	Emax (%)	MrgX1 EC$_{50}$ (µM)
16a		53.5 ± 15.1	ND
16b		7.0 ± 6.5	ND
16c		0.4 ± 5.4	ND
16d		18.1 ± 22.4	ND
16e		1.5 ± 13.6	ND
16f		0.3 ± 10.6	ND
16g		-25.5 ± 12.7	ND
16h		63.1 ± 7.5	ND
16i		-9.6 ± 15.5	ND
16j		9.1 ± 11.1	ND
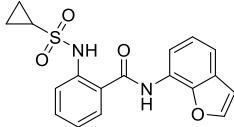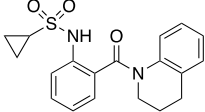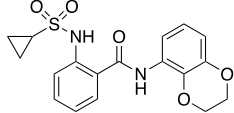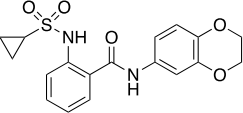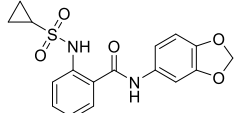
^aAssays were carried out in the presence of 10 nm BAM8-22; data are the mean ± SEM of n = 2 experiments; E_{max} values are normalized to the control compound ML382; ND/blank: not determined, as E_{max} is too low.
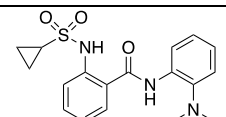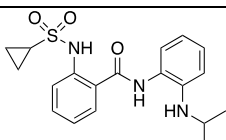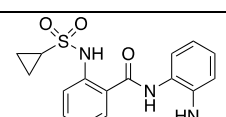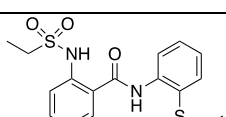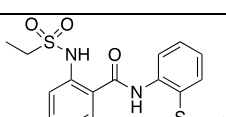
Class III: Ethoxy modifications
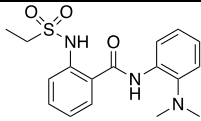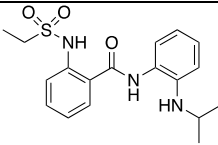
To prevent ether metabolism and assess the potency, we evaluated cyclized versions of the right-hand side of the molecule and also branching of the ethoxy moiety. For the cyclized version, we tried to mimic the ethoxy in ML382 and made *N*-linked heterocycles to impart 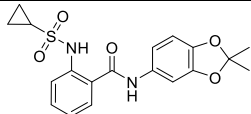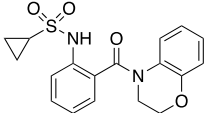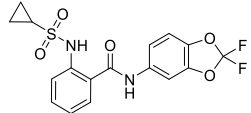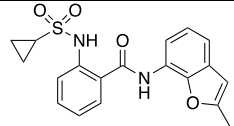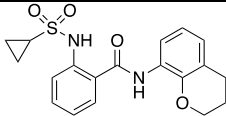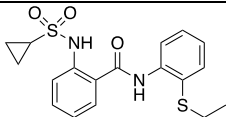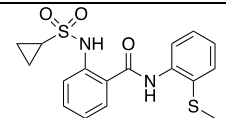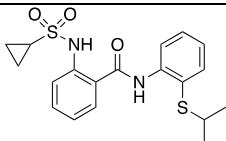rigidity to the molecule. In the cyclized ethoxy version only benzofuran containing molecules, **18a** and **18i**, -(2,3-dihydrobenzo[*b*][1,4]dioxin) moiety **18c**, and chromane moiety **18j**, retained some activity. Out of these 2-methyl benzofuran, **18i**, had a reasonable EC_{50} of 0.98 µM. The remainder of the cyclic compounds, such as tetrahydroquinoline, **18b**, benzo[d][1,3]dioxol, **18e**, 2,2-dimethylbenzo[d][1,3]dioxol, **18f**, and 2,2-difluorobenzo[*d*][1,3]dioxol **18h**, had no activity at all.

Next we moved towards replacing the ether with sulfide since both of them have two lone pair of electrons and sulfur has been used to replace oxygen. However, all of the trial compounds containing ethyl, methyl, and isopropyl sulfide, **18k**, **18m**, and **18n**, were moderately active. Thus, we moved towards using alkylated anilines to mimic the ether as in the case of **18n**-**18q**. These analogs did show some response but not sufficient to get an EC_{50}. In order to confirm the results and remove any bias in the combinations, we also used ethyl sulfonamide containing moiety to try with the sulfide and aniline containing right-hand side **18r**-**18u**; however, these also gave the same results. Overall sulfide containing moiety were slightly more active than alkylated anilines, as shown in **Table 2.5**.

Table 2.5. Class III ethoxy modifications

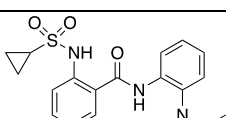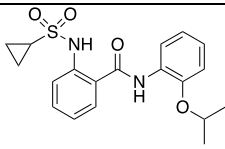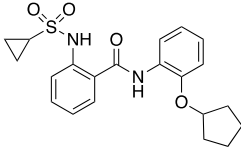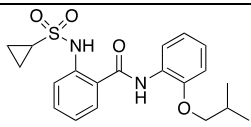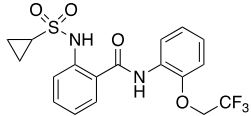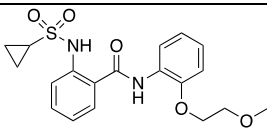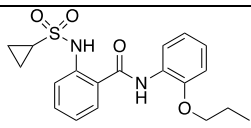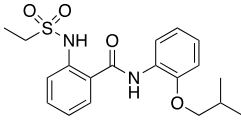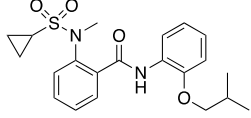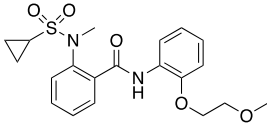| Cmpd.	Structure	Emax (%)	MrgX1 EC$_{50}$ (μM)
18a		53.4 ± 14.6	6.055
18b		6.8 ± 6.7	ND
18c		37.9 ± 15.3	19.17
18d		2.1 ± 13.9	ND
18e		7.4 ± 10.9	ND
18f		-25.6 ± 5.0	ND
18g		2.7 ± 12.2	ND
18h		14.6 ± 13.8	ND
18i		310.8 ± 94.4	0.940
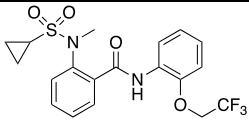
18j		126.8 ± 33.6	ND
18k		63.2 ± 7.5	ND
18l		31.1 ± 8.6	ND
18m		37.8 ± 8.2	ND
18n		19.7 ± 5.5	ND
18o		26.5 ± 9.1	ND
18p		4.1 ± 3.2	ND
18q		-11.0 ± 6.4	ND
18r		32.7 ± 7.6	ND
18s		25.9 ± 10.4	ND

18t		9.0 ± 3.6	ND
18u		5.5 ± 4.9	ND
[a]Assays were carried out in the presence of 10 nm BAM8-22; data are the mean ± SEM of n = 2 experiments; E_{max} values are normalized to the control compound ML382; ND/blank: not determined, as E_{max} is too low.			

We tried to investigate ethoxy replacements by branching, elongating the chain, and addition of a trifluoromethyl group. The introduction of a branched group produced active compounds; however, these lost ~10-fold activity compared to the ethyl group (**19a**, EC_{50} = 2.6 µM; **19b**, EC_{50} = 1.1 µM) and **19c**. The 2,2,2-trifluoroethyl group (**19d**, EC_{50} = 0.53 µM) or adding an additional methylene group (Propyl, **19f**, EC_{50} = 0.51 µM) were active compounds, although not as potent as ML382. Moving to the methoxyethyl **19e** lost all activity. We tried to introduce these changes into ethyl sulfonamide **19g,** which was not fruitful, but the *N*-methyl cyclopropyl sulfonamide group brought activity back to the molecule (**19h**, EC_{50} = 1.4 µM), (**19i**, EC_{50} = 0.76 µM), (**19j**, EC_{50} = 0.74 µM). Overall *N*-methyl cyclopropyl sulfonamide containing molecules were much better at tolerating the changes to the ethoxy, but even the best of them did not had potency comparable to it, as shown in **Table 2.6**.

Table 2.6. Class III ethoxy replacements

Cmpd.	Structure	Emax (%)	MrgX1 EC$_{50}$ (μM)
19a		389.6 ± 106.9	2.592
19b		375.5 ± 13.7	1.085
19c		18.8 ± 7.3	ND
19d		181.7 ± 60.5	0.529
19e		20.7 ± 6.9	ND
19f		378.7 ± 62.4	0.51
19g		56.5 ± 27.5	ND
19h		145.4 ± 54.3	1.125
19i		104.1 ± 74.5	0.763

| 19j | | 79.8 ± 15.4 | 0.747 |

[a]Assay were carried out in the presence of 10 nm BAM8-22; data are the mean ± SEM of n = 2 experiments; E_{max} values are normalized to the control compound ML382; ND/blank: not determined, as E_{max} is too low.

Class IV: ML382 cyclization

We envisioned closing the amide of the sulfonamide with the carbonyl of the amide to form a five-membered ring system as our first attempt to scaffold hop within this series. From our previous work, we knew the NH of the sulfonamide was not critical as alkylation of this nitrogen was tolerated. Thus, we started with commercially available indazole or aza-indazole starting material, **22** to make cyclized derivatives **24a-d**. Unfortunately, these compounds did not show any activity against MrgX1. Next, we tried out a bicyclic compound **24e**, which had come out as an impurity during some reaction trials to see if there are multiple interaction sites available at the allosteric center, but this was also not active. Like our attempt to cap the free NH into a 5-membered ring we tried out to make a 6-membered benzo[*e*][1,2,4]thiadiazine oxide ring, but two different ether modifications in this cyclized version **24f** and **24g** both came out to be inactive. So far, almost all of our attempts to cyclize the core amide to the right-hand side ethoxy were not fruitful, as shown in **Table 2.7**.

Table 2.7. Class IV ML382 cyclization

Cmpd.	Structure	Emax (%)	MrgX1 EC$_{50}$ (µM)
24a		-5.7 ± 4.1	ND
24b		1.9 ± 16.6	ND
24c		-11.7 ± 8.7 (57)	ND
24d		-4.2 ± 2.6	ND
24e		-38.1 ± 7.5	ND
24f		-19.6 ± 16.4	ND
24g		6.6 ± 21.1	ND

[a]Assays were carried out in the presence of 10 nm BAM8-22; data are the mean ± SEM of n = 2 experiments; E$_{max}$ values are normalized to the control compound ML382; ND/blank: not determined, as E$_{max}$ is too low.
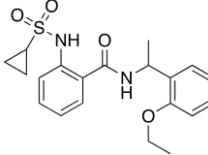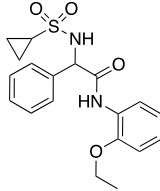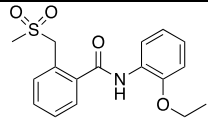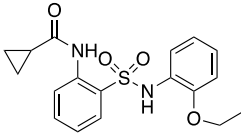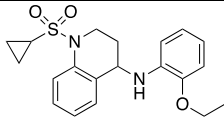
Class V: Amide replacement and bioisosteres
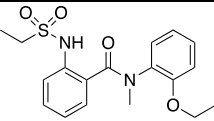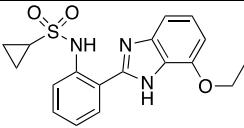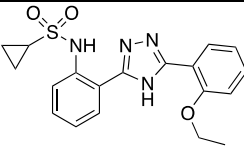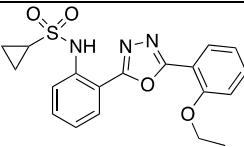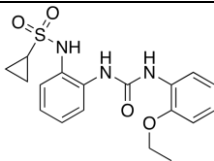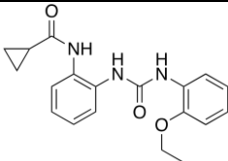
Class V compounds were aimed at identifying the role of the center amide in imparting activity to the molecule and also to find suitable ways to mask that in order to prevent its hydrolysis and to identify bioisosteres replacements. To begin with, we tried to change the position of the amide bond from ortho of the sulfonamide as in the case of ML382 to meta position **28a** and para position **28b**. **28a** was not active at all, while **28b** was only slightly active. For compound **28c**, we tried to add a carbon to shift the amide to the right, and it retained very little activity. An attempt to remove the carbonyl, as in the case of **28d,** was also not fruitful. The incorporation of a branched ethylene group on the right-hand side **28e** was also not active.

Next, we attempted to shift the sulfonamide as in **28f**, using an extra carbon and replace sulfonamide with just a sulfone as in **28f** or swapping the positions of two different amidic group **28h** were not active, and also making a cyclic sulphonamide **28i** was also not active. Making of an *N*-methylated as in **28j** was also not beneficial.

From the above study, it was clear that the amide at its native position in ML382 is absolutely essential for the activity. Any small modifications to mask it for preventing its metabolism was not fruitful, so we shifted to making some bioisosteric replacement for the amide, which shall keep the amide spatial geometry. Unfortunately, ours attempt to make benzimidazole, **28k**, triazole, **28l**, oxadiazole, **28m** and urea derivatives, **28n** and **28o**, did not result in any active compounds.

Table 2.8. Class V Amide modification and bio-isosteres

Cmpd.	Structure	Emax (%)	MrgX1 EC$_{50}$ (μM)
28a		-44.4 ± 77.3	ND
28b		70.6 ± 56.1	ND
28c		55.4 ± 73.1	ND
28d		3.3 ± 6.8	ND
28e		-16.3 ± 7.8	ND
28f		-12.8 ± 8.2	ND
28g		-15.4 ± 30.9	ND
28h		-3.3 ± 9.9	ND
28i		-20.1 ± 13.3	ND
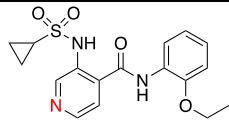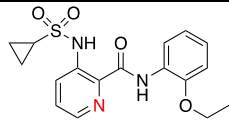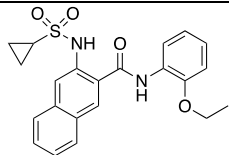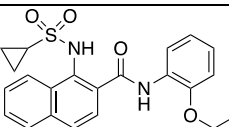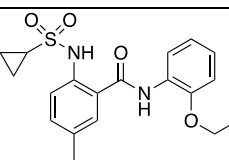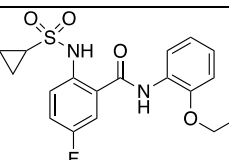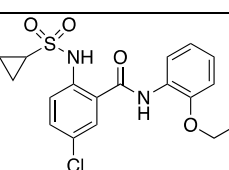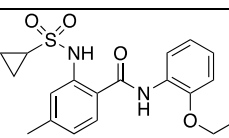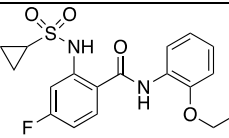
28j		-7.1 ± 2.2	ND
28k		23.8 ± 8.9	ND
28l		7.5 ± 7.4	ND
28m		6.7 ± 4.6	ND
28n		-14.3 ± 7.6	ND
28o		-28.6 ± 8.1	ND

[a]Assays were carried out in the presence of 10 nm BAM8-22; data are the mean ± SEM of n = 2 experiments; E_{max} values are normalized to the control compound ML382; ND/blank: not determined, as E_{max} is too low.
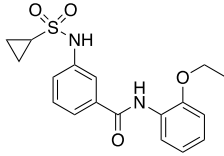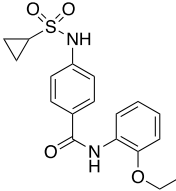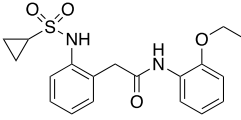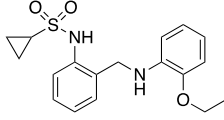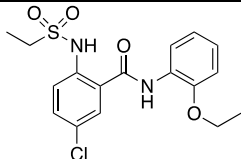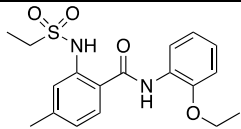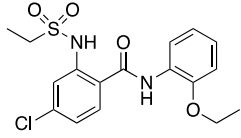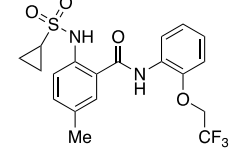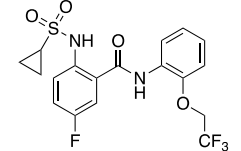
Class VI: Left-hand side modifications
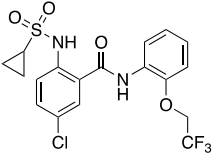
The most prominent metabolites identified from MetID studies were from oxidation of the phenyl rings. We envisioned that both the aromatic rings might be prone to oxidation, and thus these compounds were designed to introduce heterocycles and halogen substitutions to avoid oxidation. Also, incorporating halogenated substituents shall impart better stability against metabolism.

We started with pyridine moieties **34a** and **34b**; and expanding the molecule by making naphthyl derivatives **34c** and **34d**, none of which were active. From there, we moved to perform an alkyl and halogen substitution study, and we tried to incorporate methyl, fluoro, and chloro at both 5- and 4- position, respectively. On the 5-position methyl, **34e**, EC_{50} = 0.024 µM was the most active compared to fluoro, **34f**, EC_{50} = 0.13 µM, and chloro, **34g**, EC_{50} = 0.04 µM. This was a significant improvement in activity compared to ML382. Substitution at the 4-position, **34h-34j**, were not as active. 5-position substitutions with ethyl sulfonamide, **34k-34m**, also came out to be equipotent with 5-fluoro, **34l,** EC_{50} = 0.07 µM and were some of the better analogs. This contrasted with the cyclopropyl version, where 5-methyl, **34e**, was the most potent. 4-position substitutions with ethyl sulfonamide, **34n**, was not active. Additional, 5-position substitutions with trifluoro ethyl ether rather than an ethoxy, **34o-31q**, were also active, with the 5-methyl, **34o**, EC_{50} = 0.43 µM being the most active. An active compound with the trifluoroethyl group instead of plain ethoxy should help in slowing down the metabolism. Overall left-hand side modifications were very fruitful, providing many potent compounds compared to ML382, as shown in **Table 2.9**.

Table 2.9. Class VI Left-hand side modifications

Cmpd.	Structure	Emax (%)	MrgX1 EC$_{50}$ (μM)
34a		12.1 ± 4.0	ND
34b		0.1 ± 10.9	ND
34c		29.7 ± 18.3	ND
34d		8.9 ± 13.1	ND
34e		104.0 ± 8.9	0.024
34f		102.1 ± 3.8	0.133
34g		110.0 ± 3.4	0.039
34h		3.2 ± 20.7	ND
34i		67.6 ± 10.5	0.452
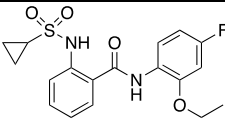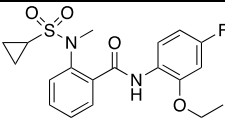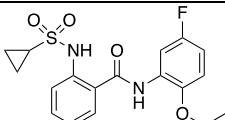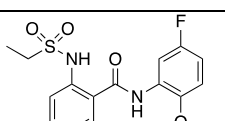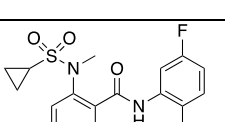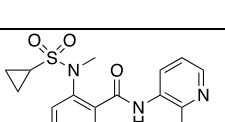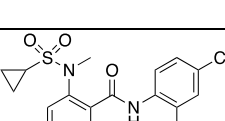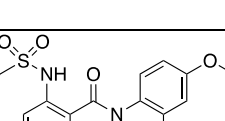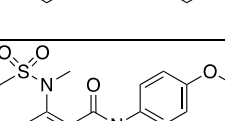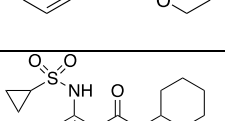
34j		36.1 ± 14.1	ND
34k		108.5 ± 2.1	0.181
34l		106.7 ± 3.3	0.070
34m		89.2 ± 6.5	0.280
34n		89.2 ± 6.5	0.280
34o		-0.5 ± 16.7	ND
34p		0.2 ± 6.9	ND
34r		89.9 ± 4.0	0.432
34s		59.8 ± 5.9	ND

34t		103.4 ± 9.1	0.840

[a]Assays were carried out in the presence of 10 nm BAM8-22; data are the mean ± SEM of n = 2 experiments; E_{max} values are normalized to the control compound ML382; ND/blank: not determined, as E_{max} is too low.

Class VII: Right-hand side modifications

In a similar fashion as the left-hand modifications, heterocycles and halogen substitutions were employed to find potent compounds which then can impart protection against ring oxidation. 4-fluoro substitution, **35a**, was not active, interestingly, when incorporated with the *N*-methyl cyclopropylsulfonamide containing moiety, **35b**, $EC_{50} = 0.62$ µM, the compound retained activity. 5-fluoro substitutions were highly active in the regular cyclopropyl sulfonamide, **35c**, $EC_{50} = 0.62$ µM, ethyl sulfonamide, **35d**, $EC_{50} = 0.079$ µM, and *N*-methyl cyclopropylsulfonamide, **35e**, $EC_{50} = 0.12$ µM. As the *N*-methyl cyclopropylsulfonamide containing group was able to tolerate a diverse set of modifications, we made a pyridine containing derivative, **35f,** $EC_{50} = 0.49$ µM, however, a 4-chloro, **35g**, was not active. Next, the diethoxy compound, **35h**, did retain activity similar to that of ML382. But, replacing the aromatic ring with a cyclohexyl **35j** resulted in an inactive compound. From this study, 5-fluoro substitution came out to be the best on right-hand side and was well tolerated by diverese sulfonamide groups as well, as shown in **Table 2.10**.

Table 2.10. Class VII Right side modifications

Cmpd.	Structure	Emax (%)	MrgX1 EC$_{50}$ (μM)
35a		-10.5 ± 8.9	ND
35b		292.2 ± 200.8	0.617
35c		189.6 ± 59.2	0.0026
35d		188.3 ± 68.1	0.079
35e		184.4 ± 70.8	0.116
35f		107.5 ± 27.4	0.497
35g		-8.9 ± 9.3	ND
35h		73.2 ± 5.6	0.185
35i		42.6 ± 8.7	ND
35j		24.2 ± 13.5	ND

[a]Assays were carried out in the presence of 10 nm BAM8-22; data are the mean ± SEM of n = 2 experiments; E_{max} values are normalized to the control compound ML382; ND/blank: not determined, as E_{max} is too low.
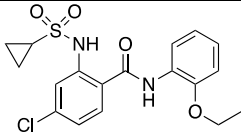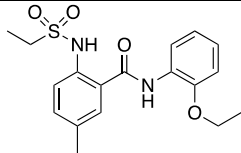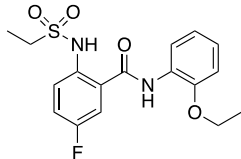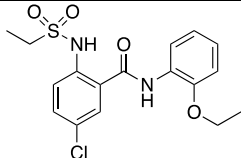
Class VI & VII combined.

Finally, we attempted to combine the best traits from the above two series for modifications on the left- and right-hand sides. For the right-hand side, we picked the 5-fluoro, which was the most potent imparting substitution, and compared its combination with various active 5-position substitutions on the left-hand side. Compound containing 5-methyl **36a**, $EC_{50} = 0.044\ \mu M$, 5-fluoro **36b**, $EC_{50} = 0.014\ \mu M$, and 5-chloro **36c**, $EC_{50} = 0.025\ \mu M$ were all very potent with low nanomolar EC_{50}. A similar study on ethyl sulfonamide bearing molecules also produced highly active compounds, **36d**-**36f**, with 5-fluoro combination **36e**, $EC_{50} = 0.041\ \mu M$ being the best in the set. We also tried a left-hand side 4-fluoro bearing combination, **36g,** which was active but not as potent $EC_{50} = 0.63\ \mu M$. This series gave us the most potent derivatives of ML382 with 5-fluoro substitution on both left and right-hand side, **36b**, being the most potent allosteric activator developed with an $EC_{50} = 0.014\ \mu M$ or 13.9 nM, as shown in **Table 2.11**.

Table 2.11. Class-VI amd VII Combined heterocyclic derivatives

Cmpd.	Structure	Emax (%)	MrgX1 EC$_{50}$ (µM)
36a		105.6 ± 3.7	~0.0446
36b		126.8 ± 25.2	0.0139
36c		103.5 ± 3.6	0.025
36d		127.6 ± 26.8	0.0916
36e		136.3 ± 26.8	~0.0411
36f		118.4 ± 21.9	0.164
36g		137.0 ± 29.1	0.633

[a]Assays were carried out in the presence of 10 nm BAM8-22; data are the mean ± SEM of n = 2 experiments; E$_{max}$ values are normalized to the control compound ML382; ND/blank: not determined, as E$_{max}$ is too low.

Pharmacokinetics

Having identified several compounds that showed EC_{50} values of <100 nM, we next profiled select compounds in an *in vitro* DMPK assays to assess their human and mouse liver microsomal intrinsic clearance and plasma protein binding, **Table 2.12**. All the compounds evaluated displayed high intrinsic clearance and were predicted to have high hepatic clearance *in vivo* (CL_{HEP} > 75% Q_H). From the metabolite identification study, we anticipated that the major metabolite pathway of ML382, was oxidation of the phenyl ring, which was confirmed by the MetID study. Thus, it was disappointing to see compounds that incorporated a halogen substituent on that ring did not translate to improved clearance in series **35** and **36**. Incorporation of a trifluoro ethyl group instead of the ethyl did show some improvement in hCL_{INT} in preventing *O*-dealkylation in compound **19d** (hCL_{INT} = 40.2 vs 61.9 ML382)**.** But not much improvement was seen in mice clearance data. Converting ethoxy into a cyclized version **18i** or increasing the chain length **19f** had no beneficial effect on metabolism. In fact, **19f** was even readily metabolized compared to ML382.

Using equilibrium dialysis, the plasma protein binding of the selected compounds were determined in human and mouse plasma. The results revealed that all the tested compounds were highly protein bound in human plasms (%f_u < 0.5). However, the compounds showed a better plasma protein binding profile in mouse plasma with several compounds displaying moderate free fraction (> 2%).

Finally, we evaluated a smaller set of selected compounds, **35c**, **36a**, and **36b**, in a rat IV cassette study to assess their ability to cross the blood-brain barrier and evaluate their *in vivo* clearance as shown in **Table 2.13**. The cassette study was done in a 5-in-1 format where five compounds are dosed in a single cassette (IV, 0.25 mg/kg) and then evaluated for their plasma and brain concentrations. These compounds had varying levels of brain penetrance, with **35c** being the best (Total plasma:total brain, K_p = 0.57). However, **36b**, had the better overall plasma profile with low clearance (CL = 14.1 mL/min/kg) and better overall plasma exposure (AUC = 304 h*ng/mL).

Table 2.12. In vitro DMPK properties of selected compounds.

Cmpd.	MrgX1, EC$_{50}$ (μM)	Intrinsic Clearance (mL/min/kg)[c]				Plasma Protein Binding (%f_u)[b]	
		hCL$_{INT}$	hCL$_{HEP}$[a]	mCL$_{INT}$	mCL$_{HEP}$[a]	Human	Mouse
5, Ml382	0.190	61.9	15.2	1,065	83.1	0.4	1.7
18i	0.940	74.9	15.8	1457.3	84.9	<0.3	2.6
19d	0.529	40.2	13.4	979.1	82.5	0.4	2.2
19f	0.514	115.6	17.1	4888.6	88.5	<0.3	1.5
35c	0.030	79.1	16.0	1659	85.5	0.4	2.2
36a	~0.045	114.3	17.1	1,101.6	83.3	0.3	1.2
36b	0.0139	59.4	15.0	979.5	82.5	0.2	1.1
36c	0.025	138.4	17.6	>2,400	86.8	0.1	0.3
36d	0.0916	69.3	15.6	1,004.3	82.7	0.3	1.4
36e	~0.041	69.1	15.6	1,235.7	84.0	0.2	0.1

[a]Predicted hepatic clearance based on intrinsic clearance in human and mouse liver microsomes using the well-stirred organ CL model (binding terms excluded). [b]%fu = percent fraction unbound. [c]*In vitro* DMPK studies were performed at Q2 Solutions, Indianapolis, IN.

Table 2.13. In vivo rat cassette.

Cmpd.	IV Bolus (0.25 mg/kg)[a]				Plasma:Brain partitioning (0.25 mg/kg, t = 15 min)[a]		
	CL (mL/min/kg)	$T_{1/2}$ (h)	AUC (h∗ng/mL)	Vss (L/Kg)	Plasma (ng/mL)	Brain (ng/g)	K_p[b]
35c	36.7	0.48	119	0.52	79.6	23.6	0.29
36a	63.1	0.42	66.2	1.2	61.5	35.1	0.57
36b	14.1	0.41	304	0.34	297	55.9	0.19
In vivo DMPK studies were performed at Pharmaron Laboratories, Louisville, KY. Cassette dosing (5-in-1) dose of 0.25 mg/kg (IV) of each test article to male Sprague-Dawley rats. Formulation: DMSO:PEG400:EtOH:Saline (5:48:10:37). Plasma blood sampling at 0.0833, 0.25, 0.5, 1, 3, 4, 8 and 24 h and Day 2 0.25 h post dose. Brain sample on Day 2 at 0.25 h. [b]K_p = total brain/plasma ratio.							

2.4. Summary and Conclusions

As discussed in the introduction, allosteric sites are very specific and the development of allosteric modulators presents a better approach to target the GPCR's due to the tolerance for a variety of chemical diversity. SAR studies on the allosteric modulators could be challenging, as seen with our study of ML382; not many modifications or derivatizations are tolerated. The binding site of ML382 appears to be very small and requires free rotation around the amide bond to achieve desired interactions. As seen with many of the examples, the free NH in sulfonamide is not necessary, but the bulk obtained through alkylation of that NH or the change in the shape and loss of flexibility of the molecule due to cyclization affects the activity. Similarly, in the case of ethoxy, very few modifications are tolerated, and two chain length appears to be the best fitting

Halogenated derivatives proved to be the best compound and thus have better interactions in a wide variety of molecules and drugs. Especially fluorine substitutions, as they are well tolerated due to their smaller size and favorable interactions. It could be possible that this hetero and halogen substitution on the aromatic ring might have stopped the oxidation, but other metabolic pathways, *O*-dealkylation and amide bond hydrolysis, might have taken over. The best molecule out of the series, **36b**, is more than eight times potent compared to the lead molecule ML382. For future improvement, another MetID study needs to be performed to assess metabolically labile positions on **36b**. Even though amide hydrolysis is not shown to be one of the metabolites, trials need to be performed to replace the primary amide with either a suitable bioisostere or some hydrogen bonding functional groups like ether or a vinyl. Rotation around the amide bond appears to be a necessary phenomenon in aligning the molecule with the allosteric binding site. Thus any approach to replace the amide should have the capacity to freely rotate around the bond, which might be difficult to identify since most of the bioisosteres are 5-membered heterocycles which in most cases helps in reducing the rotation around the bonds. We even saw some decline in brain penetration of **36b** compared to ML382, even though not many changes have been made to the molecule. Although theoretically by calculations, ML382 has desired physicochemical properties for CNS active

molecules. The polarity imparted by the sulfonamide and amide can be a deterrent towards brain penetration. In addition, the number of hydrogen bonding sites needs to be reduced. This could be challenging especially while making allosteric modulators, as not many changes will be tolerated. Due to the limitations in PK properties, these newly identified compounds will be limited to non-oral dosage regiments; still, they represent a significant improvement in potency. Future *in vivo* potency studies will highlight the improvement in dose reduction of the activators required to achieve similar behavioral outcomes.

2.5. Synthesis Protocols and Experimental

In-vitro Pharmacology

      Cell based Ca2+ imaging assay to determine MrgX1 PAM activities was carried out in the lab of Dr. Xinghong Dong at the Department of Neuroscience, Johns Hopkins University School of Medicine, Baltimore, MD. Ca^{2+} imaging assay was employed to determine the effect of PAMs on MrgX1 activation by its agonist BAM8-22 using a HEK293 cell line that stably expresses MrgX1 protein. MrgX1-expressing HEK293 cells were plated into 96-well plates. On the following day, cells were incubated with $Ca2^+$ sensitive dye Fluo4 solution at 37 °C for 30 min and at RT for 30 min after removing media. 5 µM PAM compounds were added to the assay buffer with dye for 80 sec followed by adding 10 nM BAM8-22 (EC_{20} of the agonist activating MrgX1) for 75 sec and recorded the change of fluorescence by Flexstation3 imaging plate reader. A previously characterized MrgX1 PAM ML382 was included on each plate as a positive control. PAM effect on MrgX1 activation was evaluated by the calculated fluorescence ratio and compared to the effect of ML382. If a new PAM compound exhibited a comparable or stronger effect as ML382 did, the EC_{50}s of the compound effect (i.e., enhancing MrgX1 activation by BAM8-22) was then determined from a dose response curve by repeating the assay with a series of 10 doses (from 0.04 nM to 10 µM) of the compound. The Emax of a new PAM was determined by normalizing its maximum effect with that of ML382.

DMPK Studies

Were performed in the similar manner as shown in **Chapter-1.**

Synthesis Procedure and Experimental data

      Instrumentation, chemical procuring, processing remains same as shown. Compounds **5; 15h-k; 19c,d,e,h,i,j; 24e; 28a-c,f,g,k; 34c-t and 35a-c,e-g,j** were synthesized by previous Post docs in the lab Dr. Anish Vadukoot, Dr. Christopher Aretz and rotation students Aaron Jensen and Alexander Wallick.

A.

Reagents and Conditions: (a) T3P, TEA; (b) Pyridine, RT

R1 = Me or H
13   14   15a-k (sulfonamide)
16a-j (Caronbonamide)
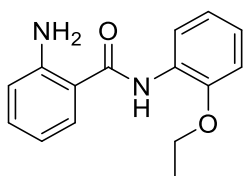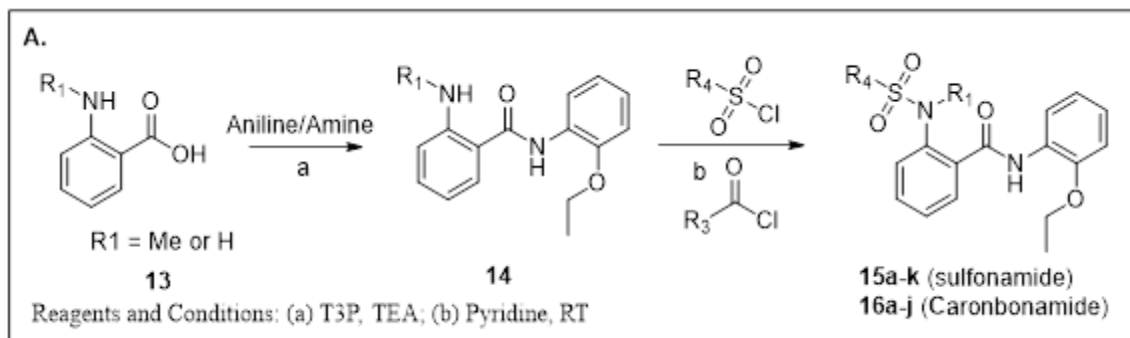
Step-1, 2-amino-*N*-(2-ethoxyphenyl)benzamide (14a'): : To a solution of anthranilic acid (0.50 g, 3.6 mmol), *O*-Phenitidine (0.42 g, 3.1 mmol) and triethylamine (1.50 mL, 10.9 mmol) in dichloromethane (5.0 mL) was dropwise added T3P (50% wt/v in ethyl acetate) (3.0 mL, 4.7 mmol). The reaction was stirred at rt for 6 hours. To the reaction mixture was added 200 mL of aqueous 1N NaOH, the product was extracted with ethyl acetate (100 mL*3). Combined organic layer was washed with brine, concentrated and used as such. Yield = 0.60 g (65%). ^{1}H NMR (500 MHz, CDCl$_3$) δ 8.54 (s, 1H), 8.47 (dd, *J* = 7.9, 1.5 Hz, 1H), 7.53 – 7.49 (m, 1H), 7.31 – 7.25 (m, 1H), 7.08 (td, *J* = 7.8, 1.7 Hz, 1H), 7.02 (td, *J* = 7.7, 1.1 Hz, 1H), 6.93 (dd, *J* = 8.0, 1.0 Hz, 1H), 6.76 (t, *J* = 7.2 Hz, 2H), 5.61 (s, 2H), 4.17 (q, *J* = 7.0 Hz, 2H), 1.50 (t, *J* = 7.0 Hz, 3H).

Step-2, Respective anilines (1.0 equiv.) and carbonyl or sulfonyl chlorides (1.0 equiv.) in pyridine (0.5 M) were stirred from rt to 45 °C over 12 hours. The crude was purified by Prep-HPLC (Water: CH$_3$CN) or normal flash chromatography (Hexane:Ethyl-acetate)
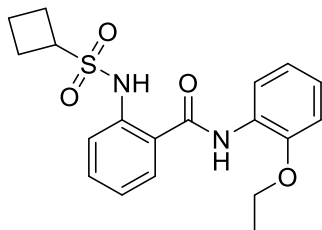
2-(cyclobutanesulfonamido)-*N*-(2-ethoxyphenyl)benzamide (15a). Yield = 22.0 mg (37.6%, off-white solid). LCMS: R_T = 2.84 min., >95% @ 215 and 254 nm, *m/z* = 375.1 [M + H]$^+$. ^{1}H NMR (500 MHz, CDCl$_3$) δ 10.46 (s, 1H), 8.66 (s, 1H), 8.42 (dd, *J* = 8.0, 1.4 Hz, 1H), 7.84 (d, *J* = 8.1 Hz, 1H), 7.63 (dd, *J* = 7.9, 1.1 Hz, 1H), 7.55 – 7.49 (m, 1H), 7.23 – 7.19 (m, 1H), 7.13 (td, *J* = 7.9, 1.5 Hz, 1H), 7.03 (td, *J* = 7.9, 1.0 Hz, 1H), 6.95 (d, *J* = 8.1 Hz, 1H), 4.19 (q, *J* = 7.0 Hz, 2H), 3.92 (p, *J* = 8.3 Hz, 1H), 2.64 – 2.53 (m, 2H), 2.22 (tdd, *J* = 11.4, 8.7, 4.1 Hz, 2H), 2.04 – 1.89 (m, 2H), 1.52 (t, *J* = 7.0 Hz, 3H). ^{13}C NMR (125 MHz, CDCl$_3$) δ 166.15, 147.72, 139.91, 133.05, 126.92, 126.70, 124.77, 123.43, 121.53, 121.08, 120.94, 120.14, 111.05, 64.36, 54.46, 23.87, 16.90, 14.91.
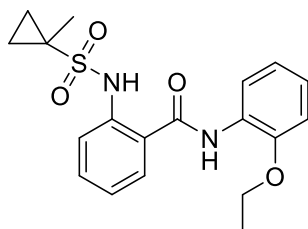
***N*-(2-ethoxyphenyl)-2-((1-methylcyclopropane)-1-sulfonamido)benzamide (15b).** Yield = 21.0 mg (35.9%, off-white solid). LCMS: R_T = 2.82 min., >95% @ 215 and 254 nm, *m/z* = 375.1 [M + H]$^+$. ^{1}H NMR (500 MHz, CDCl$_3$) δ 10.57 (s, 1H), 9.50 (s, 1H), 8.51 (d, *J* = 8.2 Hz, 1H), 7.88 (d, *J* = 8.3 Hz, 1H), 7.77 (d, *J* = 7.8 Hz, 1H), 7.60 (d, *J* = 7.7 Hz, 1H), 7.57 (t, *J* = 7.9 Hz, 1H), 7.43 (t, *J* = 7.8 Hz, 1H), 7.29 – 7.24 (m, 1H), 7.18 (t, *J* = 7.6 Hz, 1H), 2.85 (q, *J* = 7.3 Hz, 2H), 2.59 – 2.53 (m, 1H), 1.27 (t, *J* = 7.2 Hz, 5H), 0.98 – 0.93 (m, 2H). ^{13}C NMR (125 MHz, CDCl$_3$) δ 166.44, 140.02, 138.88, 135.19, 133.28, 129.80, 126.80, 124.94, 123.70, 123.65, 121.54, 121.51, 120.42, 30.64, 30.43, 14.89, 5.73.
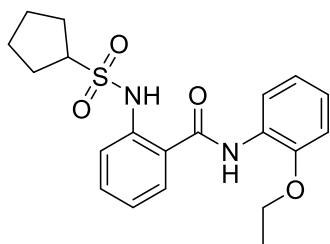
2-(cyclopentanesulfonamido)-*N*-(2-ethoxyphenyl)benzamide (15c). Yield = 20.0 mg (33.3%, clear oil). LCMS: R$_T$ = 2.93 min., >95% @ 215 and 254 nm, *m/z* = 389.1 [M + H]$^+$. ^{1}H NMR (500 MHz, CDCl$_3$) δ 10.58 (s, 1H), 8.68 (s, 1H), 8.44 (d, *J* = 8.0 Hz, 1H), 7.91 (d, *J* = 8.3 Hz, 1H), 7.65 (d, *J* = 7.3 Hz, 1H), 7.53 (dd, *J* = 11.5, 4.2 Hz, 1H), 7.20 (t, *J* = 7.6 Hz, 1H), 7.16 – 7.11 (m, 1H), 7.04 (t, *J* = 7.4 Hz, 1H), 6.96 (d, *J* = 8.1 Hz, 1H), 4.20 (q, *J* = 7.0 Hz, 2H), 3.64 – 3.56 (m, 1H), 2.13 (td, *J* = 13.7, 6.7 Hz, 2H), 1.95 (dt, *J* = 13.1, 7.7 Hz, 2H), 1.85 – 1.76 (m, 2H), 1.65 – 1.56 (m, 2H), 1.52 (t, *J* = 7.0 Hz, 3H). ^{13}C NMR (125 MHz, CDCl$_3$) δ 166.25, 147.72, 140.23, 133.14, 126.97, 126.78, 124.74, 123.11, 121.13, 121.05, 120.31, 120.20, 111.05, 64.36, 61.31, 27.90, 25.89, 14.92.

N-(2-ethoxyphenyl)-2-(*N*-methylcyclopropanesulfonamido)benzamide (15d). Yield = 11.1 mg (18.9%, yellow oil). LCMS: R$_T$ = 2.69 min., >95% @ 215 and 254 nm, *m/z* = 375.0 [M + H]$^+$. ^{1}H NMR (500 MHz, CDCl$_3$) δ 9.34 (s, 1H), 8.58 (dd, *J* = 8.0, 1.1 Hz, 1H), 7.96 (dd, *J* = 7.6, 1.3 Hz, 1H), 7.59 (dt, *J* = 7.4, 3.8 Hz, 1H), 7.55 (td, *J* = 7.6, 1.6 Hz, 1H), 7.50 (td, *J* = 7.5, 1.2 Hz, 1H), 7.09 (td, *J* = 8.0, 1.6 Hz, 1H), 7.01 (t, *J* = 7.4 Hz, 1H), 6.93 (d, *J* = 8.1 Hz, 1H), 4.19 (q, *J* = 7.0 Hz, 2H), 3.40 (s, 3H), 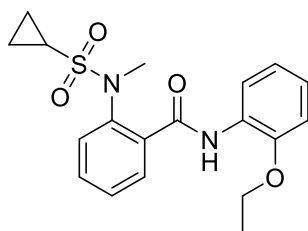2.51 (tt, *J* = 8.0, 4.8 Hz, 1H), 1.46 (t, *J* = 7.0 Hz, 3H), 1.13 – 1.08 (m, 2H), 0.99 – 0.94 (m, 2H). ^{13}C NMR (125 MHz, CDCl$_3$) δ 164.63, 147.64, 138.96, 136.14, 131.52, 130.47, 128.95, 128.81, 127.89, 124.13, 120.85, 120.43, 110.99, 64.18, 39.56, 28.07, 14.73, 5.53.
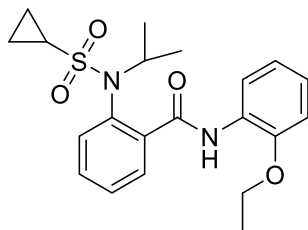
N-(2-ethoxyphenyl)-2-(N-isopropylcyclopropanesulfonamido)benzamide (15e). Yield = 11.1 mg (26.1%, white solid). LCMS: R_T = 2.75 min., >95% @ 215 and 254 nm, *m/z* = 403.10 [M + H]$^+$. ^{1}H NMR (500 MHz, CDCl$_3$) δ 9.52 (s, 1H), 8.50 (dd, *J* = 8.0, 1.0 Hz, 1H), 7.87 (dd, *J* = 7.1, 2.1 Hz, 1H), 7.56 – 7.49 (m, 2H), 7.47 – 7.43 (m, 1H), 7.11 – 7.05 (m, 1H), 6.99 (t, *J* = 7.4 Hz, 1H), 6.92 (d, *J* = 8.0 Hz, 1H), 4.48 – 4.39 (m, 1H), 4.14 (qd, *J* = 7.0, 3.3 Hz, 2H), 2.62 – 2.55 (m, 1H), 1.43 (t, *J* = 7.0 Hz, 3H), 1.27 (d, *J* = 6.7 Hz, 3H), 1.20 (ddd, *J* = 15.1, 9.3, 4.5 Hz, 2H), 1.15 (d, *J* = 6.7 Hz, 3H), 1.08 (dt, *J* = 10.1, 7.4 Hz, 1H), 1.05 – 0.99 (m, 1H). ^{13}C NMR (125 MHz, CDCl$_3$) δ 165.88, 148.28, 140.24, 132.29, 132.07, 131.12, 130.24, 129.42, 127.99, 124.22, 120.68, 120.56, 111.26, 64.22, 52.62, 30.22, 22.04, 21.87, 14.54, 6.76, 5.48.
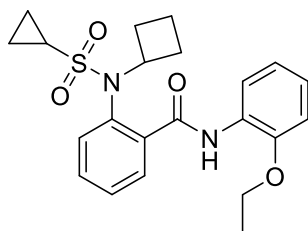
2-(N-cyclobutylcyclopropanesulfonamido)-N-(2-ethoxyphenyl)benzamide (15f). Yield = 16.0 mg (5%, yellow oil). LCMS: R_T = 3.0 min., >95% @ 215 and 254 nm, *m/z* = 415.1 [M + H]$^+$. ^{1}H NMR (500 MHz, CDCl$_3$) δ 9.37 (s, 1H), 8.51 (dd, *J* = 8.0, 1.4 Hz, 1H), 7.95 (dt, *J* = 7.0, 3.1 Hz, 1H), 7.57 – 7.52 (m, 2H), 7.47 – 7.44 (m, 1H), 7.08 (td, *J* = 7.9, 1.6 Hz, 1H), 6.99 (dt, *J* = 12.4, 2.8 Hz, 1H), 6.92 (d, *J* = 8.1 Hz, 1H), 4.67 – 4.57 (m, 1H), 4.22 – 4.15 (m, 2H), 2.53 (dq, *J* = 8.0, 4.9 Hz, 1H), 2.24 – 2.16 (m, 1H), 2.10 (ddd, *J* = 15.2, 11.1, 5.9 Hz, 1H), 2.05 – 2.00 (m, 1H), 1.94 (dd, *J* = 20.5, 10.2 Hz, 1H), 1.60 – 1.51 (m, 2H), 1.44 (t, *J* = 7.0 Hz, 3H), 1.24 – 1.18 (m, 1H), 1.08 (ddd, *J* = 13.9, 7.6, 2.8 Hz, 1H), 0.99 (dddd, *J* = 20.4, 18.0, 8.1, 5.1 Hz, 2H). ^{13}C NMR (125 MHz,

CDCl$_3$) δ 165.03, 148.04, 138.83, 133.87, 131.21, 130.82, 130.73, 129.23, 127.90, 124.20, 120.81, 120.60, 111.16, 64.13, 54.14, 30.09, 29.71, 29.41, 14.83, 14.54, 6.41, 5.53.
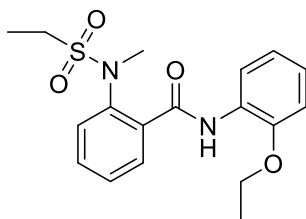
N-(2-ethoxyphenyl)-2-(N-methylethylsulfonamido)benzamide (15g). Yield = 25.0 mg (31.3%, off-white solid). LCMS: R$_T$ = 2.5 min., >95% @ 215 and 254 nm, *m/z* = 363.1[M + H]$^+$. ^{1}H NMR (500 MHz, CDCl$_3$) δ 8.85 (s, 1H), 8.54 (d, *J* = 7.8 Hz, 1H), 7.79 (d, *J* = 7.5 Hz, 1H), 7.58 – 7.46 (m, 3H), 7.10 (t, *J* = 7.4 Hz, 1H), 7.02 (t, *J* = 7.7 Hz, 1H), 6.93 (d, *J* = 8.0 Hz, 1H), 4.17 (q, *J* = 7.0 Hz, 2H), 3.38 (s, 3H), 3.18 (q, *J* = 7.4 Hz, 2H), 1.45 (t, *J* = 7.0 Hz, 3H), 1.38 (t, *J* = 7.4 Hz, 3H). ^{13}C NMR (125 MHz, CDCl$_3$) δ 165.14, 147.63, 138.65, 136.76, 131.46, 129.54, 129.52, 128.85, 127.72, 124.27, 120.88, 120.25, 111.02, 64.21, 45.82, 39.80, 14.75, 7.76.
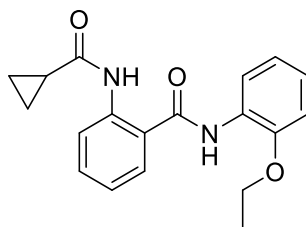
2-(cyclopropanecarboxamido)-N-(2-ethoxyphenyl)benzamide (16a). Yield = 15.0 mg (23.8%, off-white solid). LCMS: R$_T$ = 2.8 min., >95% @ 215 and 254 nm, *m/z* = 325.1[M + H]$^+$. ^{1}H NMR (500 MHz, CDCl$_3$) δ 11.20 (s, 1H), 8.66 (d, *J* = 8.4 Hz, 1H), 8.61 (s, 1H), 8.42 (d, *J* = 8.0 Hz, 1H), 7.64 (d, *J* = 7.8 Hz, 1H), 7.53 (t, *J* = 7.9 Hz, 1H), 7.14 (ddd, *J* = 13.5, 10.4, 4.5 Hz, 2H), 7.05 (t, *J* = 7.7 Hz, 1H), 6.96 (d, *J* = 8.1 Hz, 1H), 4.18 (q, *J* = 7.0 Hz, 2H), 1.70 – 1.63 (m, 1H), 1.50 (t, *J* = 7.0 Hz, 3H), 1.12 – 1.07 (m, 2H), 0.90 – 0.85 (m, 3H). ^{13}C NMR (125 MHz, CDCl$_3$) δ 172.61, 167.03, 147.83, 140.10, 132.83, 127.17, 126.38, 124.61, 122.70, 121.84, 120.98, 120.95, 120.16, 111.12, 64.34, 16.56, 14.88, 8.18.
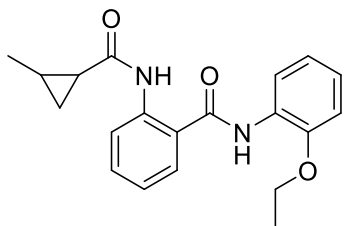
N-(2-ethoxyphenyl)-2-(2-methylcyclopropane-1-carboxamido)benzamide (16b). Yield = 27.0

mg (40.9%, white solid). LCMS: R_T = 3.1 min., >95% @ 215 and 254 nm, m/z = 339.1[M + H]$^+$.

^{1}H NMR (500 MHz, CDCl$_3$) δ 11.15 (s, 1H), 8.67 (d, J = 8.4 Hz, 1H), 8.60 (s, 1H), 8.42 (d, J = 7.9

Hz, 1H), 7.64 (d, J = 7.8 Hz, 1H), 7.52 (t, J = 7.9 Hz, 1H), 7.18 – 7.11 (m, 2H), 7.05 (t, J = 7.6 Hz,

1H), 6.96 (d, J = 8.1 Hz, 1H), 4.18 (q, J = 7.0 Hz, 2H), 1.53 – 1.46 (m, 4H), 1.38 (dt, J = 8.2, 4.2

Hz, 1H), 1.27 (dt, J = 8.6, 4.2 Hz, 1H), 1.17 (d, J = 6.0 Hz, 3H), 0.73 – 0.68 (m, 1H). ^{13}C NMR

(125 MHz, CDCl$_3$) δ 172.36, 167.08, 147.86, 140.19, 132.84, 127.17, 126.39, 124.62, 122.58,

121.71, 120.98, 120.81, 120.20, 111.14, 64.34, 25.20, 17.97, 16.91, 16.66, 14.88.
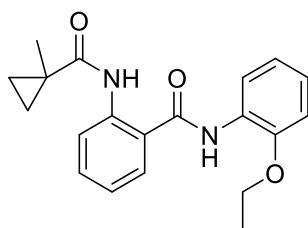
N-(2-ethoxyphenyl)-2-(1-methylcyclopropane-1-carboxamido)benzamide (16c). Yield = 22.0

mg (33.3%, off-white solid). LCMS: R_T = 3.0 min., >95% @ 215 and 254 nm, m/z = 339.1[M +

H]$^+$. ^{1}H NMR (500 MHz, CDCl$_3$) δ 11.33 (s, 1H), 8.66 (d, J = 8.4 Hz, 1H), 8.62 (s, 1H), 8.47 (d, J

= 7.9 Hz, 1H), 7.64 (d, J = 7.7 Hz, 1H), 7.53 (t, J = 7.9 Hz, 1H), 7.14 (ddd, J = 15.6, 12.0, 4.3 Hz,

2H), 7.05 (t, J = 7.6 Hz, 1H), 6.95 (d, J = 8.1 Hz, 1H), 4.18 (q, J = 7.0 Hz, 2H), 1.56 (s, 3H), 1.50

(t, J = 7.0 Hz, 3H), 1.33 (q, J = 3.9 Hz, 2H), 0.71 (q, J = 3.9 Hz, 2H). ^{13}C NMR (125 MHz, CDCl$_3$)

δ 174.38, 166.93, 147.72, 140.11, 132.71, 127.33, 126.32, 124.47, 122.78, 121.93, 121.47, 120.99,

120.07, 111.05, 64.34, 20.56, 19.63, 16.90, 14.89.

2-(cyclobutanecarboxamido)-*N*-(2-ethoxyphenyl)benzamide (16d). Yield = 39.0 mg (76.0%, white solid). LCMS: R_T = 2.93min., >95% @ 215 and 254 nm, m/z = 361.1[M + Na]$^+$. ^{1}H NMR (500 MHz, CDCl$_3$) δ 10.95 (s, 1H), 8.73 (d, *J* = 8.3 Hz, 1H), 8.61 (s, 1H), 8.42 (dd, *J* = 8.0, 1.4 Hz, 1H), 7.63 (dd, *J* = 7.9, 1.2 Hz, 1H), 7.56 – 7.52 (m, 1H), 7.18 – 7.09 (m, 2H), 7.04 (td, *J* = 7.8, 1.1 Hz, 1H), 6.95 (dd, *J* = 8.1, 1.0 Hz, 1H), 4.17 (q, *J* = 7.0 Hz, 3H), 3.30 – 3.23 (m, 1H), 2.43 (dtd, *J* = 18.0, 9.2, 2.4 Hz, 2H), 2.33 – 2.24 (m, 2H), 2.07 – 1.99 (m, 1H), 1.96 – 1.89 (m, 1H), 1.49 (t, *J* = 7.0 Hz, 3H). ^{13}C NMR (125 MHz, CDCl$_3$) δ 174.13, 166.89, 147.79, 140.09, 132.83, 127.20, 126.39, 124.56, 122.81, 121.75, 121.14, 120.98, 120.12, 111.09, 64.33, 41.59, 25.44, 18.06, 14.88.
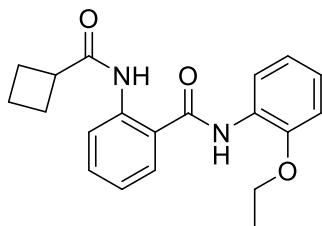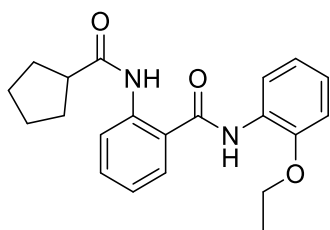

2-(cyclopentanecarboxamido)-*N*-(2-ethoxyphenyl)benzamide (16e). Yield = 31.0 mg (72.0%, brown solid). LCMS: R_T = 3.07 min., >95% @ 215 and 254 nm, m/z = 375.1[M + H]$^+$. ^{1}H NMR (500 MHz, CDCl$_3$) δ 11.03 (s, 1H), 8.73 (s, 1H), 8.72 (dd, *J* = 8.4, 0.7 Hz, 1H), 8.58 (d, *J* = 23.4 Hz, 1H), 8.42 (dd, *J* = 8.0, 1.5 Hz, 1H), 7.63 (dd, *J* = 7.9, 1.3 Hz, 1H), 7.55 – 7.50 (m, 1H), 7.19 – 7.10 (m, 2H), 7.06 – 7.02 (m, 1H), 6.95 (dd, *J* = 8.1, 1.1 Hz, 1H), 4.18 (q, *J* = 7.0 Hz, 2H), 2.81 (p, *J* = 8.2 Hz, 1H), 2.06 – 1.97 (m, 2H), 1.97 – 1.88 (m, 2H), 1.86 – 1.76 (m, 2H), 1.69 – 1.61 (m, 2H), 1.50 (t, *J* = 7.0 Hz, 3H). ^{13}C NMR (125 MHz, CDCl$_3$) δ 175.34, 166.95, 147.81, 140.23, 132.82, 127.21, 126.39, 124.56, 122.72, 121.77, 121.10, 120.98, 120.14, 111.10, 64.34, 47.69, 30.44, 25.92, 14.89.
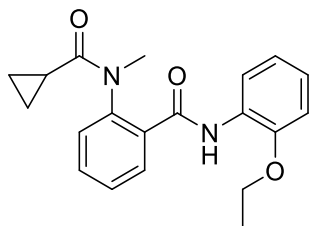
N-(2-ethoxyphenyl)-2-(N-methylcyclopropanecarboxamido)benzamide (16f). Yield = 33.0 mg (84.0%, clear oil). LCMS: R_T = 2.53 min., >95% @ 215 and 254 nm, m/z = 331.1[M + H]$^+$. ^{1}H NMR (500 MHz, CDCl$_3$) δ 8.97 (s, 1H), 8.58 (d, J = 7.7 Hz, 1H), 8.10 (d, J = 7.6 Hz, 1H), 7.59 (td, J = 7.7, 1.2 Hz, 1H), 7.51 (t, J = 7.2 Hz, 1H), 7.34 (d, J = 7.7 Hz, 1H), 7.08 (dt, J = 8.1, 4.0 Hz, 1H), 7.00 (t, J = 7.5 Hz, 1H), 6.91 (d, J = 8.0 Hz, 1H), 4.20 (q, J = 7.0 Hz, 2H), 3.35 (s, 3H), 1.43 (t, J = 7.0 Hz, 3H), 1.37 (td, J = 7.9, 4.0 Hz, 1H), 1.08 – 0.99 (m, 2H), 0.67 (p, J = 9.7 Hz, 2H). ^{13}C NMR (125 MHz, CDCl$_3$) δ 174.32, 163.55, 147.20, 141.61, 133.34, 132.31, 130.95, 129.24, 128.44, 127.66, 124.16, 120.85, 120.24, 110.71, 63.97, 37.78, 14.66, 13.13, 9.03, 8.77.
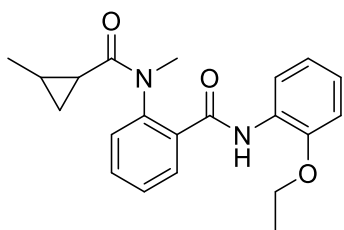

2-(N,2-dimethylcyclopropane-1-carboxamido)-N-(2-ethoxyphenyl)benzamide (16g). Yield = 31.0 mg (81.0%, brown solid). LCMS: R_T = 2.80 min., >95% @ 215 and 254 nm, m/z = 353.1[M + H]$^+$. ^{1}H NMR (500 MHz, CDCl$_3$) δ 9.09 (s, 1H), 8.59 (dd, J = 12.3, 8.0 Hz, 1H), 8.15 (ddd, J = 10.2, 9.1, 3.6 Hz, 1H), 7.61 – 7.56 (m, 1H), 7.54 – 7.49 (m, 1H), 7.33 – 7.28 (m, 1H), 7.08 (ddd, J = 8.0, 4.2, 2.1 Hz, 1H), 6.99 (dd, J = 10.7, 4.6 Hz, 1H), 6.91 (dd, J = 7.3, 4.5 Hz, 1H), 4.23 – 4.16 (m, 2H), 3.33 (d, J = 17.1 Hz, 3H), 1.41 (qd, J = 8.7, 4.7 Hz, 3H), 1.36 – 1.30 (m, 1H), 1.29 – 1.23 (m, 1H), 1.23 – 1.10 (m, 1H), 1.06 (dd, J = 7.3, 3.5 Hz, 1H), 0.91 (t, J = 6.1 Hz, 3H), 0.54 – 0.45 (m, 1H). ^{13}C NMR (125 MHz, CDCl$_3$) δ 174.11, 163.44, 147.20, 141.72, 141.66, 133.05, 132.96, 132.43, 132.13, 131.15, 129.43, 129.22, 128.45, 128.41, 127.71, 127.68, 124.13, 124.10, 120.83,

120.81, 120.23, 120.19, 110.69, 63.96, 37.76, 37.69, 22.16, 21.67, 17.80, 17.70, 17.67, 17.48, 17.27, 16.94, 14.63, 14.61.

N-(2-ethoxyphenyl)-2-(N-methylcyclobutanecarboxamido)benzamide (16h). Yield = 42.0 mg (64.1%, white solid). LCMS: R_T = 2.67 min., >95% @ 215 and 254 nm, m/z = 375.0 [M +Na]$^+$. ^{1}H NMR (500 MHz, CDCl$_3$) δ 8.96 (s, 1H), 8.55 (d, J = 7.9 Hz, 1H), 8.12 (dd, J = 7.5, 1.2 Hz, 1H), 7.14 (dd, J = 7.5, 0.8 Hz, 2H), 7.08 (td, J = 8.1, 1.4 Hz, 1H), 6.99 (t, J = 7.4 Hz, 1H), 6.91 (d, J = 7.7 Hz, 1H), 4.23 (q, J = 7.0 Hz, 2H), 3.31 (s, 3H), 3.11 – 3.01 (m, 1H), 2.43 – 2.24 (m, 2H), 1.81 – 1.70 (m, 4H), 1.44 (dd, J = 9.1, 4.9 Hz, 3H). ^{13}C NMR (125 MHz, CDCl$_3$) δ 175.54, 163.22, 147.17, 141.29, 132.83, 132.22, 130.94, 129.28, 128.63, 127.58, 124.20, 120.82, 120.34, 110.67, 63.95, 38.30, 37.66, 26.42, 25.08, 17.84, 14.63.
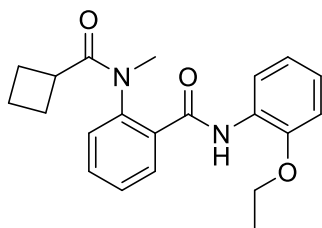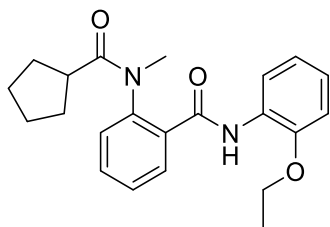

N-(2-ethoxyphenyl)-2-(N-methylcyclopentanecarboxamido)benzamide (16i). Yield = 32.0 mg (79.0%, white solid). LCMS: R_T = 2.67 min., >95% @ 215 and 254 nm, m/z = 367.1 [M + H]$^+$. ^{1}H NMR (500 MHz, CDCl$_3$) δ 9.02 (s, 1H), 8.56 (d, J = 7.9 Hz, 1H), 8.16 – 8.11 (m, 1H), 7.58 (td, J = 7.6, 1.5 Hz, 1H), 7.55 – 7.50 (m, 1H), 7.22 (d, J = 7.0 Hz, 1H), 7.08 (td, J = 8.0, 1.4 Hz, 1H), 7.00 (t, J = 7.7 Hz, 1H), 6.91 (d, J = 7.9 Hz, 1H), 4.22 (q, J = 7.0 Hz, 2H), 3.33 (s, 3H), 2.55 (p, J = 8.1 Hz, 1H), 1.86 – 1.55 (m, 8H), 1.44 (t, J = 7.0 Hz, 3H). ^{13}C NMR (125 MHz, CDCl$_3$) δ 177.90,

163.25, 147.21, 141.88, 132.93, 132.34, 130.93, 129.27, 128.62, 127.56, 124.21, 120.82, 120.41, 110.65, 63.91, 42.71, 37.73, 31.46, 31.05, 26.23, 26.11, 14.62.
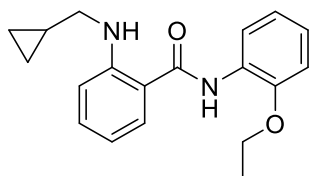
2-((cyclopropylmethyl)amino)-*N*-(2-ethoxyphenyl)benzamide (16j). Yield = 8.0 mg (13.3%, yellow oil). LCMS: R_T = 3.25 min., >95% @ 215 and 254 nm, *m/z* = 311.1[M + H]$^+$. ^{1}H NMR (500 MHz, CDCl$_3$) δ 8.50 (s, 1H), 8.44 (dd, *J* = 7.8, 1.4 Hz, 1H), 7.67 (s, 1H), 7.53 (d, *J* = 7.0 Hz, 1H), 7.36 (dd, *J* = 11.4, 4.2 Hz, 1H), 7.10 – 7.00 (m, 2H), 6.93 (d, *J* = 7.9 Hz, 1H), 6.73 (d, *J* = 8.4 Hz, 1H), 6.67 (t, *J* = 7.4 Hz, 1H), 4.16 (q, *J* = 7.0 Hz, 2H), 3.06 (d, *J* = 3.7 Hz, 2H), 1.49 (t, *J* = 7.0 Hz, 3H), 1.22 – 1.14 (m, 1H), 0.60 (q, *J* = 5.6 Hz, 2H), 0.31 (q, *J* = 4.8 Hz, 2H). ^{13}C NMR (125 MHz, CDCl$_3$) δ 167.83, 150.12, 147.64, 133.03, 128.00, 127.45, 123.59, 120.99, 119.92, 115.54, 114.66, 111.83, 111.00, 64.23, 48.12, 14.92, 10.62, 3.69.
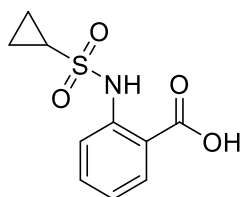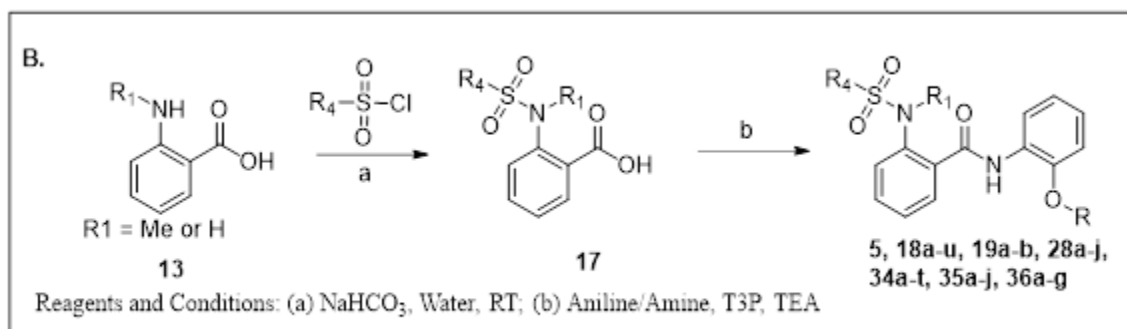
2-(cyclopropanesulfonamido)benzoic acid (17a'). To an ice-cold solution of anthranilic acid (2.00 g, 14.5 mmol) and sodium bicarbonate (2.35 g, 29.2 mmol) in water (30.0 mL) was added

cyclopropane sulfonyl chloride (1.70 mL, 16.8 mmol) dropwise. Reaction was stirred at rt for 12 hours. Crude was acidified up to pH 2 using concentrated HCl, acid product precipitates out, the solid was filtered and washed with cold water followed by hexane. Solids dried and used as such.

Yield = 2.80 g (80%). LCMS: R_T = 2.14 min., >95% @ 215 and 254 nm, m/z = 242.0 [M + H]$^+$. ^{1}H NMR (500 MHz, DMSO) δ 10.72 (s, 1H), 8.02 (d, J = 7.7 Hz, 1H), 7.67 – 7.61 (m, 2H), 7.24 – 7.17 (m, 1H), 2.86 – 2.79 (m, 1H), 1.05 – 0.97 (m, 4H). ^{13}C NMR (125 MHz, DMSO) δ 170.34, 140.99, 135.03, 132.04, 123.47, 119.23, 117.04, 30.44, 5.80.
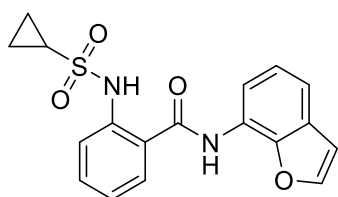
N-(benzofuran-7-yl)-2-(cyclopropanesulfonamido)benzamide (18a). To a solution of carboxylic acid (1.0 equiv.), substituted aniline (1.0 equiv.) and triethylamine (3.0 equiv.) in dichloromethane [0.1 M] was dropwise added T3P (50% wt/v in ethyl acetate) (1.50 equiv.). The reaction was stirred at rt for 6 hours. The reaction was concentrated under reduced pressure. The crude product was purified by flash column chromatography 0 to 50% ethyl acetate:hexanes to afford desired product.

Yield = 12.0 mg (25.5%, clear oil). LCMS: R_T = 2.63 min., >95% @ 215 and 254 nm, m/z = 357.1 [M + H]$^+$. ^{1}H NMR (500 MHz, CDCl$_3$) δ 10.29 (s, 1H), 8.40 (s, 1H), 8.22 (d, J = 7.9 Hz, 1H), 7.89 (d, J = 8.3 Hz, 1H), 7.80 (d, J = 7.8 Hz, 1H), 7.67 (d, J = 2.0 Hz, 1H), 7.58 (t, J = 7.9 Hz, 1H), 7.46 (d, J = 7.8 Hz, 1H), 7.32 (t, J = 7.9 Hz, 1H), 7.29 (d, J = 4.0 Hz, 1H), 6.88 (d, J = 1.9 Hz, 1H), 2.58 – 2.52 (m, 1H), 1.28 – 1.24 (m, 2H), 0.98 – 0.92 (m, 2H). ^{13}C NMR (125 MHz, CDCl$_3$) δ 166.64, 145.27, 144.70, 139.68, 133.38, 127.83, 126.95, 123.76, 123.68, 122.53, 121.85, 121.71, 117.78, 115.91, 107.64, 30.40, 5.72.

Reagents and Conditions: (a) PyClU, DMF, DIPEA
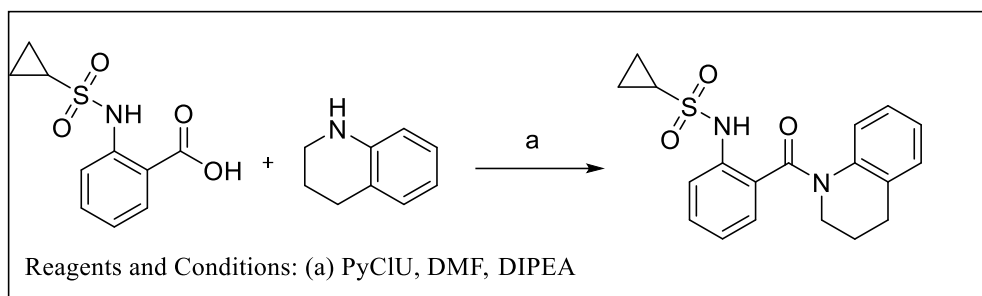
N-(2-(1,2,3,4-tetrahydroquinoline-1-carbonyl)phenyl)cyclopropanesulfonamide **(18b).** A solution of 2-(cyclopropanesulfonamido)benzoic acid (50 mg, 0.22 mmol), PyClU (85 mg, 0.26 mmol) and DIPEA (117 µL, 0.660 mmol) in DMF (1.0 mL) was stirred for 15 minutes at rt followed by addition of 1,2,3,4-tetrahydroquinoline (29 mg, 0.22 mmol). The reaction was stirred at 50º C for 12h. Product was worked up between water (20.0 mL) and ethyl acetate (20.0 mL*2). Organic layer was washed with brime, dried over sodium sulphate, concentrated and purified by flash chromatography. 0-50% hexane:ethyl acetate.

Yield = 11.0 mg (14.2%, clear oil). LCMS: R_T = 2.54 min., >95% @ 215 and 254 nm, m/z = 357.1.1 [M + H]$^+$. ^{1}H NMR (500 MHz, CDCl$_3$) δ 8.61 (s, 1H), 7.73 (d, J = 8.3 Hz, 1H), 7.35 (t, J = 7.8 Hz, 1H), 7.20 (d, J = 7.5 Hz, 1H), 7.06 (t, J = 7.5 Hz, 1H), 6.94 (t, J = 6.8 Hz, 1H), 6.89 (dd, J = 13.7, 6.5 Hz, 2H), 6.72 (d, J = 7.5 Hz, 1H), 3.94 (t, J = 6.5 Hz, 2H), 2.88 (t, J = 6.6 Hz, 2H), 2.67 – 2.61 (m, 1H), 2.09 (p, J = 6.6 Hz, 2H), 1.34 – 1.29 (m, 2H), 1.07 – 1.01 (m, 2H). ^{13}C NMR (125 MHz, CDCl$_3$) δ 169.02, 138.65, 137.61, 131.78, 131.39, 129.79, 128.66, 126.02, 125.31, 125.12, 123.17, 121.59, 44.52, 30.76, 26.84, 24.06, 6.04.
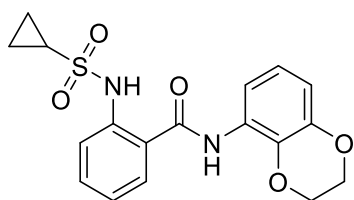
2-(cyclopropanesulfonamido)-N-(2,3-dihydrobenzo[b][1,4]dioxin-5-yl)benzamide **(18c).**

Yield = 8.0 mg (12.3%, clear oil). LCMS: R_T = 2.53 min., >95% @ 215 and 254 nm, m/z = 375.1 [M + H]$^+$. ^{1}H NMR (500 MHz, CDCl$_3$) δ 10.34 (s, 1H), 8.38 (s, 1H), 7.98 (d, J = 8.2 Hz, 1H), 7.86

(d, J = 8.3 Hz, 1H), 7.68 (d, J = 7.7 Hz, 1H), 7.55 (t, J = 7.8 Hz, 1H), 7.23 (t, J = 7.6 Hz, 1H), 6.93

(t, J = 8.3 Hz, 1H), 6.75 (d, J = 8.2 Hz, 1H), 4.42 – 4.37 (m, 2H), 4.36 – 4.31 (m, 2H), 2.57 – 2.50

(m, 1H), 1.28 – 1.23 (m, 2H), 0.98 – 0.92 (m, 2H). ^{13}C NMR (125 MHz, CDCl$_3$) δ 166.32, 143.28,

139.61, 133.08, 126.87, 123.63, 122.15, 121.77, 121.23, 113.32, 112.95, 64.92, 64.12, 30.38, 5.71.
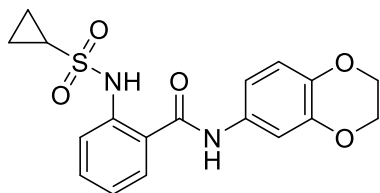
2-(cyclopropanesulfonamido)-*N*-(2,3-dihydrobenzo[b][1,4]dioxin-6-yl)benzamide **(18d).**

Yield = 31.0 mg (47.7%, clear oil). LCMS: R_T = 2.45 min., >95% @ 215 and 254 nm, m/z = 375.1

[M + H]$^+$. ^{1}H NMR (500 MHz, CDCl$_3$) δ 10.27 (s, 1H), 7.93 (s, 1H), 7.79 (d, J = 8.3 Hz, 1H), 7.64

(d, J = 7.8 Hz, 1H), 7.50 (t, J = 7.8 Hz, 1H), 7.23 (d, J = 2.3 Hz, 1H), 7.20 (t, J = 7.6 Hz, 1H), 6.99

(dd, J = 8.7, 2.4 Hz, 1H), 6.88 (d, J = 8.7 Hz, 1H), 4.31 – 4.25 (m, 4H), 2.54 – 2.48 (m, 1H), 1.25

– 1.19 (m, 2H), 0.97 – 0.91 (m, 2H). ^{13}C NMR (125 MHz, CDCl$_3$) δ 166.64, 143.63, 141.30, 139.33,

132.97, 130.51, 126.96, 123.64, 121.93, 121.53, 117.42, 114.49, 110.76, 64.43, 64.32, 30.38, 5.75.

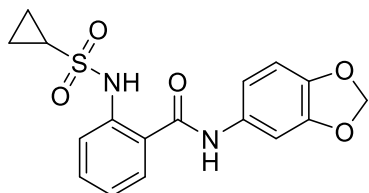***N*-(benzo[d][1,3]dioxol-5-yl)-2-(cyclopropanesulfonamido)benzamide (18e).** Yield = 20.0 mg

(31.7%, clear oil). LCMS: R_T = 2.47 min., >95% @ 215 and 254 nm, m/z = 361.0 [M + H]$^+$. ^{1}H

NMR (500 MHz, CDCl$_3$) δ 10.25 (s, 1H), 7.95 (s, 1H), 7.80 (d, J = 8.3 Hz, 1H), 7.65 (d, J = 7.8

Hz, 1H), 7.51 (t, J = 7.8 Hz, 1H), 7.20 (t, J = 7.6 Hz, 1H), 6.91 (dd, J = 8.3, 1.9 Hz, 1H), 6.82 (d, J

= 8.3 Hz, 1H), 6.01 (s, 2H), 2.56 – 2.49 (m, 1H), 1.26 – 1.21 (m, 2H), 0.98 – 0.92 (m, 2H). ^{13}C

NMR (125 MHz, CDCl$_3$) δ 166.69, 148.03, 145.19, 139.37, 133.05, 131.05, 126.94, 123.60,

121.75, 121.44, 114.30, 108.23, 103.56, 101.53, 30.45, 5.78.
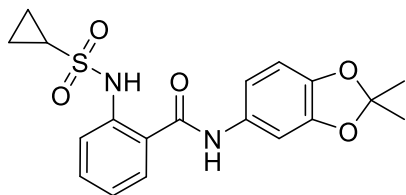
2-(cyclopropanesulfonamido)-*N*-(2,2-dimethylbenzo[d][1,3]dioxol-5-yl)benzamide **(18f).**,

Yield = 23.0 mg (33.8%, clear oil). LCMS: R_T = 2.66 min., >95% @ 215 and 254 nm, *m/z* = 389.1

[M + H]$^+$. ^{1}H NMR (500 MHz, CDCl$_3$) δ 10.27 (s, 1H), 7.89 (s, 1H), 7.81 (d, *J* = 8.3 Hz, 1H), 7.64

(d, *J* = 7.8 Hz, 1H), 7.51 (t, *J* = 7.8 Hz, 1H), 7.20 (t, *J* = 7.6 Hz, 1H), 7.16 (d, *J* = 1.6 Hz, 1H), 6.85

(dd, *J* = 8.3, 1.9 Hz, 1H), 6.73 (d, *J* = 8.3 Hz, 1H), 2.56 – 2.49 (m, 1H), 1.71 (s, 6H), 1.26 – 1.21

(m, 2H), 0.98 – 0.92 (m, 2H). ^{13}C NMR (125 MHz, CDCl$_3$) δ 166.67, 147.85, 145.19, 139.40,

133.00, 130.40, 126.89, 123.59, 121.85, 121.49, 118.79, 113.89, 107.99, 103.50, 30.41, 25.87, 5.75.

Reagents and Conditions: (a) PyClU, DMF, DIPEA
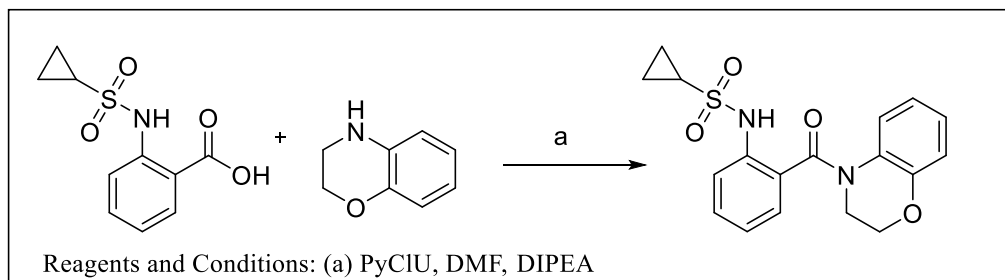
N-**(2-(3,4-dihydro-2H-benzo[*b*][1,4]oxazine-4-carbonyl)phenyl)cyclopropanesulfonamide**

(18g). Yield = 10.0 mg (13.5%, clear oil). LCMS: R_T =3.28min., >95% @ 215 and 254 nm, *m/z* =

359.1 [M + H]$^+$. ^{1}H NMR (500 MHz, CDCl$_3$) δ 8.42 (s, 1H), 7.77 (d, *J* = 8.3 Hz, 1H), 7.45 (t, *J* =

7.9 Hz, 1H), 7.26 (d, *J* = 7.7 Hz, 1H), 7.07 – 7.03 (m, 2H), 6.95 (d, *J* = 8.2 Hz, 1H), 6.70 (t, *J* = 7.5

Hz, 1H), 4.42 (t, *J* = 4.6 Hz, 2H), 4.05 (s, 2H), 2.67 – 2.59 (m, 1H), 1.30 (tt, *J* = 8.3, 4.3 Hz, 2H),
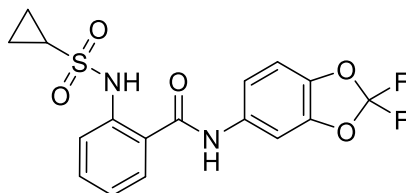
1.06 – 1.00 (m, 2H).

2-(cyclopropanesulfonamido)-*N*-(2,2-difluorobenzo[*d*][1,3]dioxol-5-yl)benzamide (18h).

Yield = 8.0 mg (12.3%, clear oil). LCMS: R_T = 2.75 min., >95% @ 215 and 254 nm, *m/z* = 397.0

[M + H]+. 1H NMR (500 MHz, CDCl3) δ 10.11 (s, 1H), 8.02 (s, 1H), 7.81 (d, *J* = 8.3 Hz, 1H), 7.66

(dd, *J* = 8.7, 1.6 Hz, 1H), 7.56 – 7.51 (m, 2H), 7.24 – 7.20 (m, 1H), 7.14 – 7.10 (m, 1H), 7.08 (d, *J*

= 8.5 Hz, 1H), 2.56 (tt, *J* = 8.0, 4.8 Hz, 1H), 1.29 – 1.24 (m, 2H), 0.98 (tt, *J* = 5.9, 2.9 Hz, 2H).
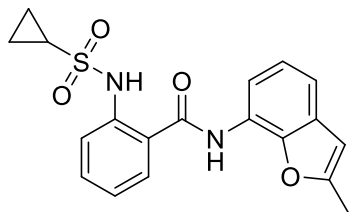
2-(cyclopropanesulfonamido)-*N*-(2-methylbenzofuran-7-yl)benzamide (18i). Yield = 15.0 mg

(19.5%, yellow oil). LCMS: R_T = 2.80 min., >95% @ 215 and 254 nm, *m/z* = 371.0 [M + H]+. 1H

NMR (500 MHz, CDCl3) δ 10.30 (s, 1H), 8.33 (s, 1H), 8.10 (d, *J* = 7.8 Hz, 1H), 7.89 (d, *J* = 8.2

Hz, 1H), 7.80 (d, *J* = 7.7 Hz, 1H), 7.58 (t, *J* = 7.4 Hz, 1H), 7.28 (ddd, *J* = 21.6, 14.5, 7.6 Hz, 4H),

6.46 (s, 1H), 2.57 – 2.53 (m, 1H), 2.51 (s, 3H), 1.27 – 1.23 (m, 2H), 0.98 – 0.92 (m, 2H). 13C NMR

(125 MHz, CDCl3) δ 166.61, 155.49, 144.94, 139.64, 133.28, 129.55, 126.97, 123.75, 123.26,

121.90, 121.87, 121.79, 116.85, 115.00, 103.61, 30.39, 14.12, 5.72.
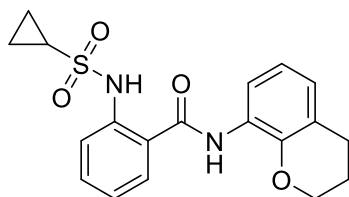
_N_-(chroman-8-yl)-2-(cyclopropanesulfonamido)benzamide (18j). Yield = 30.0 mg (38.9%,

light yellow solid). LCMS: R_T = 2.72 min., >95% @ 215 and 254 nm, *m/z* = 373.1[M + H]+. 1H

NMR (500 MHz, CDCl3) δ 10.42 (s, 1H), 8.55 (s, 1H), 8.24 (d, *J* = 7.5 Hz, 1H), 7.84 (d, *J* = 8.3

Hz, 1H), 7.69 (d, *J* = 7.7 Hz, 1H), 7.53 (t, *J* = 7.5 Hz, 1H), 7.24 (t, *J* = 7.5 Hz, 1H), 6.90 (dd, *J* =

14.0, 7.3 Hz, 2H), 4.35 – 4.30 (m, 2H), 2.85 (t, *J* = 6.4 Hz, 2H), 2.55 – 2.47 (m, 1H), 2.11 – 2.04

(m, 2H), 1.25 – 1.20 (m, 2H), 0.95 – 0.89 (m, 2H). 13C NMR (125 MHz, CDCl3) δ 166.28, 143.87,

139.49, 132.89, 126.95, 126.16, 125.34, 123.76, 122.56, 122.06, 121.87, 120.17, 117.91, 67.27, 30.26, 24.48, 22.20, 5.66.
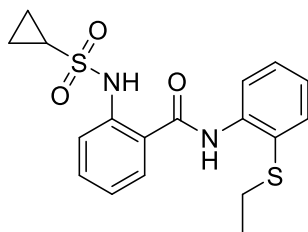
2-(cyclopropanesulfonamido)-*N*-(2-(ethylthio)phenyl)benzamide (18k). Yield = 17.0 mg (22.0%, clear oil). LCMS: R_T = 2.72 min., >95% @ 215 and 254 nm, *m/z* = 377.1[M + H]$^+$. ^{1}H NMR (500 MHz, CDCl$_3$) δ 10.57 (s, 1H), 9.50 (s, 1H), 8.51 (d, *J* = 8.2 Hz, 1H), 7.88 (d, *J* = 8.3 Hz, 1H), 7.77 (d, *J* = 7.2 Hz, 1H), 7.63 – 7.53 (m, 2H), 7.44 (dd, *J* = 11.4, 4.2 Hz, 1H), 7.27 (t, *J* = 7.8 Hz, 1H), 7.18 (td, *J* = 7.6, 0.9 Hz, 1H), 2.85 (q, *J* = 7.3 Hz, 2H), 2.55 (td, *J* = 8.0, 4.0 Hz, 1H), 1.27 (dd, *J* = 9.6, 4.9 Hz, 5H), 0.98 – 0.93 (m, 2H). ^{13}C NMR (125 MHz, CDCl$_3$) δ 166.44, 140.02, 138.88, 135.19, 133.28, 129.80, 126.80, 124.94, 123.70, 123.65, 121.55, 121.51, 120.43, 30.64, 30.43, 14.89, 5.73.
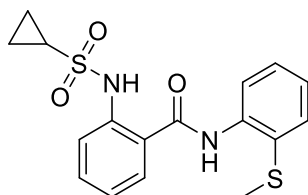
2-(cyclopropanesulfonamido)-*N*-(2-(methylthio)phenyl)benzamide (18l). Yield = 22.0 mg (29.7%, light brown solid). LCMS: R_T = 2.63 min., >95% @ 215 and 254 nm, *m/z* = 363.0[M + H]$^+$. ^{1}H NMR (500 MHz, CDCl$_3$) δ 10.51 (s, 1H), 9.21 (s, 1H), 8.40 (d, *J* = 8.1 Hz, 1H), 7.88 (d, *J* = 8.3 Hz, 1H), 7.77 (d, *J* = 7.6 Hz, 1H), 7.60 – 7.53 (m, 2H), 7.40 (t, *J* = 7.8 Hz, 1H), 7.26 (t, *J* = 7.6 Hz, 1H), 7.20 (dd, *J* = 11.0, 4.1 Hz, 1H), 2.58 – 2.52 (m, 1H), 2.47 (s, 3H), 1.29 – 1.23 (m, 2H), 0.99 – 0.93 (m, 2H). ^{13}C NMR (125 MHz, CDCl$_3$) δ 166.56, 139.95, 137.42, 133.30, 132.81, 128.98, 126.85, 126.54, 125.41, 123.73, 121.58, 121.56, 121.03, 30.42, 19.06, 5.73.
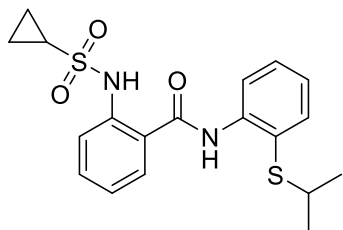
2-(cyclopropanesulfonamido)-*N*-(2-(isopropylthio)phenyl)benzamide (18m). Yield = 13.0 mg (16.1%, light yellow oil). LCMS: R_T = 2.97 min., >95% @ 215 and 254 nm, *m/z* = 390.1 [M + H]$^+$.

^{1}H NMR (500 MHz, CDCl$_3$) δ 10.61 (s, 1H), 9.66 (s, 1H), 8.56 (d, *J* = 8.2 Hz, 1H), 7.89 (d, *J* = 8.3 Hz, 1H), 7.77 (d, *J* = 7.8 Hz, 1H), 7.63 – 7.54 (m, 2H), 7.46 (t, *J* = 7.8 Hz, 1H), 7.26 (d, *J* = 7.5 Hz, 1H), 7.17 (t, *J* = 7.5 Hz, 1H), 3.21 (hept, *J* = 6.7 Hz, 1H), 2.59 – 2.51 (m, 1H), 1.29 (t, *J* = 7.1 Hz, 6H), 1.28 – 1.24 (m, 2H), 0.98 – 0.93 (m, 2H). ^{13}C NMR (125 MHz, CDCl$_3$) δ 166.34, 140.08, 139.62, 136.64, 133.27, 130.31, 126.73, 124.67, 123.65, 122.67, 121.54, 121.46, 120.09, 40.96, 30.43, 23.30, 5.72.
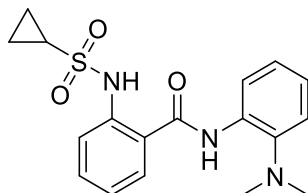
2-(cyclopropanesulfonamido)-*N*-(2-(dimethylamino)phenyl)benzamide (18n). Yield = 18.0 mg (24.3%, off-white solid) LCMS: R_T = 2.48 min., >95% @ 215 and 254 nm, *m/z* = 360.1 [M + H]$^+$.

^{1}H NMR (500 MHz, CDCl$_3$) δ 10.71 (s, 1H), 9.54 (s, 1H), 8.46 (d, *J* = 7.9 Hz, 1H), 7.88 (d, *J* = 8.3 Hz, 1H), 7.68 (d, *J* = 7.8 Hz, 1H), 7.55 (dd, *J* = 11.5, 4.1 Hz, 1H), 7.28 (s, 1H), 7.26 – 7.21 (m, 2H), 7.17 (t, *J* = 7.3 Hz, 1H), 2.74 (s, 6H), 2.59 – 2.52 (m, 1H), 1.30 – 1.24 (m, 2H), 0.97 – 0.92 (m, 2H). ^{13}C NMR (125 MHz, CDCl$_3$) δ 166.29, 143.38, 139.97, 132.98, 132.85, 126.74, 125.44, 124.70, 123.56, 121.87, 121.49, 120.29, 119.67, 45.08, 30.40, 5.70.
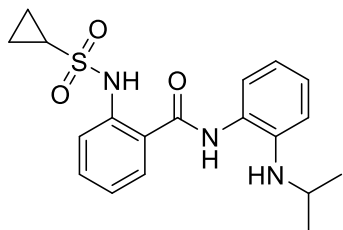
2-(cyclopropanesulfonamido)-*N*-(2-(isopropylamino)phenyl)benzamide (18o). Yield = 47.0 mg (61.0%, dark brown solid) LCMS: R$_T$ = 2.53 min., >95% @ 215 and 254 nm, *m/z* = 374.1 [M + H]$^+$. ^{1}H NMR (500 MHz, CDCl$_3$) δ 10.53 (s, 1H), 8.27 (s, 1H), 7.83 (d, *J* = 8.3 Hz, 1H), 7.73 (d, *J* = 7.4 Hz, 1H), 7.54 (dd, *J* = 16.2, 8.0 Hz, 2H), 7.21 (dt, *J* = 14.6, 7.5 Hz, 2H), 6.89 (dd, *J* = 15.4, 7.8 Hz, 2H), 3.58 (dq, *J* = 12.3, 6.1 Hz, 1H), 2.58 – 2.50 (m, 1H), 1.23 (d, *J* = 6.2 Hz, 8H), 0.99 – 0.93 (m, 2H). ^{13}C NMR (125 MHz, CDCl$_3$) δ 167.19, 140.86, 139.74, 133.14, 127.36, 127.25, 125.15, 124.84, 123.53, 121.26, 121.19, 119.32, 116.11, 45.43, 30.46, 23.03, 5.76.
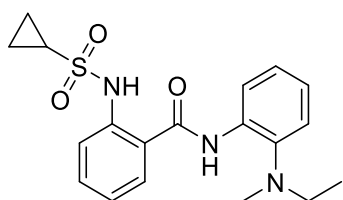
2-(cyclopropanesulfonamido)-*N*-(2-(ethyl(methyl)amino)phenyl)benzamide (18p). Yield = 12.0 mg (15.6%, yellow solid) LCMS: R$_T$ = 2.50 min., >95% @ 215 and 254 nm, *m/z* = 374.1 [M + H]$^+$. ^{1}H NMR (500 MHz, CDCl$_3$) δ 10.76 (s, 1H), 9.80 (s, 1H), 8.50 (d, *J* = 7.4 Hz, 1H), 7.87 (d, *J* = 8.3 Hz, 1H), 7.67 (d, *J* = 6.9 Hz, 1H), 7.55 (t, *J* = 7.8 Hz, 1H), 7.25 (dd, *J* = 14.0, 6.7 Hz, 3H), 7.17 (t, *J* = 7.3 Hz, 1H), 2.97 (d, *J* = 6.7 Hz, 2H), 2.71 (s, 3H), 2.60 – 2.52 (m, 1H), 1.31 – 1.24 (m, 2H), 1.09 (t, *J* = 6.8 Hz, 3H), 0.94 (q, *J* = 6.9 Hz, 2H). ^{13}C NMR (125 MHz, CDCl$_3$) δ 166.28, 140.03, 132.95, 126.68, 125.82, 124.51, 123.51, 121.71, 121.46, 119.29, 51.43, 42.82, 30.41, 13.25.
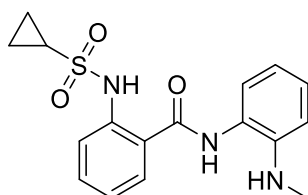
2-(cyclopropanesulfonamido)-*N*-(2-(methylamino)phenyl)benzamide (18q). Yield = 40.0 mg (56.0%, yellow solid) LCMS: R_T = 2.39 min., >95% @ 215 and 254 nm, *m/z* = 346.1 [M + H]$^+$. ^{1}H NMR (500 MHz, CDCl$_3$) δ 10.43 (s, 1H), 8.04 (s, 1H), 7.78 (d, *J* = 8.4 Hz, 1H), 7.72 (d, *J* = 7.5 Hz, 1H), 7.50 (t, *J* = 7.7 Hz, 1H), 7.32 – 7.29 (m, 1H), 7.25 (t, *J* = 7.8 Hz, 1H), 7.19 (t, *J* = 7.5 Hz, 1H), 6.81 (t, *J* = 6.7 Hz, 2H), 2.86 (s, 3H), 2.56 – 2.49 (m, 1H), 1.23 – 1.17 (m, 2H), 0.98 – 0.92 (m, 2H). ^{13}C NMR (125 MHz, CDCl$_3$) δ 167.50, 143.78, 139.52, 133.18, 128.23, 127.58, 125.75, 123.58, 122.89, 121.26, 121.06, 118.01, 112.55, 30.85, 30.42, 5.78.
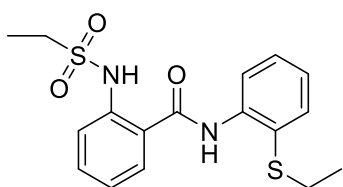
2-(ethylsulfonamido)-*N*-(2-(ethylthio)phenyl)benzamide (18r). Yield = 18.0 mg (22.7%, clear oil) LCMS: R_T = 2.79 min., >95% @ 215 and 254 nm, *m/z* = 365.0 [M + H]$^+$. ^{1}H NMR (500 MHz, CDCl$_3$) δ 10.71 (s, 1H), 9.55 (s, 1H), 8.50 (d, *J* = 8.2 Hz, 1H), 7.86 (d, *J* = 8.4 Hz, 1H), 7.77 (d, *J* = 7.9 Hz, 1H), 7.60 (d, *J* = 7.7 Hz, 1H), 7.57 (t, *J* = 7.9 Hz, 1H), 7.43 (t, *J* = 7.8 Hz, 1H), 7.24 (t, *J* = 7.6 Hz, 1H), 7.17 (t, *J* = 7.6 Hz, 1H), 3.21 (q, *J* = 7.4 Hz, 2H), 2.85 (q, *J* = 7.3 Hz, 2H), 1.39 (t, *J* = 7.4 Hz, 3H), 1.27 (t, *J* = 7.3 Hz, 3H). ^{13}C NMR (125 MHz, CDCl$_3$) δ 166.40, 140.26, 138.86, 135.26, 133.54, 129.81, 127.03, 124.96, 123.70, 123.23, 120.46, 120.14, 119.64, 46.59, 30.67, 14.90, 8.19.
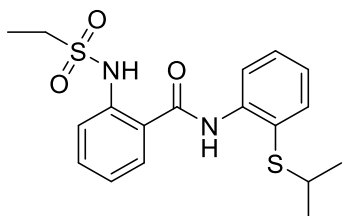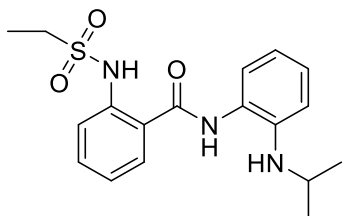

2-(ethylsulfonamido)-*N*-(2-(isopropylthio)phenyl)benzamide (18s). Yield = 30.0 mg (36.4%, clear oil) LCMS: R_T = 2.96 min., >95% @ 215 and 254 nm, *m/z* = 379.1 [M + H]$^+$. ^{1}H NMR (500 MHz, CDCl$_3$) δ 10.76 (s, 1H), 9.68 (s, 1H), 8.54 (d, *J* = 8.3 Hz, 1H), 7.86 (d, *J* = 8.3 Hz, 1H), 7.77

(d, *J* = 7.9 Hz, 1H), 7.61 (dd, *J* = 7.7, 1.2 Hz, 1H), 7.57 (t, *J* = 7.9 Hz, 1H), 7.47 – 7.42 (m, 1H),

7.24 (t, *J* = 7.6 Hz, 1H), 7.16 (td, *J* = 7.6, 1.0 Hz, 1H), 3.24 – 3.16 (m, 3H), 1.39 (t, *J* = 7.4 Hz, 3H),

1.29 (d, *J* = 6.7 Hz, 6H). ^{13}C NMR (125 MHz, CDCl$_3$) δ 166.31, 140.31, 139.58, 136.68, 133.54,

130.30, 126.98, 124.70, 123.21, 122.74, 120.15, 120.11, 119.65, 46.58, 40.98, 23.31, 8.19.
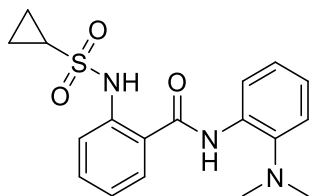
2-(cyclopropanesulfonamido)-*N*-(2-(dimethylamino)phenyl)benzamide (18t). Yield = 45.0 mg

(59.5%, light yellow oil) LCMS: R$_T$ = 2.47 min., >95% @ 215 and 254 nm, *m/z* = 348.1 [M + H]$^+$.

^{1}H NMR (500 MHz, CDCl$_3$) δ 11.10 – 11.09 (m, 1H), 10.86 (s, 1H), 9.56 (s, 1H), 8.44 (d, *J* = 8.0

Hz, 1H), 7.85 (d, *J* = 8.3 Hz, 1H), 7.69 (d, *J* = 7.8 Hz, 1H), 7.55 (t, *J* = 7.9 Hz, 1H), 7.30 – 7.26 (m,

1H), 7.25 – 7.21 (m, 2H), 7.17 (dd, *J* = 10.9, 4.2 Hz, 1H), 3.19 (t, *J* = 7.4 Hz, H), 2.73 (s, 6H), 1.39

(t, *J* = 7.4 Hz, 3H). ^{13}C NMR (125 MHz, CDCl$_3$) δ 166.26, 143.46, 140.18, 133.24, 132.79, 127.00,

125.41, 124.75, 123.17, 120.56, 120.31, 119.72, 119.62, 46.51, 45.08, 8.19.

2-(ethylsulfonamido)-*N*-(2-(isopropylamino)phenyl)benzamide (18u). Yield = 42.0 mg (53.4%,

light brown solid) LCMS: R$_T$ = 2.52 min., >95% @ 215 and 254 nm, *m/z* = 362.1 [M + H]$^+$. ^{1}H

NMR (500 MHz, CDCl$_3$) δ 10.67 (s, 1H), 8.22 (s, 1H), 8.22 (s, 1H), 7.82 (d, *J* = 8.3 Hz, 1H), 7.73

(d, *J* = 7.0 Hz, 1H), 7.60 – 7.51 (m, 2H), 7.20 (dd, *J* = 11.1, 4.3 Hz, 2H), 6.90 (t, *J* = 9.4 Hz, 2H),

3.63 – 3.55 (m, 1H), 3.19 (q, *J* = 7.4 Hz, 2H), 1.38 (t, *J* = 7.4 Hz, 3H), 1.24 (d, *J* = 6.3 Hz, 6H). ^{13}C

NMR (125 MHz, CDCl$_3$) δ 167.12, 140.70, 140.08, 133.43, 127.35, 125.27, 124.77, 123.06,

119.88, 119.56, 116.35, 46.63, 45.56, 23.04, 8.20.
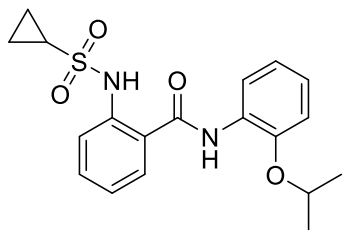
2-(cyclopropanesulfonamido)-*N*-(2-isopropoxyphenyl)benzamide (19a). Yield = 31.0 mg (40.2%, clear oil). LCMS: R_T = 2.82 min., >95% @ 215 and 254 nm, *m/z* = 375.1 [M + H]⁺. ¹H NMR (500 MHz, CDCl₃) δ 10.49 (s, 1H), 8.71 (s, 1H), 8.46 (dd, *J* = 8.0, 1.4 Hz, 1H), 7.86 (dd, *J* = 8.3, 0.7 Hz, 1H), 7.64 (dd, *J* = 7.9, 1.2 Hz, 1H), 7.57 – 7.51 (m, 1H), 7.25 (td, *J* = 7.8, 1.0 Hz, 1H), 7.13 (td, *J* = 8.0, 1.6 Hz, 1H), 7.06 – 7.00 (m, 1H), 6.99 – 6.95 (m, 1H), 4.69 (hept, *J* = 6.0 Hz, 1H), 2.53 (tt, *J* = 8.0, 4.8 Hz, 1H), 1.44 (d, *J* = 6.1 Hz, 6H), 1.25 (tt, *J* = 5.7, 3.0 Hz, 2H), 0.94 (qd, *J* = 5.8, 1.0 Hz, 2H). ¹³C NMR (125 MHz, CDCl₃) δ 166.17, 146.61, 139.71, 132.96, 127.79, 126.55, 124.68, 123.76, 122.35, 121.82, 121.10, 120.20, 112.61, 71.52, 30.35, 22.29, 5.69.
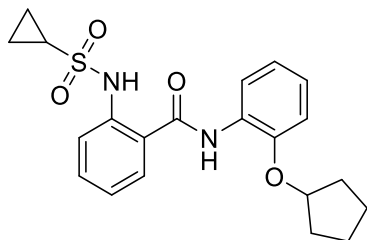
***N*-(2-(cyclopentyloxy)phenyl)-2-(cyclopropanesulfonamido)benzamide (19b).** Yield = 45.0 mg (54.3%, off-white solid). LCMS: R_T = 2.99 min., >95% @ 215 and 254 nm, *m/z* = 401.1[M + H]⁺. ¹H NMR (500 MHz, CDCl₃) δ 10.52 (s, 1H), 8.67 (s, 1H), 8.44 (dd, *J* = 8.0, 1.2 Hz, 1H), 7.86 (d, *J* = 8.3 Hz, 1H), 7.62 (dd, *J* = 7.9, 0.9 Hz, 1H), 7.57 – 7.51 (m, 1H), 7.26 – 7.21 (m, 1H), 7.12 (td, *J* = 8.0, 1.5 Hz, 1H), 7.04 – 6.99 (m, 1H), 6.96 (d, *J* = 8.1 Hz, 1H), 2.53 (tt, *J* = 8.0, 4.8 Hz, 1H), 2.01 (dt, *J* = 13.6, 6.9 Hz, 2H), 1.96 – 1.89 (m, 2H), 1.87 – 1.78 (m, 2H), 1.77 – 1.70 (m, 2H), 1.26 – 1.23 (m, 2H), 0.97 – 0.92 (m, 2H). ¹³C NMR (125 MHz, CDCl₃) δ 166.14, 146.76, 139.75, 132.99, 127.52, 126.45, 124.64, 123.77, 122.30, 121.83, 120.87, 120.07, 112.40, 80.56, 33.01, 30.35, 24.00, 5.69.

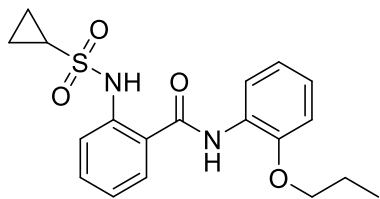**2-(cyclopropanesulfonamido)-*N*-(2-propoxyphenyl)benzamide (19f).** Yield = 27.0 mg (35.0%, light brown solid). LCMS: R_T = 2.86 min., >95% @ 215 and 254 nm, *m/z* = 375.1 [M + H]$^+$. ^{1}H NMR (500 MHz, CDCl$_3$) δ 10.47 (s, 1H), 8.71 (s, 1H), 8.47 – 8.43 (m, 1H), 7.86 (d, *J* = 8.2 Hz, 1H), 7.65 (d, *J* = 7.7 Hz, 1H), 7.55 (dd, *J* = 11.5, 4.1 Hz, 1H), 7.24 (dd, *J* = 11.2, 3.9 Hz, 1H), 7.14 (td, *J* = 8.0, 1.3 Hz, 1H), 7.04 (t, *J* = 7.4 Hz, 1H), 6.96 (d, *J* = 8.0 Hz, 1H), 4.09 (t, *J* = 6.5 Hz, 2H), 2.56 – 2.50 (m, 1H), 1.91 (dt, *J* = 14.0, 7.0 Hz, 2H), 1.27 – 1.23 (m, 2H), 1.11 (t, *J* = 7.4 Hz, 3H), 0.96 – 0.91 (m, 2H). ^{13}C NMR (125 MHz, CDCl$_3$) δ 166.20, 147.76, 139.69, 132.98, 127.03, 126.54, 124.74, 123.75, 122.34, 121.86, 121.10, 120.04, 111.07, 70.19, 30.34, 22.58, 10.56, 5.68, 0.01.
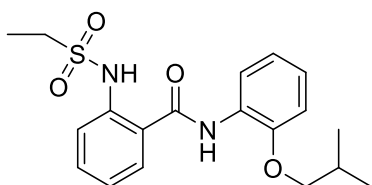
2-(ethylsulfonamido)-*N*-(2-isobutoxyphenyl)benzamide (19g). Yield = 40.0 mg (24.5%). LCMS: R_T = 3.00 min., >95% @ 215 and 254 nm, *m/z* = 377.1 [M + H]$^+$. ^{1}H NMR (500 MHz, CDCl$_3$) δ 10.67 (s, 1H), 8.74 (s, 1H), 8.44 (d, *J* = 7.9 Hz, 1H), 7.85 (d, *J* = 8.4 Hz, 1H), 7.65 (d, *J* = 7.9 Hz, 1H), 7.54 (t, *J* = 7.8 Hz, 1H), 7.20 (t, *J* = 7.6 Hz, 1H), 7.13 (t, *J* = 7.8 Hz, 1H), 7.03 (t, *J* = 7.8 Hz, 1H), 6.95 (d, *J* = 8.1 Hz, 1H), 3.89 (d, *J* = 6.5 Hz, 2H), 3.19 (q, *J* = 7.4 Hz, 2H), 2.21 (dp, *J* = 13.3, 6.7 Hz, 1H), 1.38 (t, *J* = 7.4 Hz, 3H), 1.11 (d, *J* = 6.7 Hz, 6H). ^{13}C NMR (125 MHz, CDCl$_3$) δ 166.13, 147.85, 140.01, 133.28, 126.99, 126.69, 124.78, 123.19, 121.07, 120.73, 120.03, 119.78, 111.07, 74.92, 46.55, 28.29, 19.31, 8.17.

D.
Reagents and Conditions: (a) Aniline, MW; (b) Pyridine, RT

22 → **23** → **24a-d**
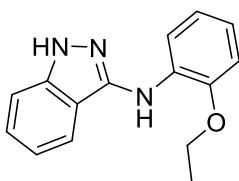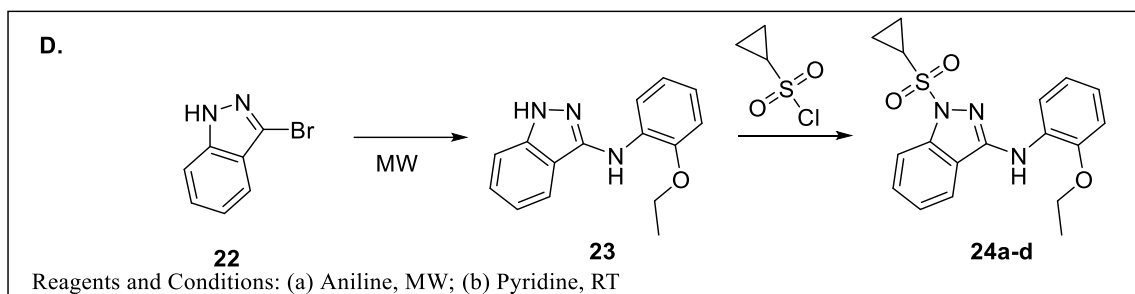
3-(2-ethoxyphenyl)-1*H*-indazole (23). 3-bromo-1*H*-indazole (0.20 g, 1.0 mmol) in *O*-phenitdine (0.2 mL) was subjected to microwave irradiation at 210 °C for 2 hours. The crude was absorbed on silica gel and purified by flash chromatography 0 to 15% ethyl acetate:hexanes. Yield = 50.0 mg (19.6%). LCMS: R_T = 2.7 min., >95% @ 215 and 254 nm, m/z = 254.1 [M + H]$^+$. ^{1}H NMR (500 MHz, CDCl$_3$) δ 9.30 (s, 1H), 8.11 (d, J = 7.9 Hz, 1H), 7.68 (d, J = 8.1 Hz, 1H), 7.44 − 7.39 (m, 2H), 7.15 (t, J = 7.1 Hz, 1H), 7.07 (s, 1H), 7.00 (t, J = 7.6 Hz, 1H), 6.95 − 6.87 (m, 2H), 4.22 (q, J = 7.0 Hz, 2H), 1.56 (t, J = 6.9 Hz, 3H).
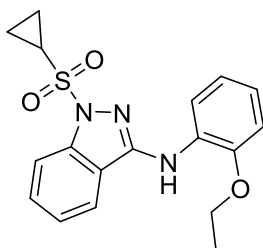
1-(cyclopropylsulfonyl)-3-(2-ethoxyphenyl)-1*H*-indazole (24a). Cyclopropane sulfonyl chloride (28 µL, 0.28 mmol) was added to a solution of 3-(2-ethoxyphenyl)-1*H*-indazole (0.060 g, 0.23 mmol) and pyridine (0.093 mg, 1.18 mmol) in CH$_3$CN (1.50 mL). The reaction was heated at 45 ºC for 24 hours. All volatiles were evaporated and crude was purified via Prep-HPLC (water: CH$_3$CN). Yield = 20.0 mg (23.8%, light brown solid). LCMS: R_T = 3.12 min., >95% @ 215 and 254 nm, m/z = 358.1 [M + H]$^+$. ^{1}H NMR (500 MHz, CDCl$_3$) δ 8.50 (dd, J = 7.9, 1.1 Hz, 1H), 8.06

(d, *J* = 8.4 Hz, 1H), 7.67 (d, *J* = 8.0 Hz, 1H), 7.57 (t, *J* = 7.8 Hz, 1H), 7.43 (s, 1H), 7.40 (t, *J* = 7.4

Hz, 1H), 7.07 (dd, *J* = 11.0, 4.2 Hz, 1H), 7.01 – 6.91 (m, 2H), 4.23 (q, *J* = 6.9 Hz, 2H), 2.69 – 2.63

(m, 1H), 1.57 (t, *J* = 7.0 Hz, 3H), 1.44 – 1.39 (m, 2H), 1.01 – 0.95 (m, 2H). ^{13}C NMR (125 MHz,

CDCl$_3$) δ 149.62, 146.40, 141.74, 129.79, 129.72, 123.69, 121.36, 121.25, 119.92, 118.62, 117.27,

114.21, 110.66, 64.30, 29.70, 15.01, 5.64.
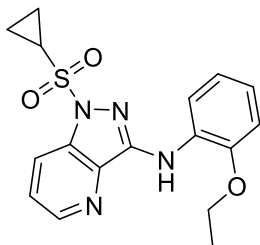
1-(cyclopropylsulfonyl)-3-(2-ethoxyphenyl)-1*H*-pyrazolo[4,3-*b*]pyridine (24b). Yield = 15.0

mg (21.7%, brown solid). LCMS: R$_T$ = 3.04 min., >95% @ 215 and 254 nm, *m/z* = 359.0 [M + H]$^+$.

^{1}H NMR (500 MHz, CDCl$_3$) δ 8.68 (dd, *J* = 4.5, 1.1 Hz, 1H), 8.56 (dd, *J* = 7.9, 1.3 Hz, 1H), 8.31

(dd, *J* = 8.4, 1.1 Hz, 1H), 8.07 (s, 1H), 7.49 (dd, *J* = 8.5, 4.5 Hz, 1H), 7.08 (dd, *J* = 11.1, 4.2 Hz,

1H), 7.01 (td, *J* = 7.8, 1.4 Hz, 1H), 6.97 – 6.94 (m, 1H), 4.25 (q, *J* = 7.0 Hz, 2H), 2.73 – 2.65 (m,

1H), 1.58 (t, *J* = 7.0 Hz, 3H), 1.46 – 1.41 (m, 2H), 1.06 – 1.01 (m, 2H).
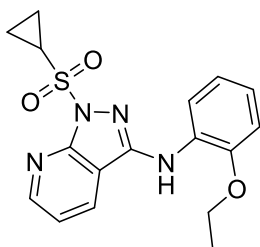
1-(cyclopropylsulfonyl)-3-(2-ethoxyphenyl)-1*H*-pyrazolo[3,4-*b*]pyridine (24c). Yield = 36.0

mg (27.8%, brown solid). LCMS: R$_T$ = 2.78 min., >95% @ 215 and 254 nm, *m/z* = 359.1 [M + H]$^+$.

^{1}H NMR (500 MHz, CDCl$_3$) δ 8.72 (dd, *J* = 4.6, 1.2 Hz, 1H), 8.34 (dd, *J* = 7.8, 1.3 Hz, 1H), 8.03

(dd, *J* = 7.9, 1.3 Hz, 1H), 7.32 (dd, *J* = 7.7, 4.9 Hz, 2H), 7.05 – 7.01 (m, 1H), 6.98 (td, *J* = 7.7, 1.4

Hz, 1H), 6.92 (d, *J* = 7.9 Hz, 1H), 4.20 (q, *J* = 7.0 Hz, 2H), 2.93 – 2.86 (m, 1H), 1.58 – 1.51 (m,

5H), 1.06 – 1.01 (m, 2H). ^{13}C NMR (125 MHz, CDCl$_3$) δ 152.68, 150.94, 146.76, 146.53, 129.42, 128.76, 121.67, 121.25, 118.70, 117.37, 111.83, 110.72, 64.25, 30.96, 14.97, 5.98.
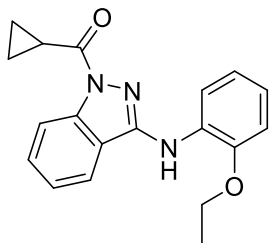
cyclopropyl(3-((2-ethoxyphenyl)amino)-1*H*-indazol-1-yl)methanone (24d). Yield = 8.0 mg (31.1%, light brown solid). LCMS: R$_T$ = 3.28 min., >95% @ 215 and 254 nm, *m/z* = 322.1 [M + H]$^+$. ^{1}H NMR (500 MHz, CDCl$_3$) δ 8.49 (d, *J* = 8.3 Hz, 1H), 7.67 (d, *J* = 7.9 Hz, 1H), 7.60 (t, *J* = 7.6 Hz, 1H), 7.40 (dd, *J* = 14.1, 6.5 Hz, 2H), 7.07 (dd, *J* = 11.0, 4.2 Hz, 1H), 6.97 (dt, *J* = 8.0, 6.9 Hz, 2H), 4.24 (q, *J* = 7.0 Hz, 2H), 3.25 (td, *J* = 8.1, 4.1 Hz, 1H), 1.58 (t, *J* = 7.0 Hz, 3H), 1.33 (dt, *J* = 7.7, 3.7 Hz, 2H), 1.17 – 1.12 (m, 2H). ^{13}C NMR (125 MHz, CDCl$_3$) δ 173.59, 147.80, 146.52, 139.19, 130.04, 129.97, 123.72, 121.20, 121.06, 120.11, 117.98, 116.96, 116.25, 110.76, 64.31, 15.01, 12.76, 10.10.
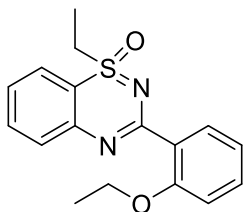
3-(2-ethoxyphenyl)-1-ethyl-1lλ^4-benzo[*e*][1,2,4]thiadiazine 1-oxide (24f). Yield = 15.0 mg (28.1%). LCMS: R$_T$ = 2.03 min., >95% @ 215 and 254 nm, *m/z* = 315.0 [M + H]$^+$. ^{1}H NMR (500 MHz, CDCl$_3$) δ 7.78 (dd, *J* = 8.0, 1.1 Hz, 1H), 7.74 – 7.70 (m, 1H), 7.67 – 7.62 (m, 2H), 7.45 – 7.41 (m, 1H), 7.36 (td, *J* = 8.4, 1.7 Hz, 1H), 7.02 (t, *J* = 7.5 Hz, 1H), 6.98 (d, *J* = 8.3 Hz, 1H), 4.17 – 4.07 (m, 2H), 3.72 (dq, *J* = 14.5, 7.3 Hz, 1H), 3.54 (dq, *J* = 14.8, 7.4 Hz, 1H), 1.40 (t, *J* = 7.0 Hz, 3H), 1.25 (t, *J* = 7.3 Hz, 3H). ^{13}C NMR (125 MHz, CDCl$_3$) δ 160.40, 156.76, 135.12, 130.80, 130.16, 128.44, 126.44, 123.66, 120.51, 113.22, 109.26, 64.48, 52.63, 14.90, 8.22.
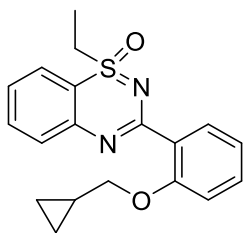
3-(2-(cyclopropylmethoxy)phenyl)-1-ethyl-1lλ^4-benzo[*e*][1,2,4]thiadiazine 1-oxide (24g).

Yield = 12.0 mg (20.7%). LCMS: R_T = 2.16 min., >95% @ 215 and 254 nm, *m/z* = 341.1 [M + H]$^+$.

]$^+$. ^{1}H NMR (500 MHz, CDCl$_3$) δ 7.78 (dd, *J* = 8.0, 1.1 Hz, 1H), 7.72 – 7.68 (m, 1H), 7.68 – 7.63

(m, 2H), 7.46 – 7.41 (m, 1H), 7.35 (td, *J* = 8.4, 1.7 Hz, 1H), 7.03 (t, *J* = 7.5 Hz, 1H), 6.95 (d, *J* =

8.3 Hz, 1H), 3.97 (d, J = 7.0 Hz, 2H), 3.72 (dq, *J* = 14.5, 7.3 Hz, 1H), 3.54 (dq, *J* = 14.8, 7.4 Hz,

1H), 1.25 (t, *J* = 7.3 Hz, 3H), 0.75 – 0.67 (m, 2H), 0.44 – 0.38 (m, 2H). ^{13}C NMR (125 MHz,

CDCl$_3$) δ 160.42, 156.76, 135.14, 130.78, 130.16, 128.44, 126.47, 123.66, 120.51, 113.21, 109.26,

73.83 52.65, 10.33, 8.21, 5.70,
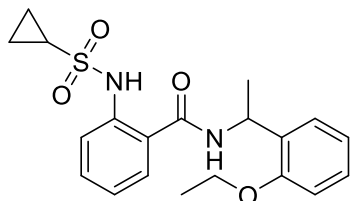
2-(cyclopropanesulfonamido)-*N*-(1-(2-ethoxyphenyl)ethyl)benzamide (28e). Yield = 18.0 mg

(17.4%, clear oil). LCMS: R_T = 2.9 min., >95% @ 215 and 254 nm, *m/z* = 389.0 [M + H]$^+$. ^{1}H NMR

(500 MHz, CDCl$_3$) δ 10.69 (s, 1H), 7.79 (d, *J* = 8.2 Hz, 1H), 7.54 (t, *J* = 12.9 Hz, 1H), 7.51 – 7.45

(m, 2H), 7.26 (dd, *J* = 4.4, 2.7 Hz, 1H), 7.15 (t, *J* = 7.6 Hz, 1H), 6.95 (dd, *J* = 13.1, 8.0 Hz, 2H),

5.40 (dq, *J* = 14.0, 7.0 Hz, 1H), 4.24 – 4.10 (m, 2H), 2.40 (td, *J* = 8.1, 4.0 Hz, 1H), 1.60 (d, *J* = 6.9

Hz, 3H), 1.53 (t, *J* = 7.0 Hz, 3H), 1.19 – 1.12 (m, 2H), 0.86 – 0.75 (m, 2H). ^{13}C NMR (125 MHz,

CDCl$_3$) δ 167.10, 156.37, 139.48, 132.49, 129.91, 128.81, 128.63, 126.44, 123.36, 122.03, 121.59,

121.09, 111.97, 63.63, 48.81, 30.15, 21.51, 15.13, 5.64, 5.40.
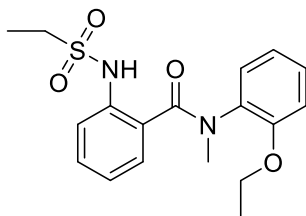
N-(2-ethoxyphenyl)-2-(ethylsulfonamido)-N-methylbenzamide (28j). Yield = 19.0 mg (25.7%,

light yellow solid). LCMS: R_T = 2.61 min., >95% @ 215 and 254 nm, m/z = 365.0 [M + H]$^+$. ^{1}H

NMR (500 MHz, CDCl$_3$) δ 8.41 (s, 1H), 7.55 (d, J = 7.9 Hz, 1H), 7.17 (d, J = 6.3 Hz, 2H), 7.03 (s,

2H), 6.82 (s, 2H), 6.75 (s, 1H), 4.05 (d, J = 6.5 Hz, 2H), 3.40 (d, J = 15.7 Hz, 3H), 3.26 – 3.18 (m,

2H), 1.44 (dd, J = 14.5, 7.2 Hz, 6H). ^{13}C NMR (125 MHz, CDCl$_3$) δ 170.31, 153.42, 136.57, 132.66,

130.64, 129.11, 128.91, 124.70, 122.39, 120.86, 119.13, 112.61, 64.06, 46.53, 14.56, 8.15.

Reagents and Conditions: (a) hydrazine hydrate, MW, 160 °C, 1h; (b) K2CO3, tBuOH, MW, 150 °C, 2h
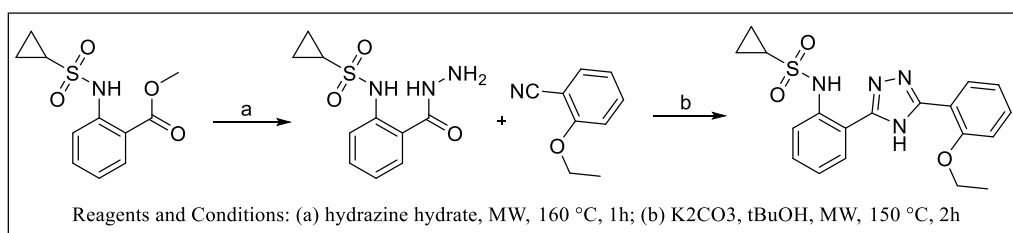
N-(2-(hydrazinecarbonyl)phenyl)cyclopropanesulfonamide A solution of methyl 2-

(cyclopropanesulfonamido)benzoate (0.15 g, 0.59 mmol) in hydrazine hydrate (80%) (117 μL,

2.35 mmol) and ethanol (0.20 mL) was subjected to microwave irradiation at 160 °C for 1 hour.

After TLC confirmation of starting material finish, volatiles were evaporated, and crude used as

such.

N-(2-(5-(2-ethoxyphenyl)-4H-1,2,4-triazol-3-yl)phenyl)cyclopropanesulfonamide (28l). A

solution of 2-ethoxybenzonitrile (0.17 μL, 1.2 mmol) N-(2-

(hydrazinecarbonyl)phenyl)cyclopropanesulfonamide (0.10 g, 0.40 mmol) and K$_2$CO$_3$ (55 mg, 0.40

mmol) in tBuOH (0.10 mL) was subjected to microwave irradiation at 150 ºC for 2 hour. Crude

purified by Prep-HPLC. Yield = 10.0 mg (6.5%, white solid). LCMS: R_T = 2.92 min., >95% @ 215
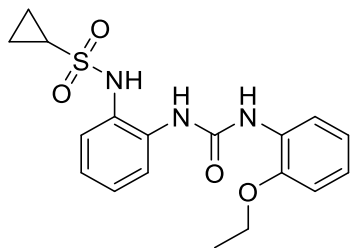
and 254 nm, *m/z* = 385.0 [M + H]$^+$. ^{1}H NMR (500 MHz, CDCl$_3$) δ 11.85 (s, 1H), 11.16 (s, 1H), 8.41 (dd, *J* = 7.8, 1.6 Hz, 1H), 8.36 (dd, *J* = 7.9, 1.4 Hz, 1H), 7.86 (d, *J* = 8.2 Hz, 1H), 7.53 – 7.47 (m, 1H), 7.45 – 7.41 (m, 1H), 7.28 – 7.23 (m, 1H), 7.21 (t, *J* = 7.3 Hz, 1H), 7.11 (d, *J* = 8.4 Hz, 1H), 4.37 (q, *J* = 7.0 Hz, 2H), 2.49 – 2.43 (m, 1H), 1.68 (t, *J* = 7.0 Hz, 3H), 1.20 – 1.15 (m, 2H), 0.83 – 0.78 (m, 2H). ^{13}C NMR (125 MHz, CDCl$_3$) δ 160.41, 156.31, 152.89, 136.79, 132.20, 130.33, 129.73, 128.24, 124.00, 121.99, 120.83, 119.30, 114.40, 112.08, 64.77, 29.87, 15.10, 5.44.
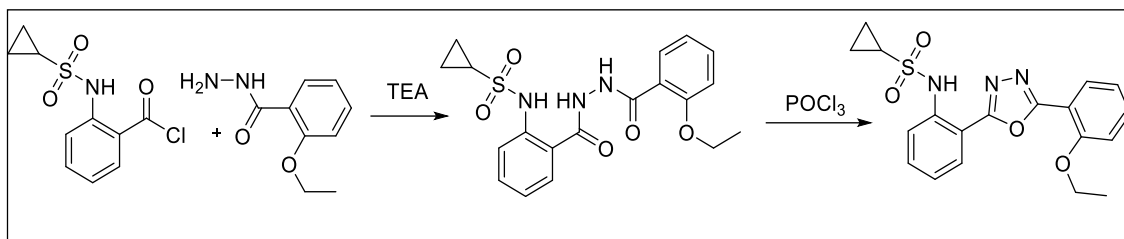

***N*-(2-(2-(2-ethoxybenzoyl)hydrazine-1-carbonyl)phenyl)cyclopropanesulfonamide.** To a solution of 2-ethoxybenzohydrazide (0.85 g, 0.47 mmol) and TEA in DCM was added 2 (cyclopropanesulfonamido)benzoyl chloride (0.13 g, 0.51 mmol) and the reaction was stirred for 2 hours at rt. Product was partitioned between water and ethyl acetate, organic layer were collected, washed with brine, concentrated and used as such. Yield = 170.0 mg (crude). LCMS: R$_T$ = 2.53 min., >95% @ 215 and 254 nm, *m/z* = 404.1 [M + H]$^+$.

***N*-(2-(5-(2-ethoxyphenyl)-1,3,4-oxadiazol-2-yl)phenyl)cyclopropanesulfonamide (28m).** A solution of *N*-(2-(2-(2-ethoxybenzoyl)hydrazine-1-carbonyl)phenyl)cyclopropanesulfonamide (0.17 g crude) in POCl$_3$ was refluxed at 80º C for 12 hours. Volatiles were evaporated under vacuum; mixture was neutralized with saturated NaHCO$_3$ aqueous solution and product extracted with ethyl acetate. Organic layer purified by flash chromatography 0-80% Ethyl acetate:Hexane. Yield = 30.0 mg (off-white solid) LCMS: R$_T$ = 2.96 min., >95% @ 215 and 254 nm, *m/z* = 386.0 [M + H]$^+$. ^{1}H NMR (500 MHz, CDCl$_3$) δ 10.46 (s, 1H), 8.10 (d, *J* = 7.6 Hz, 1H), 8.03 (d, *J* = 7.7 Hz, 1H), 7.98 (d, *J* = 8.4 Hz, 1H), 7.55 (dd, *J* = 12.9, 7.7 Hz, 2H), 7.26 (d, *J* = 7.6 Hz, 1H), 7.12 (dd, *J* = 15.0, 7.9 Hz, 2H), 4.26 (q, *J* = 6.9 Hz, 2H), 2.64 – 2.56 (m, 1H), 1.58 (t, *J* = 6.9 Hz, 3H),

1.33 – 1.27 (m, 2H), 0.97 – 0.91 (m, 2H). ^{13}C NMR (125 MHz, CDCl$_3$) δ 163.35, 157.40, 137.91, 133.58, 132.63, 130.58, 127.87, 123.55, 120.78, 119.83, 112.97, 112.41, 111.84, 64.49, 30.67, 14.87, 5.79.


N-(2-(3-(2-ethoxyphenyl)ureido)phenyl)cyclopropanesulfonamide (28n). Yield = 30.0 mg (44.4%, orange solid). LCMS: R$_T$ = 2.37 min., >95% @ 215 and 254 nm, *m/z* = 362.0 [M + H]$^+$. ^{1}H NMR (500 MHz, CDCl$_3$) δ 8.07 (dd, *J* = 8.0, 1.3 Hz, 1H), 7.76 (s, 1H), 7.61 (dd, *J* = 8.0, 1.3 Hz, 1H), 7.49 (dd, *J* = 7.9, 1.3 Hz, 1H), 7.24 (td, *J* = 7.8, 1.4 Hz, 1H), 7.18 (td, *J* = 7.8, 1.4 Hz, 1H), 7.00 (td, *J* = 7.8, 1.5 Hz, 1H), 6.93 (td, *J* = 7.8, 1.2 Hz, 1H), 6.87 – 6.83 (m, 1H), 4.05 (q, *J* = 7.0 Hz, 2H), 2.51 – 2.46 (m, 1H), 1.36 (t, *J* = 7.0 Hz, 3H), 1.12 – 1.08 (m, 2H), 0.92 – 0.87 (m, 2H). ^{13}C NMR (125 MHz, CDCl$_3$) δ 153.97, 147.86, 132.76, 129.45, 127.55, 127.50, 126.73, 125.91, 125.10, 123.52, 121.05, 120.13, 111.26, 64.22, 29.87, 14.75, 5.70.
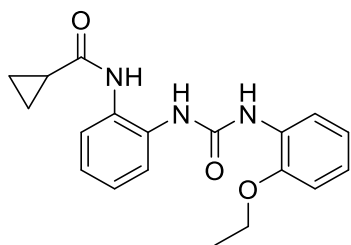
N-(2-(3-(2-ethoxyphenyl)ureido)phenyl)cyclopropanecarboxamide (28o). Yield = 28.0 mg (45.7%, white solid). LCMS: R$_T$ = 2.37 min., >95% @ 215 and 254 nm, *m/z* = 362.0 [M + H]$^+$. ^{1}H NMR (500 MHz, CDCl$_3$) δ 8.74 (s, 1H), 8.13 (d, *J* = 7.8 Hz, 1H), 7.60 (d, *J* = 6.7 Hz, 1H), 7.28 (s, 1H), 7.11 (dd, *J* = 13.5, 6.8 Hz, 1H), 6.97 (dt, *J* = 7.8, 3.9 Hz, 2H), 6.92 (td, *J* = 7.7, 1.2 Hz, 2H), 6.84 (d, *J* = 8.0 Hz, 1H), 4.05 (q, *J* = 7.0 Hz, 2H), 1.59 (d, *J* = 3.9 Hz, 1H), 1.38 (t, *J* = 7.0 Hz, 3H), 1.01 (dd, *J* = 7.4, 3.4 Hz, 2H), 0.79 (dd, *J* = 7.4, 2.8 Hz, 2H). ^{13}C NMR (125 MHz, CDCl$_3$) δ 173.32,

154.16, 147.50, 128.05, 126.04, 125.86, 125.53, 124.44, 122.85, 120.90, 119.37, 116.46, 111.05, 64.16, 15.37, 14.78, 8.14.
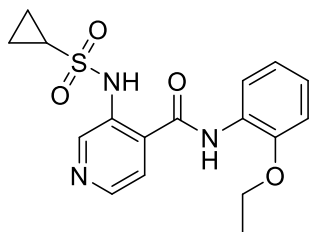
3-(cyclopropanesulfonamido)-*N*-(2-ethoxyphenyl)isonicotinamide (34a). Yield = 15.0 mg (27.3%, yellow oil). LCMS: R_T = 2.37 min., >95% @ 215 and 254 nm, *m/z* = 362.0 [M + H]$^+$. ^{1}H NMR (500 MHz, CDCl$_3$) δ 10.03 (s, 1H), 9.15 (s, 1H), 8.76 (s, 1H), 8.55 (d, *J* = 5.1 Hz, 1H), 8.41 (d, *J* = 7.9 Hz, 1H), 7.45 (d, *J* = 5.1 Hz, 1H), 7.17 (td, *J* = 8.1, 1.3 Hz, 1H), 7.04 (t, *J* = 7.6 Hz, 1H), 6.97 (d, *J* = 8.2 Hz, 1H), 4.20 (q, *J* = 6.9 Hz, 2H), 2.62 – 2.53 (m, 1H), 1.52 (dd, *J* = 8.9, 5.1 Hz, 3H), 1.30 – 1.26 (m, 2H), 1.03 – 0.98 (m, 2H). ^{13}C NMR (125 MHz, CDCl$_3$) δ 164.13, 147.74, 145.04, 144.46, 134.61, 128.26, 126.27, 125.49, 121.14, 120.28, 119.23, 111.12, 64.44, 30.89, 14.90, 5.97.
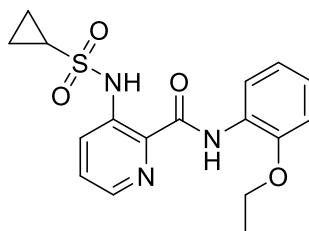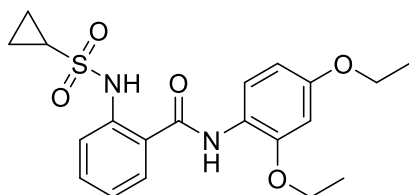

3-(cyclopropanesulfonamido)-*N*-(2-ethoxyphenyl)picolinamide (34b). Yield = 17.0 mg (30.4%, yellow solid). LCMS: R_T = 2.97 min., >95% @ 215 and 254 nm, *m/z* = 362.0 [M + H]$^+$. ^{1}H NMR (500 MHz, CDCl$_3$) δ 11.69 (s, 1H), 10.92 (s, 1H), 8.49 (dd, *J* = 8.0, 1.4 Hz, 1H), 8.37 (dd, *J* = 4.4, 1.3 Hz, 1H), 8.26 (dd, *J* = 8.5, 1.2 Hz, 1H), 7.47 (dd, *J* = 8.5, 4.4 Hz, 1H), 7.13 (td, *J* = 8.0, 1.6 Hz, 1H), 7.04 (dd, *J* = 11.2, 4.3 Hz, 1H), 6.97 (d, *J* = 8.1 Hz, 1H), 4.20 (q, *J* = 7.0 Hz, 2H), 2.58 (td, *J* = 8.0, 4.0 Hz, 1H), 1.55 (t, *J* = 7.0 Hz, 3H), 1.33 – 1.28 (m, 2H), 1.03 – 0.98 (m, 2H). ^{13}C NMR (125 MHz, CDCl$_3$) δ 164.70, 148.39, 142.56, 138.17, 134.26, 127.83, 127.49, 126.97, 124.68, 121.05, 119.93, 111.51, 64.48, 30.90, 14.85, 5.78.
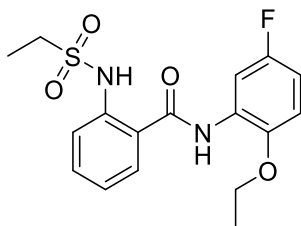
N-(2-ethoxy-5-fluorophenyl)-2-(ethylsulfonamido)benzamide (35d). Yield = 33.8 mg (40.2%, off-white solid). LCMS: R_T = 2.82 min., >95% @ 215 and 254 nm, m/z = 389.0 [M + Na]$^+$. 1 H NMR (500 MHz, CDCl3) δ 10.54 (s, 1H), 8.73 (s, 1H), 8.30 (dd, J = 10.4, 3.0 Hz, 1H), 7.85 (d, J = 8.3 Hz, 1H), 7.64 (dd, J = 7.9, 1.2 Hz, 1H), 7.58 – 7.53 (m, 1H), 7.24 – 7.19 (m, 1H), 6.87 (dd, J = 9.0, 4.9 Hz, 1H), 6.84 –6.79 (m, 1H), 4.17 (q, J = 7.0 Hz, 2H), 3.21 (q, J = 7.4 Hz, 2H), 1.51 (t, J = 7.0 Hz, 3H), 1.40 (t, J = 7.4 Hz, 3H). 13C NMR (125 MHz, CDCl3) δ 166.24, 157.81, 155.91, 143.72, 140.10, 133.50, 126.81, 123.16, 120.34, 119.74, 111.46, 111.38, 110.26, 110.08, 107.97, 107.73, 64.97, 46.70, 14.91, 8.19.
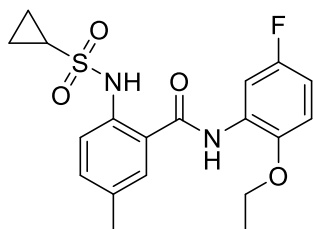

2-(cyclopropanesulfonamido)-N-(2,4-diethoxyphenyl)benzamide (35h). Yield = 18.0 mg (42.8%, white solid). LCMS: R_T = 2.88 min., >95% @ 215 and 254 nm, *m/z* = 405.0[M + H]$^+$. ^{1}H NMR (500 MHz, CDCl$_3$) δ 10.49 (s, 1H), 8.43 (s, 1H), 8.29 (d, *J* = 9.5 Hz, 1H), 7.85 (d, *J* = 8.2 Hz, 1H), 7.63 (d, *J* = 7.1 Hz, 1H), 7.55 – 7.51 (m, 1H), 7.23 (t, *J* = 7.6 Hz, 1H), 6.53 (dd, *J* = 7.3, 2.3 Hz, 2H), 4.15 (q, *J* = 7.0 Hz, 2H), 4.06 (q, *J* = 7.0 Hz, 2H), 2.55 – 2.49 (m, 1H), 1.49 (t, *J* = 7.0 Hz, 3H), 1.44 (t, *J* = 7.0 Hz, 3H), 1.26 – 1.21 (m, 2H), 0.95 – 0.91 (m, 2H). ^{13}C NMR (125 MHz, CDCl$_3$) δ 165.87, 156.46, 149.06, 139.54, 132.76, 126.58, 123.71, 122.54, 121.80, 121.06, 120.30, 104.55, 100.01, 64.34, 63.80, 30.30, 14.83, 5.66.
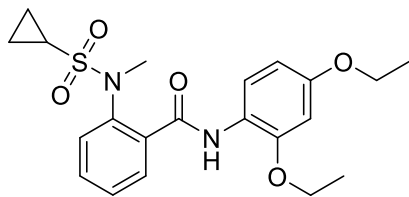
N-(2,4-diethoxyphenyl)-2-(N-methylcyclopropanesulfonamido)benzamide (35i). Yield = 16.0 mg (39.0%, white solid). LCMS: R_T = 2.7 min., >95% @ 215 and 254 nm, m/z = 419.1[M + H]$^+$. ^{1}H NMR (500 MHz, CDCl$_3$) δ 9.17 (s, 1H), 8.43 (d, J = 8.5 Hz, 1H), 7.95 (dd, J = 7.6, 1.3 Hz, 1H), 7.58 (d, J = 7.8 Hz, 1H), 7.53 (tt, J = 6.3, 3.1 Hz, 1H), 7.49 (t, J = 7.4 Hz, 1H), 6.53 – 6.49 (m, 2H), 4.15 (q, J = 7.0 Hz, 2H), 4.05 (q, J = 7.0 Hz, 2H), 3.39 (s, 3H), 2.54 – 2.48 (m, 1H), 1.44 (dt, J = 9.6, 7.0 Hz, 6H), 1.13 – 1.08 (m, 2H), 0.98 – 0.93 (m, 2H). ^{13}C NMR (125 MHz, CDCl$_3$) δ 164.19, 155.98, 149.02, 138.89, 136.17, 131.37, 130.46, 128.93, 128.84, 121.35, 121.21, 104.35, 99.93, 64.21, 63.74, 39.55, 28.14, 14.87, 14.66, 5.54.
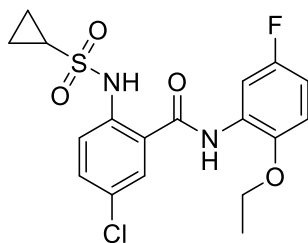

2-(cyclopropanesulfonamido)-N-(2-ethoxy-5-fluorophenyl)-5-methylbenzamide (36a). Yield = 19.0 mg (27.1%, white solid). LCMS: R_T = 2.98 min., >95% @ 215 and 254 nm, m/z = 393.0 [M + H]$^+$. ^{1}H NMR (500 MHz, CDCl$_3$) δ 10.11 (s, 1H), 8.70 (s, 1H), 8.28 (dd, J = 10.3, 3.0 Hz, 1H), 7.75 – 7.70 (m, 1H), 7.42 (s, 1H), 7.38 – 7.33 (m, 1H), 6.86 (dd, J = 9.0, 4.9 Hz, 1H), 6.82 – 6.77 (m, 1H), 4.17 (q, J = 7.0 Hz, 2H), 2.48 (ddt, J = 11.0, 7.9, 3.9 Hz, 1H), 2.42 (s, 1H), 1.52 (t, J = 7.0 Hz, 3H), 1.25 – 1.20 (m, 2H), 0.95 – 0.89 (m, 2H). ^{13}C NMR (125 MHz, CDCl$_3$) δ 166.28, 157.81, 155.91, 143.73, 143.71, 137.05, 133.92, 133.76, 127.87, 127.78, 127.03, 122.43, 122.33, 111.48, 111.41, 110.16, 109.97, 107.83, 107.59, 64.95, 30.15, 20.90, 14.88, 5.65
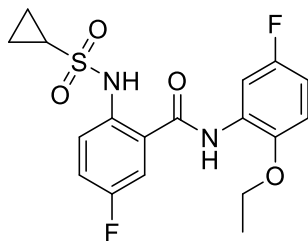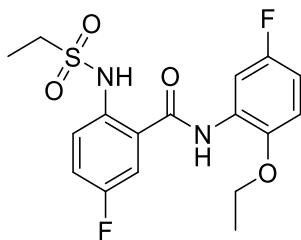
2-(cyclopropanesulfonamido)-*N*-(2-ethoxy-5-fluorophenyl)-5-fluorobenzamide (36b). Yield = 19.0 mg (26.5%, off-white solid). LCMS: R_T = 2.87 min., >95% @ 215 and 254 nm, *m/z* = 397.0 [M + H]$^+$. ^{1}H NMR (500 MHz, CDCl$_3$) δ 9.93 (s, 1H), 8.62 (s, 1H), 8.28 (dd, *J* = 10.2, 2.9 Hz, 1H), 7.84 (dd, *J* = 9.1, 4.9 Hz, 1H), 7.33 (dd, *J* = 8.5, 2.8 Hz, 1H), 7.31 – 7.27 (m, 1H), 6.88 (dd, *J* = 9.0, 5.0 Hz, 1H), 6.86 – 6.81 (m, 1H), 4.18 (q, *J* = 7.0 Hz, 2H), 2.51 – 2.44 (m, 1H), 1.52 (t, *J* = 7.0 Hz, 3H), 1.25 – 1.20 (m, 2H), 0.96 – 0.92 (m, 2H). ^{13}C NMR (125 MHz, CDCl$_3$) δ 164.99, 159.68, 157.74, 155.84, 143.69, 135.48, 127.44, 127.35, 125.06, 125.00, 124.09, 124.05, 120.30, 120.12, 113.34, 113.15, 111.48, 111.40, 110.62, 110.44, 107.98, 107.74, 64.99, 30.21, 14.87, 5.70.

5-chloro-2-(cyclopropanesulfonamido)-*N*-(2-ethoxy-5-fluorophenyl)benzamide (36c). Yield = 18.0 mg (24.3%, yellow solid). LCMS: R_T = 3.02 min., >95% @ 215 and 254 nm, *m/z* = 413.0 [M + H]$^+$. ^{1}H NMR (500 MHz, CDCl$_3$) δ 10.17 (s, 1H), 8.64 (s, 1H), 8.24 (dd, *J* = 10.2, 2.9 Hz, 1H), 7.82 (d, *J* = 8.9 Hz, 1H), 7.61 (d, *J* = 2.3 Hz, 1H), 7.51 (dd, *J* = 8.9, 2.3 Hz, 1H), 6.89 – 6.80 (m, 2H), 4.21 – 4.15 (m, 2H), 2.56 – 2.49 (m, 1H), 1.53 (dd, *J* = 9.1, 4.8 Hz, 3H), 1.26 (dt, *J* = 5.7, 4.5 Hz, 2H), 1.00 – 0.95 (m, 2H). ^{13}C NMR (125 MHz, CDCl$_3$) δ 164.99, 157.75, 155.85, 143.79, 138.23, 133.07, 129.11, 127.44, 127.34, 126.71, 123.28, 123.23, 111.54, 111.47, 110.66, 110.47, 108.02, 107.78, 65.03, 30.53, 14.86, 5.80.
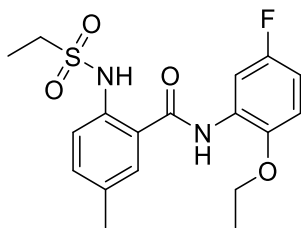
N-(2-ethoxy-5-fluorophenyl)-2-(ethylsulfonamido)-5-methylbenzamide (36d). Yield = 22.0 mg (32.0%, off-white solid). LCMS: R_T = 2.97 min., >95% @ 215 and 254 nm, *m/z* = 381.0 [M + H]⁺. ¹H NMR (500 MHz, CDCl₃) δ 10.31 (s, 1H), 8.72 (s, 1H), 8.26 (dd, *J* = 10.4, 3.0 Hz, 1H), 7.72 (d, *J* = 8.5 Hz, 1H), 7.41 (s, 1H), 7.35 (d, *J* = 8.5 Hz, 1H), 6.86 (dd, *J* = 9.0, 4.9 Hz, 1H), 6.82 – 6.76 (m, 1H), 4.17 (q, *J* = 7.0 Hz, 2H), 3.15 (q, *J* = 7.4 Hz, 2H), 2.41 (s, 3H), 1.52 (t, *J* = 7.0 Hz, 3H), 1.36 (t, *J* = 7.4 Hz, 3H). ¹³C NMR (125 MHz, CDCl₃) δ 166.24, 157.78, 155.89, 143.77, 143.75, 137.42, 134.17, 133.11, 127.81, 127.72, 127.25, 120.64, 120.21, 111.49, 111.41, 110.18, 109.99, 107.84, 107.60, 64.97, 46.39, 20.83, 14.88, 8.14.

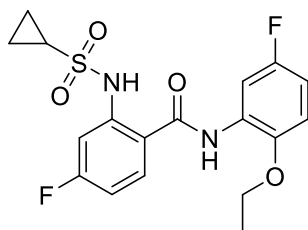**N-(2-ethoxy-5-fluorophenyl)-2-(ethylsulfonamido)-5-fluorobenzamide (36e).** Yield = 18.0 mg (25.8%, off-white solid). LCMS: R_T = 2.87 min., >95% @ 215 and 254 nm, *m/z* = 385.0 [M + H]⁺. ¹H NMR (500 MHz, CDCl₃) δ 10.15 (s, 1H), 8.64 (s, 1H), 8.24 (dd, *J* = 10.2, 2.9 Hz, 1H), 7.83 (dd, *J* = 9.1, 4.8 Hz, 1H), 7.32 (dd, *J* = 8.5, 2.8 Hz, 1H), 7.28 (ddd, *J* = 10.3, 6.7, 2.9 Hz, 1H), 6.90 – 6.85 (m, 1H), 6.85 – 6.79 (m, 1H), 4.18 (q, *J* = 7.0 Hz, 2H), 3.16 (q, *J* = 7.4 Hz, 2H), 1.52 (t, *J* = 7.0 Hz, 3H), 1.38 (t, *J* = 7.4 Hz, 3H). ¹³C NMR (125 MHz, CDCl₃) δ 165.00, 164.99, 159.16, 157.70, 157.20, 155.80, 143.77, 143.75, 135.90, 135.88, 127.38, 127.29, 122.62, 122.56, 122.24, 122.20, 120.54, 120.36, 113.57, 113.38, 111.50, 111.43, 110.64, 110.46, 107.99, 107.75, 65.01, 46.74, 14.86, 8.12.
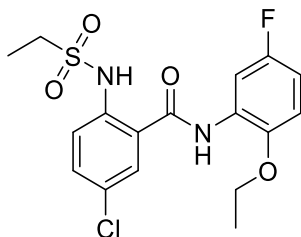
5-chloro-*N*-(2-ethoxy-5-fluorophenyl)-2-(ethylsulfonamido)benzamide (36f). Yield = 17.0 mg (23.4%, yellow oil). LCMS: R_T = 3.0 min., >95% @ 215 and 254 nm, *m/z* = 401.0 [M + H]$^+$. ^{1}H NMR (500 MHz, CDCl$_3$) δ 10.32 (s, 1H), 8.65 (s, 1H), 8.23 (dd, *J* = 10.2, 2.9 Hz, 1H), 7.82 – 7.79 (m, 1H), 7.60 (d, *J* = 2.3 Hz, 1H), 7.50 (dd, *J* = 8.9, 2.3 Hz, 1H), 6.87 (dd, *J* = 9.0, 4.9 Hz, 1H), 6.85 – 6.80 (m, 1H), 4.18 (dt, *J* = 11.5, 4.8 Hz, 2H), 3.19 (q, *J* = 7.4 Hz, 2H), 1.55 – 1.51 (m, 3H), 1.39 (t, *J* = 7.4 Hz, 3H). ^{13}C NMR (125 MHz, CDCl$_3$) δ 164.96, 157.72, 155.82, 143.81, 138.48, 133.26, 128.56, 127.37, 127.28, 126.89, 121.82, 121.31, 111.54, 111.46, 110.68, 110.49, 108.04, 107.80, 65.04, 46.92, 14.85, 8.16.

2-(cyclopropanesulfonamido)-*N*-(2-ethoxy-5-fluorophenyl)-4-fluorobenzamide (36g): Yield = 21.0 mg (29.2%, white solid). LCMS: R_T = 2.97 min., >95% @ 215 and 254 nm, *m/z* = 397.0 [M + H]$^+$. ^{1}H NMR (500 MHz, CDCl$_3$) δ 10.76 (s, 1H), 8.63 (s, 1H), 8.27 (dd, *J* = 10.3, 2.9 Hz, 1H), 7.66 – 7.61 (m, 1H), 6.93 – 6.89 (m, 1H), 6.87 (dd, *J* = 9.0, 4.9 Hz, 1H), 6.84 – 6.79 (m, 1H), 4.17 (q, *J* = 7.0 Hz, 2H), 2.63 – 2.57 (m, 1H), 1.51 (t, *J* = 7.0 Hz, 3H), 1.34 – 1.30 (m, 2H), 1.05 – 0.99 (m, 2H). ^{13}C NMR (125 MHz, CDCl$_3$) δ 166.23, 165.65, 164.21, 157.81, 155.91, 143.67, 142.49, 128.77, 128.69, 127.68, 127.59, 116.90, 111.47, 111.39, 110.59, 110.41, 110.34, 110.15, 107.98, 107.75, 64.97, 30.76, 14.91, 5.88.

2.6. References:

1.   Volkow, N. D.; McLellan, A. T. Opioid abuse in chronic pain—misconceptions and mitigation strategies. *N. Engl. J. Med.* **2016,** 374, 1253-1263.

2.   Institute of Medicine Committee on Advancing Pain Research, C.; Education. The National Academies Collection: Reports funded by National Institutes of Health. In *Relieving Pain in America: A Blueprint for Transforming Prevention, Care, Education, and Research*, National Academies Press (US) National Academy of Sciences.: Washington (DC), 2011.

3.   Johannes, C. B.; Le, T. K.; Zhou, X.; Johnston, J. A.; Dworkin, R. H. The prevalence of chronic pain in United States adults: results of an Internet-based survey. *J Pain* **2010,** 11, 1230-1239.

4.   *Centers for Disease Control and Prevention. FastStats. Therapeutic drug use* 2014

5.   Akil, H.; Watson, S. J.; Young, E.; Lewis, M. E.; Khachaturian, H.; Walker, J. M. Endogenous opioids: biology and function. *Annu. Rev. Neurosci.* **1984,** 7, 223-255.

6.   Pattinson, K. T.; Governo, R. J.; MacIntosh, B. J.; Russell, E. C.; Corfield, D. R.; Tracey, I.; Wise, R. G. Opioids depress cortical centers responsible for the volitional control of respiration. *J. Neurosci.* **2009,** 29, 8177-8186.

7.   Skolnick, P.; Volkow, N. D. Re-energizing the development of pain therapeutics in light of the opioid epidemic. *Neuron* **2016,** 92, 294-297.

8.   Scholz, J.; Woolf, C. J. Can we conquer pain? *Nat. Neurosci.* **2002,** 5, 1062-1067.

9.   Pope, J. E.; Deer, T. R.; Kramer, J. A systematic review: current and future directions of dorsal root ganglion therapeutics to treat chronic pain. *Pain Med* **2013,** 14, 1477-1496.

10.   He, S. Q.; Li, Z.; Chu, Y. X.; Han, L.; Xu, Q.; Li, M.; Yang, F.; Liu, Q.; Tang, Z.; Wang, Y.; Hin, N.; Tsukamoto, T.; Slusher, B.; Tiwari, V.; Shechter, R.; Wei, F.; Raja, S. N.; Dong, X.; Guan, Y. MrgC agonism at central terminals of primary sensory neurons inhibits neuropathic pain. *Pain* **2014,** 155, 534-44.

11.   Atlanta, G. C., National Center for Health Statistics. Wide-ranging online data for epidemiologic research (WONDER). http://wonder.cdc.gov.

12.   Campos, L. W.; Pope, J. E.; Deer, T. R. Dorsal Root Ganglion Stimulation for the Treatment of Pain in the Rehabilitation Patient. In *Comprehensive Pain Management in the Rehabilitation Patient*, Springer: 2017; pp 671-679.

13.   Caterina, M. J.; Julius, D. Sense and specificity: a molecular identity for nociceptors. *Curr. Opin. Neurobiol.* **1999,** 9, 525-530.

14.   Millan, M. J. The induction of pain: an integrative review. *Prog. Neurobiol.* **1999,** 57, 1-164.

15.   Dong, X.; Han, S.-k.; Zylka, M. J.; Simon, M. I.; Anderson, D. J. A diverse family of GPCRs expressed in specific subsets of nociceptive sensory neurons. *Cell* **2001,** 106, 619-632.

16.   Sikand, P.; Dong, X.; LaMotte, R. H. BAM8-22 peptide produces itch and nociceptive sensations in humans independent of histamine release. *J. Neurosci.* **2011,** 31, 7563-7.

17.   Liu, Q.; Tang, Z.; Surdenikova, L.; Kim, S.; Patel, K. N.; Kim, A.; Ru, F.; Guan, Y.; Weng, H.-J.; Geng, Y. Sensory neuron-specific GPCR Mrgprs are itch receptors mediating chloroquine-induced pruritus. *Cell* **2009,** 139, 1353-1365.

18.   Guan, Y.; Liu, Q.; Tang, Z.; Raja, S. N.; Anderson, D. J.; Dong, X. Mas-related G-protein–coupled receptors inhibit pathological pain in mice. *Proc. Natl. Acad. Sci. U.S.A.* **2010,** 107, 15933-15938.

19.   Li, Z.; Tseng, P.-Y.; Tiwari, V.; Xu, Q.; He, S.-Q.; Wang, Y.; Zheng, Q.; Han, L.; Wu, Z.; Blobaum, A. L. Targeting human Mas-related G protein-coupled receptor X1 to inhibit persistent pain. *Proc. Natl. Acad. Sci. U.S.A.* **2017,** 114, E1996-E2005.

20.   Conn, P. J.; Christopoulos, A.; Lindsley, C. W. Allosteric modulators of GPCRs: a novel approach for the treatment of CNS disorders. *Nat. Rev. Drug Discov.* **2009,** 8, 41-54.

21.   May, L. T.; Leach, K.; Sexton, P. M.; Christopoulos, A. Allosteric modulation of G protein–coupled receptors. *Annu. Rev. Pharmacol. Toxicol.* **2007,** 47, 1-51.

22.   Jiang, J.; Wang, D.; Zhou, X.; Huo, Y.; Chen, T.; Hu, F.; Quirion, R.; Hong, Y. Effect of M as-related gene (Mrg) receptors on hyperalgesia in rats with CFA-induced inflammation via direct and indirect mechanisms. *Br. J. Pharmacol.* **2013,** 170, 1027-1040.

23.   He, S.-Q.; Han, L.; Li, Z.; Xu, Q.; Tiwari, V.; Yang, F.; Guan, X.; Wang, Y.; Raja, S. N.; Dong, X. Temporal changes in MrgC expression after spinal nerve injury. *Neuroscience* **2014,** 261, 43-51.

24.   Han, L.; Ma, C.; Liu, Q.; Weng, H.-J.; Cui, Y.; Tang, Z.; Kim, Y.; Nie, H.; Qu, L.; Patel, K. N. A subpopulation of nociceptors specifically linked to itch. *Nat. Neurosci.* **2013,** 16, 174-182.

25.   Cai, M.; Chen, T.; Quirion, R.; Hong, Y. The involvement of spinal bovine adrenal medulla 22-like peptide, the proenkephalin derivative, in modulation of nociceptive processing. *European J. Neurosci.* **2007,** 26, 1128-1138.

26.   Höllt, V.; Haarmann, I.; Grimm, C.; Herz, A.; Tulunay, F. C.; Loh, H. H. Pro-enkephalin intermediates in bovine brain and adrenal medulla: characterization of immunoreactive peptides related to BAM-22P and peptide F. *Life Sci.* **1982,** 31, 1883-1886.

27.   Information., N. C. f. B. "PubChem Bioassay Record for AID 588675, Source: Johns Hopkins Ion Channel Center" PubChem, . https://pubchem.ncbi.nlm.nih.gov/bioassay/588675

28.   Wen, W.; Wang, Y.; Li, Z.; Tseng, P. Y.; McManus, O. B.; Wu, M.; Li, M.; Lindsley, C. W.; Dong, X.; Hopkins, C. R. Discovery and characterization of 2-(cyclopropanesulfonamido)-N-(2-ethoxyphenyl)benzamide, ML382: a potent and selective positive allosteric modulator of MrgX1. *ChemMedChem* **2015,** 10, 57-61.

29.   Kamohara, M.; Matsuo, A.; Takasaki, J.; Kohda, M.; Matsumoto, M.; Matsumoto, S.-i.; Soga, T.; Hiyama, H.; Kobori, M.; Katou, M. Identification of MrgX2 as a human G-protein-coupled receptor for proadrenomedullin N-terminal peptides. *Biochem. Biophys. Res. Commun.* **2005,** 330, 1146-1152.

30.   Bao, J.; Li, J. J.; Perl, E. R. Differences in Ca2+ channels governing generation of miniature and evoked excitatory synaptic currents in spinal laminae I and II. *Journal of Neuroscience* **1998,** 18, 8740-8750.

31.   Klotz, U. Ziconotide-a novel neuron-specific calcium channel blocker for the intrathecal treatment of severe chronic pain-a short review. *International Journal of Clinical Pharmacology & Therapeutics* **2006,** 44.

32.   Li, Z.; Tseng, P. Y.; Tiwari, V.; Xu, Q.; He, S. Q.; Wang, Y.; Zheng, Q.; Han, L.; Wu, Z.; Blobaum, A. L.; Cui, Y.; Tiwari, V.; Sun, S.; Cheng, Y.; Huang-Lionnet, J. H.; Geng, Y.; Xiao, B.; Peng, J.; Hopkins, C.; Raja, S. N.; Guan, Y.; Dong, X. Targeting human Mas-related G protein-coupled receptor X1 to inhibit persistent pain. *Proc Natl Acad Sci U S A* **2017,** 114, E1996-e2005.

33.   Wroblowski, B.; Wigglesworth, M. J.; Szekeres, P. G.; Smith, G. D.; Rahman, S. S.; Nicholson, N. H.; Muir, A. I.; Hall, A.; Heer, J. P.; Garland, S. L. The discovery of a selective, small molecule agonist for the MAS-related gene X1 receptor. *J. Med. Chem.* **2009,** 52, 818-825.

34.   Malik, L.; Kelly, N. M.; Ma, J.-N.; Currier, E. A.; Burstein, E. S.; Olsson, R. Discovery of non-peptidergic MrgX1 and MrgX2 receptor agonists and exploration of an initial SAR using solid-phase synthesis. *Bioorg. Med. Chem. Lett.* **2009,** 19, 1729-1732.

35.   Rankovic, Z. CNS Physicochemical Property Space Shaped by a Diverse Set of Molecules with Experimentally Determined Exposure in the Mouse Brain: Miniperspective. *J. Med. Chem.* **2017,** 60, 5943-5954.

36.   Hin, N.; Alt, J.; Zimmermann, S. C.; Delahanty, G.; Ferraris, D. V.; Rojas, C.; Li, F.; Liu, Q.; Dong, X.; Slusher, B. S. Peptidomimetics of Arg-Phe-NH2 as small molecule agonists of Mas-related gene C (MrgC) receptors. *Biorg. Med. Chem.* **2014,** 22, 5831-5837.

37.   Prchalová, E.; Hin, N.; Thomas, A. G.; Veeravalli, V.; Ng, J.; Alt, J.; Rais, R.; Rojas, C.; Li, Z.; Hihara, H. Discovery of Benzamidine-and 1-Aminoisoquinoline-Based Human MAS-Related G-Protein-Coupled Receptor X1 (MRGPRX1) Agonists. *J. Med. Chem.* **2019,** 62, 8631-8641.

38. Wen, W.; Wang, Y.; Li, Z.; Tseng, P. Y.; McManus, O. B.; Wu, M.; Li, M.; Lindsley, C. W.; Dong, X.; Hopkins, C. R. Discovery and Characterization of 2-(Cyclopropanesulfonamido)-N-(2-ethoxyphenyl) benzamide, ML382: a Potent and Selective Positive Allosteric Modulator of MrgX1. *ChemMedChem* **2015,** 10, 57-61.

39. Zeng, L.; Fu, H.; Qiao, R.; Jiang, Y.; Zhao, Y. Efficient Copper-Catalyzed Synthesis of N-Alkylanthranilic Acids via an ortho-Substituent Effect of the Carboxyl Group of 2-Halobenzoic Acids at Room Temperature. *Adv. Synth. Catal.* **2009,** 351, 1671-1676.

40. Ma, D.; Geng, Q.; Zhang, H.; Jiang, Y. Assembly of Substituted Phenothiazines by a Sequentially Controlled CuI/l-Proline-Catalyzed Cascade C☐S and C☐N Bond Formation. *Angew. Chem. Int. Ed.* **2010,** 49, 1291-1294.

41. Sharma, S., Qi Peng, Anish Vadukoot, Christopher Aretz, Aaron Jensen, Alexander Wallick, Xinzhong Dong, and Corey Hopkins. Further Synthesis and Biological Characterization of a Series of 2-Sulfonamidebenzamides as Allosteric Modulators of MrgX1. In Cambridge: Cambridge Open Engage: ChemRxiv, 2021.

42. Xie, H.; Lan, J.; Gui, J.; Chen, F.; Jiang, H.; Zeng, W. Ru (II)-Catalyzed Coupling-Cyclization of Sulfoximines with alpha-Carbonyl Sulfoxonium Ylides as an Approach to 1, 2-Benzothiazines. *Adv. Synth. Catal.* **2018,** 360, 3534-3543.

43. Wu, C.; Huang, R.; Zhang, M.; Chen, Z. Copper-Catalyzed Synthesis of Thiadiazine-1-oxides in Reusable Aqueous Medium under External [Ag]/Ligand/Base-Free Conditions. *J. Org. Chem.* **2019,** 85, 841-850.

44. Kumari, S.; Carmona, A. V.; Tiwari, A. K.; Trippier, P. C. Amide bond bioisosteres: Strategies, synthesis, and successes. *J. Med. Chem.* **2020,** 63, 12290-12358.

45. Moulin, A.; Bibian, M.; Blayo, A.-L.; El Habnouni, S.; Martinez, J.; Fehrentz, J.-A. Synthesis of 3, 4, 5-Trisubstituted-1, 2, 4-triazoles. *Chem. Rev.* **2010,** 110, 1809-1827.

Chapter 3. TRPC5 Inhibitors

3.1. Introduction

TRP channel family

Transient receptor potential (TRP) channels act as molecular sensors of extracellular and intracellular environmental changes and maintain homeostasis.[1] Throughout the animal kingdom TRPs are found engaged in various roles across multiple locations. Mammalian TRP channels are classified into six subfamilies, TRPC (canonical), TRPV (vanilloid), TRPM (melastatin), TRPA (ankyrin), TRPP (polycystin), and TRPML (mucoliptin), based on their sequence similarities.[2] Human TRPC channels are most closely homologous to the *Drosophila* TRP, the first channel identified and responsible for phototransduction.[3] Mammalian TRPC are Ca^{2+} permeable nonselective cation channels activated by downstream stimulation of phospholipase C (PLC) pathways via G protein-coupled receptors (GPCRs).[4] Mammalian TRPC channels are a collection of seven different proteins subdivided into four subgroups: TRPC1, TRPC2, TRPC3,6,7, and TRPC4,5 based on sequence similarity. TRPC4 and 5 share a similarly close homology as well as functional similarities. Primary activation of TRPC4,5 is achieved due to internal and external Ca^{+2} levels.

TRPC5 and Disease.

The TRPC1,4,5 channels have potential involvement in treating central nervous system diseases (anxiety, depression, epilepsy, memory, addiction) and pain.[5] TRPC4 and 5 are expressed in the brain regions associated with anxiety and fear, and knockout mice (TRPC4$^{-/-}$ and TRPC5$^{-/-}$) show decreased fear behavior compared to wild-type mice.[6-8] TRPC5 channels are implicated in epilepsy as they are expressed in rat hippocampal CA1

neurons.[9] Studies using the TRPC4,5 antagonist, ML204, **1** has also shown positive results (similar to knockout animal) in models of neuropathic pain.[10, 11] The role of TRPC5 in chronic kidney disease (CKD) and focal segmental glomerulosclerosis (FSGS) has gained significant attention over the last few years, as it could lead to a drug for treating kidney related disorders, which has been challenging..

Chronic kidney disease (CKD) and Focal Segmenal Glomerulosclerosis (FSGS)

Progressive chronic kidney disease (CKD) is a global health concern, affecting over 26 million people in the US alone.[12] CKD ultimately leads to cardiovascular disease (CVD). Focal segmental glomerulosclerosis (FSGS) is associated with the nephrotic syndrome characterized by symptomatic proteinuria (excretion of > 3.5 g protein per day through urine) in adults, scarring of the glomerulus, and loss of terminally differentiated podocytes. Currently, there are only a few treatment options for FSGS, and they primarily deal with the symptoms. Many patients are treated chronically with steroids, which have undesirable side effects. Podocytes are the functional unit of kidneys and can be divided into a cell body, major processes, and foot processes. The foot processes of adjacent podocytes form a unique form of cell junction called the slit diaphragm that covers the outer aspect of the glomerulus. Podocyte dysfunction and cytoskeletal disorganization leads to a disruption of these foot processes. This disruption of the slit diaphragm causes proteinuria, the spilling of essential proteins into the urine as shown in **Figure 3.1**.[13, 14]

TRPC5 translocation to podocyte membranes induces loss through cytoskeletal changes and thereby compromises the filtration barrier in CKD.

Kidney   Nephron   Glomerulus

Podocyte injury

1 Damage to podocytes activates RAC1, leading to translocation of sequestered TRPC5 to the cell surface.

2 This enhances AT1R-induced Ca^{2+} entry, further stimulating RAC1 activity.

3 RAC1 activation induces actin remodeling and detachment from the glomerulus.

4 Loss of podocytes disrupts the filtration barrier, allowing serum proteins to spill into the urinary space.

Healthy glomeruli
TRPC5 is sequestered in the cytoplasm and the filtration barrier is maintained.

TRPC5

Vesicle

Glomerular basement membrane

TRPC5

RAC1

AT1R

Ca^{2+}

RAC1

Cytoskeletal changes

Foot processes of neighboring podocytes

Endothelial cell

Figure 3.1. Mechanism of TRPC5 mediated podocyte injury and proteinuria

(image taken from Chung et al. Science 2017, 358, 1256-1257).[14]

Role of TRPC5 in CKD

TRPC5 channels are activated by G-protein coupled receptors (GPCRs), such as the angiotensin II type 1 receptor (AT1R), and TRPC5 activation has been shown to induce podocyte apoptosis. Some forms of FSGS are caused by mutations in genes involved in actin cytoskeleton regulation. These mutations generally result in excess Ras-related C3 botulinum toxin substrate 1 (Rac1) signaling in podocytes, causing vesicular insertion of TRPC5 into the podocyte plasma membrane. Thus, more TRPC5 channels are available for activation by receptors, such as the AT1R. This increases Ca^{2+} influx into the podocyte, causing further Rac1 activation, thus completing a self-sustaining circuit that promotes podocyte cytoskeletal remodeling. Rac1 promotes cytoskeletal remodeling and podocyte death through the elevation of reactive oxygen species. Therefore, inhibiting the overactivity of TRPC5 in an injured kidney can be of therapeutic value.[15]

3.2. TRPC5 inhibitors

ML204

In an effort to find potent and selective modulators of TRPC4, a high-throughput screen (HTS) of 305,000 compounds of the Molecular Libraries Small Molecule Repository (MLSMR) was carried out. The hits from the HTS were remade, and their SAR was explored to obtain one of the first selective molecular probes for the TRPC channel, ML204, **1**, as shown in **Figure 3.2**. Compound **1** was moderately potent with an $IC_{50} = 0.96$ µM against TRPC4β channels. **1** also inhibited TRPC5, activated through co-stimulation of $G_{i/o}$ and $G_{q/11}$ signaling by µ-opioid and M_3-like muscarinic receptors due to very close similarity between TRPC4 and C5. ML204 reversed podocyte loss and proteinuria in a rat model of FSGS, which specifically expresses human AT1R in podocytes.[16] Due to poor specificity, ML204 could not be further used as a tool compound. Due to high homology between TRPC4 and 5 channels, it's important to identify TRPC5 selective inhibitors.
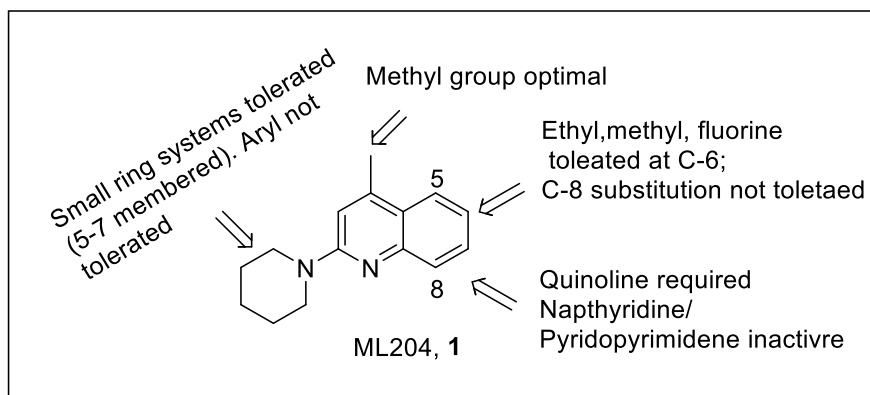
Figure 3.2. Structure of ML204, 1 and the SAR observations
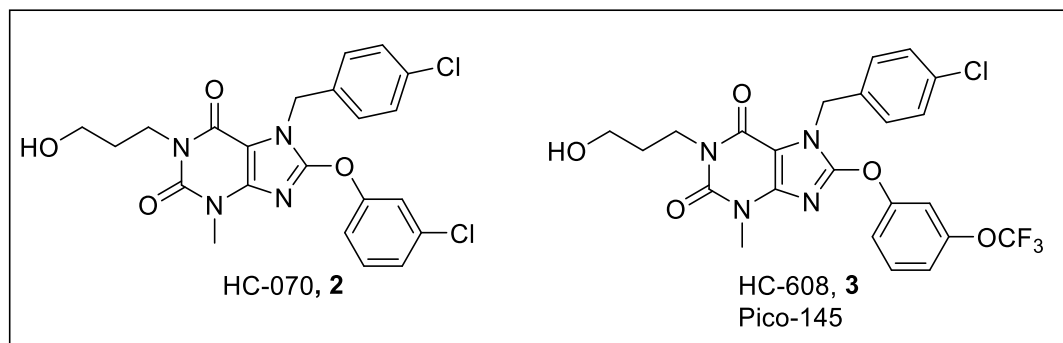
Figure 3.3. Structure of Hydra Biosciences xanthene based TRPC5 inhibitors

Hydra Biosciences

Hydra Biosciences performed a high-throughput screen of ~65,000 compounds, and subsequent modifications of the lead molecule led to the identification of a variety of low nanomolar and, in some cases, picomolar inhibitors of TRPC4 and 5 homo- and heterotetramers. Based on the results, >600 xanthine analogs were synthesized and characterized for their inhibitory activity on TRPC4,5.[17] HC-070, **2**, and HC-608, **3**, were among the best compounds out of the study as shown in **Figure 3.3**. **3** has also been reported as Pico-145 due to its picomolar range activity in some assays. **3** has an IC_{50} of 1.3 nM against tetracycline inducible exogenous human TRPC5, IC_{50} of 0.34 nM against TRPC4, 0.19 nM against TRPC5-1 and 0.033 nM against TRPC4-1.[18] **2** inhibited recombinantly-expressed human TRPC5 (hTRPC5) with an IC_{50} = 9.3 nM and TRPC4 with an IC_{50} = 46.0 nM. In whole-cell manual patch clamp, **2** inhibited lanthanum-activated hTRPC5-mediated currents with an IC_{50} = 0.52 nM. Increased potency in electrophysiological compared to fluorometric assays has often been observed and reported for other TRP channels.[19]

Clemizole

Clemizole, **4** was identified as a TRPC5 inhibitor from a medium-throughout screen of the Spectrum collection and LOPAC1280 compound libraries at the University of Leipzig as shown in **Table 3.1**. **4** is a direct channel inhibitor with IC$_{50}$ of 1.1 μM and does not modulate the GPCR activation cascade. **4** is slightly selective for TRPC5 compared to TRPC4 (6-fold selective) and nearly 10-fold selective against TRPC3,6,7. Originally it was developed as a histamine H$_1$ receptor antagonist. It also inhibits monoamine reuptake inhibitor and hERG channels at a concentration of 10 μM. Such off-target activity limit its use as the IC$_{50}$ for activity on TRPC5 varies widely based upon the assay condition, and it can be right- or left-shifted in the case of native channels.[20]
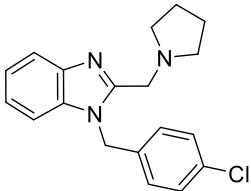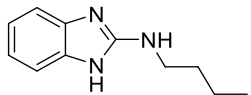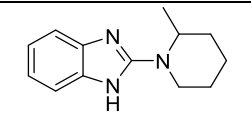
2-Aminobenzimidazole

In addition to **1** from the HTS of the MLSMR library, another lead M084, **5**, was identified as TRPC4,5 inhibitor, as shown in **Table 3.1**. Although **5** was less potent than **1**, it had better PK properties and provided an alternate structural class. Overall IC$_{50}$ values against TRPC4 and TRPC5 were 8.2 μM and 10.3 μM, respectively, as determined by the FMP assay using Ala^2-MePhe^4-Glyol^5-Enkephalin (DAMGO) to stimulate G$_{i/o}$ via the co-expressed μ-receptor. Interestingly, **5** displayed a weak inhibitory effect on TRPC3, with an IC$_{50}$ of ~50 μM. SAR studies around **5** revealed position 2 of the benzimidazole backbone to be an absolute requirement for activity. This could be either a primary or secondary amine in the form of a ring structure either as a piperidine or a pyrrolidine. Any other changes at the 2-position such as an aromatic group, extra amine, alcohol or ether were not tolerated. Out of the SAR studies, **6** came out to be the most potent compound

(IC$_{50}$ = 4.3 µM) and had excellent selectivity towards TRPC6 and C3, as shown in **Table 3.1.**[21]

Table 3.1. Clemizole and aminobenzimidazole selectivity profile

No.	Structure	TRPC4β	TRPC5	TRPC6	TRPC3
		IC$_{50}$ (µM)			
4	CLEMIZOLE	6.4	1.1	11.3	9.1
5	M084	10.3	8.2	59.6	48.6
6		4.3	3.5	>100	>100

Goldfinch Bio

A screening of a structurally diverse library of ~400,000 compounds against TRPC5, using a Fluorescent Imaging Plate Reader (FLIPR) assay, resulted in the identification of pyridazinone **7,** as shown in **Figure 3.4** with an IC_{50} of 5.0 µM against TRPC5. From the SAR study around the lower aromatic ring, central core and the brominated pyridazinone, GFB-8438, **8**, with piperazinone core was identified to be a potent TRPC5 inhibitor IC_{50} = 0.18 µM.[22] Apart from this published paper, the organization has developed many pyridazinones bearing highly potent TRPC5 inhibitors. The series had multiple compounds with reported potency of <50 nM. Though exact details of the activity is not provided.[23] One of the inhibitors, GFB-887, is in clinical trials, but its structure is not disclosed yet; it could be something similar to **9** and **10**.[24] GFB-887 is undergoing a phase 2a, double-blind, placebo-controlled, multiple−ascending dose study of GFB-887 in patients with focal segmental glomerulosclerosis (FSGS), treatment-resistant minimal change disease (TR-MCD), or diabetic nephropathy (DN). Adult patients on stable renin−angiotensin system blockade and/or immunosuppression with persistent proteinuria are being dosed in 3 ascending dose levels to GFB-887 or placebo for 12 weeks.[25, 26]
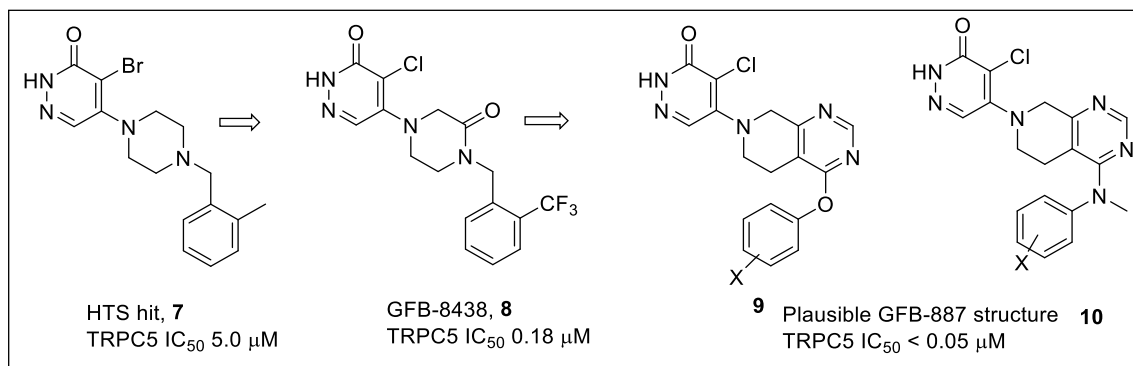
Figure 3.4. Pyridazinone containing TRPC5 inhibitors from Goldfinch Bio

3.3. Design of new benzimidazole based TRPC5 inhibitors

Very few TRPC5 inhibitors have been reported till date, most of which published within the last decade. These include ML204, **1** in 2011, Hydra Biosciences compounds (**2,3**) in 2015 and Goldfinch biosciences compounds (**7-10**) since 2019. ML204 was the first TRPC5 inhibitor be developed by in the lab Dr. Hopkins and collaborators. Although ML204 showed *in vivo* effectiveness in slowing down the progression of podocyte failure, its nonselective inhibition hampered its utility. From a high-throughput screen performed at the Johns Hopkins Ion Channel Center (JHICC) utilizing the >300,000 NIH Molecular Library Small Molecule Repository (MLSMR) compound collection, several benzimidazole containing compounds were identified as TRPC4,5 inhibitors. These molecules afforded an excellent starting point for a medicinal chemistry effort as they were low MW (<300), offered multiple points of diversification, and satisfied many parameters for tool compound development (e.g., cLogP <3). AC1903, **13a** ($IC_{50} = 4.06$ µM) was one of the best HIT compounds and was used as a template to optimize and develop more potent and selective inhibitor. First, we tried to replace the furan moiety on the right-hand side with various other 5- and 6-membered heterocycles as in compounds **13a-13s**, **Table 3.2.** This study allowed us to assess a suitable replacement for the PK labile fragment like furan from the structure, and find an equal or more potent replacement. After that, we tried to optimize the lower benzylic group with various substituted benzyl and cyclohexyl groups, e.g., compounds **15a-15I**, as shown in **Table 3.3**. Next, we replaced the core benzimidazole with azabenzimidazole **16a-b** and C-5,6 substituted benzimidazoles **16c-d.**

Synthesis of benzimidazole based inhibitors

To synthesize the desired benzimidazole compounds, we designed a two-way modular approach as shown in **Scheme 3.1**. The initial library centered around keeping the southern benzyl group constant while modifying the right-hand furan moiety and these were made by reacting the 2-chlorobenzimidazole (or substituted benzimidazole), **11**, with benzyl bromide under basic

conditions (sodium hydride, NaH). Next, the resulting compounds, **12**, were reacted with the appropriate amine (neat) under microwave heating to yield the desired compounds **13a-s**, **22a-j**, and **24a-f**. To scan the benzylic substitution, 2-chlorobenzimidazole, **11**, was first reacted under microwave with the appropriate amine to give **14**, which was benzylated under basic condition (K$_2$CO$_3$) using microwave irradiation.[27]

To make azabenzimidazole core as in **16a-b** or C-5,6 substituted benzimidazoles **25d-q**, not available commercially, we built the ring using appropriately substituted starting material. Substituted 2-nitro aniline, **17**, is benzylated under basic conditions, followed by nitro reduction to give diamine compound, **19**, which is further cyclized using *N,N'*-carbonyldiimidazole (CDI) to give substituted imidazo[4,5-*b*]pyridine-2-one, **20**. **20** is converted to the appropriate 2-chloro compound **21** utilizing POCl$_3$, which then undergoes nucleophilic substitution with various amines under microwave irradiation to give final compounds.[28] Utilizing appropriate handles on C-5/6 position further derivatization and substitution of the core ring was achieved. Such as making new C-C and C-N bonds using C-5/6 -bromo derivative and making various ethers using C-5/6 -hydroxy derivatives. C-5/6 hydroxy-containing core was obtained through *O*-demethylation of C-5/6 methoxy derivatives as shown in **Scheme 3.1.C.**. The experimental section shows the synthesis of other core rings such as indazole, **25r** and quinazoline, **25s**.[29]

The furfuryl amine substituent, AC1903 **13a**, was used as the standard control, and the % inhibition at 3 µM was normalized to 100%. We utilized the first triage of % inhibition of the TRPC5 channel using the Syncropatch instrument to have a higher throughput capacity for SAR, which was then followed up with IC$_{50}$ determinations of active compounds.

A.

Reagents and conditions: (a) DMF, NaH, 6h; (b) R_1R_1NH, MW; (c) K_2CO_3, ACN, MW, 1h

B.

Reagents and conditions: (a)Cs_2CO_3, Dioxane, 100°C, 2 h; (b) H_2/Pd, RT, 3 h; (c) CDI, THF, RT, 12 h; d) $POCl_3$, PCl_5, 90°C, 6 h; (d) MW. 200°C, 30 min

C.

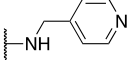Reagents and conditions: (a) BBr_3, DCM, -10-0 °C, (b)Cs_2CO_3, DMF, 60°C, 6 h;
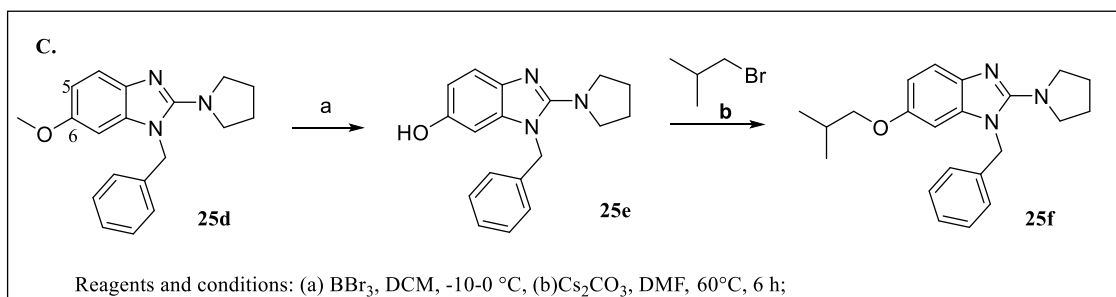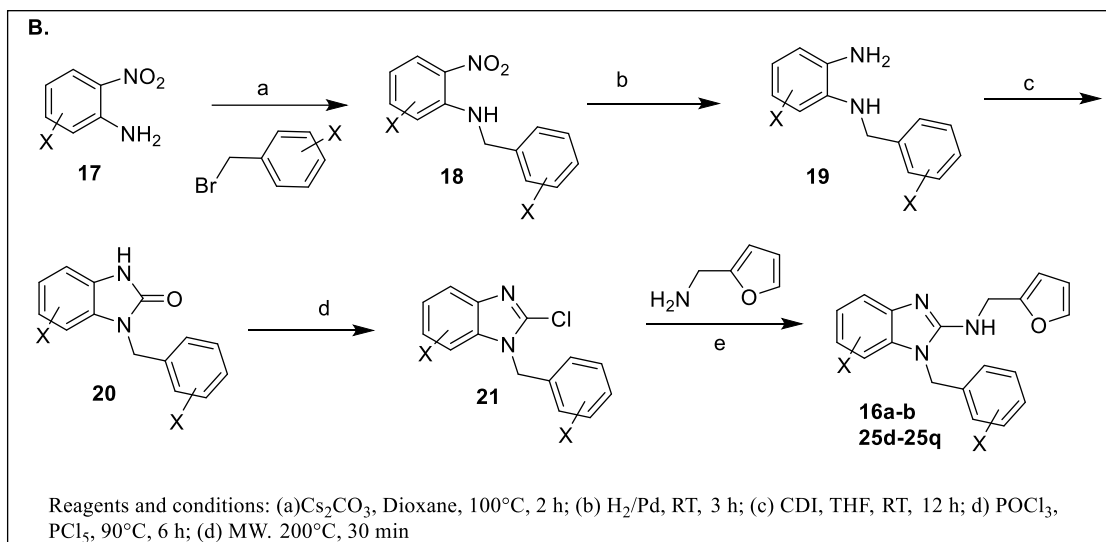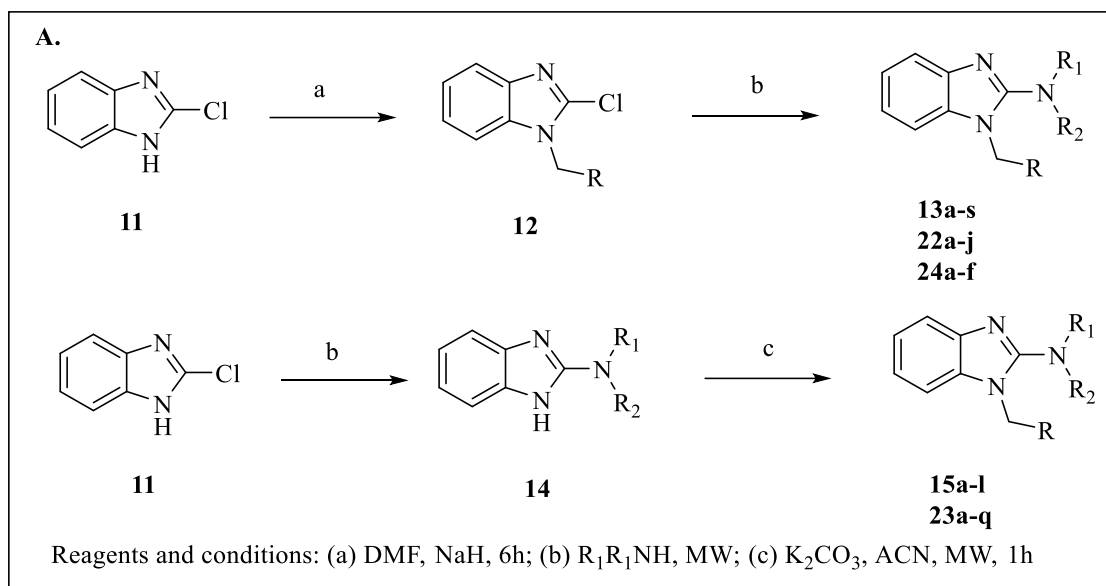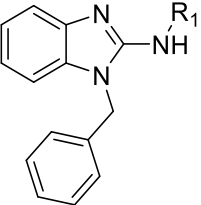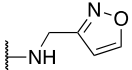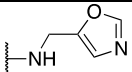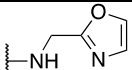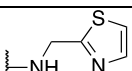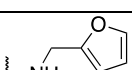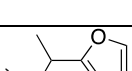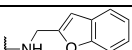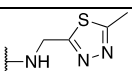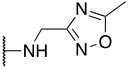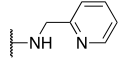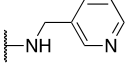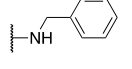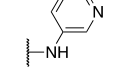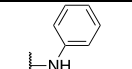
Scheme 3.1. Synthesis of benzimidazole based TRPC5 inhibitors

3.4. Results

Knowing the furan moiety is prone to oxidation, we set out to investigate furan replacements. Moving from the furan to the 2-thiophene led to a compound that was active (**13b**, 150% inhibition), but the IC_{50} was not improved**.** The incorporation of various 5-membered heterocycles such as isoxazole **13c**, oxazole **13d-e,** or thiazole, **13f** did not result in active compounds. 3-methyl-2-furyl derivative (**13g**, IC_{50} = 6.93 µM) and the methine branched furan (**13h**, IC_{50} = 4.44 µM) were the only two active modifications. Inserting a carbonyl group **13j** or methylating other heterocycles **13l-m** did not yield active compounds. Replacing the furan with a 2-pyridyl compound or its isomer **13n-p** was not an effective change. Replacing the 2-thiophene **13b** with a phenyl bioisostere led to a reduction in activity (**13q,** 33% inhibition). Direct attachment of pyridine or phenyl **13r-s** was also not tolerated, as shown in **Table 3.2**.

Table 3.2. SAR studies around AC1903 furan replacements
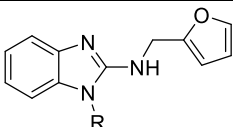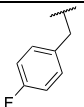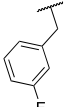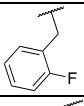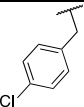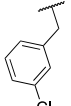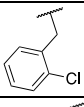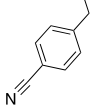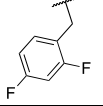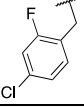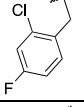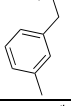
Cmpd	R1	Syncropatch (@ 3 μM)[a]	TRPC5 IC$_{50}$ (μM)
13a		1.00	4.06 ± 0.91
13b		1.498	6.26 ± 1.59
13c		0.4697	ND
13d		0.3325	ND
13e		0.1908	ND
13f		0.4249	ND
13g		0.8230	6.93 ± 1.53
13h		0.9136	4.44 ± 1.12
13i		0.4170	ND
13j		0.3853	ND
13k		0.1798	ND
13l		0.2996	ND
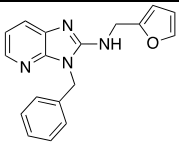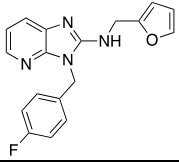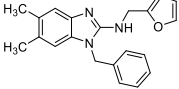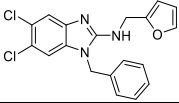
13m		0.1978	ND
13n		-0.0181	ND
13o		0.1199	ND
13p		0.1739	ND
13q		0.3281	ND
13r		0.1993	ND
13s		0.1894	ND

[a]Inhibition values were recorded in cells (n > 10) using the Syncropatch (Nanion). Experiments were recorded (minimum) on one session over two different assay plates. AC1903 and DMSO were added as control compounds on every assay plate. ND-Not determined

Next, we evaluated the southern benzimidazole benzyl substituents by keeping the furan-2-yl-methylamine group constant as shown in **Table 3.3**. We started by examining the effect of halogen substitution on the benzyl ring. For fluoro substitution, 4-fluoro, **15a**, came out to be the best position compared to 3- and 2-fluoro positions, **15b** and **15c,** respectively. **15a** showed 167% inhibition with an IC_{50} of 1.82 µM. A similar trend was observed with chloro but the best active substitution, 4-chloro **15d,** showed only 71% inhibition. 4-cyano, **15g**, had approximately 50% inhibitory activity. 2,4-difluoro, **15h**, showed 86% inhibition but a 2-fold drop in $IC_{50} = 8.42$ µM, 4-chloro-2-fluoro **15i** had 127% activity but did not translate equally well to $IC_{50} = 18.1$ µM.

Surprisingly 2-chloro 4-fluoro, **15j**, lost all activity. 3-methyl, **15k**, was almost equipotent to the original phenyl with an $IC_{50} = 4.80$ µM. The incorporation of non-aromatic groups such as cyclohexyl methyl, **15l**, led to a significant loss in activity. Changing the core scaffold from the benzimidazole to the azabenzimidazole, **16a** and **16b**, led to compounds with reduced activity (20-30% inhibition). The addition of substituents on the phenyl ring of the benzimidazole (5- and 6-positions) showed an interesting trend. 5,6-dimethylbenzimidazole (**16c**, 123% inhibition, $IC_{50} = 12.3$ µM) was significantly more potent than the 5,6-dichlorobenzimidazole (**16d**, 28% inhibition) suggesting an electronic effect of the substituent groups. Wherein electron-donating group (EDG) might be a more favorable substitution compared to electron withdrawing group (EWG).

Table 3.3. SAR studies around AC1903 benzyl replacement

Cmpd	R	Syncropatch (@ 3 μM)	TRPC5 IC$_{50}$ (μM)
13a		1.00	4.06 ± 0.91
15a		1.668	1.82 ± 0.32
15b		0.6189	ND
15c		0.5438	ND
15d		0.7092	ND
15e		0.7018	ND
15f		0.0261	ND
15g		0.5051	ND
15h		0.8696	8.42 ± 3.07
15i		1.278	18.1 ± 9.7
15j		0.2358	ND
15k		0.9456	4.80 ± 1.14
15l		0.6156	ND

16a		0.3115	ND
16b		0.2174	ND
16c		1.226	12.3 ± 7.0
16d		0.2821	ND

[a]Inhibition values were recorded in cells (n > 10) using the Syncropatch (Nanion). Experiments were recorded (minimum) on one session over two different assay plates. AC1903 and DMSO were added as control compounds on every assay plate. ND-Not determined

Looking at the SAR studies around AC1903, **13a,** it appears that the benzimidazole core scaffold, which is conserved across many known inhibitors **4**, **5**, and **6** is favored for activity. However, **13a** is more selective for TRPC5 (IC$_{50}$ = 4.1 μM) compared to the other known benzimidazoles. Modifications of the 2-benzimidazole right-hand side portion revealed tolerance for some 5-membered heteroaryl methyl groups, with furan being the most potent heterocycles. Amide replacements were not active, and *N*-methylation was less active. The left-hand phenyl portion of the benzimidazole was also resistant to change, with the azabenzimidazole losing all activity. The southern part of the molecule provided more SAR information wherein selective 4-position fluoro substitution yields highly active compound and also established the importance of benzyl group for maintaining the activity, as shown in **Figure 3.5**.

In vivo pharmacokinetic study (IP dosing, 25 mg/kg, 0–24 h) showed AC1903, **13a** having similar PK properties as of ML204 with C$_{max}$ of 687 (ng/mL) and T$_{max}$ was at 0.11 hour. **13a** also showed very good selectivity against TRPC4 and TRPC6, which was a significant leap given the high sequence homology between TRPC4 and TRPC5, and previous difficulty in finding compounds that preferentially inhibited TRPC5.[30, 31]

Single channel recordings in acutely isolated rat glomeruli showed that **13a** was effective in blocking TRPC5 channel activity in the glomeruli of proteinuric rats. Chronic administration of **13a** suppressed severe proteinuria and prevented podocyte loss, and thus also helped toestablish the pharmacology of TRPC5 inhibition as an effective podocyte-preserving therapeutic strategy. The efficacy of **13a** was also demonstrated in another animal model of kidney disease: Dahl salt-sensitive (Dahl S) rats. Dahl S rats exhibit progressive kidney injury as they age, with moderate hypertension when raised on a low-salt diet. On a high-salt diet, these rats develop progressive proteinuria and decline in kidney function with significant angiotensin II-mediated hypertension. Inhibiting TRPC5 with **13a** at the time of severe, established proteinuria, but before creatinine is elevated (indicating irreversible kidney damage) rescued podocytes and attenuated the progression of morphologic and molecular changes that characterize FSGS.[30]
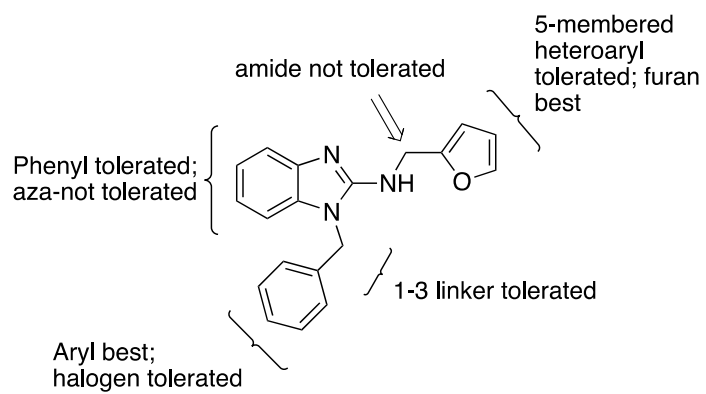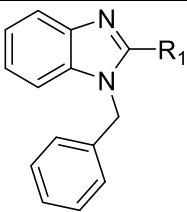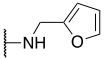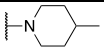
Figure 3.5. SAR studies around selective TRPC5 inhibitor AC1903, 13a

New class of benzimidazole compounds

The furan bearing benzimidazole compound AC1903, **13a** played a significant role in establishing the role of TRPC5 inhibition to prevent and reverse podocyte injury in FSGS. However, much improvement needs to be made toward its potency and pharmacokinetic liabilities owi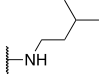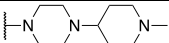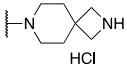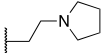ng to the presence of the furan ring. In this study to identify new class of inhibitors, we focused our attention on additional hits from the HTS and some previous inhibitors such as the **5** and **6**. These compounds included a 2-position *N*-linked alkyl or a saturated *N*-heterocycle containing benzimidazole but lacked the southern benzyl moiety found in the **13a** class of molecules. We started our exploration on an *N*-1-benzyl containing benzimidazole and tried various 2-position substitutions.
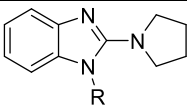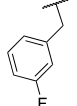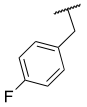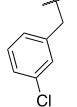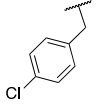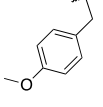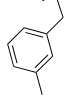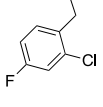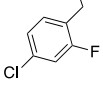
4-methyl piperidine **22a** and piperidine **22b** were only moderately active (~50%) compared to **13a**. Pyrrolidine **22c** was almost equipotent to **13a** with an $IC_{50} = 4.30\,\mu M$. Since pyrrolidine can also be susceptible to oxidative metabolism, we tried to incorporate 2-methyl substitution on the pyrrolidine which were almost 100% active with no significant difference between the (*S*)-**22d** or *(R)*-**22e** stereoisomers. *N*-propyl, **22f**, and *N*-isopentyl, **22g**, containing compounds came out to be potent with an IC_{50} of 0.72 µM and 1.3 µM, respectively. Any attempt to elongate the right hand side with the help of even bulkier heterocycles such as *N*-4-(1-methylpiperidin-4-yl)piperazine, **22h**, and diazaspiro[3.5]nonane, **22i**, were not productive. However, adding an extra carbon to the clemizole, **4,** to further elongate the molecule in **22j** resulted in almost 91% active molecule, as shown in **Table 3.4**.

Table 3.4. SAR studies around benzimidazole C-2 substitution

Compd	R1	Syncropatch (@ 3 μM)[a]	TRPC5 IC$_{50}$ (μM)
13a		1.00	4.06 ± 0.91
22a		0.4912	ND
22b		0.6491	ND
22c		1.146	4.30 ± 1.63
22d		0.9295	ND
22e		1.0177	ND
22f		1.199	0.720 ± 0.213
22g		0.9434	1.298 ± 0.306
22h		-0.1468	ND
22i		0.0298	ND
22j		0.9162	ND

[a]Inhibition values were recorded in cells (n > 10) using the Syncropatch (Nanion). Experiments were recorded (minimum) on one session over two different assay plates. AC1903 and DMSO were added as control compounds on every assay plate. ND-Not determined

Moving forward, we tried to explore the southern benzylic substitution on the active pyrrolidine moiety, **22c**. Similar to studies with **13a**, we started with identifying ideal fluoro substitution similar to **15a**, compound **23c** bearing the 4-fluoro was the most active compound (IC_{50} = 0.59 µM) compared to the 2- and 3-fluoro, **23a** and **23b**. However, the opposite trend was observed in previous series, 4-chloro substitution in **23e** (IC_{50} = 0.44 µM) was more active than fluorinated **22c.** It seems that 2-pyrrolidine containing benzimidazole could tolerate a diverse set of benzylic substitutions. 4-methoxy, **23f** (IC_{50} = 1.15 µM) and 4-methyl, **23g** (IC_{50} = 0.9 µM) also had very good inhibitory activity. In the dihalo series 4-chloro-2-fluoro compound, **23j** (IC_{50} = 0.84 µM) was more active but had lost 2-fold potency compared to just 4-chloro, **23e**. The pyridyl series of compounds showed an interesting trend with activity increasing while moving from position 4 to 2, **23k < 23l < 23m**. Incorporation of the active 4-chloro position into the pyridyl study as in the case of **23n**, led to a moderately active 298ompound with an IC50 = 3.11 µM. Any attempt to mask the benzylic methylene with a carbonyl or sulfone, **23o** and **23p**, yielded inactive compounds. An attempt to diversify from benzyl to alkyl sulfonamide such as **23q** resulted in a complete loss of activity, as shown in **Table 3.5.**

Table 3.5. SAR studies around benzimidazole *N*-1 substitution

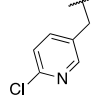| Cmpd	R	Syncropatch (@ 3μM)	TRPC5 IC$_{50}$ (μM)
23a		1.948	2.69
23b		2.263	1.49 ± 0.31
23c		2.544	0.59 ± 0.14
23d		2.168	0.72 ± 0.21
23e		2.770	0.44 ± 0.14
23f		2.133	1.15 ± 0.25
23g		1.367	0.902 ± 0.340
23h		1.640	1.90
23i		0.8675	ND
23j		2.421	0.84 ± 0.23

23k		-0.0518	ND
23l		0.4124	ND
23m		0.9744	ND
23n		1.268	3.11 ± 0.94
23o		0.1876	ND
23p		-0.4296	ND
23q		0.0221	ND

[a]Inhibition values were recorded in cells (n > 10) using the Syncropatch (Nanion). Experiments were recorded (minimum) on one session over two different assay plates. AC1903 and DMSO were added as control compounds on every assay plate. ND-Not determined

Moving forward, we tried to merge the active *N*-1 substitution 4-chloro benzyl with some active and diverse C-2 substitution. 2- or 4-methyl piperidine, **24a** and **24b**, were only moderately active. In the case of 2-methyl pyrrolidine, the *R* stereoisomer **24d** (IC_{50} = 2.89 µM) was more active compared to *S*, **24C**. The most significant improvement was observed while merging the most active compounds from **Table 3.4** and **3.5**. The *N*-propyl containing moiety, **24e**, came out to be the most active compound in the series with an IC_{50} = 0.068 µM or 68 nM. **24e** is the first nanomolar potent compound in the benzimidazole core containing series of molecules. 1,1-dioxothiomorpholine, **24f** resulted in an inactive compound as shown in **Table 3.5.**

Next, we tried to diversify the benzimidazole core itself by incorporating various substituents on the C-5 and C-6 positions of the phenyl ring in the benzimidazole compound. Similar, as in the case of **13a**, 5,6-dimethylbenzimidazole (**25b**, 123% inhibition, IC_{50} = 12.3 µM) was significantly more potent than the 5,6-dichlorobenzimidazole (**25a**, 28% inhibition), but the theory of EDG being better over EWG was proved wrong as can be seen with multiple examples of C-5 and C-5 substituents of both EDG and EWG class having very good activity, **25c-25n**. Overall it is hard to say if the C-5 or C-6 position is better for diversification and molecular elongation, but the trend lies on the side of C-5 being a better position for diversification. Various halogens are well tolerated, with C-5 chloro, **25m** being the better one. C-5 or C-6 methoxy showed a bit more activity compared to the free hydroxy, **25d** vs. **25e** and **25h** vs. **25i.** Free hydroxy provided a excellent handle to make ethers of varied length, but as it seems in the case of **25f** vs. **25g**, elongation of more than 3-carbon length results in a reduction of activity. Overall, 5-methyl came out to be the best in this class with an IC_{50} = 0.24 µM. Next, we tried to incorporate the chloro pyridazinone moiety from the Goldfinch Bio compounds to see if it would be tolerated. We attached it to C-5 via a C-C bond as in **25o** and C-O bond, **25p; 25p** was more active compared to **25o**, but the activity did not yield a good IC_{50} value. Since this new class of pyrrolidines were able to tolerate a diverse set of modifications compared to the previous AC1903 series, we tried to change the

benzimidazole core with an azabenzimidazole, **25q**; indazole, **25r** and quinazoline, **25s** but none of them were active, as shown in **Table 3.7.**

Table 3.6. SAR studies towards combined C-2 and *N*-1 substitution
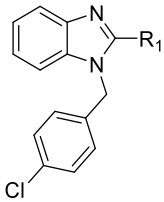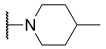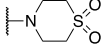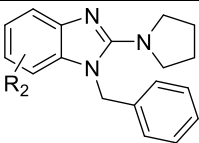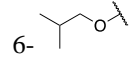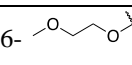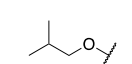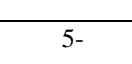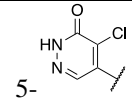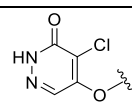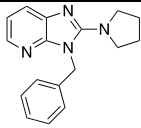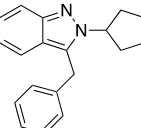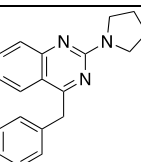
Cmpd	R1	Syncropatch (@ 3 µM)	TRPC5 IC$_{50}$ (µM)
24a		0.1185	ND
24b		0.4607	ND
24c		1.004	ND
24d		1.191	2.89 ± 0.70
24e		1.265	0.068 ± 0.106
24f		0.1554	ND

[a]Inhibition values were recorded in cells (n > 10) using the Syncropatch (Nanion). Experiments were recorded (minimum) on one session over two different assay plates. AC1903 and DMSO were added as control compounds on every assay plate. ND-Not determined

Table 3.7. SAR studies towards C-5/6 susbtitution

Cmpd	R2	Syncropatch (@ 3 µM)	TRPC5 IC$_{50}$ (µM)
25a	5,6-diCl	0.1905	ND
25b	5,6-diMe	1.008/1.075	ND
25c	6-F	0.7637	ND
25d	6-OMe	1.202	ND
25e	6-OH	1.198	ND
25f		1.111	ND
25g		0.7795	ND
25h	5-OMe	1.251	1.15 ± 0.33
25i	5-OH	1.191	ND
25j		0.5668	ND
25k		0.6808	ND
25l	5-Br	0.6381	ND
25m	5-Cl	1.083	ND
25n	5-Me	2.149	0.243 ± 0.160
25o		0.7867	ND
25p		1.152	7.55 ± 2.52

25q		0.0074	ND
25r		0.1078	ND
25s		-0.9366	ND
Inhibition values were recorded in cells (n > 10) using the Syncropatch (Nanion). Experiments were recorded (minimum) on one session over two different assay plates. AC1903 and DMSO were added as control compounds on every assay plate. ND-Not determined			

3.5. Summary and Conclusion

The development of therapeutics aimed at treating chronic kidney diseases is of prime importance. TRPC channels present a promising gateway for pharmacological intervention to stop and reverse kidney damage. There have been controversies regarding whether TRPC5 or TRPC6 is associated with FSGS and CKD and which channel to target.[32] However, a majority of the growing evidence is making the role of TRPC5 clear and concise. One of the essential steps in clearing the confusion and assigning the mechanism is the availability of highly potent and selective molecular probes. ML204 and AC1903 played that role in establishing some of the fundamental pharmacology and role of the TRPC5 channel, as did GFB887.[33]

The involvement of TRPC5 in the process of FSGS is mainly attributed to certain mutations, which increase the RAC1 activity. Due to various research groups evaluating their inhibitors on different TRPC5 mutants, use of varied TRPC5 activators, and difference in technique (automation vs. manual patch clamp), there is a high discrepancy in the data obtained. Unless all the molecules are tested *in vivo* on a similar platform, it is difficult discern which compounds are "better". Our group has been involved with developing TRPC5 inhibitors from the very beginning. The initial HTS to identify ML204 and its subsequent use to see actual improvement in the disease state was of very prime importance in the journey towards establishing TRPC5 as a prime target to treat CKD. The discovery of a selective inhibitor, AC1903 **13a**, was even a bigger step, and it helped establish the pharmacology and underlying mechanisms of TRPC5 overactivation leading to podocyte injury. From there, we developed our current best active compound, **24e**, which had potency in the nanomolar range, **Figure 3.5**. In the final study, we identified multiple inhibitors with low micromolar potency, which are better than AC1903. The present study remains incomprehensive moving forward, as we still need to merge some of the potency imparting trends. We merged the best benzylic moiety with the best C-2 substitution to get the most active compound. However, still, we are missing incorporating the C-5, C-6 substitutions imparting high potency such as the 5-Me substitution. The most active compounds are currently being tested for their selectivity

against other TRPC channels. Primary pharmacokinetic studies suggest that the molecules, even though might show *in vivo* efficacy, are highly susceptible to metabolism. Moving forward, we need to address this issue also along with the identification of even potent targets.

One facet that shall help realize the development of TRPC5 targeting therapeutics is the recent advances in Cryo-EM and computational techniques for structural determination. Recent studies using Cryo-EM highlights structures of the human TRPC5 channel alone (resolution: 3.0 Å) or complexed with the two structurally diverse inhibitors clemizole,**4** (resolution: 2.7 Å) and HC-070, **2** (resolution: 2.7 Å).[34] Moreover, a binding pocket for the lipid second messenger diacylglycerol (DAG) was identified structurally for the first time. The clemizole binding pocket is located within the so alled S1-S4 segment close to the loop of the voltage sensing-like domain (VSLD). AC1903 and GFB-8438, **8** also interact at this same pocket. Being present in the VSLD, this pocket cannot be accessed directly from outside, and molecules need to penetrate inside the cell to get access to this pocket.[34]

In contrast, the HC-070, **2** binding pocket is formed by two adjacent TRPC5 channel subunits near the pore forming loop. This binding site appears to be accessible extracellularly. DAG contact site partially overlaps this pocket. Interaction of **2** with the channel displaces the polar head group of DAG. That could be a possible reason for the picomolar activity of **2**. It can directly interact with the binding pockets without passing through the cellular membranes. Displacement of DAG molecules out of their place, could be a secondary mechanism of action working in its favor. Availability of such high-quality structure and data points will help in the design and development of better TRPC5 inhibitors.[34-36]
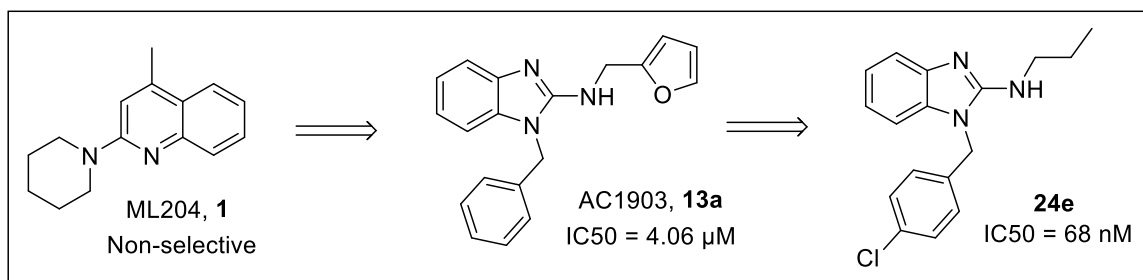
Figure 3.5. Progress made towards TRPC5 inhibitors

3.6. Synthesis Protocols and Experimental

In vitro Pharmacology

In vitro inhibition assays were performed in the lab of Dr. Anna Greka at Broad Institute of MIT and Harvard, Cambridge. TRPC5 was stably expressed by cloning mouse TRPC5 into the pCDNA5/FRT/TO plasmid then co-transfecting with the pOG44 plasmid into Flp-In T-REx -293 cells (Invitrogen) followed by 200 ug/mL HygromycinB selection. Cells were maintained in Advanced DMEM/F12 (Invitrogen #10565-042) supplemented with 10% FBS along with 15 µg/mL Blasticidin S (Life #A11139-03) and 200 µg/mL Hygromycin B (Life #10687-010). For Syncropatch experiments 0.5-1 µg/mL Doxycycline (1 mg/mL stock doxycycline hyclate, Sigma #D9891-10G) was added 3 days prior to Syncropatch recordings. On the day of Syncropatch recordings, the cells were lifted using 4 minute incubations at 37 o C with accutase (Sigma #A6964-100ML). Syncropatch pharmacology The potency of the compounds was measured by inhibition of riluzole-induced TRPC5 currents as measured on the automated patch clamp platform Syncropatch 384PE (Nanion). Extracellular solution was composed of: 140 mM NaCl, 5 mM KCl, 10 mM HEPES, 2 mM $MgCl_2$, 2 mM $CaCl_2$ and 10 mM glucose. Intracellular solution was composed of: 20 mM CsCl, 90 mM $CsSO_4$, 5 mM EGTA, 2 mM $CaCl_2$, 10 mM HEPES, 10 mM glucose, 4 mM Na_2-ATP and 0.5 mM Na-GTP. A ramp protocol of 200 ms from -100mV to +100 mV was pulsed at 5-10s intervals to measure TRPC5 currents. Baseline currents were recorded followed by addition of riluzole to a final concentration of 30 µM to activate currents. Only cells that developed the characteristic doublyrectifying current of TRPC5 homomers were taken for subsequent analysis. The compound being tested was then added while maintaining 30 µM of riluzole in solution. Cells were discarded if there was noticeable runup or rundown in the current generated from the last 3 voltage ramps before compound addition. Percent inhibition was calculated as the average of the 3 ramps after compound addition (once the current had stabilized)

divided by the average of the 3 ramps before compound addition. IC50's were calculated by using the three parameters nonlinear regression (curve fit) function of Prism 7 (GraphPad).

Synthesis Procedure and Experimental data

Instrumentation, chemical procuring, processing remains same as shown in Chapter 1. Compounds **13b,i,n,o,p** and **15b,c,d,f,g,h,l** were synthesized by Dr. Hopkins. Compounds **22a-e**, **23a-j,o,p,q** and **24a-d,f** were synthesize by roation students Kirsten T. Tolentino, Wacey Gallegos, Kathy Hecker, Jennifer Hinman, Mackenzie Asche and Madie Beninato.

General Procedure A:

Reagents and conditions: (a) DMF, NaH, 6h; (b) R_1R_1NH, MW
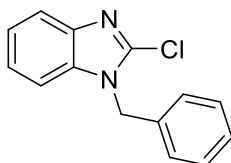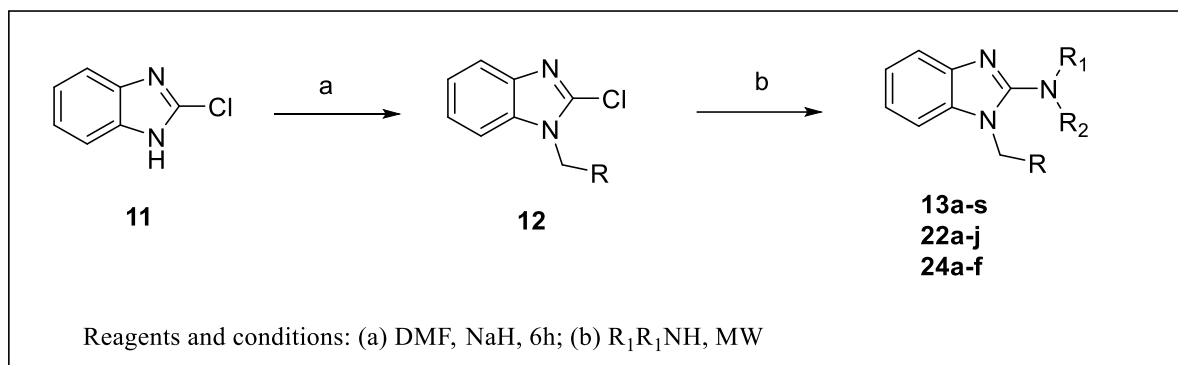
Step-a: 1-benzyl-2-chloro-1*H*-benzo[*d*]imidazole (12a). In a round bottom flask fitted with magnetic stirrer, 2-chloro-1*H*-benzimidazole (0.50 g, 3.2 mmol) was dissolved in DMSO (3 mL), and then NaH (60%; 0.19 g, 4.9 mmol) was added at 0 °C and stirred for 1h. Benzyl bromide (670 mg, 3.9 mmol) was added to the suspension and the reaction was stirred at rt for 12 h. Ice cold water (15 mL) was added to the mixture the product precipitates, collected via filtration. Filtrate was washed with water and dried under vacuum to give desired product as white solid. Yield = 0.75 g, (88%, white solid). LCMS: R_T = 2.69 min., >98% @ 215 and 254 nm, *m/z* = 243.0 [M +

H]⁺. ¹H NMR (500 MHz, CDCl₃) δ 7.68 (d, *J* = 7.4 Hz, 1H), 7.35 – 7.24 (m, 5H), 7.16 (d, *J* = 6.8

Hz, 2H), 5.38 (s, 2H). ¹³C NMR (125 MHz, CDCl₃) δ 141.33, 134.83, 128.99, 128.22, 126.76,

123.53, 123.05, 119.18, 109.98, 47.94.
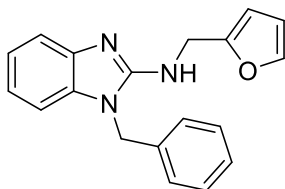
Step-b: 1-Benzyl-*N*-(furan-2-ylmethyl)-1*H*-benzo[*d*]imidazol-2-amine   (13a). A   10   mL

microwave vial with stir bar was charged with 1-benzyl-2-chloro-1*H*-benzo[*d*]imidazole (50 mg,

0.2 mmol) and furfuryl amine (0.20 g, 2.0 mmol). The mixture was subjected to microwave

irradiation at 200 °C for 30 min. The mixture was diluted with ethyl acetate (50 mL) and washed

with water (25 mL) and brine (25 mL). The organic layer was dried over sodium sulphate,

evaporated, and purified by reverse phase chromatography (0-100% water/ CH₃CN). Fractions

collected were evaporated to yield desired product. Yield = 30 mg (48%, white solid). LCMS: R_T =

2.07 min., >98% @ 215 and 254 nm, *m/z* = 304.1 [M + H]⁺. ¹H NMR (500 MHz, CDCl₃) δ 7.58

(d, *J* = 7.8 Hz, 1H), 7.34 (m, 4H), 7.17 (t, *J* = 9.2 Hz, 3H), 7.13 – 7.05 (m, 2H), 6.31 (s, 1H), 6.23

(s, 1H), 5.13 (s, 2H), 4.71 (d, *J* = 5.4 Hz, 2H), 4.34 (s, 1H). ¹³C NMR (125 MHz, CDCl₃) δ 153.76,

151.70, 142.14, 135.29, 134.88, 129.19, 128.14, 126.43, 121.56, 120.03, 116.85, 110.40, 107.46,

107.41, 45.72, 40.51.

All intermediates of series **12** prepared as shown in General Procedure A, Step-a.
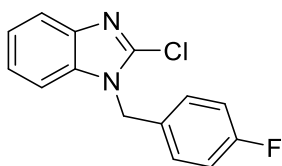
2-chloro-1-(4-fluorobenzyl)-1*H*-benzo[*d*]imidazole (12a'). Yield = 0.80 g (83%). LCMS: R_T =

2.58 min., >98% @ 215 and 254 nm, *m/z* = 261.1.0 [M + H]⁺. ¹H NMR (500 MHz, CDCl₃) δ 7.73

(d, *J* = 6.9 Hz, 1H), 7.31 – 7.22 (m, 3H), 7.18 (dd, *J* = 8.0, 5.3 Hz, 2H), 7.02 (dd, *J* = 11.8, 5.2 Hz,

2H), 5.36 (s, 2H). ^{13}C NMR (125 MHz, CDCl$_3$) δ 163.46, 161.49, 140.62, 134.95, 130.79, 128.67, 128.60, 123.49, 123.00, 119.61, 116.10, 115.92, 109.74.
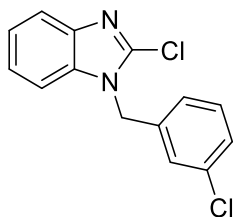
2-chloro-1-(3-chlorobenzyl)-1*H*-benzo[*d*]imidazole (12f). Yield = 0.76 g (84%). LCMS: R$_T$ = 2.72 min., >98% @ 215 and 254 nm, *m/z* = 277.0 [M + H]$^+$. ^{1}H NMR (500 MHz, CDCl$_3$) δ 7.72 (d, *J* = 7.2 Hz, 1H), 7.27 (dt, *J* = 9.4, 7.9 Hz, 4H), 7.22 (d, *J* = 7.6 Hz, 1H), 7.18 (s, 1H), 7.04 (t, *J* = 11.8 Hz, 1H), 5.34 (s, 2H). ^{13}C NMR (125 MHz, CDCl$_3$) δ 141.57, 140.64, 136.93, 134.96, 134.89, 130.36, 128.51, 126.92, 124.88, 123.67, 123.16, 119.51, 109.72, 47.28.

2-chloro-1-(4-chloro-2-fluorobenzyl)-1*H*-benzo[*d*]imidazole (12i). Yield = 0.81 g (83%) LCMS: R$_T$ = 2.78 min., >98% @ 215 and 254 nm, *m/z* = 294.9 [M + H]$^+$. ^{1}H NMR (500 MHz, CDCl$_3$) δ 7.74 – 7.65 (m, 1H), 7.31 – 7.24 (m, 3H), 7.15 (dd, *J* = 9.8, 1.3 Hz, 1H), 7.05 (d, *J* = 8.2 Hz, 1H), 6.89 (t, *J* = 8.1 Hz, 1H), 5.40 (s, 2H). ^{13}C NMR (125 MHz, CDCl$_3$) δ 160.94, 158.94, 141.43, 140.63, 135.26, 135.18, 134.75, 129.45, 129.41, 125.16, 125.13, 123.73, 123.25, 120.85, 120.74, 119.46, 116.73, 116.53, 109.63, 41.28, 41.24.
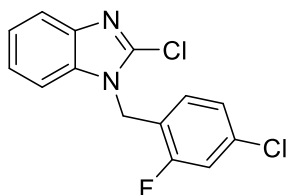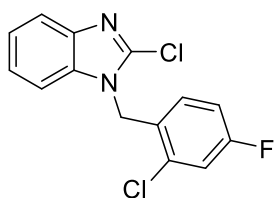

2-chloro-1-(2-chloro-4-fluorobenzyl)-1*H*-benzo[*d*]imidazole (12j). Yield = 0.78 g (80%) LCMS: R$_T$ = 2.78 min., >98% @ 215 and 254 nm, *m/z* = 295.0 [M + H]$^+$. ^{1}H NMR (500 MHz,

CDCl$_3$) δ 7.73 (d, J = 7.9 Hz, 1H), 7.28 (dt, J = 15.1, 7.3 Hz, 2H), 7.23 – 7.19 (m, 1H), 7.16 (d, J = 7.9 Hz, 1H), 6.87 (dd, J = 11.5, 4.9 Hz, 1H), 6.87 (dd, J = 11.5, 4.9 Hz, 1H), 6.67 – 6.57 (m, 1H). ^{13}C NMR (125 MHz, CDCl$_3$) δ 163.05, 161.06, 141.53, 140.90, 134.84, 133.12, 133.03, 128.51, 128.44, 128.40, 128.37, 123.76, 123.30, 119.54, 117.46, 117.27, 114.82, 114.65, 109.72, 44.91.
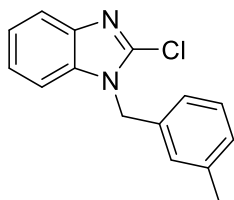
2-chloro-1-(3-methylbenzyl)-1H-benzo[d]imidazole (12k). Yield = 0.75 g (89%) LCMS: R$_T$ = 2.69 min., >98% @ 215 and 254 nm, m/z = 257.0 [M + H]$^+$. ^{1}H NMR (500 MHz, CDCl$_3$) δ 7.74 (d, J = 7.4 Hz, 1H), 7.33 – 7.21 (m, 4H), 7.12 (d, J = 7.4 Hz, 1H), 6.99 (d, J = 12.5 Hz, 2H), 5.36 (s, 2H), 2.35 (d, J = 29.5 Hz, 4H). ^{13}C NMR (125 MHz, CDCl$_3$) δ 141.79, 140.84, 138.84, 135.18, 134.96, 128.97, 128.88, 127.41, 123.87, 123.35, 122.84, 119.48, 109.94, 47.92, 21.41.
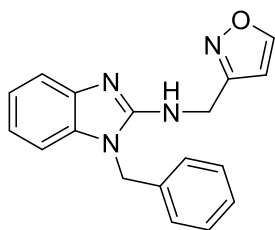
1-benzyl-N-(isoxazol-3-ylmethyl)-1H-benzo[d]imidazol-2-amine (13c). Yield = 25 mg (40%, yellow oil) LCMS: R$_T$ = 1.91 min., >98% @ 215 and 254 nm, m/z = 305.1 [M + H]$^+$. ^{1}H NMR (500 MHz, CDCl$_3$) δ 8.34 (s, 1H), 7.57 (d, J = 7.9 Hz, 2H), 7.37 – 7.30 (m, 4H), 7.24 – 7.16 (m, 4H), 7.14 – 7.07 (m, 3H), 6.39 (d, J = 1.0 Hz, 2H), 5.17 (s, 3H), 4.84 (s, 3H). ^{13}C NMR (125 MHz, CDCl$_3$) δ 160.13, 158.90, 152.95, 139.56, 134.72, 134.09, 129.26, 128.36, 126.56, 122.25, 120.95, 116.05, 108.02, 103.83, 45.97, 39.27.
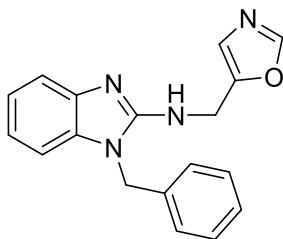
1-benzyl-*N*-(oxazol-5-ylmethyl)-1*H*-benzo[*d*]imidazol-2-amine (13d). Yield = 10 mg (27%, light yellow solid) LCMS: R_T = 1.88 min., >98% @ 215 and 254 nm, *m/z* = 305.0 [M + H]$^+$. ^{1}H NMR (500 MHz, CDCl$_3$) δ 7.79 (d, *J* = 19.2 Hz, 1H), 7.58 (d, *J* = 7.9 Hz, 1H), 7.40 – 7.31 (m, 3H), 7.19 (dt, *J* = 12.8, 3.5 Hz, 1H), 7.17 – 7.07 (m, 4H), 6.95 (s, 1H), 5.17 (d, *J* = 21.0 Hz, 2H), 4.78 (s, 2H). ^{13}C NMR (125 MHz, CDCl$_3$) δ 153.22, 150.79, 149.14, 141.48, 135.06, 134.75, 129.29, 128.33, 126.40, 124.08, 121.84, 120.44, 116.88, 107.60, 45.79, 38.09.
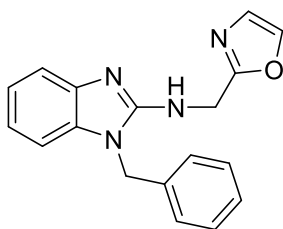
1-benzyl-*N*-(oxazol-2-ylmethyl)-1*H*-benzo[*d*]imidazol-2-amine (13e). Yield = 25 mg (40%) LCMS: R_T = 1.86 min., >98% @ 215 and 254 nm, *m/z* = 305.1 [M + H]$^+$. ^{1}H NMR (500 MHz, CDCl$_3$) δ 7.63 (s, 1H), 7.56 (d, *J* = 7.9 Hz, 1H), 7.36 – 7.30 (m, 3H), 7.18 (dd, *J* = 14.6, 7.2 Hz, 3H), 7.10 (t, *J* = 7.5 Hz, 1H), 7.06 (t, *J* = 7.4 Hz, 1H), 7.01 (s, 1H), 5.14 (s, 2H), 4.87 (s, 2H). ^{13}C NMR (125 MHz, CDCl$_3$) δ 161.43, 152.92, 139.69, 139.34, 134.87, 134.06, 129.12, 128.16, 126.78, 126.55, 122.18, 120.88, 116.11, 108.11, 45.78, 40.56
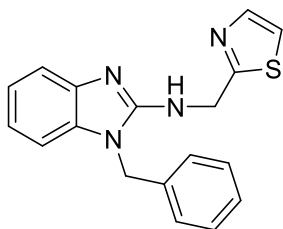
1-benzyl-*N*-(thiazol-2-ylmethyl)-1*H*-benzo[*d*]imidazol-2-amine (13f). Yield = 15 mg (22%, brown solid) LCMS: R_T = 1.90 min., >98% @ 215 and 254 nm, *m/z* = 321.1 [M + H]$^+$. ^{1}H NMR (500 MHz, CDCl$_3$) δ 7.66 (d, *J* = 3.0 Hz, 1H), 7.56 (d, *J* = 7.9 Hz, 1H), 7.34 – 7.27 (m, 4H), 7.24 (d, *J* = 3.1 Hz, 1H), 7.17 (d, *J* = 6.5 Hz, 3H), 7.12 – 7.08 (m, 2H), 5.17 (s, 2H), 5.03 (s, 2H). ^{13}C NMR (125 MHz, CDCl$_3$) δ 167.98, 153.40, 142.16, 141.68, 135.22, 134.86, 129.14, 128.12, 126.54, 121.70, 120.25, 119.40, 116.74, 107.70, 45.80, 44.71.
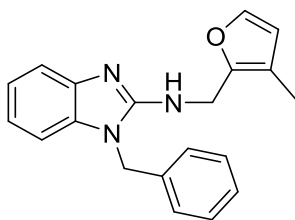
1-benzyl-*N*-((3-methylfuran-2-yl)methyl)-1*H*-benzo[*d*]imidazol-2-amine (13g). Yield = 20 mg (30%, light yellow oil) LCMS: R_T = 2.08 min., >98% @ 215 and 254 nm, *m/z* = 318.1 [M + H]$^+$. ^{1}H NMR (500 MHz, CDCl$_3$) δ 7.58 (d, *J* = 7.9 Hz, 1H), 7.35 – 7.30 (m, 3H), 7.25 (d, *J* = 1.2 Hz, 1H), 7.20 (t, *J* = 7.3 Hz, 1H), 7.14 (d, *J* = 6.5 Hz, 2H), 7.10 (d, *J* = 7.7 Hz, 1H), 7.05 (d, *J* = 7.8 Hz, 1H), 6.19 (d, *J* = 1.0 Hz, 1H), 5.09 (s, 2H), 4.67 (s, 2H), 2.12 – 1.92 (m, 3H). ^{13}C NMR (125 MHz, CDCl$_3$) δ 152.96, 146.00, 141.45, 139.16, 134.79, 133.75, 129.17, 128.22, 126.54, 122.21, 120.86, 117.58, 115.82, 113.16, 108.01, 45.87, 38.81, 9.67.
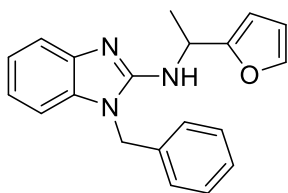
1-benzyl-*N*-(1-(furan-2-yl)ethyl)-1*H*-benzo[*d*]imidazol-2-amine (13h). Yield = 40 mg (65%, brown oil) LCMS: R_T = 2.07 min., >98% @ 215 and 254 nm, *m/z* = 318.1 [M + H]$^+$. ^{1}H NMR (500 MHz, CDCl$_3$) δ 7.57 (d, *J* = 7.9 Hz, 1H), 7.34 (q, *J* = 5.9 Hz, 3H), 7.19 (dd, *J* = 10.8, 4.0 Hz, 1H), 7.15 (d, *J* = 6.6 Hz, 2H), 7.09 (q, *J* = 7.8 Hz, 2H), 6.27 (d, *J* = 1.1 Hz, 1H), 6.15 (d, *J* = 2.8 Hz, 1H), 5.34 (q, *J* = 6.4 Hz, 1H), 5.13 (dd, *J* = 36.5, 17.0 Hz, 3H), 1.57 (d, *J* = 6.6 Hz, 3H). ^{13}C NMR

(125 MHz, CDCl₃) δ 155.35, 152.63, 141.88, 139.71, 134.86, 133.87, 129.23, 128.27, 126.47, 122.14, 120.64, 115.96, 110.18, 107.84, 105.70, 47.27, 45.91, 20.11.
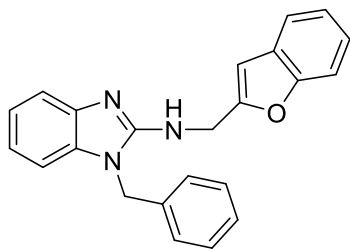
N-(benzofuran-2-ylmethyl)-1-benzyl-1*H*-benzo[*d*]imidazol-2-amine (13k). Yield = 50 mg (72%, yellow oil) LCMS: R_T = 2.17 min., >98% @ 215 and 254 nm, *m/z* = 354.1 [M + H]⁺. ¹H NMR (500 MHz, CDCl₃) δ 7.57 (d, *J* = 7.9 Hz, 2H), 7.49 (d, *J* = 7.4 Hz, 2H), 7.38 (d, *J* = 8.1 Hz, 2H), 7.28 (t, *J* = 5.1 Hz, 6H), 7.26 – 7.22 (m, 2H), 7.20 (dt, *J* = 6.8, 4.9 Hz, 3H), 7.13 (dd, *J* = 9.1, 5.7 Hz, 5H), 7.03 (d, *J* = 7.9 Hz, 2H), 6.65 (d, *J* = 8.7 Hz, 2H), 5.09 (s, 2H), 4.88 (s, 2H). ¹³C NMR (125 MHz, CDCl₃) δ 166.24, 154.91, 153.42, 152.39, 134.46, 133.31, 129.22, 128.35, 128.11, 126.59, 124.23, 122.82, 122.54, 121.30, 121.08, 115.49, 111.09, 108.23, 104.76, 45.92, 40.83.
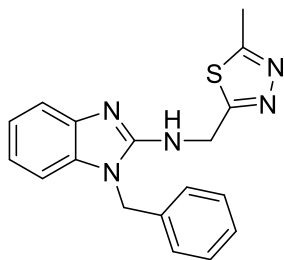
1-benzyl-*N*-((5-methyl-1,3,4-thiadiazol-2-yl)methyl)-1*H*-benzo[*d*]imidazol-2-amine (13l). Yield = 20 mg (28%, light yellow oil) LCMS: R_T = 1.85 min., >98% @ 215 and 254 nm, *m/z* = 336.1 [M + H]⁺. ¹H NMR (500 MHz, CDCl₃) δ 7.58 (d, *J* = 7.9 Hz, 1H), 7.35 – 7.30 (m, 3H), 7.23 – 7.18 (m, 1H), 7.17 – 7.09 (m, 4H), 5.45 (d, *J* = 12.5 Hz, 1H), 5.19 (s, 2H), 5.06 (s, 2H), 2.68 (d, *J* = 37.1 Hz, 3H). ¹³C NMR (125 MHz, CDCl₃) δ 167.40, 166.60, 152.76, 140.38, 134.84, 134.51, 129.19, 128.27, 126.51, 122.08, 120.79, 116.40, 108.00, 77.28, 77.02, 76.77, 45.91, 41.94, 15.51.
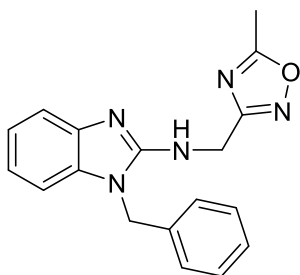
1-benzyl-*N*-((5-methyl-1,2,4-oxadiazol-3-yl)methyl)-1*H*-benzo[*d*]imidazol-2-amine (13m).

Yield = 25 mg (38%, brown oil) LCMS: R_T = 1.88 min., >98% @ 215 and 254 nm, *m/z* = 320.1 [M + H]⁺. ¹H NMR (500 MHz, CDCl₃) δ 7.51 (t, *J* = 10.1 Hz, 1H), 7.37 – 7.29 (m, 3H), 7.24 – 7.16 (m, 3H), 7.12 (t, *J* = 7.6 Hz, 1H), 7.10 – 7.02 (m, 1H), 5.20 (s, 2H), 4.88 (s, 2H), 2.72 – 2.16 (m, 4H). ¹³C NMR (125 MHz, CDCl₃) δ 177.22, 167.47, 152.33, 137.39, 134.46, 133.26, 129.15, 128.30, 126.72, 122.64, 121.54, 115.39, 108.49, 46.10, 39.33, 12.26.
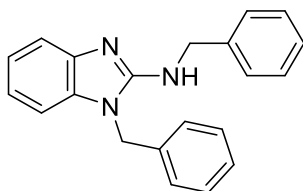
***N*,1-dibenzyl-1*H*-benzo[*d*]imidazol-2-amine (13q).** Yield = 40 mg (62%, yellow oil) LCMS: R_T = 2.104 min., >98% @ 215 and 254 nm, *m/z* = 314.1 [M + H]⁺. ¹H NMR (500 MHz, CDCl₃) δ 7.57 (d, *J* = 7.9 Hz, 1H), 7.35 – 7.23 (m, 8H), 7.17 (dd, *J* = 15.3, 7.0 Hz, 3H), 7.13 – 7.07 (m, 2H), 5.13 (s, 2H), 4.69 (s, 2H), 4.42 (s, 1H). ¹³C NMR (125 MHz, CDCl₃) δ 154.15, 142.10, 138.53, 135.37, 134.89, 129.21, 128.65, 128.16, 127.62, 127.52, 126.51, 121.58, 119.99, 116.70, 107.40, 77.33, 77.08, 76.82, 47.42, 45.73.
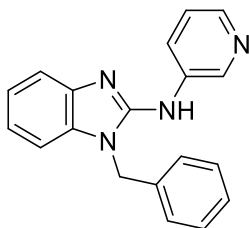
1-benzyl-*N*-(pyridin-3-yl)-1H-benzo[*d*]imidazol-2-amine (13r). Yield = 34 mg (27%, white solid) LCMS: R_T = 1.92 min., >98% @ 215 and 254 nm, *m/z* = 301.1 [M + H]⁺. ¹H NMR (500

MHz, CDCl₃) δ 8.36 (d, *J* = 2.2 Hz, 1H), 8.25 (d, *J* = 16.7 Hz, 1H), 8.21 (d, *J* = 4.4 Hz, 1H), 7.61 (s, 1H), 7.46 – 7.35 (m, 3H), 7.27 – 7.14 (m, 6H), 6.51 (s, 1H), 5.30 (s, 2H). ¹³C NMR (125 MHz, CDCl₃) δ 149.30, 143.28, 135.03, 133.94, 129.44, 128.51, 126.59, 123.84, 122.07, 121.27, 108.01, 46.19.
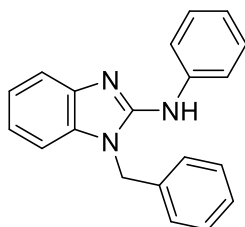
1-benzyl-*N*-phenyl-1*H*-benzo[*d*]imidazol-2-amine (13s). Yield = 35 mg (57%, white solid) LCMS: R_T = 2.04 min., >98% @ 215 and 254 nm, *m/z* = 300.1 [M + H]⁺. ¹H NMR (500 MHz, CDCl₃) δ 7.66 (d, *J* = 7.4 Hz, 1H), 7.45 (d, *J* = 7.9 Hz, 2H), 7.41 – 7.35 (m, 3H), 7.32 (t, *J* = 7.7 Hz, 2H), 7.25 – 7.15 (m, 5H), 7.02 (t, *J* = 7.3 Hz, 1H), 6.17 (s, 1H), 5.25 (s, 2H). ¹³C NMR (125 MHz, CDCl₃) δ 149.93, 135.21, 134.10, 129.37, 129.22, 128.41, 126.62, 122.47, 121.88, 120.90, 118.37, 107.85, 77.29, 77.04, 76.79, 46.24.
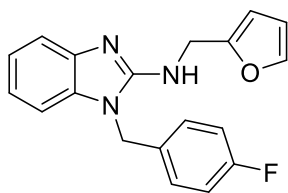
1-(4-fluorobenzyl)-*N*-(furan-2-ylmethyl)-1*H*-benzo[*d*]imidazol-2-amine (15a). Yield = 22 mg (36%, brown solid) LCMS: R_T = 2.04 min., >98% @ 215 and 254 nm, *m/z* = 322.0 [M + H]⁺. ¹H NMR (500 MHz, CDCl₃) δ 7.56 (d, *J* = 7.8 Hz, 1H), 7.33 (s, 1H), 7.21 – 7.14 (m, 1H), 7.13 – 7.06 (m, 4H), 7.01 (t, *J* = 8.5 Hz, 2H), 6.31 (d, *J* = 1.6 Hz, 1H), 6.24 (d, *J* = 2.6 Hz, 1H), 5.08 (s, 2H), 4.70 (d, *J* = 4.8 Hz, 2H), 4.45 (s, 1H). ¹³C NMR (125 MHz, CDCl₃) δ 163.40, 161.43, 153.63, 151.63, 142.16, 134.68, 131.05, 131.03, 128.18, 128.11, 121.68, 120.09, 116.89, 116.20, 116.03, 110.43, 107.52, 107.41, 45.05, 40.49.
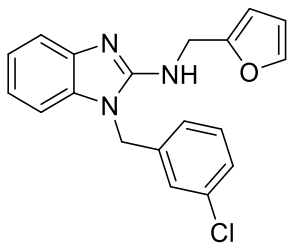
1-(3-chlorobenzyl)-*N*-(furan-2-ylmethyl)-1*H*-benzo[*d*]imidazol-2-amine (15e). Yield = 25 mg (41%, light brown oil) LCMS: R_T = 2.11 min., >98% @ 215 and 254 nm, *m/z* = 338.1 [M + H]$^+$. ^{1}H NMR (500 MHz, CDCl$_3$) δ 7.58 (d, *J* = 7.9 Hz, 1H), 7.35 (d, *J* = 0.9 Hz, 1H), 7.28 (dd, *J* = 12.3, 8.5 Hz, 2H), 7.19 (dd, *J* = 11.7, 4.7 Hz, 2H), 7.12 – 7.04 (m, 2H), 7.00 (d, *J* = 7.3 Hz, 1H), 6.32 (dd, *J* = 3.0, 1.8 Hz, 1H), 6.27 (d, *J* = 2.7 Hz, 1H), 5.09 (s, 2H), 4.72 (s, 2H), 4.42 (s, 1H). ^{13}C NMR (125 MHz, CDCl$_3$) δ 153.54, 151.51, 142.23, 142.03, 137.40, 135.19, 134.60, 130.48, 128.41, 126.57, 124.48, 121.82, 120.23, 116.93, 110.44, 107.58, 107.41, 45.20, 40.53.
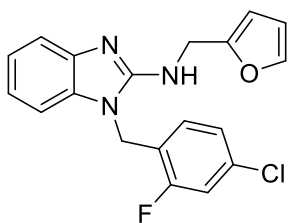
1-(4-chloro-2-fluorobenzyl)-*N*-(furan-2-ylmethyl)-1*H*-benzo[*d*]imidazol-2-amine (15i). Yield = 24 mg (39%, brown solid) LCMS: R_T = 2.14 min., >98% @ 215 and 254 nm, *m/z* = 356.0 [M + H]$^+$. ^{1}H NMR (500 MHz, CDCl$_3$) δ 7.54 (d, *J* = 7.8 Hz, 1H), 7.36 (d, *J* = 0.9 Hz, 1H), 7.19 – 7.13 (m, 2H), 7.09 – 7.06 (m, 2H), 7.04 (dd, *J* = 8.4, 0.9 Hz, 1H), 6.88 (t, *J* = 8.2 Hz, 1H), 6.34 – 6.31 (m, 1H), 6.29 (d, *J* = 2.6 Hz, 1H), 5.10 (s, 2H), 4.73 (d, *J* = 4.6 Hz, 2H), 4.67 (s, 1H). ^{13}C NMR (125 MHz, CDCl$_3$) δ 161.00, 159.01, 153.45, 151.56, 142.23, 142.18, 134.98, 134.90, 134.38, 129.22, 129.18, 125.24, 125.21, 121.86, 121.33, 121.21, 120.17, 116.94, 116.61, 116.42, 110.46, 107.65, 107.40, 40.54, 39.36, 39.33.

1-(2-chloro-4-fluorobenzyl)-*N*-(furan-2-ylmethyl)-1*H*-benzo[*d*]imidazol-2-amine (15j). Yield = 20 mg (33%, brown solid) LCMS: R_T = 2.137 min., >98% @ 215 and 254 nm, *m/z* = 356.0 [M + H]$^+$. ^{1}H NMR (500 MHz, CDCl$_3$) δ 7.55 (d, *J* = 7.9 Hz, 1H), 7.33 (d, *J* = 0.9 Hz, 1H), 7.21 – 7.15 (m, 2H), 7.09 – 7.04 (m, 1H), 7.00 (d, *J* = 7.7 Hz, 1H), 6.85 (td, *J* = 8.5, 2.5 Hz, 1H), 6.72 (dd, *J* = 8.6, 5.9 Hz, 1H), 6.31 (dd, *J* = 3.0, 1.8 Hz, 1H), 6.28 (d, *J* = 2.8 Hz, 1H), 5.14 (s, 2H), 4.71 (s, 3H). ^{13}C NMR (125 MHz, CDCl$_3$) δ 163.02, 161.02, 153.57, 151.58, 142.20, 142.18, 134.40, 133.09, 133.01, 128.72, 128.70, 128.56, 128.49, 121.89, 120.17, 117.38, 117.18, 116.88, 114.83, 114.66, 110.45, 107.67, 107.46, 42.93, 40.44.
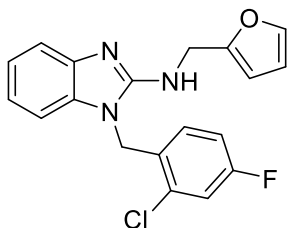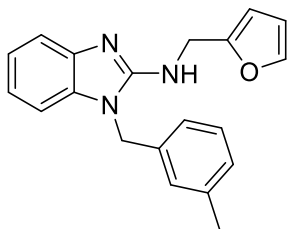

N-(furan-2-ylmethyl)-1-(3-methylbenzyl)-1*H*-benzo[*d*]imidazol-2-amine (15k). Yield = 30 mg (49%, yellow oil) LCMS: R_T = 2.103 min., >98% @ 215 and 254 nm, *m/z* = 318.1 [M + H]$^+$. ^{1}H NMR (500 MHz, CDCl$_3$) δ 7.58 (d, *J* = 7.9 Hz, 1H), 7.34 (d, *J* = 0.9 Hz, 1H), 7.23 (t, *J* = 7.9 Hz, 1H), 7.20 – 7.16 (m, 1H), 7.10 (ddd, *J* = 11.1, 8.6, 4.3 Hz, 3H), 6.96 (m, *J* = 6.9 Hz, 2H), 6.31 (dd, *J* = 3.0, 1.8 Hz, 1H), 6.22 (d, *J* = 2.5 Hz, 1H), 5.09 (s, 2H), 4.70 (s, 2H), 4.41 (s, 1H), 2.31 (s, 3H). ^{13}C NMR (125 MHz, CDCl$_3$) δ 153.82, 151.75, 142.11, 142.07, 139.09, 135.22, 134.92, 129.08, 128.93, 127.07, 123.55, 121.51, 120.01, 116.77, 110.40, 107.46, 107.35, 45.74, 40.48, 21.40.

General Procedure B for synthesis of core ring.

Reagents and conditions: (a)Cs₂CO₃, Dioxane, 100°C, 2 h; (b) H₂/Pd, RT, 3 h; (c) CDI, THF, RT, 12 h; d) POCl₃, PCl₅, 90°C, 6 h; (d) MW. 200°C, 30 min
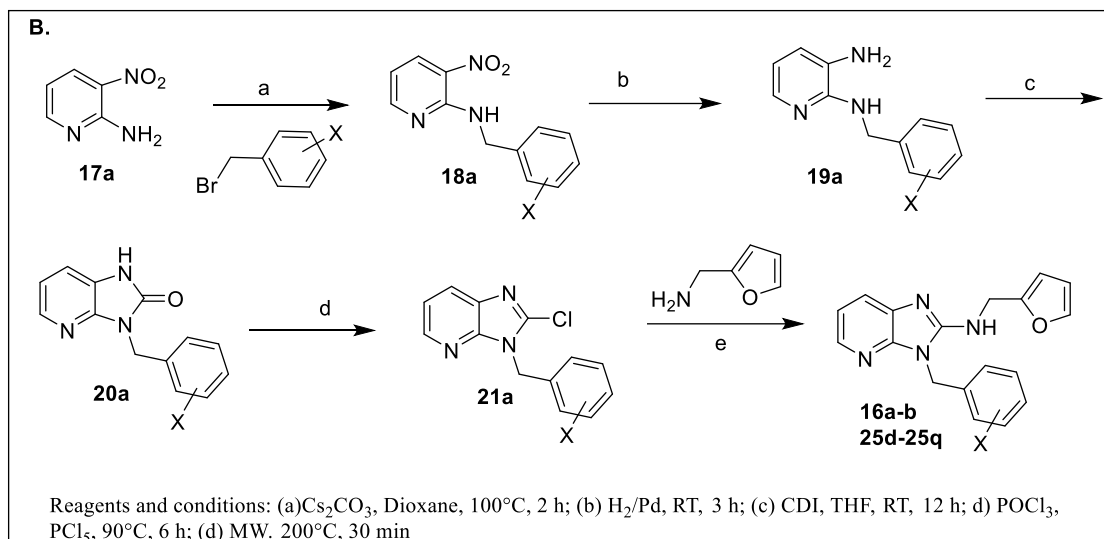
N-benzyl-3-nitropyridin-2-amine (18a). In a round bottom flask fitted with magnetic stirrer and reflux condenser, a solution of 2-chloro-3-nitropyridine (1.0 g, 6.3 mmol) and cesium carbonate (4.0 g, 12.0 mmol) in dioxane (20 mL) was added benzyl bromide (1.5 equiv.)(substituted benzyl bromide) and heated at 100 ºC for 2 h. The mixture was cooled to RT, filtered and purified by column chromatography (Biotage) with a gradient of EtOAc and hexanes (0-20%, EtOAc in Hexane) to provide desired compound Yield = 1.37 g (94%). LCMS: R_T = 2.78 min., >98% @ 215 and 254 nm, m/z = 230.0 $[M + H]^+$. ^{1}H NMR (500 MHz, CDCl₃) δ 8.55 (s, 1H), 8.47 (d, J = 7.0 Hz, 2H), 7.39 (q, J = 7.6 Hz, 4H), 7.32 (t, J = 5.9 Hz, 1H), 6.77 – 6.61 (m, 1H), 4.89 (d, J = 5.6 Hz, 2H). ^{13}C NMR (125 MHz, CDCl₃) δ 155.78, 152.44, 138.23, 135.32, 128.74, 127.63, 127.53, 112.09, 45.07.

N^2-benzylpyridine-2,3-diamine (19a). In a round bottom flask fitted with magnetic stirrer, was added *N*-benzyl-3-nitropyridin-2-amine (1.37 g, 5.90 mmol) and 10% Pd/C (50% water; 120 mg, 0.59 mmol) dissolved in MeOH (15 mL). The mixture was purged with N₂ gas and a pressurized balloon containing H₂ gas was fitted. The suspension was stirred at RT for 3 h. The filtered through

celite, evaporated and used as such. Yield = 1.13 g (97%). LCMS: R_T = 1.58 min., >98% @ 215 and 254 nm, m/z = 200.0 [M + H]$^+$. ^{1}H NMR (500 MHz, CDCl$_3$) δ 7.83 – 7.78 (m, 1H), 7.43 (d, J = 7.3 Hz, 2H), 7.37 (t, J = 7.5 Hz, 2H), 7.30 (dd, J = 12.8, 5.3 Hz, 1H), 6.93 – 6.83 (m, 1H), 6.59 (dd, J = 7.2, 5.2 Hz, 1H), 4.66 (d, J = 2.6 Hz, 2H), 4.40 (s, 1H), 3.21 (s, 2H). ^{13}C NMR (125 MHz, CDCl$_3$) δ 150.19, 139.85, 139.18, 128.58, 128.36, 128.11, 127.22, 122.09, 113.75, 46.11.

3-benzyl-1,3-dihydro-2*H*-imidazo[4,5-*b*]pyridin-2-one (20a). In a round bottom flask fitted with magnetic stirrer, N^2-benzylpyridine-2,3-diamine (1.13 g, 5.6 mmol) and CDI (1.83 g, 11.3 mmol) were dissolved in anhydrous THF (50 mL). The mixture was stirred under inert atmosphere for 12 h. The product was partitioned between water (100 mL) and ethyl acetate (100 mL X 2). The collective organic layer was washed with brine, dried over sodium sulphate and used as such. Yield = 1 g (crude). LCMS: R_T = 2.1 min., >98% @ 215 and 254 nm, m/z = 226.0 [M + H]$^+$. ^{1}H NMR (500 MHz, CDCl$_3$) δ 8.08 (d, J = 5.1 Hz, 1H), 7.71 (s, 3H), 7.49 (d, J = 7.3 Hz, 2H), 7.32 (dd, J = 14.9, 7.3 Hz, 2H), 6.99 (dt, J = 29.3, 14.7 Hz, 1H), 5.21 (s, 2H).

3-benzyl-2-chloro-3*H*-imidazo[4,5-*b*]pyridine (21a). In a round bottom flask fitted with magnetic stirrer, 3-benzyl-1,3-dihydro-2*H*-imidazo[4,5-*b*]pyridin-2-one (1.0 g, 4.40 mmol) was dissolved in POCl$_3$ (10 mL), refluxed at 100 ºC for 10 min, PCl$_5$ (0.90 g, 4.40 mmol) was added to the refluxing mixture and heated at 90 °C for 6 h. The mixture was allowed to reach rt. The crude was slowly added to ice-water and then basified with 6N NaOH solution. The product was extracted with ethyl acetate (200 mL x 2). Organic layer was dried over sodium sulphate and purified by column chromatography (0-30%, EtOAc in Hexane) fractions collected were evaporated to yield desired compound as white solid. Yield = 0.25 g (approx. 25%). LCMS: R_T = 2.42 min., >98% @ 215 and 254 nm, m/z = 244.0 [M + H]$^+$. ^{1}H NMR (500 MHz, CDCl$_3$) δ 8.42 (d, J = 4.2 Hz, 1H), 8.02 – 7.94 (m, 1H), 7.41 – 7.22 (m, 6H), 5.53 (s, 2H). ^{13}C NMR (125 MHz, CDCl$_3$) δ 147.60, 144.38, 142.50, 135.33, 134.29, 128.84, 128.17, 127.73, 126.95, 119.15, 46.46.
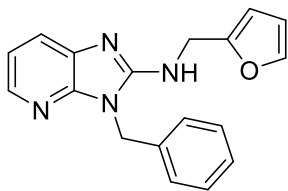
3-benzyl-*N*-(furan-2-ylmethyl)-3*H*-imidazo[4,5-*b*]pyridin-2-amine (16a). Yield = 30 mg (48%, white solid) LCMS: R_T = 1.967 min., >98% @ 215 and 254 nm, *m/z* = 305.2 [M + H]⁺. ¹H NMR (500 MHz, CDCl₃) δ 8.16 – 8.05 (m, 1H), 7.74 (dd, *J* = 7.8, 1.0 Hz, 1H), 7.38 – 7.31 (m, 4H), 7.22 (d, *J* = 6.7 Hz, 2H), 7.10 (dt, *J* = 18.3, 9.1 Hz, 1H), 6.30 (s, 1H), 6.18 (d, *J* = 2.5 Hz, 1H), 5.32 (s, 2H), 4.69 (d, *J* = 5.0 Hz, 2H), 4.60 (s, 1H). ¹³C NMR (125 MHz, CDCl₃) δ 154.03, 151.18, 148.01, 142.26, 139.84, 135.14, 129.22, 128.24, 126.93, 122.71, 117.81, 110.41, 107.45, 44.13, 39.84.
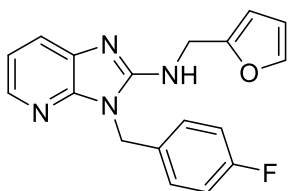
3-(4-fluorobenzyl)-*N*-(furan-2-ylmethyl)-3*H*-imidazo[4,5-*b*]pyridin-2-amine (16b). Yield = 28 mg (45%, brown oil) LCMS: R_T = 2.00 min., >98% @ 215 and 254 nm, *m/z* = 323.1 [M + H]⁺. ¹H NMR (500 MHz, CDCl₃) δ 8.10 (dd, *J* = 5.0, 1.1 Hz, 1H), 7.74 (dd, *J* = 7.8, 1.1 Hz, 1H), 7.32 (d, *J* = 15.5 Hz, 1H), 7.20 (dd, *J* = 8.2, 5.4 Hz, 2H), 7.11 (dd, *J* = 7.8, 5.1 Hz, 1H), 7.03 (t, *J* = 8.6 Hz, 2H), 6.31 (dd, *J* = 2.9, 1.8 Hz, 1H), 6.22 (d, *J* = 2.8 Hz, 1H), 5.30 (d, *J* = 16.1 Hz, 2H), 4.69 (s, 2H), 4.60 (s, 1H). ¹³C NMR (125 MHz, CDCl₃) δ 163.49, 161.52, 153.80, 151.07, 147.86, 142.32, 139.91, 130.96, 128.74, 128.68, 122.80, 117.92, 116.23, 116.06, 110.45, 107.60, 43.45, 39.84.
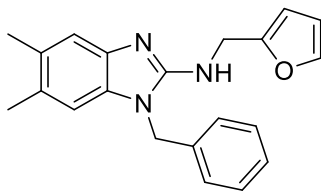
1-benzyl-*N*-(furan-2-ylmethyl)-5,6-dimethyl-1*H*-benzo[*d*]imidazol-2-amine (16c). Yield = 16 mg (32%, clear oil) LCMS: R_T = 2.23 min., >98% @ 215 and 254 nm, *m/z* = 332.1 [M + H]⁺. ¹H

NMR (500 MHz, CDCl$_3$) δ 7.30 (d, J = 6.8 Hz, 5H), 7.10 (d, J = 7.0 Hz, 5H), 6.74 (s, 1H), 6.27 (t, J = 11.1 Hz, 2H), 5.03 (s, 2H), 4.69 (s, 2H), 2.31 (d, J = 15.9 Hz, 6H). ^{13}C NMR (125 MHz, CDCl$_3$) δ 151.92, 150.93, 142.29, 134.86, 131.46, 130.95, 129.83, 129.10, 128.13, 126.53, 115.86, 110.38, 108.96, 107.93, 45.76, 40.39, 20.27, 20.07.
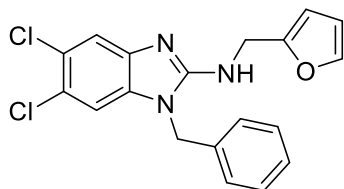
1-benzyl-5,6-dichloro-*N*-(furan-2-ylmethyl)-1*H*-benzo[*d*]imidazol-2-amine (16d). Yield = 14 mg (23%, brown solid) LCMS: R$_T$ = 2.47 min., >98% @ 215 and 254 nm, m/z = 372.0 [M + H]$^+$. ^{1}H NMR (500 MHz, CDCl$_3$) δ 7.57 (s, 1H), 7.38 – 7.30 (m, 4H), 7.15 – 7.04 (m, 3H), 6.30 (dd, J = 2.9, 1.7 Hz, 1H), 6.22 (d, J = 2.8 Hz, 1H), 5.05 (s, 2H), 4.66 (s, 2H). ^{13}C NMR (125 MHz, CDCl$_3$) δ 154.87, 151.01, 142.32, 141.41, 134.24, 134.13, 129.36, 128.47, 126.29, 125.25, 123.42, 117.72, 110.46, 108.88, 107.74, 45.98, 40.37.
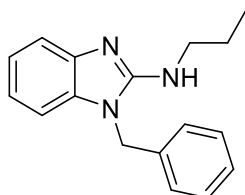
1-benzyl-*N*-propyl-1H-benzo[*d*]imidazol-2-amine (22f). Yield = 14 mg (57.5%, white solid) LCMS: R$_T$ = 2.04 min., >98% @ 215 and 254 nm, m/z = 266.1 [M + H]$^+$. ^{1}H NMR (500 MHz, CDCl$_3$) δ 7.55 (d, J = 7.8 Hz, 1H), 7.38 – 7.31 (m, 3H), 7.19 (d, J = 6.8 Hz, 2H), 7.18 – 7.14 (m, 1H), 7.11 – 7.04 (m, 2H), 5.13 (s, 2H), 4.18 (s, 1H), 3.47 (dd, J = 12.9, 6.9 Hz, 2H), 1.66 – 1.57 (m, 2H), 0.88 (t, J = 7.4 Hz, 3H). ^{13}C NMR (125 MHz, CDCl$_3$) δ 154.08, 141.89, 134.45, 133.99, 133.94, 129.31, 127.80, 121.67, 119.93, 116.42, 107.20, 45.20, 45.08, 22.94, 11.21.
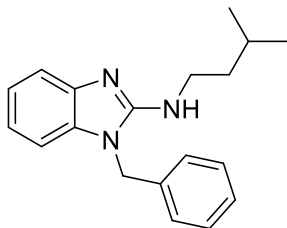
1-benzyl-*N*-isopentyl-1H-benzo[*d*]imidazol-2-amine (22g). Yield = 12 mg (11.4%, off-white solid) LCMS: R_T = 3.07 min., >98% @ 215 and 254 nm, *m/z* = 294.1 [M + H]$^+$. ^{1}H NMR (500 MHz, CDCl$_3$) δ 7.55 (d, *J* = 7.8 Hz, 1H), 7.34 (dt, *J* = 15.2, 5.2 Hz, 3H), 7.18 – 7.13 (m, 3H), 7.08 – 7.05 (m, 2H), 5.08 (s, 2H), 4.17 (s, 1H), 3.51 (dd, *J* = 12.8, 7.0 Hz, 2H), 1.58 – 1.51 (m, 1H), 1.47 (dd, *J* = 14.4, 7.0 Hz, 2H), 0.88 (d, *J* = 6.5 Hz, 6H). ^{13}C NMR (125 MHz, CDCl$_3$) δ 154.41, 142.21, 135.53, 134.80, 129.15, 128.09, 126.51, 121.39, 119.70, 116.42, 107.22, 45.66, 41.74, 38.55, 25.76, 22.50.
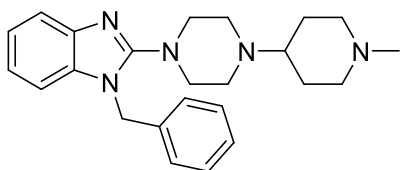
1-benzyl-2-(4-(1-methylpiperidin-4-yl)piperazin-1-yl)-1H-benzo[*d*]imidazole (22h). Yield = 15 mg (18.5%, yellow solid) LCMS: R_T = 1.73 min., >98% @ 215 and 254 nm, *m/z* = 390.2 [M + H]$^+$. ^{1}H NMR (500 MHz, CDCl$_3$) δ 7.60 (d, *J* = 7.9 Hz, 1H), 7.32 (t, *J* = 7.2 Hz, 2H), 7.29 – 7.25 (m, 1H), 7.18 (t, *J* = 7.6 Hz, 1H), 7.14 (d, *J* = 7.3 Hz, 2H), 7.08 (t, *J* = 7.6 Hz, 1H), 7.00 (d, *J* = 7.9 Hz, 1H), 5.20 (s, 2H), 3.35 (d, *J* = 9.5 Hz, 2H), 3.28 – 3.24 (m, 4H), 2.65 (s, 6H), 2.63 (s, 3H), 2.54 – 2.45 (m, 1H), 1.96 (d, *J* = 3.9 Hz, 4H). ^{13}C NMR (125 MHz, CDCl$_3$) δ 168.13, 157.65, 141.04, 135.99, 135.27, 129.03, 127.73, 125.96, 122.15, 121.70, 117.84, 109.45, 50.50, 48.59, 47.65, 43.27, 25.33. (10% CD$_3$OD was added for increasing solubility)
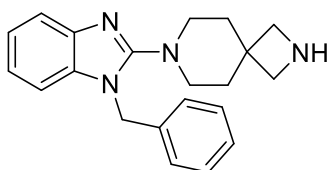
7-(1-benzyl-1H-benzo[*d*]imidazol-2-yl)-2,7-diazaspiro[3.5]nonane (22i). Yield = 13 mg (19.7%, off-white solid) LCMS: R_T = 1.72 min., >98% @ 215 and 254 nm, *m/z* = 333.1 [M + H]$^+$. ^{1}H NMR (500 MHz, DMSO-*d$_6$*) δ 7.60 (d, *J* = 7.8 Hz, 1H), 7.40 (t, *J* = 7.5 Hz, 3H), 7.36 – 7.32 (m, 2H), 7.29 (t, *J* = 6.0 Hz, 3H), 5.47 (s, 2H), 3.73 (d, *J* = 5.3 Hz, 4H), 3.49 – 3.47 (m, 4H), 1.97-1.92 (m, 4H). ^{13}C NMR (125 MHz, DMSO-*d$_6$*) δ 172.26, 135.26, 132.65, 129.47, 128.44, 126.71, 124.93, 124.34, 111.87, 55.40, 54.29, 49.26, 46.70, 36.08, 33.54.
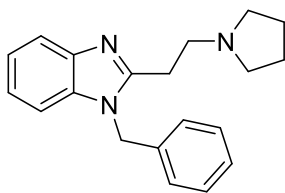
1-benzyl-2-(2-(pyrrolidin-1-yl)ethyl)-1H-benzo[*d*]imidazole (22j). Yield = 21.0 mg (29.9%, yellow solid) LCMS: R_T = 2.12 min., >98% @ 215 and 254 nm, *m/z* = 306.18 [M + H]$^+$. ^{1}H NMR (500 MHz, CDCl$_3$) δ 7.78 (d, *J* = 7.5 Hz, 1H), 7.33 – 7.27 (m,4H), 7.23 (dd, *J* = 10.9, 5.3 Hz, 2H), 7.07 (d, *J* = 7.0 Hz, 2H), 5.40 (s, 2H), 3.14 – 3.08 (m, 2H), 3.07 – 3.04 (m, 2H), 2.65 – 2.57 (m, 4H), 1.81 (dd, *J* = 6.5, 3.1 Hz, 4H). ^{13}C NMR (125 MHz, CDCl$_3$) δ 142.31, 135.75, 135.49, 129.06, 128.02, 126.51, 122.95, 122.39, 119.26, 109.81, 53.94, 52.87, 46.99, 23.39.
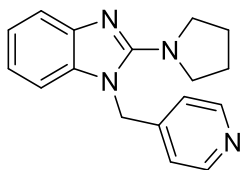
1-(pyridin-4-ylmethyl)-2-(pyrrolidin-1-yl)-1*H*-benzo[*d*]imidazole (23k). Yield = 16.0 mg (14.4%, off-white solid) LCMS: R_T = 0.94 min., >98% @ 215 and 254 nm, *m/z* = 279.1 [M + H]$^+$. ^{1}H NMR (500 MHz, CDCl$_3$) δ 8.63 (d, *J* = 4.4 Hz, 2H), 7.74 – 7.69 (m, 1H), 7.26 (t, *J* = 7.7 Hz, 1H), 7.12 (d, *J* = 6.2 Hz, 1H), 7.10 (d, *J* = 5.6 Hz, 2H), 6.97 (d, *J* = 7.9 Hz, 1H), 5.36 (s, 2H), 3.69 – 3.61 (m,4H), 2.01 – 1.96 (m, *J* = 16.3 Hz, 4H).
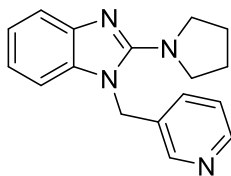
1-(pyridin-3-ylmethyl)-2-(pyrrolidin-1-yl)-1*H*-benzo[*d*]imidazole (23l). Yield = 22.0 mg (19.8%, yellow solid). LCMS: R_T = 0.94 min., >98% @ 215 and 254 nm, m/z = 279.1 [M + H]$^+$. ^{1}H NMR (500 MHz, CDCl$_3$) δ 8.58 (d, J = 5.8 Hz, 2H), 7.59 (d, J = 7.9 Hz, 1H), 7.41 (d, J = 7.9 Hz, 1H), 7.27 – 7.24 (m, 1H), 7.20 (t, J = 7.6 Hz, 1H), 7.07 (t, J = 7.6 Hz, 1H), 7.00 (d, J = 7.9 Hz, 1H), 5.34 (s, 2H), 3.59 (t, J = 6.5 Hz, 4H), 1.99 – 1.95 (m, 4H). ^{13}C NMR (125 MHz, CDCl$_3$) δ 149.51, 147.58, 133.44, 123.96, 123.13, 121.37, 116.10, 108.32, 50.95, 45.74, 25.67.

1-(pyridin-2-ylmethyl)-2-(pyrrolidin-1-yl)-1*H*-benzo[*d*]imidazole (23m). Yield = 20.0 mg (18.0%, white solid) LCMS: R_T = 1.2 min., >98% @ 215 and 254 nm, m/z = 279.1 [M + H]$^+$. ^{1}H NMR (500 MHz, CDCl$_3$) δ 8.64 – 8.61 (m, 1H), 7.65 – 7.59 (m, 2H), 7.24 (dd, J = 7.1, 5.2 Hz, 1H), 7.21 – 7.17 (m, 1H), 7.08 – 7.04 (m, 1H), 7.01 (d, J = 7.7 Hz, 1H), 6.95 (d, J = 7.9 Hz, 1H), 5.42 (s, 2H), 3.62 (t, J = 6.6 Hz, 4H), 1.97 – 1.93 (m, 4H). ^{13}C NMR (125 MHz, CDCl$_3$) δ 156.65, 149.70, 137.27, 122.64, 122.31, 120.45, 120.29, 116.38, 108.11, 50.52, 49.76, 25.65.

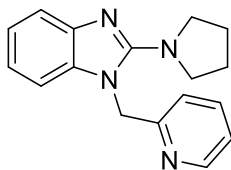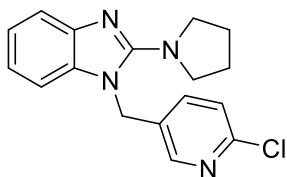**1-((6-chloropyridin-3-yl)methyl)-2-(pyrrolidin-1-yl)-1*H*-benzo[*d*]imidazole (23n).** Yield = 19.0 mg (23.4%, yellow solid) LCMS: R_T = 1.2 min., >98% @ 215 and 254 nm, m/z = 279.1 [M + H]$^+$. ^{1}H NMR (500 MHz, CDCl$_3$) δ 8.34 (s, 1H), 7.58 (d, J = 7.9 Hz, 1H), 7.36 (dd, J = 8.3, 2.4 Hz,

1H), 7.30 – 7.27 (m, 1H), 7.19 (t, J = 7.6 Hz, 1H), 7.07 (t, J = 7.6 Hz, 1H), 6.97 (d, J = 7.9 Hz, 1H),

5.30 (s, 2H), 3.58 (d, J = 6.4 Hz, 4H), 1.97 (dd, J = 8.1, 5.1 Hz, 4H). ^{13}C NMR (125 MHz, CDCl$_3$)

δ 156.27, 151.07, 147.51, 136.52, 135.22, 131.42, 124.67, 122.56, 120.72, 116.77, 108.00, 50.79,

45.01, 25.64.
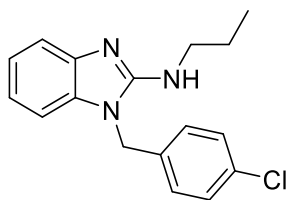
1-(4-chlorobenzyl)-*N*-propyl-1*H*-benzo[*d*]imidazol-2-amine (24e). Yield = 25.0 mg (56.8%,

white solid) LCMS: R$_T$ = 2.13 min., >98% @ 215 and 254 nm, *m/z* = 300.1 [M + H]$^+$. ^{1}H NMR

(500 MHz, CDCl$_3$) δ 7.53 (d, J = 7.9 Hz, 1H), 7.31 (d, J = 8.4 Hz, 2H), 7.17 – 7.13 (m, 1H), 7.09

(d, J = 8.4 Hz, 2H), 7.07 – 7.01 (m, 2H), 5.08 (s, 2H), 4.33 (s, 1H), 3.47 (dd, J = 12.5, 6.9 Hz, 2H),

1.67 – 1.59 (m, 2H), 0.90 (t, J = 7.4 Hz, 4H). ^{13}C NMR (125 MHz, CDCl$_3$) δ 154.08, 141.89,

134.45, 133.99, 133.94, 129.31, 127.80, 121.67, 119.93, 116.42, 107.20, 45.20, 45.08, 22.94, 11.21.
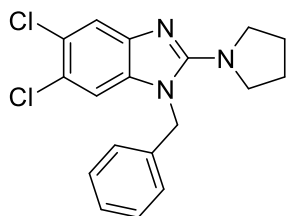
1-benzyl-5,6-dichloro-2-(pyrrolidin-1-yl)-1*H*-benzo[*d*]imidazole (25a). Yield = 27.0 mg

(48.3%, white solid) LCMS: R$_T$ = 2.24 min., >98% @ 215 and 254 nm, *m/z* = 346.0[M + H]$^+$. ^{1}H

NMR (500 MHz, CDCl$_3$) δ 7.61 (s, 1H), 7.40 – 7.35 (m, 1H), 7.34 – 7.31 (m, 1H), 7.11 (d, J = 7.2

Hz, 2H), 7.01 (s, 1H), 5.26 (s, 2H), 3.62 – 3.56 (m, 4H), 1.95 (d, J = 6.2 Hz, 4H). ^{13}C NMR (125

MHz, CDCl$_3$) δ 156.79, 135.80, 135.14, 129.21, 127.97, 125.78, 125.45, 123.52, 116.98, 109.59,

50.36, 48.11, 25.67.
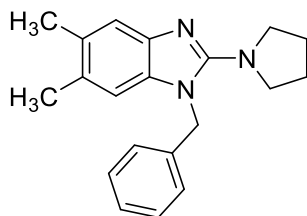
**1-benzyl-5,6-dimethyl-2-(pyrrolidin-1-yl)-1*H*-benzo[*d*]imidazole (25b).** Yield = 14.0 mg (41.8%, white solid) LCMS: R_T = 2.17 min., >98% @ 215 and 254 nm, *m/z* = 306.1 [M + H]⁺. ¹H NMR (500 MHz, CDCl₃) δ 7.67 (s, 1H), 7.42 – 7.34 (m, 3H), 7.10 (d, *J* = 7.1 Hz, 2H), 6.82 (s, 1H), 5.43 (s, 2H), 3.87 (t, *J* = 6.5 Hz, 4H), 2.30 (s, 3H), 2.26 (s, 3H), 2.01 (t, *J* = 6.5 Hz, 4H). ¹³C NMR (125 MHz, CDCl₃) δ 148.55, 134.79, 133.81, 132.65, 130.13, 129.57, 128.51, 127.95, 125.13, 114.17, 109.71, 51.20, 48.09, 25.68, 20.33, 19.84.
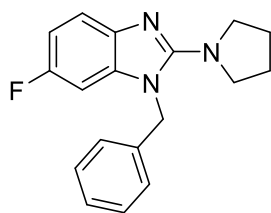
1-benzyl-6-fluoro-2-(pyrrolidin-1-yl)-1*H*-benzo[*d*]imidazole (25c) Yield = 25.0 mg (44.1%, white solid) LCMS: R_T = 2.12 min., >98% @ 215 and 254 nm, *m/z* = 296.1 [M + H]⁺. ¹H NMR (500 MHz, CDCl₃) δ 7.44 (dd, *J* = 8.6, 4.7 Hz, 0.5H), 7.35 (dd, *J* = 13.8, 7.6 Hz, 2H), 7.33 – 7.30 (m, 1H), 7.23 (dd, *J* = 9.7, 2.0 Hz, 0.5H), 7.16 (d, *J* = 7.3 Hz, 2H), 6.91 – 6.82 (m, 1H), 6.75 – 6.66 (m, 1H), 5.27 (d, *J* = 10.7 Hz, 2H), 3.61 – 3.49 (m, 4H), 1.94 (t, *J* = 6.5 Hz, 4H). ¹³C NMR (125 MHz, CDCl₃) 158.5, 143.2, 138.5, 136.58, 128.98, 127.63, 125.71, 109.9, 108.08, 106.87, 103.15, 95.9, 50.5, 47.97, 25.64

1-benzyl-6-methoxy-2-(pyrrolidin-1-yl)-1*H*-benzo[*d*]imidazole (25d). Yield = 26.0 mg (46.5%, white solid) LCMS: R_T = 2.1 min., >98% @ 215 and 254 nm, *m/z* = 308.1 [M + H]$^+$. ^{1}H NMR (500 MHz, CD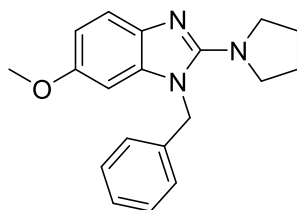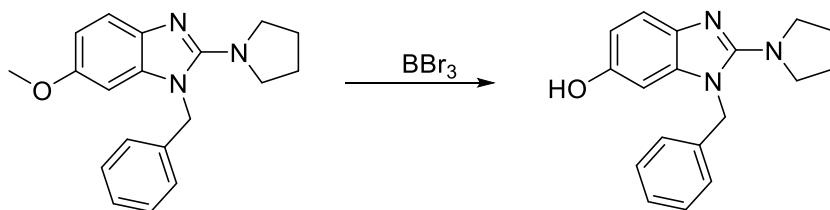Cl$_3$) δ 7.45 (d, *J* = 8.6 Hz, 1H), 7.35 (t, *J* = 7.3 Hz, 2H), 7.31 (d, *J* = 7.1 Hz, 1H), 7.19 (d, *J* = 7.3 Hz, 2H), 6.78 (dd, *J* = 8.6, 2.4 Hz, 1H), 6.54 (d, *J* = 2.3 Hz, 1H), 5.25 (s, 2H), 3.77 (s, 3H), 3.50 (d, *J* = 6.7 Hz, 4H), 1.95 – 1.89 (m, 4H). ^{13}C NMR (125 MHz, CDCl$_3$) δ 157.07, 154.81, 136.86, 136.73, 136.51, 128.90, 127.46, 125.82, 116.92, 108.62, 94.50, 55.98, 50.66, 47.82, 25.56.

1-benzyl-2-(pyrrolidin-1-yl)-1*H*-benzo[*d*]imidazol-6-ol (25e). To a solution of **25d** (100.00 mg, 0.326 mmol) in DCM (4 mL) at -10 °C was added boron tribromide (BBr$_3$, 71.17 µL, 0.81 mmol) the reaction was stirred at 0 °C for 3 hours. Crude was evaporated and product purified by normal phase flash chromatography.

Yield = 60.0mg (63.1%, off-white solid) LCMS: R_T = 1.93 min., >98% @ 215 and 254 nm, *m/z* = 294.1 [M + H]$^+$. ^{1}H NMR (500 MHz, CDCl$_3$) δ 7.22 – 7.17 (m, 3H), 7.14 (d, *J* = 8.5 Hz, 1H), 6.96 (d, *J* = 7.1 Hz, 2H), 6.60 (d, *J* = 8.5 Hz, 1H), 6.44 (s, 1H), 5.05 (s, 2H), 3.56 – 3.49 (m, 4H), 1.87 – 1.82 (m, 4H). ^{13}C NMR (125 MHz, CDCl$_3$) δ 168.49, 153.32, 135.68, 134.51, 129.12, 127.92, 125.59, 114.41, 111.41, 96.61, 50.46, 47.72, 25.58.

1-benzyl-6-isobutoxy-2-(pyrrolidin-1-yl)-1*H*-benzo[*d*]imidazole (25f). A solution of **25e** (75.mg, 0.26 mmol), isobutyl bromide (33.3 µL, 0.307 mmol) and cesium carbonate (169 mg, 0.520

mmol) in DMF (1.5 mL) was stirred at 60 ºC for 6 hours. After the completion of reaction crude was evaporated and product purified by normal phase flash chromatography.

Yield = 30.0 mg (33.1%, off- white solid) LCMS: R_T = 2.15 min., >98% @ 215 and 254 nm, m/z = 350.1 [M + H]$^+$. ^{1}H NMR (500 MHz, CDCl$_3$) δ 7.36 (d, J = 8.6 Hz, 1H), 7.26 (t, J = 7.3 Hz, 2H), 7.22 (d, J = 6.9 Hz, 1H), 7.09 (d, J = 7.4 Hz, 2H), 6.69 (dd, J = 8.6, 2.2 Hz, 1H), 6.46 (d, J = 2.2 Hz, 1H), 5.16 (s, 2H), 3.57 (t, J = 5.6 Hz, 2H), 3.42 (t, J = 6.5 Hz, 4H), 1.95 (dt, J = 13.3, 6.6 Hz, 1H), 1.85 – 1.80 (m, 4H), 0.91 (d, J = 6.7 Hz, 6H). ^{13}C NMR (125 MHz, CDCl$_3$) δ 154.61, 136.89, 129.01, 128.93, 127.48, 125.78, 116.80, 109.53, 95.26, 75.41, 50.68, 47.79, 28.41, 25.57, 19.33.
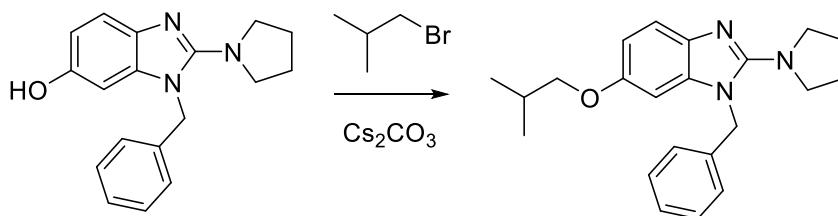

1-benzyl-6-(2-methoxyethoxy)-2-(pyrrolidin-1-yl)-1*H*-benzo[*d*]imidazole (25g). Yield = 22.0 mg (36.8%, off-white solid) LCMS: R_T = 2.15 min., >98% @ 215 and 254 nm, m/z = 352.1 [M + H]$^+$. ^{1}H NMR (500 MHz, CDCl$_3$) δ 7.35 (d, J = 8.6 Hz, 1H), 7.25 (t, J = 7.3 Hz, 2H), 7.22 – 7.19 (m, 1H), 7.07 (d, J = 7.3 Hz, 2H), 6.71 (dd, J = 8.6, 2.4 Hz, 1H), 6.50 (d, J = 2.3 Hz, 1H), 5.14 (s, 2H), 3.99 – 3.96 (m, 2H), 3.63 – 3.60 (m, 2H), 3.43 (t, J = 6.7 Hz, 4H), 3.33 (s, 3H), 1.85 – 1.81 (m, 4H). ^{13}C NMR (125 MHz, CDCl$_3$) δ 153.96, 136.74, 136.57, 128.92, 127.50, 125.77, 116.69, 109.33, 95.83, 71.20, 68.15, 59.18, 50.65, 47.83, 25.57.

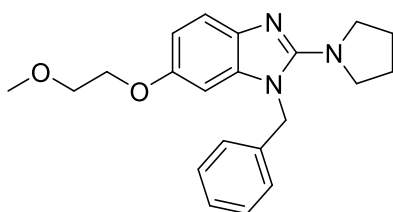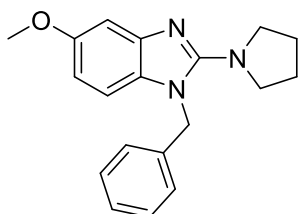**1-benzyl-5-methoxy-2-(pyrrolidin-1-yl)-1*H*-benzo[*d*]imidazole (25h).** Yield = 26.0 mg (46.5%, white solid) LCMS: R_T = 2.06 min., >98% @ 215 and 254 nm, m/z = 308.1 [M + H]$^+$. ^{1}H NMR

(500 MHz, CDCl$_3$) δ 7.25 – 7.22 (m, 2H), 7.19 (dd, *J* = 8.3, 6.2 Hz, 1H), 7.07 (d, *J* = 7.3 Hz, 2H), 7.04 (d, *J* = 2.3 Hz, 1H), 6.74 (d, *J* = 8.6 Hz, 1H), 6.54 (dd, *J* = 8.6, 2.4 Hz, 1H), 5.16 (s, 2H), 3.74 (s, 3H), 3.46 (t, *J* = 6.7 Hz, 4H), 1.84 – 1.80 (m, 4H). ^{13}C NMR (125 MHz, CDCl$_3$) δ 157.50, 156.02, 142.92, 137.05, 130.51, 128.91, 128.76, 127.65, 127.49, 127.33, 125.76, 108.48, 108.04, 100.92, 55.88, 50.49, 47.91, 25.63.
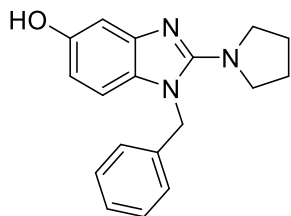
1-benzyl-2-(pyrrolidin-1-yl)-1*H*-benzo[*d*]imidazol-5-ol (25i). Yield = 175.0 mg (91.0%, white solid) LCMS: R$_T$ = 1.98 min., >98% @ 215 and 254 nm, *m/z* = 294.1 [M + H]$^+$. ^{1}H NMR (500 MHz, CDCl$_3$) δ 9.04 (s, 1H), 8.72 (s, 1H), 7.30 – 7.24 (m, 3H), 7.07 – 7.01 (m, 3H), 6.63 (d, *J* = 9.3 Hz, 2H), 5.20 (s, 2H), 3.69 – 3.61 (m, 4H), 1.94 – 1.90 (m, 4H). ^{13}C NMR (125 MHz, CDCl$_3$) δ 168.26, 155.05, 150.52, 135.64, 133.22, 129.16, 128.86, 128.12, 127.99, 125.76, 125.42, 111.01, 109.63, 99.80, 50.34, 47.78, 25.58.

1-benzyl-5-isobutoxy-2-(pyrrolidin-1-yl)-1*H*-benzo[*d*]imidazole (25j). Yield = 21.0 mg (35.4%, yellow oil) LCMS: R$_T$ = 2.45 min., >98% @ 215 and 254 nm, *m/z* = 350.1 [M + H]$^+$. ^{1}H NMR (500 MHz, CDCl$_3$) δ 7.24 (t, *J* = 7.4 Hz, 2H), 7.20 (d, *J* = 7.3 Hz, 1H), 7.08 – 7.05 (m, 2H), 7.03 (s, 1H), 6.74 (d, *J* = 8.5 Hz, 1H), 6.55 (dd, *J* = 8.5, 2.3 Hz, 1H), 5.16 (s, 2H), 3.67 (d, *J* = 6.6 Hz, 2H), 3.46 (t, *J* = 6.7 Hz, 4H), 2.05 – 1.97 (m, 1H), 1.85 – 1.82 (m, 4H), 0.94 (d, *J* = 6.7 Hz, 6H). Rotamers observed ^{13}C NMR (125 MHz, CDCl$_3$) δ 155.64, 137.09, 130.39, 128.89, 128.84,

128.66, 128.04, 127.46, 125.88, 125.77, 108.99, 108.43, 101.89, 75.38, 50.50, 47.89, 28.24, 25.63, 25.59, 19.37, 19.34.
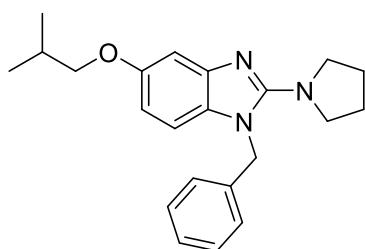

1-benzyl-5-(2-methoxyethoxy)-2-(pyrrolidin-1-yl)-1*H*-benzo[*d*]imidazole (25k). Yield = 23.0 mg (38.5%, clear oil) LCMS: R_T = 2.14 min., >98% @ 215 and 254 nm, m/z = 352.1 [M + H]$^+$. ^{1}H NMR (500 MHz, CDCl$_3$) δ 7.26 (t, J = 7.3 Hz, 2H), 7.22 – 7.20 (m, 1H), 7.08 (d, J = 4.1 Hz, 1H), 7.06 (d, J = 2.0 Hz, 2H), 6.76 – 6.73 (m, 1H), 6.61 (dd, J = 8.6, 2.3 Hz, 1H), 5.17 (s, 2H), 4.08 – 4.05 (m, 2H), 3.70 – 3.66 (m, 2H), 3.49 – 3.47 (m, 4H), 3.38 (s, 3H), 1.84 (d, J = 2.0 Hz, 4H). ^{13}C NMR (125 MHz, CDCl$_3$) δ 155.21, 136.92, 128.94, 127.54, 125.74, 109.34, 108.56, 101.67, 71.20, 68.04, 59.18, 50.52, 47.93, 25.63.
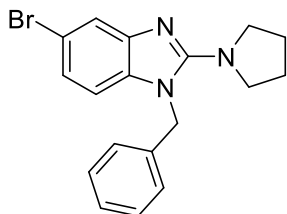
1-benzyl-5-bromo-2-(pyrrolidin-1-yl)-1*H*-benzo[*d*]imidazole (25l). Yield = 130.0 mg (77.8%, yellow solid) LCMS: R_T = 2.5 min., >98% @ 215 and 254 nm, m/z = 356.1 [M + H]$^+$. ^{1}H NMR (500 MHz, CDCl$_3$) δ 7.55 (d, J = 1.7 Hz, 1H), 7.25 (t, J = 7.2 Hz, 2H), 7.22 (d, J = 7.1 Hz, 1H), 7.04 (d, J = 7.3 Hz, 2H), 7.01 (dd, J = 8.3, 1.8 Hz, 1H), 6.72 (d, J = 8.3 Hz, 1H), 5.18 (s, 2H), 3.48 (t, J = 6.7 Hz, 4H), 1.86 – 1.83 (m, 4H). ^{13}C NMR (125 MHz, CDCl$_3$) δ 157.60, 144.00, 136.56, 135.29, 129.01, 127.67, 125.65, 122.51, 119.35, 114.61, 109.28, 50.36, 47.91, 25.67.
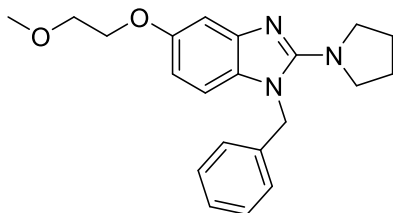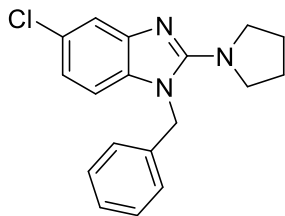
1-benzyl-5-chloro-2-(pyrrolidin-1-yl)-1*H*-benzo[*d*]imidazole (25m). Yield = 180.0 mg (80.0%, white solid) LCMS: R_T = 2.2 min., >98% @ 215 and 254 nm, *m/z* = 312.1 [M + H]⁺. ¹H NMR (500 MHz, CDCl₃) δ 7.52 (d, *J* = 1.9 Hz, 1H), 7.37 – 7.33 (m, 2H), 7.31 (t, *J* = 5.0 Hz, 1H), 7.13 (d, *J* = 7.1 Hz, 2H), 6.97 (dd, *J* = 8.4, 1.9 Hz, 1H), 6.85 (d, *J* = 8.4 Hz, 1H), 5.28 (s, 2H), 3.59 (t, *J* = 6.7 Hz, 4H), 1.96 – 1.92 (m, 4H). ¹³C NMR (125 MHz, CDCl₃) δ 157.25, 136.44, 129.03, 127.71, 127.36, 125.61, 120.03, 116.24, 108.83, 50.41, 47.94, 25.66.
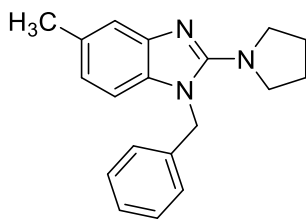
1-benzyl-5-methyl-2-(pyrrolidin-1-yl)-1*H*-benzo[*d*]imidazole (25n). Yield = 50.0 mg (48.3%, white solid) LCMS: R_T = 2.31 min, >98% @ 215 and 254 nm, *m/z* = 292.1 [M + H]⁺. ¹H NMR (500 MHz, CDCl₃) δ 7.37 (d, *J* = 8.7 Hz, 1H), 7.34 (t, *J* = 7.2 Hz, 2H), 7.31 – 7.28 (m, 1H), 7.16 (d, *J* = 7.2 Hz, 2H), 6.86 (s, 2H), 5.27 (s, 2H), 3.56 (t, *J* = 6.7 Hz, 4H), 2.44 (s, 3H), 1.95 – 1.90 (m, 4H). ¹³C NMR (125 MHz, CDCl₃) δ 156.74, 136.98, 133.91, 131.53, 128.90, 127.48, 125.73, 121.18, 116.74, 107.87, 50.54, 47.83, 25.62, 21.58.
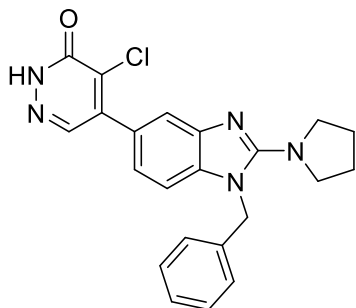
5-(1-benzyl-2-(pyrrolidin-1-yl)-1*H*-benzo[d]imidazol-5-yl)-4-chloropyridazin-3(2*H*)-one

(25o). Yield = 7.0 mg (14.0%, white solid) LCMS: R_T = 2.54 min., >98% @ 215 and 254 nm, *m/z* = 406.1 [M + H]$^+$. ^{1}H NMR (500 MHz, DMSO-d_6) δ 13.48 (s, 1H), 7.98 (s, 1H), 7.53 (d, *J* = 1.4 Hz, 1H), 7.35 (t, *J* = 7.1 Hz, 2H), 7.29 (t, *J* = 6.4 Hz, 2H), 7.19 – 7.12 (m, 3H), 5.48 (s, 2H), 3.55 – 3.54 (m, 4H), 1.87 (t, *J* = 6.6 Hz, 4H). ^{13}C NMR (125 MHz, DMSO-d_6) δ 158.34, 157.42, 142.89, 138.84, 138.02, 137.69, 131.47, 129.27, 127.80, 126.37, 126.02, 120.58, 116.50, 109.09, 50.13, 47.35, 25.60.
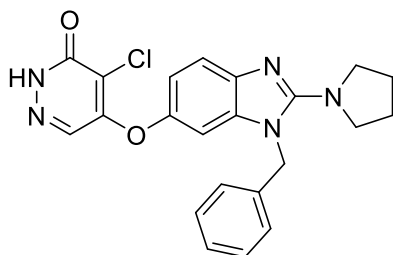
5-((1-benzyl-2-(pyrrolidin-1-yl)-1*H*-benzo[d]imidazol-6-yl)oxy)-4-chloropyridazin-3(2*H*)-one (25p). Yield = 9.0 mg (20.9%, clear oil) LCMS: R_T = 2.54 min., >98% @ 215 and 254 nm, *m/z* = 422.1 [M + H]$^+$. ^{1}H NMR (500 MHz, CDCl$_3$) δ 10.66 (s, 1H), 8.03 (d, *J* = 8.5 Hz, 1H), 7.43 (dd, *J* = 18.2, 8.0 Hz, 4H), 7.09 (d, *J* = 7.6 Hz, 3H), 6.88 (s, 1H), 5.46 (s, 2H), 3.97 (s, 4H), 2.09 (s, 4H).
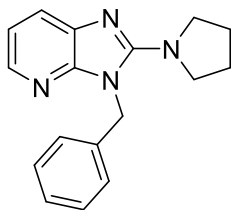
3-benzyl-2-(pyrrolidin-1-yl)-3*H*-imidazo[4,5-b]pyridine (25q). Yield = 8.0 mg (28.0%, white

solid) LCMS: R_T = 1.8 min., >98% @ 215 and 254 nm, *m/z* = 279.1 [M + H]$^+$. ^{1}H NMR (500 MHz,

CDCl$_3$) δ 8.06 (d, *J* = 4.1 Hz, 1H), 7.70 (d, *J* = 7.0 Hz, 1H), 7.34 – 7.29 (m, *J* = 14.4, 6.8 Hz, 3H),

7.13 (d, *J* = 7.3 Hz, 2H), 7.09 (dd, *J* = 7.7, 5.1 Hz, 1H), 5.54 (s, 2H), 3.62 (t, *J* = 6.5 Hz, 4H), 1.93

(t, *J* = 6.5 Hz, 4H). ^{13}C NMR (125 MHz, CDCl$_3$) δ 155.45, 139.34, 137.42, 128.81, 127.38, 125.81,

122.04, 117.95, 49.56, 46.08, 25.59.

Reagents and conditions: PdCl$_2$, tBu$_3$PHBF$_4$, Cs$_2$CO$_3$, DMF 130°C, 5 h
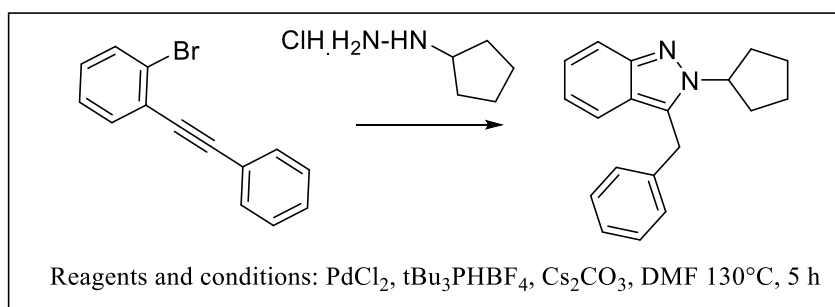
3-benzyl-2-cyclopentyl-2H-indazole (25r). PdCl$_2$ (5 mol%), tBu$_3$PHBF$_4$ (10 mol%), Cs$_2$CO$_3$ (3.0

equiv), and anhydrous DMF (3.0 mL) were placed in an oven dried Schlenk tube with a magnetic

stirring bar, and the resulting mixture was stirred under argon at ambient temperature for 30 min.

Next, (2-bromophenyl) acetylene (215 mg, 0.830 mmol) and the appropriate hydrazine (160 mg,

1.17 mmol) were added, and the mixture was heated at 130 °C for 5 h. The reaction mixture was

then cooled to rt, diluted with water, and extracted twice with EtOAc. The organic phase was dried

over Na$_2$SO$_4$ and concentrated, and the crude product was purified by flash chromatography

EtOAc:Hexane..

Yield = 18.0 mg (7.8%, yellow oil) LCMS: R_T = 3.06 min., >98% @ 215 and 254 nm, m/z = 277.1

[M + H]$^+$. ^{1}H NMR (500 MHz, CDCl$_3$) δ 7.65 (d, J = 8.7 Hz, 1H), 7.43 (d, J = 8.4 Hz, 1H), 7.22 –

7.18 (m, 3H), 7.15 (t, J = 7.3 Hz, 1H), 7.03 (d, J = 7.3 Hz, 2H), 6.97 – 6.93 (m, 1H), 4.71 (p, J =

7.7 Hz, 1H), 4.36 (s, 2H), 2.16 – 2.07 (m, 2H), 1.97 – 1.90 (m, J = 9.8, 5.5 Hz, 2H), 1.89 – 1.82

(m, J = 11.7, 8.2, 2.0 Hz, 2H), 1.59 – 1.51 (m, J = 10.2, 7.9, 4.5 Hz, 2H). ^{13}C NMR (125 MHz,

CDCl$_3$) δ 157.79, 149.72, 133.21, 129.83, 128.92, 128.62, 128.14, 127.04, 119.64, 60.85, 33.99,

33.14, 30.52, 24.78.

Reagents and conditions: (a) Benzyl boronic acid, K$_3$PO$_4$, tetrakis, Dioxane:water 120°C, 2 h;
(b) Pyrrolidine, MW,120°C, 1 h
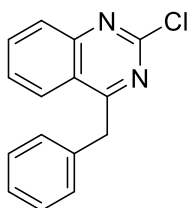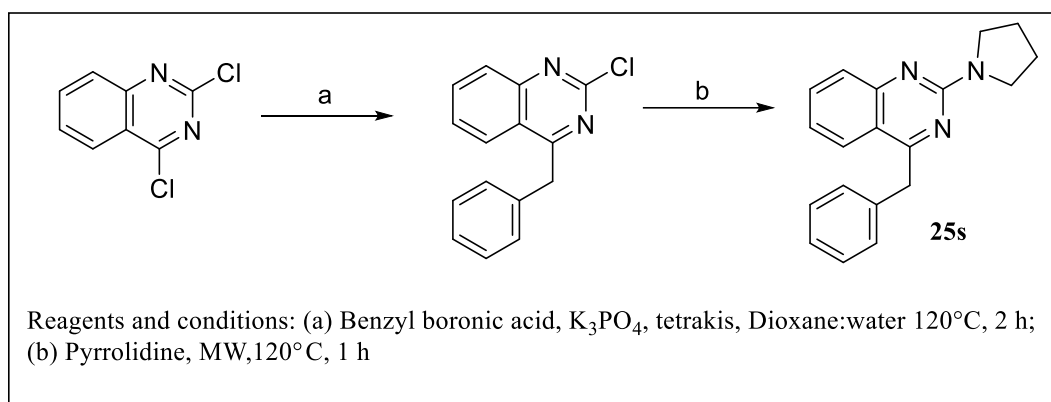
4-benzyl-2-chloroquinazoline. 2,4-dichloroquinazoline (200.0 mg, 1.0 mmol), benzyl boronic

acid (203 mg, 1.50 mmol), and K$_3$PO$_4$ (0.42 g, 2.0 mmol) in dioxane:water (4:1, 3 mL) were

degassed using Ar gas for 10 min, *tetrakis*(*triphenylphosphine*)*palladium*(*0*) (28.0 mg, 0.025 mmol)

was added the reaction vessel was purged with argon and subjected to microwave irradiation at 120

°C for 2 h. The crude reaction mixture was filtered over celite and the filtrate purified by normal

phase flash chromatography EtOAc:Hexane. Yield = 70.0 mg (27.5%) LCMS: R_T = 2.8 min., >98%

@ 215 and 254 nm, m/z = 255.1 [M + H]$^+$. ^{1}H NMR (500 MHz, CDCl$_3$) δ 8.17 (d, J = 8.4 Hz,

1H), 8.13 (d, J = 7.2 Hz, 1H), 8.00 (d, J = 8.5 Hz, 1H), 7.90 (t, J = 7.7 Hz, 1H), 7.61 (t, J = 8.2 Hz,

1H), 7.50 (t, J = 7.8 Hz, 1H), 7.34 (t, J = 5.0 Hz, 2H), 7.24 (t, J = 7.0 Hz, 1H), 4.64 (s, 2H).

4-benzyl-2-(pyrrolidin-1-yl)quinazoline (25s). Yield = 15.0 mg (26.3%, yellow oil) LCMS: R_T =

2.42 min., >98% @ 215 and 254 nm, m/z = 290.1 [M + H]$^+$. ^{1}H NMR (500 MHz, CDCl$_3$) δ 7.80

(d, J = 8.2 Hz, 1H), 7.50 (t, J = 7.4 Hz, 1H), 7.26 (t, J = 6.9 Hz, 2H), 7.23 – 7.19 (m, 3H), 7.12 (t,

J = 7.3 Hz, 1H), 7.03 (t, J = 7.5 Hz, 1H), 4.37 (s, 2H), 3.65 (s, 4H), 1.94 (t, J = 6.6 Hz, 4H). ^{13}C

NMR (125 MHz, CDCl$_3$) δ 180.80, 178.72, 152.47, 133.47, 128.91, 128.47, 126.50, 125.47, 46.97,

41.24, 25.57.

3.7. References

1.   Clapham, D. E. TRP channels as cellular sensors. *Nature* **2003,** 426, 517-524.

2.   Montell, C.; Birnbaumer, L.; Flockerzi, V. The TRP channels, a remarkably functional family. *Cell* **2002,** 108, 595-598.

3.   Montell, C.; Rubin, G. M. Molecular characterization of the Drosophila trp locus: a putative integral membrane protein required for phototransduction. *Neuron* **1989,** 2, 1313-1323.

4.   Plant, T. D.; Schaefer, M. TRPC4 and TRPC5: receptor-operated Ca^{2+}-permeable nonselective cation channels. *Cell Calcium* **2003,** 33, 441-450.

5.   Alawi, K. M.; Russell, F. A.; Aubdool, A. A.; Srivastava, S.; Riffo-Vasquez, Y.; Baldissera, L.; Thakore, P.; Saleque, N.; Fernandes, E. S.; Walsh, D. A. Transient receptor potential canonical 5 (TRPC5) protects against pain and vascular inflammation in arthritis and joint inflammation. *Ann. Rheum. Dis.* **2017,** 76, 252-260.

6.   Riccio, A.; Li, Y.; Tsvetkov, E.; Gapon, S.; Yao, G. L.; Smith, K. S.; Engin, E.; Rudolph, U.; Bolshakov, V. Y.; Clapham, D. E. Decreased anxiety-like behavior and Gαq/11-dependent responses in the amygdala of mice lacking TRPC4 channels. *J. Neurosci.* **2014,** 34, 3653-3667.

7.   Riccio, A.; Li, Y.; Moon, J.; Kim, K.-S.; Smith, K. S.; Rudolph, U.; Gapon, S.; Yao, G. L.; Tsvetkov, E.; Rodig, S. J. Essential role for TRPC5 in amygdala function and fear-related behavior. *Cell* **2009,** 137, 761-772.

8.   Just, S.; Chenard, B. L.; Ceci, A.; Strassmaier, T.; Chong, J. A.; Blair, N. T.; Gallaschun, R. J.; del Camino, D.; Cantin, S.; D'Amours, M.; Eickmeier, C.; Fanger, C. M.; Hecker, C.; Hessler, D. P.; Hengerer, B.; Kroker, K. S.; Malekiani, S.; Mihalek, R.; McLaughlin, J.; Rast, G.; Witek, J.; Sauer, A.; Pryce, C. R.; Moran, M. M. Treatment with HC-070, a potent inhibitor of TRPC4 and TRPC5, leads to anxiolytic and antidepressant effects in mice. *PloS One* **2018,** 13, e0191225.

9.   Tai, C.; Hines, D. J.; Choi, H. B.; MacVicar, B. A. Plasma membrane insertion of TRPC5 channels contributes to the cholinergic plateau potential in hippocampal CA1 pyramidal neurons. *Hippocampus* **2011,** 21, 958-967.

10.   Wei, H.; Sagalajev, B.; Yüzer, M. A.; Koivisto, A.; Pertovaara, A. Regulation of neuropathic pain behavior by amygdaloid TRPC4/C5 channels. *Neurosci. Lett.* **2015,** 608, 12-17.

11.   Sadler, K. E.; Moehring, F.; Shiers, S. I.; Laskowski, L. J.; Mikesell, A. R.; Plautz, Z. R.; Mecca, C. M.; Dussor, G.; Price, T. J.; McCorvy, J. D. Transient receptor potential canonical 5 (TRPC5) mediates inflammatory mechanical pain. *bioRxiv* **2020**.

12.   Hill, N. R.; Fatoba, S. T.; Oke, J. L.; Hirst, J. A.; O'Callaghan, C. A.; Lasserson, D. S.; Hobbs, F. R. Global prevalence of chronic kidney disease–a systematic review and meta-analysis. *PloS one* **2016,** 11, e0158765.

13.   Greka, A.; Mundel, P. Cell biology and pathology of podocytes. *Annu. Rev. Physiol.* **2012,** 74, 299-323.

14.   Chung, J.-J.; Shaw, A. S. TRP'ing up chronic kidney disease. *Science* **2017,** 358, 1256-1257.

15.   Greka, A.; Mundel, P. Balancing calcium signals through TRPC5 and TRPC6 in podocytes. *J. Am. Soc. Nephrol.* **2011**, ASN. 2011040370.

16.   Miller, M.; Shi, J.; Zhu, Y.; Kustov, M.; Tian, J.-b.; Stevens, A.; Wu, M.; Xu, J.; Long, S.; Yang, P. Identification of ML204: a novel potent antagonist that selectively modulates native TRPC4/C5 channels. *J. Biol. Chem.* **2011**, jbc. M111. 274167.

17.   Chenard, B. L.; Gallaschun, R. J. Substituted xanthines and methods of use thereof. 2016.

18.   Just, S.; Chenard, B. L.; Ceci, A.; Strassmaier, T.; Chong, J. A.; Blair, N. T.; Gallaschun, R. J.; del Camino, D.; Cantin, S.; D'Amours, M. Treatment with HC-070, a potent inhibitor of TRPC4 and TRPC5, leads to anxiolytic and antidepressant effects in mice. *PloS one* **2018,** 13, e0191225.

19.   McNamara, C. R.; Mandel-Brehm, J.; Bautista, D. M.; Siemens, J.; Deranian, K. L.; Zhao, M.; Hayward, N. J.; Chong, J. A.; Julius, D.; Moran, M. M. TRPA1 mediates formalin-induced pain. *Proc. Natl. Acad. Sci. USA* **2007,** 104, 13525-13530.

20.   Richter, J. M.; Schaefer, M.; Hill, K. Clemizole hydrochloride is a novel and potent inhibitor of transient receptor potential channel TRPC5. *Mol. Pharmacol.* **2014,** 86, 514-521.

21.   Zhu, Y.; Lu, Y.; Qu, C.; Miller, M.; Tian, J.; Thakur, D. P.; Zhu, J.; Deng, Z.; Hu, X.; Wu, M.; McManus, O. B.; Li, M.; HOng, X.; Zhu, M. X.; Luo, H.-R. Identification and optimization of 2-aminobenzimidazole derivatives as novel inhibitors of TRPC4 and TRPC5 channels. *Br. J. Pharmacol.* **2015,** 172, 3495-3509.

22.   Yu, M.; Ledeboer, M. W.; Daniels, M.; Malojcic, G.; Tibbitts, T. T.; Coeffet-Le Gal, M.; Pan-Zhou, X.-R.; Westerling-Bui, A.; Beconi, M.; Reilly, J. F. Discovery of a potent and selective TRPC5 inhibitor, efficacious in a focal segmental glomerulosclerosis model. *ACS Med. Chem. Lett.* **2019,** 10, 1579-1585.

23.   Harmange, M. W. L. H. D. Y.-C. P. Pyridazinones and methods of use thereof. 2021.

24.   Sabnis, R. W. Novel Pyridazinones as TRPC5 Inhibitors for Treating Kidney Diseases. *ACS Med. Chem. Lett.* **2021,** 12, 526-527.

25.   Walsh, L.; Reilly, J. F.; Cornwall, C.; Gaich, G. A.; Gipson, D. S.; Heerspink, H. J.; Johnson, L.; Trachtman, H.; Tuttle, K. R.; Farag, Y. M. Safety and Efficacy of GFB-887, a TRPC5 Channel Inhibitor, in Patients with Focal Segmental Glomerulosclerosis, Treatment-Resistant Minimal Change Disease, or Diabetic Nephropathy: TRACTION-2 Trial Design. *Kidney Int. Rep.* **2021**.

26.   Goldfinch Bio, I. A Study of TRPC5 Channel Inhibitor in Patients With Diabetic Nephropathy, Focal Segmental Glomerulosclerosis, and Treatment-Resistant Minimal Change Disease. https://clinicaltrials.gov/ct2/show/NCT04387448 (08/18).

27.   Sharma, S. H.; Pablo, J. L.; Montesinos, M. S.; Greka, A.; Hopkins, C. R. Design, synthesis and characterization of novel N-heterocyclic-1-benzyl-1H-benzo [d] imidazole-2-amines as selective TRPC5 inhibitors leading to the identification of the selective compound, AC1903. *Bioorg. Med. Chem. Lett.* **2019,** 29, 155-159.

28.   Stockley, M. L.; Macdonald, E. C.; Shah, P.; Jordan, A.; Hitchin, J.; Hamilton, N. Autotaxin inhibitory compounds. In Google Patents: 2020.

29.   Halland, N.; Nazare, M.; R'kyek, O.; Alonso, J.; Urmann, M.; Lindenschmidt, A. A General and Mild Palladium-Catalyzed Domino Reaction for the Synthesis of 2H-Indazoles. *Angew. Chem. Int. Ed.* **2009,** 48, 6879-6882.

30.   Zhou, Y.; Castonguay, P.; Sidhom, E.-H.; Clark, A. R.; Dvela-Levitt, M.; Kim, S.; Sieber, J.; Wieder, N.; Jung, J. Y.; Andreeva, S. A small-molecule inhibitor of TRPC5 ion channels suppresses progressive kidney disease in animal models. *Science* **2017,** 358, 1332-1336.

31.   Richter, J. M.; Schaefer, M.; Hill, K. Clemizole hydrochloride is a novel and potent inhibitor of transient receptor potential channel TRPC5. *Mol. Pharmacol.* **2014**, mol. 114.093229.

32.   Wang, X.; Dande, R. R.; Yu, H.; Samelko, B.; Miller, R. E.; Altintas, M. M.; Reiser, J. TRPC5 does not cause or aggravate glomerular disease. *J. Am. Soc. Nephrol.* **2018,** 29, 409-415.

33.   Pablo, J. L.; Greka, A. Charting a TRP to novel therapeutic destinations for kidney diseases. *Trends Pharmacol. Sci.* **2019,** 40, 911-918.

34.   Song, K.; Wei, M.; Guo, W.; Quan, L.; Kang, Y.; Wu, J.-X.; Chen, L. Structural basis for human TRPC5 channel inhibition by two distinct inhibitors. *Elife* **2021,** 10, e63429.

35.   Wright, D. J.; Simmons, K. J.; Johnson, R. M.; Beech, D. J.; Muench, S. P.; Bon, R. S. Human TRPC5 structures reveal interaction of a xanthine-based TRPC1/4/5 inhibitor with a conserved lipid binding site. *Communications biology* **2020,** 3, 1-11.

36.   Storch, U.; y Schnitzler, M. M.; Gudermann, T. A greasy business: Identification of a diacylglycerol binding site in human TRPC5 channels by cryo-EM. *Cell Calcium* **2021,** 97, 102414.